(12) INTERNATIONAL APPLICATION PUBLISHED UNDER THE PATENT COOPERATION TREATY (PCT)

(19) World Intellectual Property Organization
International Bureau

(43) International Publication Date
18 July 2013 (18.07.2013)

WIPO | PCT

(10) International Publication Number
WO 2013/106852 A1

(51) International Patent Classification:
A61K 39/39 (2006.01) *A61K 9/16* (2006.01)

(21) International Application Number:
PCT/US2013/021478

(22) International Filing Date:
14 January 2013 (14.01.2013)

(25) Filing Language: English

(26) Publication Language: English

(30) Priority Data:
61/586,624 13 January 2012 (13.01.2012) US

(71) Applicants: **PRESIDENT AND FELLOWS OF HARVARD COLLEGE** [—/US]; 17 Quincy Street, Cambridge, MA 02138 (US). **DANA-FARBER CANCER INSTITUTE, INC.** [—/US]; 450 Brookline Avenue, Boston, MA 02215 (US).

(72) Inventors; and

(71) Applicants *(for US only)*: **ALI, Omar, Abdel-Rahman** [US/US]; 700 Huron Ave., Apt. 15, Cambridge, MA 02138 (US). **DRANOFF, Glenn** [US/US]; 28 Outlook Drive, Lexington, MA 02421 (US). **MOONEY, David, J.** [US/US]; 27 Powers Road, Sudbury, MA 01776 (US).

(74) Agents: **BEATTIE, Ingrid, A.** et al.; Mintz Levin Cohn Ferris Glovsky and Popeo, P.C., One Financial Center, Boston, MA 02111 (US).

(81) Designated States *(unless otherwise indicated, for every kind of national protection available)*: AE, AG, AL, AM, AO, AT, AU, AZ, BA, BB, BG, BH, BN, BR, BW, BY, BZ, CA, CH, CL, CN, CO, CR, CU, CZ, DE, DK, DM, DO, DZ, EC, EE, EG, ES, FI, GB, GD, GE, GH, GM, GT, HN, HR, HU, ID, IL, IN, IS, JP, KE, KG, KM, KN, KP, KR, KZ, LA, LC, LK, LR, LS, LT, LU, LY, MA, MD, ME, MG, MK, MN, MW, MX, MY, MZ, NA, NG, NI, NO, NZ, OM, PA, PE, PG, PH, PL, PT, QA, RO, RS, RU, RW, SC, SD, SE, SG, SK, SL, SM, ST, SV, SY, TH, TJ, TM, TN, TR, TT, TZ, UA, UG, US, UZ, VC, VN, ZA, ZM, ZW.

(84) Designated States *(unless otherwise indicated, for every kind of regional protection available)*: ARIPO (BW, GH, GM, KE, LR, LS, MW, MZ, NA, RW, SD, SL, SZ, TZ, UG, ZM, ZW), Eurasian (AM, AZ, BY, KG, KZ, RU, TJ, TM), European (AL, AT, BE, BG, CH, CY, CZ, DE, DK, EE, ES, FI, FR, GB, GR, HR, HU, IE, IS, IT, LT, LU, LV, MC, MK, MT, NL, NO, PL, PT, RO, RS, SE, SI, SK, SM, TR), OAPI (BF, BJ, CF, CG, CI, CM, GA, GN, GQ, GW, ML, MR, NE, SN, TD, TG).

[Continued on next page]

(54) Title: CONTROLLED DELIVERY OF TLR AGONISTS IN STRUCTURAL POLYMERIC DEVICES

(57) Abstract: The present invention comprises compositions, methods, and devices for creating an stimulating an antigen-specific dendritic cell immune response. Devices and methods provide prophylactic and therapeutic immunity to subjects against cancer and infectious agents.

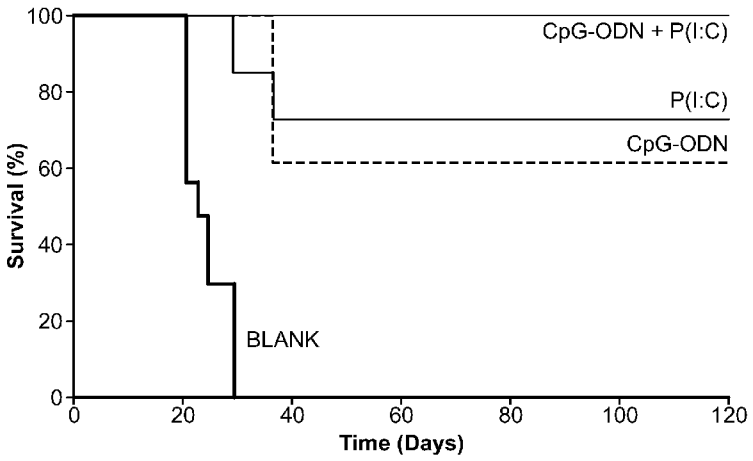


FIG. 22

WO 2013/106852 A1

Published:

— *with international search report (Art. 21(3))*

CONTROLLED DELIVERY OF TLR AGONISTS IN STRUCTURAL POLYMERIC DEVICES

RELATED APPLICATIONS

This application claims priority to U.S. Provisional Application No. 61/586,624, filed January 13, 2012. This application is incorporated herein by reference in its entirety.

GOVERNMENT SUPPORT

This invention was made with Government support awarded by the National Institutes of Health. The Government has certain rights in the invention.

BACKGROUND OF THE INVENTION

Dendritic cells (DCs) collect and process antigens for presentation to T cells. DCs are the most potent activators of the immune system among antigen presenting cells. Research focused on using dendritic cells for a therapeutic benefit has been slow because dendritic cells are rare and difficult to isolate.

SUMMARY OF THE INVENTION

The invention features a device and method for stimulating immune cells such as dendritic cells, *in situ*. For example, presentation of Toll-like receptor (TLR) agonists in the context of the device is used for cancer vaccination. Incorporation and presentation of the TLR agonists embedded in structural polymeric devices specifically stimulates CD8(+) dendritic cells (DCs) (corresponding to CD141+ DCs in humans) and plasmacytoid DCs, which subsets of DCs are critical for cancer vaccination.

Accordingly, the invention provides a device comprising a porous polymeric structure composition, a tumor antigen, and a toll-like receptor (TLR) agonist. For example, the device comprises a polymeric structure composition, a tumor antigen, and a combination of toll-like receptor (TLR) agonists, wherein the TLR agonist is selected from the group consisting of TLR1, TLR2, TLR3, TLR4, TLR5, TLR6, TLR7, TLR8, TLR9, TLR10, TLR11, TLR12, and TLR13. For example, the polymeric structure comprises poly (D,L-lactide-co-glycolide) (PLG). Exemplary TLR agonists include pathogen associated molecular patterns (PAMPs), e.g., an infection-mimicking composition such as a bacterially-derived immunomodulator. TLR agonists include nucleic acid or lipid compositions [e.g., monophosphoryl lipid A (MPLA)].

SUBSTITUTE SHEET (RULE 26)

Certain nucleic acids function as TLR agonists, e.g., TLR1 agonists, TLR2 agonists, TLR3 agonists, TLR4 agonists, TLR5 agonists, TLR6 agonists, TLR7 agonists, TLR8 agonists, TLR9 agonists, TLR10 agonists, TLR11 agonists, TLR12 agonists, or TLR13 agonists. In one example, the TLR agonist comprises a TLR9 agonist such as a cytosine-guanosine oligonucleotide (CpG-ODN), a poly(ethylenimine) (PEI)-condensed oligonucleotide (ODN) such as PEI-CpG-ODN, or double stranded deoxyribonucleic acid (DNA). TLR9 agonists are useful to stimulate plasmacytoid DCs. For example, the device comprises 5 μg, 10μg, 25μg, 50 μg, 100 μg, 250μg, or 500 μg of CpG-ODN.

In another example, the TLR agonist comprises a TLR3 agonist such as polyinosine-polycytidylic acid (poly I:C), PEI-poly (I:C), polyadenylic–polyuridylic acid (poly (A:U)), PEI-poly (A:U), or double stranded ribonucleic acid (RNA).

TLR3 agonists are useful to stimulate CD8+ DCs in mice and CD141+ DCs in humans. A plurality of TLR agonists, e.g, a TLR3 agonist such as poly I:C and a TLR9 agonist such as CpG act in synergy to activate an anti-tumor immune response. For example, the device comprises a TLR3 agonist such as poly (I:C) and the TLR9 agonist (CpG-ODN) or a PEI-CpG-ODN. Preferably, the TLR agonist comprises the TLR3 agonist, poly (I:C) and the TLR9 agonist, CpG-ODN. The combination of poly (I:C) and CpG-ODN act synergistically as compared to the vaccines incorporating CpG-ODN or P(I:C) alone.

In some cases, the TLR agonist comprises a TLR4 agonist selected from the group consisting of lipopolysaccharide (LPS), monophosphoryl lipid A (MPLA), a heat shock protein, fibrinogen, heparin sulfate or a fragment threof, hyaluronic acid or a fragment thereof, nickel, an opoid, α1-acid glycoprotein (AGP), RC-529, murine β-defensin 2, and complete Freund's adjuvant (CFA). In other cases, the TLR agonist comprises a TLR5 agonist, wherein the TLR5 agonist is flagellin. Other suitable TLR agonists include TRL7 agonists selected from the group consisting of single-stranded RNA, guanosine anologs, imidazoqinolines, and loxorbine.

Preferably, the TLR agonist is present at a concentration effective to induce the local production of interleukin-12 (IL-12) by dendritic cells.

The invention also provides a device comprising a porous polymeric structure composition, a disease-associated antigen, and a toll-like receptor (TLR) agonist, wherein the TLR agonist preferentially binds to TLR3. In some cases, the polymeric structure composition comprises poly-lactide-co-glycolide (PLG). The TLR3 agonist is present in an amount to preferentially stimulate CD8+ dendritic cells or CD141+ dendritic cells.

Preferably, the TLR agonist comprises a TLR3 agonist. In some cases, the TLR3 agonist comprises polyinosine-polycytidylic acid (poly I:C) or PEI- poly (I:C). For example, the TLR agonist comprises a nucleic acid. In other cases, the TLR agonist further comprises a TLR9 agonist. For example, the TLR9 agonist comprises a cytosine-guanosine oligonucleotide (CpG-ODN) or a PEI-CpG-ODN. Optionally, the device comprises a combination of TLR agonists, the combination comprising a TLR3 agonist and a TLR9 agonist. For example, the TLR3 agonist comprises poly (I:C) and the TLR9 agonist comprises CpG-ODN.

Alternatively, the device comprises a combination of TLR agonists, the combination comprising a TLR3 agonist and a TLR4 agonist. For example, the TLR3 agonist comprises poly (I:C) and the TLR4 agonist comprises MPLA.

Optionally, the device further comprises a recruitment composition. Exemplary recruitment compositions include granulocyte macrophage colony stimulating factor (GM-CSF), Flt3L, and CCL20. For example, the recruitment composition comprises encapsulated GM-CSF.

In some cases, the disease-associated antigen comprises a tumor antigen. For example, the tumor antigen comprises a tumor lysate, purified protein tumor antigen, or synthesized tumor antigen.

Optionally, the TLR agonist further comprises pathogen associated molecular patterns (PAMPs). For example, the PAMP comprises a monophosphoryl lipid A (MPLA).

Also provided is a device comprising a polymeric structure composition, a tumor antigen, and a combination of TLR agonists, wherein the TLR agonist is selected from the group consisting of TLR1, TLR2, TLR3, TLR4, TLR5, TLR6, TLR7, TLR8, TLR9, TLR10, TLR11, TLR12, and TLR13.

A method for eliciting an anti-tumor immune response is carried out by contacting or implanting into a subject a device comprising a polymeric structure composition, a tumor antigen, and a TLR agonist, wherein the TLR agonist preferentially binds to TLR3. For example, the TLR agonist comprises a TLR3 agonist. Alternatively, the TLR agonist comprises a TLR3 agonist and a TLR9 agonist.

Preferably, the anti-tumor immune response comprises activation of a CD8+ dendritic cell or a CD141+ dendritic cell. In some cases, the anti-tumor immune response comprises

activation of a plasmacytoid dendritic cell or a CD141+ dendritic cell. Alternatively, the anti-tumor immune response comprises a reduction in tumor burden.

Preferably, the TLR agonist is present at a concentration effective to induce production of interleukin-12 (IL-12) by dendritic cells.

Optionally, the device further comprises granulocyte macrophage colony stimulating factor (GM-CSF). In some examples, the GM-CSF is encapsulated. Another optional recruitment composition is a cytokine. For example, the device comprises 1 μg, 3 μg, 5 μg, 10 μg, 25 μg, or 50 μg of GM-CSF.

The device also contains a tumor antigen, e.g., in the form of a tumor lysate (cultured cells or patient-derived primary cells) or purified tumor antigen such as a synthesized/synthetic recombinant protein or biochemically-purified antigen from a tumor cell.

Also with in the invention is a method for eliciting an anti-tumor immune response by contacting a subject, e.g., implanting into a subject, a device comprising a porous polymeric structure composition, a tumor antigen, and a TLR agonist. For example, the TLR agonist is selected from the group consisting of TLR1, TLR2, TLR3, TLR4, TLR5, TLR6, TLR7, TLR8, TLR9, TLR10, TLR11, TLR12, and TLR13. The device described above is associated with advantages over earlier vaccines. The most significant advantage is its ability to stimulate critical subsets of DCs that mediate potent anti-tumor activity. The the method involves administering to a subject a device that contains a TLR3 agonist and/or a TLR9 agonist, which leads to elicitation of an anti-tumor immune response characterized by activation of plasmacytoid DCs and/or CD141+ DCs in the subject to which the vaccine was administered. The vaccine is useful for prophylaxis as well as therapy.

The device is administered, e.g., topically applied or implanted, and is present over a period of time, e.g., in-dwelling, while constantly recruiting, educating, and dispersing or sending cells forth to lymph nodes or sites of disease or infection in the body. Improvements over existing devices include long term, ongoing activation of cells that enter the device and concomitant long term, ongoing egress of immunologically activated, e.g., antigen primed cells. The device includes a scaffold composition, a recruitment composition, and a deployment composition. The deployment composition that mediates prolonged and continuous egress of primed cells is an infection-mimicking composition such as a bacterially-derived immunomodulator. In preferred embodiments, the bacterially-derived

immunomodulator is a nucleic acid such as a cytosine-guanosine oligonucleotide (CpG-ODN).

The methods are used to treat a wide variety of diseases and to develop vaccines against a wide variety of antigens. In a preferred embodiment, the present invention is used to develop a cancer vaccine. Another preferred embodiment of the present invention comprises an infection-mimicking microenvironment with means to activate the host immune system and subsequently induce an immune response. The use of a synthetic cytosine-guanosine oligodeoxynucleotide (CpG-ODN) sequence with exogenous granulocyte macrophage colony stimulating factor (GM-CSF) provides a method for precisely controlling dendritic cell migration and modulating antigen-specific immune responses. In fact, the approach of using of this synthetic cytosine-gyanosine oligonucleotide (CpG-ODN) sequence and/or poly (I:C) demonstrates significant improvements over earlier immune therapies.

Various components of the device are tabulated and described below.

Table 1

	FUNCTION		
EXEMPLARY DEVICE	Attract a DC to Device	Present an Immunogenic Factor	Induce DC Migration from Device
1	**Scaffold Composition**	**Scaffold Composition**	**Scaffold Composition**
2	Bioactive Composition	Bioactive Composition	Bioactive Composition
3	**Scaffold Composition**	Bioactive Composition	Bioactive Composition
4	**Scaffold Composition**	**Scaffold Composition**	Bioactive Composition
5	Bioactive Composition	**Scaffold Composition**	**Scaffold Composition**
6	Bioactive Composition	Bioactive Composition	**Scaffold Composition**
7	Bioactive Composition	**Scaffold Composition**	Bioactive Composition
8	**Scaffold Composition**	Bioactive Composition	**Scaffold Composition**

Devices perform three primary functions, e.g. attracting cells to the device, presenting an immunogenic factor, and inducing cell migration away from the device. Each of these primary functions are performed by the scaffold (bold font) and/or biological (standard font) composition(s). Table 1 provides exemplary combinations of either the scaffold or biological composition paired with at least one primary function in exemplary devices (1-8). For

example, the scaffold composition performs all three primary functions (device 1). In an alternative example, the scaffold composition performs one primary function, e.g. attracts cells to the device (preferably, dendritic cells), whereas the biological composition performs two primary functions, e.g. presents an immunogenic factor and induces cells (preferably, dendritic cells) to migrate away from the device (device 3). Device 5, for instance, is the inverse combination of device 3. Exemplary secondary functions of the scaffold and/or biological compositions include, but are not limited to, targeting the device to a particular cell or tissue type, adhering/releasing the device to/from the surface of one or more cells or tissues, and modulating the stability/degradation of the device.

The invention comprises a device comprising a scaffold composition and bioactive composition, the bioactive composition being incorporated into or conjugated onto the scaffold composition, wherein the scaffold composition attracts a dendritic cell, introduces a immunogenic factor into the dendritic cell thereby activating the dendritic cell, and induces the dendritic cell to migrate away from the scaffold composition. Alternatively the bioactive composition incorporated into or coated onto the scaffold composition attracts a dendritic cell, introduces an immunogenic factor into the dendritic cell thereby activating the dendritic cell, and induces the dendritic cell to migrate away from the scaffold composition. In other preferred embodiments, the scaffold composition or bioactive composition separately attract a dendritic cell to the device, introduce an immunogenic factor into the dendritic cell, and induce the dendritic cell to migrate away from the device.

DCs include conventional DCs as well as specific subsets of DCs. The TLR agonists, e.g., TLR3 agonists, preferentially attract and stimulate CD141+ DCs in the human (CD8+ DCs in the mouse). The TLR9 agonisst, e.g., CpG, preferentially attract and stimulate plasmacytoid DCs.

In preferred embodiments, the recruitment composition is GM-CSF, e.g., encapsulated GM-CSF. The device temporally controls local GM-CSF concentration, thereby controlling recruitment, residence, and subsequent dispersement/deployment of immune cells to lymph nodes or tissue sites distant from location of the device, e.g., sites of infection or tumor location. The concentration of GM-CSF determines whether if functions as a recruitment element or a deployment element. Accordingly, a method of programming dendritic cells *in situ* is carried out by introducing to a subject a device comprising scaffold composition and encapsulated recruitment composition. A pulse of recruitment composition is released from the device within 1-7 days of introduction of the device, leaving a residual

amount of the recruitment composition in or on the device. The pulse is followed by slow release of the residual amount over several weeks. The local concentration of the recruitment composition and the temporal pattern of release mediates recruitment, retention, and subsequent release of dendritic cells from the device. For example, the pulse comprises at least 50, 60, 75, 90 or 95 % of the amount of the recruitment composition associated with the device. An exemplary temporal release profile comprises a pulse characterized by release of at least 60% of the amount of the recruitment composition associated with the device in 1-5 days following the introduction of the device to a subject. Following the pulse, the residual amount is slowly released over an extended period of time (e.g., 1, 2, 3, 4, 5, 6, 7, 8, 9, 10, 12 days or 2, 3, 4, 5 or more weeks) following the pulse period. Other recruitment compositions include Flt3L and/or CCL20. The recruitment compounds are used individually or in combination.

The method of making a scaffold is carried out by providing a scaffold composition, incorporating into or coating onto the scaffold composition a first bioactive composition comprising polypeptides with means for attracting or repelling a dendritic cell, and contacting the scaffold composition with a second bioactive composition, wherein the second bioactive composition is covalently or non-covalently associated with the scaffold composition wherein the second bioactive composition comprises a immunogenic factor. In an alternate embodiment of this method, the linking and contacting steps are repeated to yield a plurality of layers, wherein the second bioactive composition comprises a combination of compounds with means to activate a dendritic cell.

Methods comprise continuous *in situ* dendritic cell programming, comprising administering to a subject, a device comprising a scaffold composition and bioactive composition, the bioactive composition being incorporated into or conjugated onto the scaffold composition, wherein the scaffold composition attracts a dendritic cell, introduces a immunogenic factor into the dendritic cell thereby activating the dendritic cell, and induces the dendritic cell to migrate away from the scaffold composition. The devices recruit and stimulate a heterogeneous population of dendritic cells. Each subset is specialized and contributes significantly to the generation of an immune response. For example, the device mediates CpG-ODN presentation and enrichment of a subset of dendritic cells, plasmacytoid DC (pDC), or CD141+ DCs, which are particularly important in development of anti-tumor immunity.

Methods comprise increasing vaccine efficacy, comprising administering to a subject, a device comprising a scaffold composition and bioactive composition, the bioactive composition being incorporated into or conjugated onto the scaffold composition, wherein the scaffold composition attracts a dendritic cell, introduces a immunogenic factor into the dendritic cell thereby activating the dendritic cell, and induces the dendritic cell to migrate away from the scaffold composition, thereby increasing the effectiveness of a vaccination procedure.

Methods comprise vaccinating a subject against cancer, comprising administering to a subject, a device comprising a scaffold composition and bioactive composition, the bioactive composition being incorporated into or conjugated onto the scaffold composition, wherein the scaffold composition attracts a dendritic cell, introduces a immunogenic factor into the dendritic cell thereby activating the dendritic cell, and induces the dendritic cell to migrate away from the scaffold composition, thereby conferring upon a subject anti-tumor immunity, e.g., IL-12 production, and reduced tumor burden. In the case of a localized or solid tumor, the device is administered or implanted at or near the tumor site or site from which the tumor was excised or surgically removed. For example, the device is implanted at a distance of 1, 3, 5, 10, 15, 20, 25, 40 mm from a tumor site or site of excision, e.g., the PLG vaccine device is administered 16-21 mm away from a tumor mass.

Immunogenic factors include TLR ligands. For example, the immunogenic factor used is a modified TLR-9 ligand sequence, PEI-CpG-ODN. Preferably, the TLR ligand is a TLR3 agonist such as poly (I:C) or condensed PEI-poly (I:C).

Scaffold compositions comprise a non-biodegradable material. Exemplary non-biodegradable materials include, but are not limited to, metal, plastic polymer, or silk polymer. Moreover, scaffold compositions are composed of a biocompatible material. This biocompatible material is non-toxic or non-immunogenic.

Bioactive compositions are covalently or non-covalently linked to the scaffold composition. Bioactive compositions comprise an element, either covalently or non-covalently bonded to the surface of the scaffold composition, with means to attract a dendritic cell. Alternatively, or in addition, bioactive compositions comprise an element, either covalently or non-covalently bonded to the surface of the scaffold composition, with means to introduce an immunogenic factor into a dendritic cell. Alternatively, or further in addition, bioactive compositions comprises an element, either covalently or non-covalently bonded to

the surface of the scaffold composition, with means to induce a dendritic cell to migrate away from the scaffold composition.

The element of the bioactive composition with means to manipulate a dendritic cell is a secreted or membrane-bound amino acid, peptide, polypeptide, protein, nucleotide, dinucleotide, oligonucleotide, polynucleotide, polymer, small molecule or compound. In a preferred embodiment, this element is granulocyte macrophage colony stimulating factor (GM-CSF), because this element attracts dendritic cells to the scaffold composition. In another preferred embodiment, this element is a PEI-CpG-ODN sequence because this element has means to introduce CpG-ODN sequences into a dendritic cell thereby activating the cell. In some embodiments, this element is a polynucleotide or polypeptide encoding for CCR7, a chemokine receptor that mediates dendritic cell migration towards lymph nodes and away from the scaffold composition. The CCR7 element is introduced into a dendritic cell simultaneously or sequentially with PEI-CpG-ODN sequences to enhance dendritic cell migration away from the scaffold composition.

Scaffold compositions of the present invention contain an external surface. Scaffold compositions of the present invention alternatively, or in addition, contain an internal surface. External or internal surfaces of the scaffold compositions are solid or porous. Pore size is less than about 10 nm, in the range of about 100 nm-20 μm in diameter, or greater than about 20 μm. In preferred embodiments, the size of the pores allows the migration into and subsequent exit of cells such as DCs from the device. For example, the pores are nanoporous, microporous, or macroporous. For example, the diameter of nanopores are less than about 10 nm; micropore are in the range of about 100 μm-20 μm in diameter; and, macropores are greater than about 20 μm (preferably greater than about 100 μm and even more preferably greater than about 400 μm). In one example, the scaffold is macroporous with open, interconnected pores of about 100-500 μm in diameter, e.g., 100-200, 200-400, or 400-500 μm. The size of the pores and the interconnected architecture allows the cells to enter, traverse within the volume of the device via the interconnected pores, and then leave the device via the pores to go to locations in the body outside of the device, e.g. to a tumor site, where an immune response is mounted against tumor cells. The activated DCs migrate away from the device and mount an immune response to solid tumors at discrete locations or throughout the body in the case of metastatic tumor cells or blood tumors such as leukemias.

Scaffold compositions of the present invention comprise one or more compartments.

Devices of the present invention are administered or implanted orally, systemically, sub- or trans-cunataneously, as an arterial stent, or surgically.

The devices and methods of the invention provide a solution to several problems associated with protocols for continuous cell programming in situ. In situ cell programming systems that stimulate immune responses of the cells and induce their outward migration to populate infected or diseased bodily tissues enhance the success of recovery, e.g., the specific elimination of diseased tissue. Such a device that controls cell function and/or behavior, e.g., locomotion, contains a scaffold composition and one or more bioactive compositions. The bioactive composition is incorporated into or coated onto the scaffold composition. The scaffold composition and/or bioactive composition temporally and spatially (directionally) controls dendritic cell attraction, programming, and migration.

The devices mediate active recruitment, modification, and release of host cells from the material *in vivo*, thereby improving the function of cells that have contacted the scaffold. For example, the device attracts or recruits cells already resident in the body to the scaffold material, and programs or reprograms the resident cells to a desired fate (e.g., immune activation).

This device includes a scaffold composition which incorporates or is coated with a bioactive composition; the device regulates attraction, activation, and migration of dendritic cells. Depending on the application for which the device is designed, the device regulates attraction, activation, and/or migration of dendritic cells through the physical or chemical characteristics of the scaffold itself. For example, the scaffold composition is differentially permeable, allowing cell migration only in certain physical areas of the scaffold. The permeability of the scaffold composition is regulated, for example, by selecting or engineering a material for greater or smaller pore size, density, polymer cross-linking, stiffness, toughness, ductility, or viscoelascticity. The scaffold composition contains physical channels or paths through which cells can move more easily towards a targeted area of egress of the device or of a compartment within the device. The scaffold composition is optionally organized into compartments or layers, each with a different permeability, so that the time required for a cell to move through the device is precisely and predictably controlled. Migration is also regulated by the degradation, de- or re-hydration, oxygenation, chemical or pH alteration, or ongoing self-assembly of the scaffold composition.

Attraction, activation, and/or migration are regulated by a bioactive composition. The device controls and directs the activation and migration of cells through its structure.

Chemical affinities are used to channel cells towards a specific area of egress. For example, cytokines are used to attract or retard the migration of cells. By varying the density and mixture of those bioactive substances, the device controls the timing of the migration. The density and mixture of these bioactive substances is controlled by initial doping levels or concentration gradient of the substance, by embedding the bioactive substances in scaffold material with a known leaching rate, by release as the scaffold material degrades, by diffusion from an area of concentration, by interaction of precursor chemicals diffusing into an area, or by production/excretion of compositions by resident support cells. The physical or chemical structure of the scaffold also regulates the diffusion of bioactive agents through the device.

The bioactive composition includes one or more compounds that regulate cell function and/or behavior. The bioactive composition is covalently linked to the scaffold composition or non-covalently associated with the scaffold.

Signal transduction events that participate in the process of cell migration are initiated in response to immune mediators. Thus, the device optionally contains a second bioactive composition that comprises GM-CSF, a CpG-ODN or poly (I:C) sequence, a cancer antigen, and/or an immunomodulator.

In some cases, the second bioactive composition is covalently linked to the scaffold composition, keeping the composition relatively immobilized in or on the scaffold composition. In other cases, the second bioactive composition is noncovalently associated with the scaffold. Noncovalent bonds are generally one to three orders of magnitude weaker than covalent bonds permitting diffusion of the factor out of the scaffold and into surrounding tissues. Noncovalent bonds include electrostatic, hydrogen, van der Waals, π aromatic, and hydrophobic.

The scaffold composition is biocompatible. The composition is bio-degradable/erodable or resistant to breakdown in the body. Relatively permanent (degradation resistant) scaffold compositions include metals and some polymers such as silk. Preferably, the scaffold composition degrades at a predetermined rate based on a physical parameter selected from the group consisting of temperature, pH, hydration status, and porosity, the cross-link density, type, and chemistry or the susceptibility of main chain linkages to degradation or it degrades at a predetermined rate based on a ratio of chemical polymers. For example, a high molecular weight polymer comprised of solely lactide degrades over a period of years, e.g., 1-2 years, while a low molecular weight polymer comprised of a 50:50 mixture of lactide and glycolide degrades in a matter of weeks, e.g., 1,

2, 3, 4, 6, 10 weeks. A calcium cross-linked gels composed of high molecular weight, high guluronic acid alginate degrade over several months (1, 2, 4, 6, 8, 10, 12 months) to years (1, 2, 5 years) *in vivo*, while a gel comprised of low molecular weight alginate, and/or alginate that has been partially oxidized, will degrade in a matter of weeks.

Exemplary scaffold compositions include polylactic acid, polyglycolic acid, PLGA polymers, alginates and alginate derivatives, gelatin, collagen, fibrin, hyaluronic acid, laminin rich gels, agarose, natural and synthetic polysaccharides, polyamino acids, polypeptides, polyesters, polyanhydrides, polyphosphazines, poly(vinyl alcohols), poly(alkylene oxides), poly(allylamines)(PAM), poly(acrylates), modified styrene polymers, pluronic polyols, polyoxamers, poly(uronic acids), poly(vinylpyrrolidone) and copolymers or graft copolymers of any of the above. One preferred scaffold composition includes an RGD-modified alginate.

Another preferred scaffold composition a macroporous poly-lactide-co-glycolide (PLG). For example, the PLG matrix includes GM-CSF, danger signals, and a target antigen, e.g., a cancer antigen and serves as a residence for recruited DCs as they are programmed. The recruitment element, GM-CSF, is encapsulated into the PLG scaffolds. PLG matrices that comprise the encapsulated GM-CSF provide a pulse of the dendritic cell recruitment composition and then a gradual slower rate of release. The pulse comprises at least 40, 50, 60, 75, 80% or more of the initial amount of bioactive composition with the remaining per cent being released gradually over then next days or weeks after administration to the site in or on the subject to be treated. For example, release is approximately 60% of bioactive GM-CSF load within the first 5 days, followed by slow and sustained release of bioactive GM-CSF over the next 10 days. This release profile mediates a rate of diffusion of the factor through the surrounding tissue to effectively recruit resident DCs.

Porosity of the scaffold composition influences migration of the cells through the device. Pores are nanoporous, microporous, or macroporous. For example, the diameter of nanopores are less than about 10 nm; micropore are in the range of about 100 nm-20 μm in diameter; and, macropores are greater than about 20 μm (preferably greater than about 100 μm and even more preferably greater than about 400μm). In one example, the scaffold is macroporous with aligned pores of about 400-500μm in diameter.

The device is manufactured in one stage in which one layer or compartment is made and infused or coated with one or more bioactive compositions. Exemplary bioactive compositions comprise polypeptides or polynucleotides. Alternatively, the device is manufactured in two or more (3, 4, 5, 6, ...10 or more) stages in which one layer or

compartment is made and infused or coated with one or more bioactive compositions followed by the construction of a second, third, fourth or more layers, which are in turn infused or coated with one or more bioactive compositions in sequence. Each layer or compartment is identical to the others or distinguished from one another by the number or mixture of bioactive compositions as well as distinct chemical, physical and biological properties.

A method of making a scaffold is carried out by providing a scaffold composition and covalently linking or noncovalently associating the scaffold composition with a first bioactive composition. Exemplary devices and methods of making them are described in USSN: 12/867,426, USSN: 13/510,356, and PCT/US2012/35505, each of which is hereby incorporated by reference. The first bioactive composition preferably contains granulocyte macrophage colony stimulating factor. The scaffold composition is also contacted with a second bioactive composition, preferably one or more cytosine-guanosine oligonucleotide (CpG-ODN) sequences. The second bioactive composition is associated with the scaffold composition to yield a doped scaffold, i.e., a scaffold composition that includes one or more bioactive substances. The contacting steps are optionally repeated to yield a plurality of doped scaffolds, e.g., each of the contacting steps is characterized by a different amount of the second bioactive composition to yield a gradient of the second bioactive composition in the scaffold device. Rather than altering the amount of composition, subsequent contacting steps involve a different bioactive composition, i.e., a third, fourth, fifth, sixth…., composition or mixture of compositions, that is distinguished from the prior compositions or mixtures of prior doping steps by the structure or chemical formula of the factor(s). The method optionally involves adhering individual niches, layers, or components to one another and/or insertion of semi-permeable, permeable, or nonpermeable membranes within or at one or more boundaries of the device to further control/regulate locomotion of cells or bioactive compositions.

Therapeutic applications of the device include the instruction of immune cells. For example, the method includes the steps of providing a device that includes scaffold composition with a bioactive composition incorporated therein or thereon and a mammalian cell bound to the scaffold and contacting a mammalian tissue with the device, e.g., by implanting or affixing the device into or onto a mammalian tissue. At the time of administering or implanting the device, exemplary relative amounts of each component, recruiting composition (e.g., GM-CSF, Flt3L, or CCL20), danger signal (e.g., CpG-ODN),

and antigen (e.g., purified tumor antigen or tumor cell lysate) are as follows: GM-CSF: 0.5 μg - 500 μg; CpG-ODN: 50μg - 3,000 μg; and Tumor antigen/lysate: 100 μg - 10,000 μg.

A method of modulating an activity of a cell, e.g., a host cell, is carried out by administering to a mammal a device containing a scaffold composition and a recruitment composition incorporated therein or thereon, and then contacting the cell with a deployment signal. The cells leave the device after encountering antigen (and other factors) and thus being activated to seek out tumor cells in the body to which an immune response is mounted. The activity of the cell at egress differs from that prior to entering the device. Cells are recruited into the device and remain resident in the device for a period of time, e.g., minutes; 0.2. 0.5, 1, 2, 4, 6, 12, 24 hours; 2, 4, 6, days; weeks (1-4), months (2, 4, 6, 8, 10, 12) or years, during which the cells are exposed to structural elements and bioactive compositions that lead to a change in the activity or level of activity of the cells. Encountering the antigen and other compounds in the device induces egress of the altered (re-educated or reprogrammed) cells, and the cells migrate out of the device and into surrounding tissues or remote target locations to seek out and mediate immunity against diseased cells such as tumor cells.

The deployment signal is a composition such as protein, peptide, or nucleic acid or a state of activation of the cell. For example, having ingested antigen, DCs become activated and migrate to lymph nodes, the spleen, and other anatomical locations, where they meet up with T cells to further propagate an antigen-specific immune response, e.g., anti-cancer response. For example, cells migrating into the device only encounter the deployment signal once they have entered the device. In some cases, the deployment signal is a nucleic acid molecule, e.g., a plasmid containing sequence encoding a protein that induces migration of the cell out of the device and into surrounding tissues. The deployment signal occurs when the cell encounters the plasmid in the device, the DNA becomes internalized in the cell (i.e., the cell is transfected), and the cell manufactures the gene product encoded by the DNA. In some cases, the molecule that signals deployment is an element of the device and is released from the device in delayed manner (e.g., temporally or spatially) relative to exposure of the cell to the recruitment composition. Alternatively, the deployment signal is a reduction in or absence of the recruitment composition. For example, a recruitment composition induces migration of cells into the device, and a reduction in the concentration or depletion, dissipation, or diffusion of the recruitment composition from the device results in egress of cells out of the device. In this manner, immune cells such as T cells, B cells, or dendritic

cells (DCs) of an individual are recruited into the device, primed and activated to mount an immune response against an antigen-specific target. Optionally, an antigen corresponding to a target to which an immune response is desired is incorporated into or onto the scaffold structure. Cytokines, such as granulocyte macrophage colony stimulating factor (GM-CSF) are also a component of the device to amplify immune activation and/or induce migration of the primed cells to lymph nodes. Other cell specific recruitment compositions are described below.

The device recruit cells *in vivo*, modifies these cells, and then promotes their migration to another site in the body. This approach is exemplified herein in the context of dendritic cells and cancer vaccine development but is also useful to other vaccines such as those against microbial pathogens as well as cell therapies in general. Cells educated using the devices described herein promote regeneration of a tissue or organ immediately adjacent to the material, or at some distant site. Alternatively, the cells are educated to promote destruction of a tissue (locally or at a distant site). The methods are also useful for disease prevention, e.g., to promote cell-based maintenance of tissue structure and function to stop or retard disease progression or age-related tissue changes. The education of cells within the device, "programming" and "reprogramming" permits modification of the function or activity of any cell in the body to become a multipotent stem cell again and exert therapeutic effects.

The inability of traditional and *ex vivo* DC-based vaccination strategies to coordinate and sustain an immune response mediated by the heterogeneous DC network in cancer patients has led to limited clinical effectiveness of these approaches. The devices and methods described herein have distinct advantages, because preferential recruitment and expansion of pDCs dramatically improves immune responses to cancer antigens and reduces tumor progression compared to previous vaccine approaches.

Polynucleotides, polypeptides, or other agents are purified and/or isolated. Specifically, as used herein, an "isolated" or "purified" nucleic acid molecule, polynucleotide, polypeptide, or protein, is substantially free of other cellular material, or culture medium when produced by recombinant techniques, or chemical precursors or other chemicals when chemically synthesized. Purified compounds are at least 60% by weight (dry weight) the compound of interest. Preferably, the preparation is at least 75%, more preferably at least 90%, and most preferably at least 99%, by weight the compound of interest. For example, a purified compound is one that is at least 90%, 91%, 92%, 93%, 94%, 95%, 98%, 99%, or 100% (w/w) of the desired compound by weight. Purity is measured by any appropriate standard method,

for example, by column chromatography, thin layer chromatography, or high-performance liquid chromatography (HPLC) analysis. A purified or isolated polynucleotide (ribonucleic acid (RNA) or deoxyribonucleic acid (DNA)) is free of the genes or sequences that flank it in its naturally-occurring state. A purified or isolated polypeptide is free of the amino acids or sequences that flank it in its naturally-occurring state. Purified also defines a degree of sterility that is safe for administration to a human subject, e.g., lacking infectious or toxic agents.

Similarly, by "substantially pure" is meant a nucleotide or polypeptide that has been separated from the components that naturally accompany it. Typically, the nucleotides and polypeptides are substantially pure when they are at least 60%, 70%, 80%, 90%, 95%, or even 99%, by weight, free from the proteins and naturally-occurring organic molecules with they are naturally associated.

By "isolated nucleic acid" is meant a nucleic acid that is free of the genes which flank it in the naturally-occurring genome of the organism from which the nucleic acid is derived. The term covers, for example: (a) a DNA which is part of a naturally occurring genomic DNA molecule, but is not flanked by both of the nucleic acid sequences that flank that part of the molecule in the genome of the organism in which it naturally occurs; (b) a nucleic acid incorporated into a vector or into the genomic DNA of a prokaryote or eukaryote in a manner, such that the resulting molecule is not identical to any naturally occurring vector or genomic DNA; (c) a separate molecule such as a cDNA, a genomic fragment, a fragment produced by polymerase chain reaction (PCR), or a restriction fragment; and (d) a recombinant nucleotide sequence that is part of a hybrid gene, i.e., a gene encoding a fusion protein. Isolated nucleic acid molecules according to the present invention further include molecules produced synthetically, as well as any nucleic acids that have been altered chemically and/or that have modified backbones. For example, the isolated nucleic acid is a purified cDNA or RNA polynucleotide. Isolated nucleic acid molecules also include messenger ribonucleic acid (mRNA) molecules.

The transitional term "comprising," which is synonymous with "including," "containing," or "characterized by," is inclusive or open-ended and does not exclude additional, unrecited elements or method steps. By contrast, the transitional phrase "consisting of" excludes any element, step, or ingredient not specified in the claim. The transitional phrase "consisting essentially of" limits the scope of a claim to the specified

materials or steps "and those that do not materially affect the basic and novel characteristic(s)" of the claimed invention.

Other features and advantages of the invention will be apparent from the following description of the preferred embodiments thereof, and from the claims. Unless otherwise defined, all technical and scientific terms used herein have the same meaning as commonly understood by one of ordinary skill in the art to which this invention belongs. Although methods and materials similar or equivalent to those described herein can be used in the practice or testing of the present invention, suitable methods and materials are described below. All published foreign patents and patent applications cited herein are incorporated herein by reference. Genbank and NCBI submissions indicated by accession number cited herein are incorporated herein by reference. All other published references, documents, manuscripts and scientific literature cited herein are incorporated herein by reference. In the case of conflict, the present specification, including definitions, will control. In addition, the materials, methods, and examples are illustrative only and not intended to be limiting.

BRIEF DESCRIPTION OF THE DRAWINGS

Figure 1 is a diagram of the immune response to infection. Figure 1 is a diagram showing the mechanisms by which bacterial invasion and bacterial toxins damage resident skin cells promoting the production of inflammatory cytokines, including GM-CSF, and activation of dermal endothelium. Cytokine stimulation induces extravasation of leukocytes and recruits skin resident DCs (langerhans cells) and monocytes/preDCs. DCs, recruited to the site of inflammation encounter and injest bacterium and bacterial products including antigenic molecules and CpG-rich DNA, which stimulates TLR9 activation. As a result of TLR ligation and the inflammatory conditions, the DC rapidly matures to upregulate its expression of MHC-antigen complexes, costimulatory molecules, and CCR7 and begins to home to the lymph nodes where it initiates and propagates antigen specific T-cell responses.

Figures 2A-C. Figure 2A is a schematic representation of PEI condensation of CpG-rich oligonucleotide sequences. The PEI polycation with positively charged amine groups is mixed with CpG-ODNs consisting of negatively charged phosphate groups at charge ratios (NH3+:PO4-) resulting in positively charged PEI-CpG-ODN condensates. Figure 2B is a bar graph showingthe zeta potential (mv) of CpG-ODN 1826 and its PEI condensates at charge ratios of 4,7 and 15. Box plots represent the mean and standard deviation (n=4) Figure 2C is a bar graph showing the particle size of CpG-ODN 1826 and its PEI condensates

at charge ratios of 4,7 and 15. Values represent the average particle size and the standard deviation (n=4).

Figures 3A-D. Figures A - C show *in vitro* uptake of CpG-ODN by JAWSII DCs. Figures 3A-B are bright field images of cells and their corresponding fluorescent images displaying the uptake of TAMRA labeled CpG-ODN molecules (A) or PEI-CpG-ODN condensates (B). Figure 3C is a bar graph showing quantification of uptake of naked (**-o-**) and PEI-CpG-ODN (- ● -) condensates over a period of 110 hours. Figure 3D is a line graph showing quantification of uptake of PEI-CpG-ODN condensates and subsequent decondensation within JAWSII DCs. The number of PEI-CpGODN condensates in the cells (- ■ -), and the amount of uncondensed CpG-ODN (--□--) was monitored and quantified over a period of 70 hours. Scale bar – 20 μm. Values in C (n>10 cells) and D (n>7 cells) represent the mean and standard deviation.

Figures 4A-D. (A) Imaging DC activation. Figure 4A is a series of brightfield images of activated DC morphology in correlation with fluorescent images displaying the uptake of TAMRA labeled CpG-ODN molecules condensed with PEI (charge ratio -7). Figure 4B is a series of FACS histograms of JawsII DCs positive for the activation markers CD86, MHCII and CCR7 following no stimulation (tinted line), CpG-ODN (- - -), and PEI-CpG-ODN condensates (—). Figure 4C is a chart showing tabulated data displaying the percentage of DCs positive for the activation markers CD86, MHCII, and CCR7 following no stimulation, and stimulation with TNF-α/LPS or CpG-ODN or PEI-CpG-ODN. Figure 4D is a bar graph showing CpG-ODN and DC emigration toward CCL19. The effects of no stimulation (■), and PEI (■) or CpG-ODN (■) or PEI-CpG-ODN (■) stimulation on DC emigration from the top wells of transwell systems toward media supplemented with 300 ng/ml CCL19. Migration counts taken at 24 hours. Scale bar – 20 μm. Values in C and D (n=4) represent the mean and standard deviation. CpG-ODN activation media (5 μg/ml). * $P<0.05$** $P<0.01$.

Figures 5A-B. Figure 5A is a series of bar graphs showing the percentage of JawsII DCs positive for MHCII and CCR7 expression after PEI-CpG-ODN (5 μg/ml) stimulation in media supplemented with 0 (□), 50 (■) and 500 ng/ml GM-CSF (■). Figure 5B is a line graph showing CpG-ODN and DC emigration toward CCL19 in the presence of GM-CSF. The effects of no stimulation (- ■ -), and stimulation with PEI (---) or CpG-ODN (- ● -) or PEI-CpG-ODN (- ● -) on DC emigration from the top wells of transwell systems toward

media supplemented with 300 ng/ml CCL19. Migration counts taken at 24 hours. Values represent the mean and standard deviation (n=4).

Figures 6A-C. Figure 6A is a line graph showing the fraction of PEI-CpG-ODN condensates retained in PLG matrices over time with incubation in PBS in vitro. Figures 6B-C are bar graphs showing emigration of JAWS II DCs from CpG-ODN loaded scaffolds. (B) The total number of DCs that migrated from scaffolds loaded with 5, 50, 500 μg of CpG-ODN toward media supplemented with 300 ng/ml CCL19. (C) The total number of DCs that migrated from scaffolds loaded with 25 μg of CpG-ODN in the presence of 500ng/ml GM-CSF toward media supplemented with 300 ng/ml CCL19. Migration counts taken at 48 hours. Values represent mean and standard deviation (n=4 or 5).

Figures 7A-B. PLG-based infection mimics continuously program DCs in situ. Figure 7a is a chart showing the tabulated data of host DC recruitment (cell #) and DC activation (% expressing MHC or CCR7) in response to various dosages of PEI-CpG-ODN and GM-CSF loaded into PLG matrices. Matrices were implanted into the backs of C57/BL6J mice for 7 days. Figure 7B is a bar graph showing the number of CD11c(+)MHCII(+) and CD11c(+)CCR7(+) host DCs isolated from matrices loaded with PEI-ODN control, 10 μg PEI-CpG-ODN, 400 and 3000ng GM-CSF, and 400 and 3000ng GM-CSF in combination with 10 μg PEI-CpG-ODN at Day 7 after implantation into the backs of C57/BL6J mice. Values represent the mean and standard deviation (n=3-5). * $P<0.05$** $P<0.01$.

Figures 8A-D. Infection mimics continuously disperse programmed DCs *in situ.* Figure 8a is a bar graph showing the number of FITC(+) DCs that have homed to the inguinal lymph nodes as a function of time subsequent to their residence at FITC painted blank matrices (-□-), FITC painted GM-CSF loaded matrices (-■-), and FITC painted GM-CSF and CpG-ODN matrices (-■-). GM-CSF dose was 3000ng and CPG-ODN dose was 10μg. Figure 8B is a digital photograph of inguinal lymph nodes extracted from C57BL/6J mice (control) and at 10 days after the implantation of matrices incorporating 10 μg CpG-ODN + 3000ng GM-CSF (infection-mimic). Figures 8C-D are bar graphs showing the total number of cells (C) and CD11c+ DCs (D) isolated from inguinal lymph nodes extracted from C57BL/6J mice at 2 and 7 days after the implantation of blank matrices (□) and matrices incorporating 3000ng GM-CSF (■) or 10 μg CpG-ODN + 3000ng GM-CSF (■).Values in A, C and D represent the mean and standard deviation (n=4 or 5). * $P<0.05$** $P<0.01$.

Figure 9 is a bar graph showing infection-mimicking microenvironment confers potent anti-tumor immunity. The time to tumor occurrence after PLG cancer vaccines were

implanted into mice. A comparison between blank PLG scaffolds (Blank), scaffolds loaded with antigen alone (Lys), antigen+3000ng GM-CSF (Lys+3000ng GMCSF), antigen + PEI-CpG-ODN condensate (Lys+CpG) and the combination of antigen, 3000ng GM-CSF and PEI-CpG-ODN (Lys+3000ng+PEI-CpG-ODN). Animals were also immunized using a cell-based vaccine (cell-based) using irradiated B16-F10 melanoma cells that had been genetically modified to produce GM-CSF, for comparison. At Day 14 after vaccination, C57BL/6J mice were challenged with 10^5 B16-F10 melanoma tumor cells and monitored for the onset of tumor occurrence (n= 9 or 10).

Figures 10A-B. Vaccination efficacy of Infection mimics dependent on T cell responses. Figure 10A is a series of representative photomicrographs of tumor sections from mice vaccinated with PLG cancer vaccines that appropriately control the presentation of tumor lysates, 3000ng GM-CSF and CpG-ODN and blank (blank) scaffold controls. Sections were stained to detect for CD4(+) and CD8(+) T cell infiltrates into tumor tissue that was explanted from mice that had developed tumors at days 20-25. Figure 10B is a bar graph showing T-cell infiltrates into B16-FI0 melanoma tumors of vaccinated animals. Tumors were explanted from C57BL/6J mice treated with blank PLG scaffolds (□), or PLG scaffolds incorporating B16-F10 melanoma tumor lysates, 3000ng GM-CSF and 10 μg PEI-CpG-ODN (■) at days 20-25. T-cell infiltrates were examined in randomized sections of tumors (n=4, $1mm^3$). Scale bar – 50 μm. Values in A, D and E represent the mean and standard deviation (n=3 or 4). * $P<0.05$** $P<0.01$.

Figures 11 A-F. In vivo control of DC recruitment and programming. Figure 11A is a line graph showing cumulative release of GM-CSF from PLG matrices over a period of 23 days. Figure 11B is a photograph showing H&E staining of sectioned PLG scaffolds explanted from subcutaneous pockets in the backs of C57BL/6J mice after 14 days: Blank scaffolds, and GM-CSF (3000 ng) loaded scaffolds. Figure 11 c is a series of FACS plots of cells isolated from explanted scaffolds and stained for the DC markers, CD11c and CD86. Cells were isolated from blank and GM-CSF (3000 ng) loaded scaffolds implanted for 28 days. Numbers in FACS plots indicate the percentage of the cell population positive for both markers. Figure 11D is a bar graph showing the fractional increase in CD11c(+)CD86(+) DCs isolated from PLG scaffolds at day 14 after implantation in response to doses of 1000, 3000 and 7000ng of GM-CSF, as normalized to the blank control (Blanks). Figure 11E is a line graph showing the in vivo concentration profiles of GM-CSF at the implant site of PLG scaffolds incorporating 0 (-), 3000 (--O--), and 7000 ng (-- ● --) of GM-CSF as a function of

time post implantation. Figure 11F is a bar graph showing the percentage of CD11c(+)CCR7(+) host DCs isolated from scaffolds loaded with 0 (□), 400 (■), 3000ng (■), and 7000 ng of GM-CSF (☒) as a function of time after implantation into the backs of C57BL/6J mice. Scale bar in B – 500 μm. Values in A, D, E, and F represent mean and standard deviation (n=4 or 5). * $P<0.05$ ** $P<0.01$.

Figures 12 A-G. Antigen co-presentation with CpG-ODN to DCs infiltrating PLG matrices enhances local CD8+ cDC numbers, IL-12 production and total CD8(+) cell numbers. The number of (Figure 12A) plasmacytoid DCs, (B) CD11c(+)CD11b(+) cDCs, and (Figure 12C) CD11c(+)CD8(+) cDCs at day 10 post-implantation in blank matrices (Blanks) and in response to doses of 3000ng GM-CSF (GM) or 100 μg CpG-ODN (CpG) alone or in combination (CpG+GM) or co-presented with tumor lysates (GM+Ant, CpG+Ant and CpG+GM+Ant). The in vivo concentration of (Figure 12D) IFN-α (E) IFN-γ and (Figure 12F) IL-12 at day 10 post-implantation in blank matrices (Blanks) and in response to doses of 3000ng GM-CSF (GM) or 100 μg CpG-ODN (CpG) alone or in combination (CpG+GM) or co-presented with tumor lysates (GM+Ant, CpG+Ant and CpG+GM+Ant). (Figure 12G) . FACS histograms of CD8(+) cells infiltrating Blank PLG matrices(—), and matrices loaded with 3000ng GM-CSF and 100μg CpG-ODN alone (- - -) or with tumor antigens (tinted line). Values in A-F represent mean and standard deviation (n=4 or 5). * $P<0.05$ ** $P<0.01$.

Figures 13A-F. Tumor protection regulated by CpG-ODN presentation and plasmacytoid DC enrichment. Survival times of mice vaccinated with PLG vaccines 14 days prior to B16-F10 melanoma tumor challenge. (Figure 13A) shows a comparison of survival times in mice vaccinated with PLG matrices loaded with tumor lysates and 1, 10, 50 or 100μg of CpG-ODN. Figure 13B shows a comparison of survival times in mice vaccinated with PLG matrices loaded with tumor lysates, 3000ng GM-CSF and 1, 10, 50 or 100μg of CpG-ODN. A correlation between the number of (Figure 13C) CD11c(+)PDCA-1(+) DCs, (Figure 13D) CD11c(+)CD11b(+) DCs, and (Figure 13E) CD11c(+)CD8(+) cDCs at the PLG vaccine site at day 10 and the percent of animals surviving B16-F10 melanoma tumor challege at Day 100. Figure 13F shows the fraction of total DC population consisting of CD11c(+)CD11b(+) cDCs, CD11c(+)PDCA-1(+) pDCs, and CD11c(+)CD8(+) cDCs generated at the PLG vaccine site at day 10. Survival percentage is taken at Day 100 after challenge with B16-F10 melanoma cells.

Figures 14A-B are line graphs showing PLG vaccine efficacy against established tumors. Figure 14A shows a comparison of the survival time in C57BL/6 mice treated with blank PLG scaffolds, and PLG vaccines (3μg GM-CSF+100μg CpG-ODN+ tumor lysates). Figure 14B shows a comparison of tumor growth in C57BL/6 mice treated with blank PLG scaffolds, and PLG vaccines (3μg GM-CSF+100μg CpG-ODN+ tumor lysates). Mice were inoculated with $5x10^5$ B16-F10 melanoma tumor cells at Day 0 and tumors were allowed to grow for 7 days when mice were either implanted with blank PLG matrices or PLG vaccine. The average tumor size was expressed as one-half the product of the smallest and largest diameter.

Figures 15A- B are line graphs showing cumulative release of (A) CpG-rich oligonucleotides (CpG 1826) or (B) P(I:C) in combination with the cumulative release of GM-CSF from PLG scaffolds. Figures 15C-D are bar graphs showing bioactivity of P(I:C) and MPLA, respectively, released from PLG scaffolds presented as fold-increase over controls. Bioactivity measured by the ability of the Poly(I:C) and MPLA released from PLG scaffolds to stimulate HEK293 cells expressing TLR3 and TLR4, respectively, and stably transfected with NF-κB–dependent alkaline phosphatase reporter. Bioactivity was measured over time and compared to controls of unstimulated cells. Figure 15E is a line graph showing MPLA in combination with the cumulative release of GM-CSF from PLG scaffolds. Values represent mean and standard deviation (n=5 or 6). These data show *in vitro* release kinetics and bioactivity of various TLR agonists from GM-CSF loaded PLG scaffolds. Figure 15F is a photomicrograph showing the top surface of a macroporous PLG scaffold (scale bar - 3 mm), and SEM micrograph of a scaffold cross section (scale bar - 50 μm).

Figures 16A-D are bar graphs showing DC recruitment and Activation at Vaccine Site is regulated by TLR agonist presentation. The total numbers of (A) CD11c(+) DCs, (B) activated CD11c(+) DCs positive for MHCII and CD86 expression, (C) PDCA-1(+) plasmacytoid DCs, and (D) CD11c(+)CD8(+) DCs recruited to scaffold site at day 7 after implantation of GM-CSF loaded matrices (GM) and matrices loaded with GM-CSF in combination with CpG-ODN (CpG), MPLA (MPLA), and P(I:C) (P(IC)). Figure 16E shows FACS histograms and plots representing scaffold infiltrating dendritic cells in GM-CSF loaded scaffolds (Con) or scaffolds loaded with GM-CSF in combination with CpG-ODN (CpG), MPLA (MPLA), and P(I:C) (P(IC)) at day 7 postimplantation in mice. Histograms indicate the relative frequency of CD11c(+) dendritic cells infiltrating the indicated scaffold formulation. Density plots indicate cells stained for CD11c(+) in combination with activated,

DC markers, CD86(+) and MHCII(+). Numbers in the upper right quadrant of FACS plots indicate the percentage of CD11c(+) dendritic cells positive for activation markers. Figure 16F is a bar graph showing the total numbers of CD11c(+) DCs, and activated CD11c(+) DCs positive for MHCII and CD86 expression, at the scaffold site at day 7 after implantation of GM-CSF loaded matrices (Con) and matrices loaded with GM-CSF in combination with CpG-ODN (CpG), MPLA (MPLA), and P(I:C) (P(IC)). Values represent mean and standard deviations (n=6). * $P<0.05$ ** $P<0.01$, as compared to GM-CSF loaded matrices. ** $P<0.01$, as compared to GM-CSF loaded matrices (Con).

Figures 16G and 16H are bar charts showing that CD8(+)DC, and pDC subsets and IL-12 concentrations at vaccine site. Figure 16G shows the total numbers of CD11c(+)CD8(+) DCs and pDCs at scaffold site at day 7, and (H) the local IL-12 concentration after implantation of GM-CSF loaded scaffolds (Con) and scaffolds loaded with GM-CSF in combination with CpG-ODN (CpG), MPLA (MPLA), and P(I:C) (P(IC)). Values represent mean and standard deviations (n=6). ** $P<0.01$, as compared to GM-CSF loaded matrices (Con).

Figures 17A-C are graphs showing prophylactic vaccination and correlation to CD8(+)DC, and pDC subsets and IL-12 concentrations at vaccine site. Survival times of mice vaccinated with PLG vaccines 14 days prior to B16-F10 melanoma tumor challenge (10^5 cells). Figure 17A shows a comparison of survival times in untreated mice (Control) and mice treated with GMCSF loaded PLG scaffolds (GM-CSF) or with PLG scaffolds loaded with GM-CSF in combination with CpG-ODN (CpG), P(I:C), or MPLA. Plots of the normalized magnitude of (B) CD11c(+)CD8(+) DC infiltration, (C) pDC infiltration at the vaccine site, and (D) local IL-12 concentration versus the percent of animals surviving B16-F10 melanoma tumor challenge at Day 100 (survival data taken from experimental conditions in (A; red data points) and previously reported data with this system). r values in B-C represent the linear correlation coefficient between x-axis variable and survival percentage.

Figures 18A-D are bar graphs showing T cell Activity and cytokine production at vaccine site at Day 14 of scaffold implantation. (A)The number of CD3(+)CD8(+) cytotoxic T cells at day 14 after implantation of GM-CSF loaded matrices (GM) and matrices loaded with GM-CSF in combination with CpG-ODN (CpG), MPLA (MPLA), and P(I:C) (P(IC)). The in vivo concentration of (B) IL-12, (C) Rantes, and (D) IFN-□ at day 14 after implantation of GM-CSF loaded matrices (GM) and matrices loaded with GM-CSF in combination with CpG-ODN (CpG), MPLA (MPLA), and P(I:C) (P(IC)). Values represent

mean and standard deviations (n=5). * P<0.05 ** P<0.01, as compared to control matrices (loaded with GM-CSF).

Figures 19A-F are graphs showing therapeutic vaccination and anti-tumor T cell activity. A comparison of the (A) tumor size and (B) overall survival in mice bearing established melanoma tumors (inoculated with $5x10^5$ B16-F10 cells and allowed to develop for 9 days) and treated with either GM-CSF loaded matrices (Con) or matrices loaded with GM-CSF in combination with CpG-ODN (CpG), MPLA (MPLA), and P(I:C) (P(IC)). (C) FACS plots representing tumor infiltrating leukocytes isolated from explanted tumors at Day 18 after tumor challenge. Mice were treated with GM-CSF loaded matrices (Control) or matrices loaded with GM-CSF in combination with CpG-ODN (CpG), MPLA (MPLA), and P(I:C) (P(IC)) at Day 9 after tumor inoculation and cell isolations from tumors were prepared at Day 18 and stained for activated, cytotoxic T cell markers, CD8(+) and CD107a. Numbers in FACS plots indicate the percentage of the cell population positive for both markers. (D) The numbers of CD8(+), tumor-infiltrating T cells positive for both IFNγ and CD107a in untreated mice (naïve) or mice vaccinated with various treatments. (E) The total numbers of Trp2-specific cytotoxic T cells in splenocytes of vaccinated mice. Figure 19F is a bar chart showing a comparison of the tumor size at Day 17. * $P<0.05$ ** $P<0.01$, as compared to control matrices (loaded with GM-CSF), unless otherwise noted.

Figure 20 is a series of bar charts, line graphs and dot plots showing that vaccine efficacy is impaired in mice lacking CD8(+) DC. (A) Survival times of untreated mice (control), wildtype C57BL/6J mice (WT) and Batf3−/− mice (CD8 DC KO), vaccinated with PLG vaccines 14 days prior to B16-F10 melanoma tumor challenge (105 cells). (B) Analysis of cytotoxic and regulatory T cells at PLG vaccine site of wildtype C57BL/6J mice (WT) and Batf3−/− mice (CD8 DC KO) at day 10 post implantation. FACS dot plots indicate scaffold-infiltrating cells stained for CD3(+) and Trp2(+) tetramer. Numbers in the upper right quadrant of FACS plots indicate the percentage Trp2 specific cytotoxic T cell, and numbers in lower right quadrant represent the rest of the T cell population at the vaccine site. Graphs indicate the total numbers of Trp2-specific cytotoxic T cells at implant site and the ratio of CD8(+) cytotoxic T cells to regulatory T cells. (C) Fold increase in IL-12 concentration at vaccine site and (D) Trp(2)-specific cytotoxic T cells in spleens of vaccinated, wildtype C57BL/6J mice (WT) and Batf3−/− mice (CD8 DC KO). CpG-ODN was the adjuvant utilized in vaccines. Data represent mean and standard deviation, (n=5)* P<0.05 ** P<0.01.

Figure 21 is a series of bar charts. Figure 21A shows the local TNF-α□e local TNF-shows ts of bar chartsn, (n=5)* Pded scaffolds (Con) and scaffolds loaded with GM-CSF in combination with CpG-ODN (CpG), MPLA (MPLA), and P(I:C) (P(IC)). Values represent mean and standard deviations (n=5). ** $P<0.01$, as compared to GM-CSF loaded matrices (Con). Figure 21B shows the local IFN-α concentration after implantation of GM-CSF loaded scaffolds (Con) and scaffolds loaded with GM-CSF in combination with CpG-ODN (CpG), MPLA (MPLA), and P(I:C) (P(IC)). Values represent mean and standard deviations (n=5). **$P<0.01$, as compared to GM-CSF loaded matrices (Con). Figure 21C shows the local IL-12p70 concentration after implantation of GM-CSF loaded scaffolds (Con) and vaccine scaffolds (loaded with tumor lysate, GM-CSF and CpG-ODN)(CpG), in wildtype (vax) and Cd8atm1Mak/J mice (CD8 Tc KO). Figure 21D shows the local IFN-γ concentration after implantation of GM-CSF loaded scaffolds (Con) and vaccine scaffolds (loaded with tumor lysate, GM-CSF and CpG-ODN)(CpG), in wildtype (vax) and B6.129S2-Cd8atm1Mak/J mice (CD8 Tc KO).

Figure 22 is a line graph showing that PLG vaccines incorporating CpG-ODN and/or P(I:C) generate significant tumor protection. The overall survival of mice bearing melanoma tumors, and treated with either blank matrices [Blank] or matrices loaded with CpG-ODN or P(I:C) alone or in combination [CpG-ODN + P(I:C)] (n=8). Mice were challenged with $5x10^5$ B16-F10 cells and vaccinated 3 days later with PLG vaccines. Total dose of TLR agonist was approximately 100 μg in all vaccines.

Figure 23 is a bar chart demonstrating in vitro chemotaxis and chemokinesis of DCs. The *in vitro* (Figure 23A) chemotaxis and (Figure 23B) chemokinesis of bone marrow derived DCs in response to control media and media supplemented with GMCSF, Flt3L, and CCL20. * $P<0.05$ ** $P<0.01$, as compared to GM-CSF loaded matrices. Values represent mean and standard deviation. (n=4).

Figure 24 is a series of line graphs, bar charts, and photomicrographs demonstrating PLG scaffolds that release cytokines for DC recruitment. Figure 24A shows the cumulative release of GM-CSF, Flt3L, or CCL20 from PLG scaffolds. Figure 24B shows a representative photograph of scaffold histological sections stained for CD11(+) DC infiltrates (pink) into macroporous blank (left) and GM-CSF loaded scaffolds (right) at Day 10 after implantation. Scale bar – 100 um. Figure 24C shows the total numbers of CD11c(+) DCs at scaffold site at day 7 after implantation of Blank PLG matrices (Con) and matrices loaded

with GM-CSF (GM), Flt3L (FL3) and CCL20 (CCL20). Values represent mean and standard deviations (n=6). * $P<0.05$ ** $P<0.01$, as compared to GM-CSF loaded matrices.

Figure 25 is a series of line graphs, dot plots, and bar charts demonstrating DC recruitment and activation mediated by PLG matrices loaded with Cytokines and CpG-ODN. Figure 25A shows FACS histograms and plots representing scaffold infiltrating dendritic cells in CpG-ODN loaded PLG scaffolds (Con) or scaffolds loaded with GM-CSF (GM), Flt3L(Fl3L) or CCL20(CCL20) in combination with CpG-ODN at day 7 post-implantation in mice. Histograms indicate the relative frequency of MHCII and CD86 expression in CD11c(+) DCs infiltrating the indicated scaffold formulation. Dot plots indicate cells stained for CD11c(+) in combination with activated, plasmacytoid DC marker, PDCA-1. Numbers in the upper right quadrant of FACS plots indicate the percentage of CD11c(+)PDCA-1(+) pDCs. Figure 25B shows the total numbers of activated CD11c(+) DCs positive for MHCII and CD86 expression, and Figure 25C shows CD11c(+)PDCA-1(+) pDCs present in scaffold at day 7 after implantation of CpG-ODN loaded PLG scaffolds (Con) or scaffolds loaded with GM-CSF (GM), Flt3L(Fl3L) or CCL20(CCL20) in combination with CpG-ODN. Values represent mean and standard deviations (n=5). * $P<0.05$ ** $P<0.01$, as compared to controls (Con) unless otherwise indicated.

Figure 26 is a series of bar charts and a line graph demonstrating PLG vaccines generate immunoprotective cytokines, antigen-specific T cells, and cancer protection. Fold difference in local (Figure 26A) IL-12 and (Figure 26B) IFN-γ concentration after implantation of scaffolds loaded with B16-F10 tumor lysate, CpG-ODN in combination with with GM-CSF (GM), Flt3L(Fl3L) or CCL20(CCL20). Concentrations were normalized to the value found with control (matrices delivering lysate and CpG-ODN, no cytokines) (Figure 25C). The total numbers of Trp2-specific CD8(+) T cells in spleens of vaccinated animals at Day 10 post-implantation. (Figure 25D shows the overall survival of mice bearing melanoma tumors, and treated with either CpG-ODN loaded matrices (Blank) or matrices loaded with CpG-ODN in combination with GMCSF, Flt3L and CCL20 (n=8). Values represent mean and standard deviations (n=5). * $P<0.05$, as compared to CCL20 loaded matrices (CC20).

DETAILED DESCRIPTION OF THE INVENTION

Prior to the invention, cancer vaccines typically depended on cumbersome and expensive manipulation of cells in the laboratory, and subsequent cell transplantation resulted

in poor lymph node homing and limited efficacy. The invention solves these problems by using materials that mimic key aspects of bacterial infection to directly control immune cell trafficking and activation in the body. Presentation of TLR agonists for cancer vaccination leads to improved activation of immune cells. The vaccines and methods comprise incorporation and presentation of TLR agonists embedded in structural polymeric devices. The data described herein demonstrate the critical role of CD8(+) Dendritic cells (DCs) and plasmacytoid DCs (as well as conventional DCs) for cancer vaccination, which are preferentially recruited and activated using the TLR-agonist containing structural polymeric device. The device is manufactured as a tiny bioengineered porous disc filled with tumor-specific antigens and TLR agonists. The disc is implanted into the body, e.g., inserted under the skin, where it activates the immune system to destroy tumor cells. While typical earlier methods involved growing cells outside the body, this approach reprograms cells that are already in the body.

In some examples, the device includes a recruitment component. Thus, the device optionally includes a recruitment molecule such as a cytokine. In those situations, polymers were designed to first release a cytokine to recruit and house host dendritic cells (DCs), and subsequently present cancer antigens and danger signals to activate the resident DCs and dramatically enhance their homing to lymph nodes. Specific and protective anti-tumor immunity was generated with these materials, as 90% survival was achieved in animals that otherwise die from cancer within 25 days. These materials are useful in cancer and other vaccines to program and control the trafficking of a variety of cell types in the body.

A polymer system was designed to not only serve as a drug delivery device, but also as a physical, antigen-presenting structure to which the DCs are recruited, and where DCs reside while they are activated using a material (poly[lactide-co-glycolide]) and bioactive molecules (GM-CSF and CpG-ODN). These bioactive molecules have excellent safety profiles. The material system serves as an effective cancer vaccine, eliminating the time, expense and regulatory burden inherent to existing cell therapies and reducing or eliminating the need for multiple, systemic injections and high total drug loading. The devices described herein utilize infection-mimicking materials to program DCs *in situ*.

A quantitative understanding of the ability of GM-CSF to impact DC recruitment, activation and emigration *in vitro* was developed in order to appropriately design a material system for vaccination. GM-CSF enhanced DC recruitment and proliferation in a dose dependent manner. However, high concentrations (>100ng/ml) of GM-CSF inhibited DC

migration toward a lymph node derived chemoattractant (CCL19). Immunohistochemical staining revealed that the high concentrations of GM-CSF (500 ng/ml) also down-regulated DC expression of the CCL19 receptor CCR7 and MHCII. These results indicated that control over GM-CSF exposure was needed to both recruit and program DCs *in vivo*. If GM-CSF alone is to be used for both purposes, its local concentration is designed to decrease over time in order to release DCs that become trapped in the material. Alternatively, provision of a danger signal (e.g., CpG-ODN) in the local environment is used to release DCs from GM-CSF inhibition once they reside at the infection-mimicking site.

Based on this understanding, a macroporous poly-lactide-co-glycolide (PLG) matrix was designed to present GM-CSF, danger signals, and cancer antigens in a defined spatiotemporal manner *in vivo*, and serve as a residence for recruited DCs as they are programmed. GM-CSF was encapsulated (54% efficiency) into PLG scaffolds using a high pressure CO_2 foaming process. These matrices released approximately 60% of their bioactive GM-CSF load within the first 5 days, followed by slow and sustained release of bioactive GM-CSF over the next 10 days. This release profile allows diffusion of the factor through the surrounding tissue to effectively recruit resident DCs.

As described herein, *in situ* dendritic cell targeting systems are utilized to therapeutically manipulate the immune system with TLR agonists. As described in detail below, macroporous polymeric scaffolds were designed that deliver three different classes of TLR agonists *in vivo*: CpG--ODN, MPLA, and P(I:C) in combination with GM-CSF, Flt3L, or CCL20 to augment DC recruitment and activation. The ability of *in situ* TLR presentation from macroporous matrices to modulate DC subset generation, and cancer vaccine efficacy in a B16-F10 melanoma model was also characterized. The ability of these systems to effect immune protection and tumor regression required CD8(+) DCs and correlated strongly with plasmacytoid DCs(pDCs) and IL-12 production, regardless of the TLR agonist type or dose. Thus, the results presented herein demonstrate that 3D polymer matrices are utilized to regulate DC subsets *in situ* for immunotherapy and indicate that CD8(+) DCs, pDCs and IL-12 signaling are critical components of successful material-based vaccination protocols.

The generation of immunity requires collaboration between dendritic cells (DCs) and T cells, as the priming of cytotoxic T lymphocyte (CTL) by DCs is a crucial event in the fight against infection and tumors (Lanzavecchia A. and Sallusto F., 2001 Cell, 106: 263-266). DCs regulate immune responses by recognizing, processing, and decoding pathogen associated molecular patterns (PAMPs) and antigenic molecules (Banchereau J, and

Steinman RM., 1998 Nature, 392: 245-252; Mellman I. and Steinman R.M., 2001 Cell, 106: 255-258; Sansonetti P.J., 2006 Nat. Immunol., 7: 1237–1242; Meylan et al., 2006 Nature, 442: 39–44; Akira et al., 2006 Cell, 124: 783–801). PAMP recognition by pattern recognition receptors (PRRs) present intercellularly or at the DC surface signal the presence of infection and triggers signal transduction pathways ultimately resulting in DC activation (Sansonetti P.J., 2006 Nat. Immunol., 7: 1237–1242; Meylan et al., 2006 Nature, 442: 39–44; Akira et al., 2006 Cell, 124: 783–801). Generally, activated DCs are characterized by enhanced expression of MHC and co-stimulatory molecules and proinflammatory cytokines, which enables DCs to translate pathogenic signals to naïve T cells and trigger adaptive immune responses (Banchereau J, and Steinman RM., 1998 Nature, 392: 245-252; Mellman I. and Steinman R.M., 2001 Cell, 106: 255-258; Sansonetti P.J., 2006 Nat. Immunol., 7: 1237–1242; Meylan et al., 2006 Nature, 442: 39–44; Akira et al., 2006 Cell, 124: 783–801; Gilboa, E., 2007 J Clin Invest., 117: 1195-1203; Banchereau J. and Steinman R.M., 2007 Nature, 49: 419-426). DCs act as a network of distinct subsets that perform specialized functions to stimulate and polarize T cell responses in order to coordinate immune regulation (Naik et al., 2007 Nat Immunol, 8: 1217-1226; O'Garra1 A. and Trinchieri G. 2004 Nat Immunol, 5: 1206 -1208; D'Amico A and Wu L., 2003 J Exp Med, 2: 293-303; Villadangos JA and Schnorrer P, 2007 Nat Rev Immunol, 7: 543-555; Liu YJ, 2001 Cell, 106: 259-262; Jego et al., 2003 Immunity, 19: 225-234; Randolph et al., 2008 Annu. Rev. Immunol., 26: 293–316). Antigen processing and presentation to T cells is predominantly attributed to the conventional DC subset (cDCs), consisting of both CD8(-) DCs and CD8(+) DCs. CD8(+) DCs are especially adept at cross-presentation of exogenous antigen, IL-12 production and induction of cytotoxic T cell responses (Schnorrer P, 2006 PNAS 28: 10729-34; Skokos D. and Nussenzweig M.C., J Exp Med, 204: 1525-1531; Den Haana et al., 2000 J Exp Med, 12: 1685-1696; Moser M. and Murphy K.M., 2000 Nat. Immunol., 1: 199–205; Hildner et al., 2008 Science, 322:1097–1100). The plasmacytoid DC (pDC) subset has the capacity to produce significant amounts of type-1 interferons (IFNs) in response to microbial nucleic acids, particularly during viral infection, to facilitate T cell activation, growth and survival for disease clearance (Liu YJ, 2001 Cell, 106: 259-262; Jego et al., 2003 Immunity, 19: 225-234; Randolph et al., 2008 Annu. Rev. Immunol., 26: 293–316; Kanzler et al., 2007 Nat. Med., 13: 552–559). Moreover, the processes mediated by pDC and CD8(+) DC subsets have been associated with priming t-helper 1 (Th1) effector cells for the control of infection and tumors. A balanced distribution of activated DC subsets is associated with the control of autoimmune

disease and tumors, indicating that these cells may cooperate during the generation of protective immunity.

Prior to the invention described herein, cancer vaccines are designed to introduce antigen in combination with immunostimulatory signals to activate DCs either *ex vivo* prior to administration, or *in situ* (Gilboa E., 2007 J Clin Invest., 117: 1195-1203; Banchereau J. and Steinman R.M., 2007 Nature, 49: 419-426; Kanzler et al., 2007 Nat. Med., 13: 552–559; Hansen et al., 2013 Vaccine, 31(4), 639-46; Schuler et al., 2003 Curr Opin Immunol, 15: 138–147; Curiel T.J, 2002 J Clin Invest, 109: 311–312). A range of stimuli are used to trigger DC maturation and differentiation including proinflammatory cytokines, PAMPs recognized by the toll-like receptor (TLR) family, and feedback signals from innate and adaptive immune cells. As described in detail below, discrete combinations of these stimuli and DC subsets differentially control T cell activation and polarization, and these components are optimized and exploited to generate effective immune responses that eradicate tumors or infectious agents. However, it is currently unclear what components and DC subsets should be included in cancer vaccines, partly because current techniques limit the cell types that can be cultured or targeted (Kanzler et al., 2007 Nat. Med., 13: 552–559; Hansen et al., 2013 Vaccine, 31(4), 639-46; Schuler et al., 2003 Curr Opin Immunol, 15: 138–147; Curiel T.J, 2002 J Clin Invest, 109: 311–312). Standard DC-based protocols widely used in the clinic utilize monocyte-derived conventional DCs that are unable to cross-present antigens, or efficiently produce IL-12 or type-1 IFNs that can prime CTL-mediated immune responses and tumor cell death (Hansen et al., 2013 Vaccine, 31(4), 639-46; Schuler et al., 2003 Curr Opin Immunol, 15: 138–147; Curiel T.J, 2002 J Clin Invest, 109: 311–312). Prior to the invention described herein, there were attempts to utilize type 1 differentiated DCs in combination with TLR agonists to boost CTL priming capacity, but this maturation is accompanied by decreased migratory and stimulatory function upon implantation (Hansen et al., 2013 Vaccine, 31(4), 639-46). Described herein are macroporous polymer matrices that regulate the trafficking and activation of DCs in vivo by precisely controlling the presentation of GMCSF and CpG-oligonucleotide (CpG-ODN) adjuvants (Ali et al., 2009 Nat Mater, 2: 151–8; Ali et al., 2009 Sci Transl Med, 1:8–19). When applied as cancer vaccines, these matrices led to induce CTL-mediated eradication of melanoma tumors (Ali et al., 2009 Sci Transl Med, 1:8–19).

As described herein, matrices were modified to present 3 different classes of TLR agonists, CpG-ODN, monophosphoryl lipid A (MPLA), and polyinosinic:polycytidylic acid

(P(I:C)), all in combination with GM-CSF. The ability of each vaccine to recruit and generate activated DC subsets, in vivo was first quantified. The impact of DC induction on T cell-mediated immunity and cancer vaccine efficacy in vaccine models of B16-F10 melanoma was next assessed. These studies demonstrate that anti-tumor efficacy requires CD8(+) DCs and is strongly correlated with pDC numbers and local IL-12 production. Survival outcomes were also correlated to an array of inflammatory cytokines, which revealed a strong relationship between IL-12 production and antitumor efficacy. Altogether, the results presented herein demonstrate that various DC subsets are recruited and utilized for *in situ* vaccination, and provide important cellular and molecular insights into cancer vaccine design.

Infammatory Mediators

Dendritic Cell (DC) proliferation, migration and maturation are sensitive to inflammatory mediators, and granulocyte macrophage colony stimulating factor (GM-CSF) has been identified as a potent stimulator of immune responses, specifically against cancer antigens. GM-CSF also has the ability to recruit and program these antigen-presenting immune cells. Additionally, Cytosine-guanosine (CpG) oligonucleotide (CpG-ODN) sequences found in bacterial DNA are potent immunomodulators that stimulate DC activation, leading to specific T-cell responses. Creating an infection mimicking microenvironment by the presentation of exogenous GM-CSF and CpG-ODN provides an avenue to precisely control the number and timing of DC migration and modulate antigen specific immune responses.

The vertebrate immune system employs various mechanisms for pathogen recognition making it adept at generating antigen-specific responses and clearing infection. Immunity is controlled by antigen presenting cells (APCs), especially dendritic cells (DCs), which capture antigens and are activated by stimuli, unique 'danger signals' of the invading pathogen, such as CpG dinucleotide sequences in bacterial DNA (Banchereau J, and Steinman RM. Nature. 392, 245-252. (1998); Klinman DM. Nat. Rev. Immunol. 4, 249-58 (2004); each herein incorporated by reference).

However, cancerous cells, derived from self-tissues, are void of the danger signals required to signal DC maturation and instead promote an immunosuppressive microenvironment that allows cells to escape immunity. Key elements of infection are inflammatory cytokines and danger signals (Figure 1). A polymeric material system is ideal to present these factors in the required spatiotemporal manner to provide an infection-

mimicking microenvironment *in situ* that useful as a vaccine. These infection mimics provide the continuous programming of host DCs, providing for efficient DC activation and dispersement *in situ*. These infection-mimicking devices are used for numerous vaccine applications including melanoma cancer vaccines.

In many infections, inflammatory cytokines and danger signals stimulate specific DC responses that mediate immune recognition and pathogen clearance (Fig 1). For example, upon bacterial invasion and release of toxins, skin cells such as fibroblasts, keratinocytes and melanocytes are damaged resulting in the release of inflammatory cytokines, such as GM-CSF (Hamilton J. Trends in Immunol. 23, 403-408. (2002); Hamilton J., and Anderson G. Growth Factors. 22(4), 225-231. (2004); each herein incorporated by reference), that act to recruit Langerhans DC (skin) and DC precursors (monocytes; blood) (Hamilton J. Trends in Immunol. 23, 403-408. (2002); Hamilton J., and Anderson G. Growth Factors. 22(4), 225-231. (2004); Bowne W.B., et al. Cytokines Cell Mol Ther. 5(4), 217-25. (1999).; Dranoff, G. Nat. Rev. Cancer 4, 11-22 (2004); each herein incorporated by reference). As DCs arrive to the site of infection they begin to differentiate, and increase in phagocytic ability in response to the inflammation (Mellman I., and Steinman R.M. Cell. 106, 255-258. (2001), herein incorporated by reference), and DCs that ingest bacteria or their products begin to process antigens and DC maturation proceeds via endosomal TLR9 signaling stimulated by CpG dinucleotide sequences in bacterial DNA (Krieg A. M., Hartmann G., and Weiner G. J. CpG DNA: A potent signal for growth, activation, and maturation of human dendritic cells. Proc Natl Acad Sci U S A. 16, 9305–9310 (1999), herein incorporated by reference). Mature DCs then home to the lymph nodes where they prime antigen specific T-cell responses that clear infection.

CpG-ODNs are potent "danger signals" that upregulate DC expression of CCR7, CD80/86 costimulatory molecules, and MHC-antigen complexes. Importantly, TLR9 signaling induces DCs into promoting Th1-like, cytotoxic –Tcell responses, by cytokine production (e.g. type 1 IFN) and cross-presentation of antigen onto MHCI molecules. The presentation of these signals concurrently with tumor antigens provides the danger signal needed to promote immune responses that effectively fight cancerous cells.

Different classes of CPG-ODNs promote different immune responses depending on the ODN's specific structure and sequence. The ODN utilized in the present invention, CpG-ODN 1826, has been successfully tested in various mouse vaccination models, including melanoma. CpG-ODN 1826 has shown a beneficial effect alone or when used as adjuvant for

peptide vaccines and whole cell vaccines. Moreover, ODN 1826 has been shown to directly promote DC maturation and cytokine production. This particular CpG ODN sequence also indirectly activates Th1 cells and NK cells and, thus, enhances adaptive cellular immune responses.

Vector systems that promote CpG internalization into DCs to enhance delivery and its localization to TLR9 have been developed. The amine-rich polycation, polyethylimine (PEI) has been extensively used to condense plasmid DNA, via association with DNA phosphate groups, resulting in small, positively charge condensates facilitating cell membrane association and DNA uptake into cells (Godbey W.T., Wu K.K., and Mikos, A.G. J. of Biomed Mater Res, 1999, *45*, 268-275; Godbey W.T., Wu K.K., and Mikos, A.G. Proc Natl Acad Sci U S A. 96(9),5177-81. (1999); each herein incorporated by reference). Consequently, PEI has been utilized as a non-viral vector to enhance gene transfection and to fabricate PEI-DNA loaded PLG matrices that promoted long-term gene expression in host cells *in situ* (Huang YC, Riddle F, Rice KG, and Mooney DJ. Hum Gene Ther. 5, 609-17. (2005), herein incorporated by reference). Therefore, CpG-ODNs were condensed with PEI molecules, and the size and charge of these PEI-CpG-ODN condensates, as dependent on the amine-phosphate charge ratio, was characterized. The ability of PEI condensation to enhance DC internalization of CpG-ODN was assessed, and the subsequent decondensation of PEI-CpG-ODN within DCs and its promotion of DC activation was analyzed *in vitro*. To determine whether PEI-CpG-ODNs had the potential to improve upon the vaccination effects of the GM-CSF based system described in chapter 3, its stimulatory effects on DCs maturation and mobilization in the presence of GM-CSF was also examined.

To appropriately mimic infection and program cells in situ a PLG system was designed to not only serve as a drug delivery device, that releases inflammatory cytokines (eg. GM-CSF) but also as a physical structure to which the DCs are recruited and reside while they are activated by danger signals (eg. CpG-ODNs). The ability to control DC recruitment to and DC residence within porous PLG matrices is achieved using temporal control over the delivery of GM-CSF *in situ*, which results in batches of programmed DCs being dispersed only when GM-CSF levels were designed to subside *in situ*. This system dispersed 6% of programmed DCs to the lymph nodes and induced protective anti-tumor immunity in 23% of mice when applied as a cancer vaccine. The cell programming and dispersement efficiency is improved using an overriding secondary signal (CpG-ODN) that continuously releases DCs from GM-CSF inhibition and promotes DC maturation and

dispersement in the presence of high GM-CSF levels *in situ*. Specifically, PLG matrices were fabricated to locally present synthetic CpG-ODN with exogenous GM-CSF allowing for DCs recruited by GM-CSF to be stimulated by CpG-ODN *in situ*.

Dendritic Cells

Dendritic cells (DCs) are immune cells within the mammalian immune system and are derived from hematopoietic bone marrow progenitor cells. More specifically, dendritic cells can be categorized into lymphoid (or plasmacytoid) dendritic cell (pDC) and myeloid dendritic cell (mDC) subdivisions having arisen from a lymphoid (or plasmacytoid) or myeloid precursor cell, respectively. From the progenitor cell, regardless of the progenitor cell type, an immature dendritic cell is born. Immature dendritic cells are characterized by high endocytic activity and low T-cell activation potential. Thus, immature dendritic cells constitutively sample their immediate surrounding environment for pathogens. Exemplary pathogens include, but are not limited to, a virus or a bacteria. Sampling is accomplished by pattern recognition receptors (PRRs) such as the toll-like receptors (TLRs). Dendritic cells activate and mature once a pathogen is recognized by a pattern recognition receptor, such as a toll-like receptor.

Mature dendritic cells not only phagocytose pathogens and break them down, but also, degrade their proteins, and present pieces of these proteins, also referred to as antigens, on their cell surfaces using MHC (Major Histocompatibility Complex) molecules (Classes I, II, and III). Mature dendritic cells also upregulate cell-surface receptors that serve as co-receptors for T-cell activation. Exemplary co-receptors include, but are not limited to, CD80, CD86, and CD40. Simultaneously, mature dendritic cells upregulate chemotactic receptors, such as CCR7, that allows the cell to migrate through the blood stream or the lymphatic system to the spleen or lymph node, respectively.

Dendritic cells are present in external tissues that are in contact with the external environment such as the skin (dendritic cells residing in skin are also referred to as Langerhans cells). Alternatively, dendritic cells are present in internal tissues that are in contact with the external environment such as linings of the nose, lungs, stomach, and intestines. Finally, immature dendritic cells reside in the blood stream. Once activated, dendritic cells from all off these tissues migrate to lymphoid tissues where they present antigens and interact with T cells and B cells to initiate an immune response. One signaling system of particular importance for the present invention involves the chemokine receptor CCR7 expressed on the surface of dendritic cells and the chemokine receptor ligand CCL19

secreted by lymph node structures to attract migrating mature dendritic cells toward high concentrations of immune cells. Exemplary immune cells activated by contact with mature dendritic cells include, but are not limited to, helper T cells, killer T cells, and B cells. Although multiple cell types within the immune system present antigens, including macrophages and B lymphocytes, dendritic cells are the most potent activators of all antigen-presenting cells.

Dendritic cells earned their name from the characteristic cell shape comprising multiple dendrites extending from the cell body. The functional benefit of this cell shape is a significantly increased cell surface and contact area to the surroundings compared to the cell volume. Immature dendritic cells sometimes lack the characteristic dendrite formations and are referred to as veiled cells. Veiled cells possess large cytoplasmic veils rather than dendrites.

Plasmacytoid dendritic cells (pDCs) are innate immune cells that circulate in the blood and are found in peripheral lymphoid organs. They constitute < 0.4% of peripheral blood mononuclear cells (PBMC). In humans these cells express the surface markers CD123, BDCA-2(CD303) and BDCA-4(CD304), but do not express high levels of CD11c or CD14, which distinguishes them from conventional dendritic cells or monocytes, respectively. Mouse pDC express CD11c, B220, BST-2 (mPDCA) and Siglec-H and are negative for CD11b. As components of the innate immune system, these cells express intracellular Toll-like receptors 7 and 9 which detect ssRNA and CpG DNA motifs, respectively. Upon stimulation and subsequent activation, these cells produce large amounts of type I interferon (mainly IFN-α (alpha) and IFN-β (beta)), which are critical pleiotropic anti-viral compounds mediating a wide range of effects. The CD8− subset presents antigen using the class II pathway to CD4+ helper T cells. The CD8+ subset presents antigens using the class I pathway. The peptide/MHC class I molecules are presented to CD8+ T cells which go on to become cytotoxic T lymphocytes (CTL). The CD8 cell surface protein in the mouse corresponds to the CD141 cell surface protein in the human. CD8/CD141-positive cells express TLR3 and are preferentially activated by TLR3 agonists.

Toll-like Receptors (TLRs)

TLRs are a class of single transmembrane domain, non-catalytic, receptors that recognize structurally conserved molecules referred to as pathogen-associated molecular patterns (PAMPs). PAMPs are present on microbes and are distinguishable from host

molecules. TLRs are present in all vertebrates. Thirteen TLRs (referred to as TLRs1-13, consecutively) have been identified in humans and mice. Humans comprise TLRs 1-10.

TLRs and interleukin-1 (IL-1) receptors comprise a receptor superfamily the members of which all share a TIR domain (Toll-IL-1 receptor). TIR domains exist in three varieties with three distinct functions. TIR domains of subgroup 1 are present in receptors for interleukins produced by macrophages, monocytes, and dendritic cells. TIR domains of subgroup 2 are present in classical TLRs which bind directly or indirectly to molecules of microbial origin. TIR domains of subgroup 3 are present in cytosolic adaptor proteins that mediate signaling between proteins comprising TIR domains of subgroups 1 and 2.

TLR ligands comprise molecules that are constantly associated with and highly specific for a threat to the host's survival such as a pathogen or cellular stress. TLR ligands are highly specific for pathogens and not the host. Exemplary pathogenic molecules include, but are not limited to, lipopolysaccharides (LPS), lipoproteins, lipoarabinomannan, flagellin, double-stranded RNA, and unmethylated CpG islands of DNA.

In one preferred embodiment of the present invention, the Toll-Like receptor 9 (TLR9) is activated by specific unmethylated CpG-containing sequences in bacterial DNA or synthetic oligonucleotides (ODNs) found in the endosomal compartment of dendritic cells. Methylation status of the CpG site is a crucial distinction between bacterial and mammalian DNA, as well as between normal and cancerous tissue. Unmethylated ODNs including one or more CpG motifs mimic the effects of bacterial DNA. Alternatively, or in addition, unmethylated ODNs including one or more CpG motifs occur within oncogenes present within malignant tumor cells.

One or more sequences of the TLR-9 receptor recognizes one or more CpG-ODN sequences of the present invention. TLR-9 receptors encompassed by the present invention are described by the following sequences.

Human TLR-9, isoform A, is encoded by the following mRNA sequence (NCBI Accession No. NM_017442 and SEQ ID NO: 1; the start codon for all mRNA sequences presented herein is bolded and capitalized):

```
  1 ggaggtcttg tttccggaag atgttgcaag gctgtggtga aggcaggtgc agcctagcct
 61 cctgctcaag ctacaccctg gccctccacg catgaggccc tgcagaactc tggagatggt
121 gcctacaagg gcagaaaagg acaagtcggc agccgctgtc ctgagggcac cagctgtggt
181 gcaggagcca agacctgagg gtggaagtgt cctcttagaa tggggagtgc ccagcaaggt
241 gtacccgcta ctggtgctat ccagaattcc catctctccc tgctctctgc ctgagctctg
301 ggccttagct cctccctggg cttggtagag gacaggtgtg aggccctcat gggatgtagg
361 ctgtctgaga ggggagtgga aagaggaagg ggtgaaggag ctgtctgcca tttgactatg
421 caaatggcct ttgactcatg ggaccctgtc ctcctcactg ggggcagggt ggagtggagg
481 gggagctact aggctggtat aaaaatctta cttcctctat tctctgagcc gctgctgccc
```

```
 541 ctgtgggaag ggacctcgag tgtgaagcat ccttccctgt agctgctgtc cagtctgccc
 601 gccagaccct ctggagaagc ccctgccccc cagcATGggt ttctgccgca gcgccctgca
 661 cccgctgtct ctcctggtgc aggccatcat gctggccatg accctggccc tgggtacctt
 721 gcctgccttc ctaccctgtg agctccagcc ccacggcctg gtgaactgca actggctgtt
 781 cctgaagtct gtgccccact tctccatggc agcaccccgt ggcaatgtca ccagcctttc
 841 cttgtcctcc aaccgcatcc accacctcca tgattctgac tttgcccacc tgcccagcct
 901 gcggcatctc aacctcaagt ggaactgccc gccggttggc ctcagcccca tgcacttccc
 961 ctgccacatg accatcgagc ccagcacctt cttggctgtg cccaccctgg aagagctaaa
1021 cctgagctac aacaacatca tgactgtgcc tgcgctgccc aaatccctca tatccctgtc
1081 cctcagccat accaacatcc tgatgctaga ctctgccagc ctcgccggcc tgcatgccct
1141 gcgcttccta ttcatggacg gcaactgtta ttacaagaac ccctgcaggc aggcactgga
1201 ggtggccccg ggtgccctcc ttggcctggg caacctcacc cacctgtcac tcaagtacaa
1261 caacctcact gtggtgcccc gcaacctgcc ttccagcctg gagtatctgc tgttgtccta
1321 caaccgcatc gtcaaactgg cgcctgagga cctggccaat ctgaccgccc tgcgtgtgct
1381 cgatgtgggc ggaaattgcc gccgctgcga ccacgctccc aacccctgca tggagtgccc
1441 tcgtcacttc ccccagctac atcccgatac cttcagccac ctgagccgtc ttgaaggcct
1501 ggtgttgaag gacagttctc tctcctggct gaatgccagt tggttccgtg ggctgggaaa
1561 cctccgagtg ctggacctga gtgagaactt cctctacaaa tgcatcacta aaaccaaggc
1621 cttccagggc ctaacacagc tgcgcaagct taacctgtcc ttcaattacc aaaagagggt
1681 gtcctttgcc cacctgtctc tggccccttc cttcgggagc ctggtcgccc tgaaggagct
1741 ggacatgcac ggcatcttct tccgctcact cgatgagacc acgctccggc cactggcccg
1801 cctgcccatg ctccagactc tgcgtctgca gatgaacttc atcaaccagg cccagctcgg
1861 catcttcagg gccttccctg gcctgcgcta cgtggacctg tcggacaacc gcatcagcgg
1921 agcttcggag ctgacagcca ccatggggga ggcagatgga ggggagaagg tctggctgca
1981 gcctggggac cttgctccgg ccccagtgga cactcccagc tctgaagact tcaggcccaa
2041 ctgcagcacc ctcaacttca ccttggatct gtcacggaac aacctggtga ccgtgcagcc
2101 ggagatgttt gcccagctct cgcacctgca gtgcctgcgc ctgagccaca actgcatctc
2161 gcaggcagtc aatggctccc agttcctgcc gctgaccggt ctgcaggtgc tagacctgtc
2221 ccacaataag ctggacctct accacgagca ctcattcacg gagctaccac gactggaggc
2281 cctggacctc agctacaaca gccagccctt tggcatgcag ggcgtgggcc acaacttcag
2341 cttcgtggct cacctgcgca ccctgcgcca cctcagcctg gcccacaaca acatccacag
2401 ccaagtgtcc cagcagctct gcagtacgtc gctgcgggcc ctggacttca gcggcaatgc
2461 actgggccat atgtgggccg agggagacct ctatctgcac ttcttccaag gcctgagcgg
2521 tttgatctgg ctggacttgt cccagaaccg cctgcacacc ctcctgcccc aaaccctgcg
2581 caacctcccc aagagcctac aggtgctgcg tctccgtgac aattacctgg ccttctttaa
2641 gtggtggagc ctccacttcc tgcccaaact ggaagtcctc gacctggcag gaaaccagct
2701 gaaggccctg accaatggca gcctgcctgc tggcacccgg ctccggaggc tggatgtcag
2761 ctgcaacagc atcagcttcg tggcccccgg cttcttttcc aaggccaagg agctgcgaga
2821 gctcaacctt agcgccaacg ccctcaagac agtggaccac tcctggtttg ggcccctggc
2881 gagtgccctg caaatactag atgtaagcgc caaccctctg cactgcgcct gtggggcggc
2941 ctttatggac ttcctgctgg aggtgcaggc tgccgtgccc ggtctgccca gccgggtgaa
3001 gtgtggcagt ccgggccagc tccagggcct cagcatcttt gcacaggacc tgcgcctctg
3061 cctggatgag gccctctcct gggactgttt cgccctctcg ctgctggctg tggctctggg
3121 cctgggtgtg cccatgctgc atcacctctg tggctgggac ctctggtact gcttccacct
3181 gtgcctggcc tggcttccct ggcgggggcg gcaaagtggg cgagatgagg atgccctgcc
3241 ctacgatgcc ttcgtggtct tcgacaaaac gcagagcgca gtggcagact gggtgtacaa
3301 cgagcttcgg gggcagctgg aggagtgccg tgggcgctgg gcactccgcc tgtgcctgga
3361 ggaacgcgac tggctgcctg gcaaaaccct ctttgagaac ctgtgggcct cggtctatgg
3421 cagccgcaag acgctgtttg tgctggccca cacggaccgg gtcagtggtc tcttgcgcgc
3481 cagcttcctg ctggcccagc agcgcctgct ggaggaccgc aaggacgtcg tggtgctggt
3541 gatcctgagc cctgacggcc gccgctcccg ctatgtgcgg ctgcgccagc gcctctgccg
3601 ccagagtgtc ctcctctggc cccaccagcc cagtggtcag cgcagcttct gggcccagct
3661 gggcatggcc ctgaccaggg acaaccacca cttctataac cggaacttct gccagggacc
3721 cacggccgaa tagccgtgag ccggaatcct gcacggtgcc acctccacac tcacctcacc
3781 tctgcctgcc tggtctgacc ctcccctgct cgcctccctc accccacacc tgacacagag
3841 caggcactca ataaatgcta ccgaaggc
```

Human TLR-9, isoform A, is encoded by the following amino acid sequence (NCBI Accession No. NP_059138 and SEQ ID NO: 2):

MGFCRSALHPLSLLVQAIMLAMTLALGTLPAFLPCELQPHGLVNCNWLFLKSVPHFSMAAPRGNVTSL
SLSSNRIHHLHDSDFAHLPSLRHLNLKWNCPPVGLSPMHFPCHMTIEPSTFLAVPTLEELNLSYNNIMTV
PALPKSLISLSLSHTNILMLDSASLAGLHALRFLFMDGNCYYKNPCRQALEVAPGALLGLGNLTHLSLK
YNNLTVVPRNLPSSLEYLLLSYNRIVKLAPEDLANLTALRVLDVGGNCRRCDHAPNPCMECPRHFPQL
HPDTFSHLSRLEGLVLKDSSLSWLNASWFRGLGNLRVLDLSENFLYKCITKTKAFQGLTQLRKLNLSFN
YQKRVSFAHLSLAPSFGSLVALKELDMHGIFFRSLDETTLRPLARLPMLQTLRLQMNFINQAQLGIFRAF
PGLRYVDLSDNRISGASELTATMGEADGGEKVWLQPGDLAPAPVDTPSSEDFRPNCSTLNFTLDLSRN
NLVTVQPEMFAQLSHLQCLRLSHNCISQAVNGSQFLPLTGLQVLDLSHNKLDLYHEHSFTELPRLEALD
LSYNSQPFGMQGVGHNFSFVAHLRTLRHLSLAHNNIHSQVSQQLCSTSLRALDFSGNALGHMWAEGD
LYLHFFQGLSGLIWLDLSQNRLHTLLPQTLRNLPKSLQVLRLRDNYLAFFKWWSLHFLPKLEVLDLAG
NQLKALTNGSLPAGTRLRRLDVSCNSISFVAPGFFSKAKELRELNLSANALKTVDHSWFGPLASALQIL
DVSANPLHCACGAAFMDFLLEVQAAVPGLPSRVKCGSPGQLQGLSIFAQDLRLCLDEALSWDCFALSL
LAVALGLGVPMLHHLCGWDLWYCFHLCLAWLPWRGRQSGRDEDALPYDAFVVFDKTQSAVADWV
YNELRGQLEECRGRWALRLCLEERDWLPGKTLFENLWASVYGSRKTLFVLAHTDRVSGLLRASFLLA
QQRLLEDRKDVVVLVILSPDGRRSRYVRLRQRLCRQSVLLWPHQPSGQRSFWAQLGMALTRDNHHFY
NRNFCQGPTAE

Human TLR3 is encoded by the following mRNA sequence (GenBank Accesion No. NM_003265.2 (GI:19718735), incorporated herein by reference; SEQ ID NO: 15):

```
   1 cactttcgag agtgccgtct atttgccaca cacttccctg atgaaatgtc tggatttgga
  61 ctaaagaaaa aaggaaaggc tagcagtcat ccaacagaat cATGagacag actttgcctt
 121 gtatctactt ttgggggggc cttttgccct ttgggatgct gtgtgcatcc tccaccacca
 181 agtgcactgt tagccatgaa gttgctgact gcagccacct gaagttgact caggtacccg
 241 atgatctacc cacaaacata acagtgttga accttaccca taatcaactc agaagattac
 301 cagccgccaa cttcacaagg tatagccagc taactagctt ggatgtagga tttaacacca
 361 tctcaaaact ggagccagaa ttgtgccaga aacttcccat gttaaaagtt ttgaacctcc
 421 agcacaatga gctatctcaa ctttctgata aaacctttgc cttctgcacg aatttgactg
 481 aactccatct catgtccaac tcaatccaga aaattaaaaa taatcccttt gtcaagcaga
 541 agaatttaat cacattagat ctgtctcata atggcttgtc atctacaaaa ttaggaactc
 601 aggttcagct ggaaaatctc caagagcttc tattatcaaa caataaaatt caagcgctaa
 661 aaagtgaaga actggatatc tttgccaatt catctttaaa aaaattagag ttgtcatcga
 721 atcaaattaa agagttttct ccagggtgtt ttcacgcaat tggaagatta tttggcctct
 781 ttctgaacaa tgtccagctg ggtcccagcc ttacagagaa gctatgtttg gaattagcaa
 841 acacaagcat tcggaatctg tctctgagta acagccagct gtccaccacc agcaatacaa
 901 ctttcttggg actaaagtgg acaaatctca ctatgctcga tctttcctac aacaacttaa
 961 atgtggttgg taacgattcc tttgcttggc ttccacaact agaatatttc ttcctagagt
1021 ataataatat acagcatttg ttttctcact ctttgcacgg gcttttcaat gtgaggtacc
1081 tgaatttgaa acggtctttt actaaacaaa gtatttccct tgcctcactc cccaagattg
1141 atgatttttc ttttcagtgg ctaaaatgtt tggagcacct taacatggaa gataatgata
1201 ttccaggcat aaaaagcaat atgttcacag gattgataaa cctgaaatac ttaagtctat
1261 ccaactcctt tacaagtttg cgaactttga caaatgaaac atttgtatca cttgctcatt
1321 ctcccttaca catactcaac ctaaccaaga ataaaatctc aaaaatagag agtgatgctt
1381 tctcttggtt gggccaccta gaagtacttg acctgggcct taatgaaatt gggcaagaac
1441 tcacaggcca ggaatggaga ggtctagaaa atattttcga aatctatctt tcctacaaca
1501 agtacctgca gctgactagg aactcctttg ccttggtccc aagccttcaa cgactgatgc
1561 tccgaagggt ggcccttaaa aatgtggata gctctccttc accattccag cctcttcgta
1621 acttgaccat tctggatcta agcaacaaca acatagccaa cataaatgat gacatgttgg
1681 agggtcttga gaaactagaa attctcgatt tgcagcataa caacttagca cggctctgga
1741 aacacgcaaa ccctggtggt cccatttatt tcctaaaggg tctgtctcac ctccacatcc
1801 ttaacttgga gtccaacggc tttgacgaga tcccagttga ggtcttcaag gatttatttg
1861 aactaaagat catcgattta ggattgaata atttaaacac acttccagca tctgtcttta
1921 ataatcaggt gtctctaaag tcattgaacc ttcagaagaa tctcataaca tccgttgaga
1981 agaaggtttt cgggccagct ttcaggaacc tgactgagtt agatatgcgc tttaatccct
2041 ttgattgcac gtgtgaaagt attgcctggt ttgttaattg gattaacgag acccatacca
2101 acatccctga gctgtcaagc cactaccttt gcaacactcc acctcactat catgggttcc
```

```
2161 cagtgagact ttttgataca tcatcttgca aagacagtgc ccccttgaa ctctttttca
2221 tgatcaatac cagtatcctg ttgattttta tctttattgt acttctcatc cactttgagg
2281 gctggaggat atctttttat tggaatgttt cagtacatcg agttcttggt ttcaaagaaa
2341 tagacagaca gacagaacag tttgaatatg cagcatatat aattcatgcc tataaagata
2401 aggattgggt ctgggaacat ttctcttcaa tggaaaagga agaccaatct ctcaaatttt
2461 gtctggaaga aagggacttt gaggcgggtg tttttgaact agaagcaatt gttaacagca
2521 tcaaaagaag cagaaaaatt atttttgtta taacacacca tctattaaaa gacccattat
2581 gcaaaagatt caaggtacat catgcagttc aacaagctat tgaacaaaat ctggattcca
2641 ttatattggt tttccttgag gagattccag attataaact gaaccatgca ctctgtttgc
2701 gaagaggaat gtttaaatct cactgcatct tgaactggcc agttcagaaa gaacggatag
2761 gtgcctttcg tcataaattg caagtagcac ttggatccaa aaactctgta cattaaattt
2821 atttaaatat tcaattagca aaggagaaac tttctcaatt taaaaagttc tatggcaaat
2881 ttaagttttc cataaaggtg ttataatttg tttattcata tttgtaaatg attatattct
2941 atcacaatta catctcttct aggaaaatgt gtctccttat ttcaggccta tttttgacaa
3001 ttgacttaat tttacccaaa ataaaacata taagcacgta aaaaaaaaaa aaaaaaa
```

Human TLR3 is encoded by the following amino acid sequence (GenBank Accesion No. ABC86910.1 (GI:86161330), incorporated herein by reference; SEQ ID NO: 16):

```
   1 mrqtlpciyf wggllpfgml cassttkctv shevadcshl kltqvpddlp tnitvlnlth
  61 nqlrrlpaan ftrysqltsl dvgfntiskl epelcqklpm lkvlnlqhne lsqlsdktfa
 121 fctnltelhl msnsiqkikn npfvkqknli tldlshngls stklgtqvql enlqelllsn
 181 nkiqalksee ldifansslk klelssnqik efspgcfhai grlfglflnn vqlgpsltek
 241 lclelantsi rnlslsnsql sttsnttflg lkwtnltmld lsynnlnvvg ndsfawlpql
 301 eyffleynni qhlfshslhg lfnvrylnlk rsftkqsisl aslpkiddfs fqwlkclehl
 361 nmedndipgi ksnmftglin lkylslsnsf tslrtltnet fvslahsplh ilnltknkis
 421 kiesdafswl ghlevldlgl neigqeltgq ewrglenife iylsynkylq ltrnsfalvp
 481 slqrlmlrrv alknvdssps pfqplrnlti ldlsnnnian inddmlegle kleildlqhn
 541 nlarlwkhan pggpiyflkg lshlhilnle sngfdeipve vfkdlfelki idlglnnlnt
 601 lpasvfnnqv slkslnlqkn litsvekkvf gpafrnltel dmrfnpfdct cesiawfvnw
 661 inethtnipe lsshylcntp phyhgfpvrl fdtssckdsa pfelffmint sillifiviv
 721 llihfegwri sfywnvsvhr vlgfkeidrq teqfeyaayi ihaykdkdwv wehfssmeke
 781 dqslkfclee rdfeagvfel eaivnsikrs rkiifvithh llkdplckrf kvhhavqqai
 841 eqnldsiilv fleeipdykl nhalclrrgm fkshcilnwp vqkerigafr hklqvalgsk
 901 nsvh
```

The nucleic acid sequence of human TLR1 is provided in GenBank Accession No. NM_003263.3 (GI:41350336), incorporated herein by reference. The amino acid sequence of human TLR1 is provided in GenBank Accession No. NP_003254.2 (GI:41350337), incorporated herein by reference.

The nucleic acid sequence of human TLR2 is provided in GenBank Accession No. NM_003264.3 (GI:68160956), incorporated herein by reference. The amino acid sequence of human TLR2 is provided in GenBank Accession No. NP_003255.2 (GI:19718734), incorporated herein by reference.

The nucleic acid sequence of human TLR4 is provided in GenBank Accession No. NM_138554.4 (GI:373432600), incorporated herein by reference. The amino acid sequence of human TLR4 is provided in GenBank Accession No. NP_612564.1 (GI:19924149), incorporated herein by reference.

The nucleic acid sequence of human TLR5 is provided in GenBank Accession No. NM_003268.5 (GI:281427130), incorporated herein by reference. The amino acid sequence of human TLR5 is provided in GenBank Accession No. NP_003259.2 (GI:16751843), incorporated herein by reference.

The nucleic acid sequence of human TLR6 is provided in GenBank Accession No. NM_006068.4 (GI:318067953), incorporated herein by reference. The amino acid sequence of human TLR6 is provided in GenBank Accession No. NP_006059.2 (GI:20143971), incorporated herein by reference.

The nucleic acid sequence of human TLR7 is provided in GenBank Accession No. NM_016562.3 (GI:67944638), incorporated herein by reference. The amino acid sequence of human TLR7 is provided in GenBank Accession No. NP_057646.1 (GI:7706093), incorporated herein by reference.

The nucleic acid sequence of human TLR8 is provided in GenBank Accession No. NM_138636.4 (GI:257196253), incorporated herein by reference. The amino acid sequence of human TLR8 is provided in GenBank Accession No. NP_619542.1 (GI:20302168), incorporated herein by reference.

The nucleic acid sequence of human TLR10 is provided in GenBank Accession No. NM_030956.3 (GI:306140488), incorporated herein by reference. The amino acid sequence of human TLR10 is provided in GenBank Accession No. NP_112218.2 (GI:62865618), incorporated herein by reference.

The nucleic acid sequence of mouse TLR11 is provided in GenBank Accession No. NM_205819.3 (GI:408684412), incorporated herein by reference. The amino acid sequence of mouse TLR11 is provided in GenBank Accession No. NP_991388.2 (GI:408684413), incorporated herein by reference.

The nucleic acid sequence of mouse TLR12 is provided in GenBank Accession No. NM_205823.2 (GI:148539900), incorporated herein by reference. The amino acid sequence of mouse TLR12 is provided in GenBank Accession No. NP_991392.1 (GI:45430001), incorporated herein by reference.

The nucleic acid sequence of mouse TLR13 is provided in GenBank Accession No. NM_205820.1 (GI:45429998), incorporated herein by reference. The amino acid sequence of mouse TLR13 is provided in GenBank Accession No. NP_991389.1 (GI:45429999), incorporated herein by reference.

A representative list of TLR agonists (both synthetic and natural ligands), along with their corresponding receptor is provided in Table 2 below.

Table 2

Receptor	Pathogen Associated Ligands (PAMPS) [1]	Ligand Natural host	Synthetic Ligands
TLR 1	multiple triacyl lipopeptides	Bacteria	Pam3Cys-*
TLR 2	multiple glycolipids	Bacteria	CFA
	multiple lipopeptides	Bacteria	MALP2-**
	multiple lipoproteins	Bacteria	Pam2Cys**
	lipoteichoic acid	Gram Positive Bacteria	FSL-1
	HSP 70, or other heat shock proteins	Host cells	Hib-OMPC
	zymosan (Beta- glucan)	Fungi	
	Numerous others		
TLR 3	Double stranded RNA	viruses	Poly (I:C); Low and High molecular weight
			Poly (A:U)
TLR 4	lipopolysacharides (LPS); or LPS derivatives such as MPLA	Gram negative bacteria	AGP
	several heat shock proteins	Bacteria and host cells	MPLA
	fibrinogen	host cells	RC-529
	heparin sulfate fragments	host cells	MDF2β
	hyaluronic acid fragments	host cells	CFA
	nickel		
	Various opoid drugs		
TLR 5	Flagellin	Bacteria	Flagellin
TLR 6	multiple diacyl lipopeptides	Mycoplasma	FSL1-**
			Pam2Cys**
			MALP2-**
TLR 7	Viral ssRNA (Influenza, VSV, HIV, HCV)	RNA viruses	Guanosine analogs; imidazoquinolines (e.g. Imiquimod, Aldara ® R848, Resiquimod®), Loxoribine
TLR 8	small synthetic compounds; single-stranded RNA	RNA, Human and viral	Imidazoquinoline; Loxoribine; ssPolyU, 3M-012
TLR 9	Unmethylated CpG Oligodeoxynucleotide DNA DNA; dsDNA viruses (HSV, MCMV); Hemozoin (Plasmodium)	Bacteria, DNA viruses	CpG-oligonucleotides, numerous sequences have been synthesized (e.g CpG-ODN 2006, 1826, 2395)
TLR 10	unknown		
TLR 11	Profilin	Toxoplasma gondii	
TLR 12	Profilin	Toxoplasma gondii	
TLR 13 [2][3]	bacterial ribosomal RNA sequence 'CGGAAAGACC'	Virus, bacteria	

*Ligands recognized by TLR1 and TLR2

**Ligands recognized by TLR2 and TLR6

References

Meyer T, Stockfleth E. Clinical investigations of Toll-like receptor agonists. Expert opinion on investigational drugs. 2008;17:1051-1065. [PubMed]

van Duin D, Medzhitov R, Shaw AC. Triggering TLR signaling in vaccination. Trends in immunology. 2006;27:49-55

Kumar H, Kawai T, Akira S. Toll-like receptors and innate immunity. Biochemical and biophysical research communications. 2009;388:621-625.

Walterbaugh C, Doan T, Melvold R, Viselli S (2008). *Immunology*. Lippincott's Illustrated reviews. Philadelphia: Wolters Kluwer Health/Lippincott Williams & Wilkins. pp. 17.

Shi Z, Cai Z, Sanchez A, *et al.* (February 2011). *A novel Toll-like receptor that recognizes vesicular stomatitis virus*. 286. pp. 4517-24.

Oldenburg M, Krüger A, Ferstl R, *et al.* (August 2012). *TLR13 recognizes bacterial 23S rRNA devoid of erythromycin resistance-forming modification*. 337. pp. 1111-5.

S. Gnjatic, N.B. Sawhney, N. Bhardwaj Toll-like receptor agonists: are they good adjuvants? Cancer J., 16 (4) (2010), pp. 382-391.

Granulocyte Macrophage Colony Stimulating Factor (GM-CSF)

Granulocyte-macrophage colony-stimulating factor (GM-CSF) is a protein secreted by macrophages, T cells, mast cells, endothelial cells and fibroblasts. Specifically, GM-CSF is a cytokine that functions as a white blood cell growth factor. GM-CSF stimulates stem cells to produce granulocytes and monocytes. Monocytes exit the blood stream, migrate into tissue, and subsequently mature into macrophages.

Scaffold devices described herein comprise and release GM-CSF polypeptides to attract host DCs to the device. Contemplated GM-CSF polypeptides are isolated from endogenous sources or synthesized *in vivo* or *in vitro*. Endogenous GM-CSF polypeptides are isolated from healthy human tissue. Synthetic GM-CSF polypeptides are synthesized *in vivo* following transfection or transformation of template DNA into a host organism or cell, e.g. a mammal or cultured human cell line. Alternatively, synthetic GM-CSF polypeptides are synthesized *in vitro* by polymerase chain reaction (PCR) or other art-recognized methods Sambrook, J., Fritsch, E.F., and Maniatis, T., Molecular Cloning: A Laboratory Manual. Cold Spring Harbor Laboratory Press, NY, Vol. 1, 2, 3 (1989), herein incorporated by reference).

[01] GM-CSF polypeptides are modified to increase protein stability *in vivo*. Alternatively, GM-CSF polypeptides are engineered to be more or less immunogenic. Endogenous mature human GM-CSF polypeptides are glycosylated, reportedly, at amino acid residues 23 (leucine), 27 (asparagine), and 39 (glutamic acid) (see US Patent No. 5,073,627). GM-CSF polypeptides of the present invention are modified at one or more of these amino acid residues with respect to glycosylation state.

GM-CSF polypeptides are recombinant. Alternatively GM-CSF polypeptides are humanized derivatives of mammalian GM-CSF polypeptides. Exemplary mammalian species from which GM-CSF polypeptides are derived include, but are not limited to, mouse, rat, hamster, guinea pig, ferret, cat, dog, monkey, or primate. In a preferred embodiment, GM-CSF is a recombinant human protein (PeproTech, Catalog # 300-03). Alternatively, GM-CSF is a recombinant murine (mouse) protein (PeproTech, Catalog #315-03) . Finally, GM-CSF is a humanized derivative of a recombinant mouse protein.

Human Recombinant GM-CSF (PeproTech, Catalog # 300-03) is encoded by the following polypeptide sequence (SEQ ID NO: 3):

MAPARSPSPS TQPWEHVNAI QEARRLLNLS RDTAAEMNET VEVISEMFDL QEPTCLQTRL ELYKQGLRGS LTKLKGPLTM MASHYKQHCP PTPETSCATQ IITFESFKEN LKDFLLVIPF DCWEPVQE

Murine Recombinant GM-CSF (PeproTech, Catalog # 315-03) is encoded by the following polypeptide sequence (SEQ ID NO: 7):

MAPTRSPITV TRPWKHVEAI KEALNLLDDM PVTLNEEVEV VSNEFSFKKL TCVQTRLKIF
EQGLRGNFTK LKGALNMTAS YYQTYCPPTP ETDCETQVTT YADFIDSLKT FLTDIPFECK KPVQK

Human Endogenous GM-CSF is encoded by the following mRNA sequence (NCBI Accession No. NM_000758 and SEQ ID NO: 8):

```
  1 acacagagag aaaggctaaa gttctctgga ggatgtggct gcagagcctg ctgctcttgg
 61 gcactgtggc ctgcagcatc tctgcacccg cccgctcgcc cagccccagc acgcagccct
121 gggagcatgt gaatgccatc caggaggccc ggcgtctcct gaacctgagt agagacactg
181 ctgctgagat gaatgaaaca gtagaagtca tctcagaaat gtttgacctc caggagccga
241 cctgcctaca gacccgcctg gagctgtaca agcagggcct gcggggcagc ctcaccaagc
301 tcaagggccc cttgaccatg atggccagcc actacaagca gcactgccct ccaaccccgg
361 aaacttcctg tgcaacccag attatcacct ttgaaagttt caaagagaac ctgaaggact
421 ttctgcttgt catccccttt gactgctggg agccagtcca ggagtgagac cggccagatg
481 aggctggcca agccggggag ctgctctctc atgaaacaag agctagaaac tcaggatggt
541 catcttggag ggaccaaggg gtgggccaca gccatggtgg gagtggcctg gacctgccct
601 gggccacact gaccctgata caggcatggc agaagaatgg gaatatttta tactgacaga
661 aatcagtaat atttatatat ttatattttt aaaatattta tttatttatt tatttaagtt
721 catattccat atttattcaa gatgttttac cgtaataatt attattaaaa atatgcttct
781 a
```

Human Endogenous GM-CSF is encoded by the following amino acid sequence (NCBI Accession No. NP_000749.2 and SEQ ID NO: 9):

MWLQSLLLLGTVACSISAPARSPSPSTQPWEHVNAIQEARRLLNLSRDTAAEMNETV
EVISEMFDLQEPTCLQTRLELYKQGLRGSLTKLKGPLTMMASHYKQHCPPTPETSCA
TQIITFESFKENLKDFLLVIPFDCWEPVQE

Cytosine-Guanosine (CpG) Oligonucleotide (CpG-ODN) Sequences

CpG sites are regions of deoxyribonucleic acid (DNA) where a cysteine nucleotide occurs next to a guanine nucleotide in the linear sequence of bases along its length (the "p" represents the phosphate linkage between them and distinguishes them from a cytosine-guanine complementary base pairing). CpG sites play a pivotal role in DNA methylation, which is one of several endogenous mechanisms cells use to silence gene expression. Methylation of CpG sites within promoter elements can lead to gene silencing. In the case of cancer, it is known that tumor suppressor genes are often silences while oncogenes, or cancer-inducing genes, are expressed. Importantly, CpG sites in the promoter regions of tumor suppressor genes (which prevent cancer formation) have been shown to be methylated while CpG sites in the promoter regions of oncogenes are hypomethylated or unmethylated in certain cancers. The TLR-9 receptor binds unmethylated CpG sites in DNA.

The present invention comprises CpG dinucleotides and oligonucleotides. Contemplated CpG oligonucleotides are isolated from endogenous sources or synthesized *in vivo* or *in vitro*. Exemplary sources of endogenous CpG oligonucleotides include, but are not

limited to, microorganisms, bacteria, fungi, protozoa, viruses, molds, or parasites. Alternatively, endogenous CpG oligonucleotides are isolated from mammalian benign or malignant neoplastic tumors. Synthetic CpG oligonucleotides are synthesized *in vivo* following transfection or transformation of template DNA into a host organism. Alternatively, Synthetic CpG oligonucleotides are synthesized *in vitro* by polymerase chain reaction (PCR) or other art-recognized methods (Sambrook, J., Fritsch, E.F., and Maniatis, T., Molecular Cloning: A Laboratory Manual. Cold Spring Harbor Laboratory Press, NY, Vol. 1, 2, 3 (1989), herein incorporated by reference).

CpG oligonucleotides are presented for cellular uptake by dendritic cells. In one embodiment, naked CpG oligonucleotides are used. The term "naked" is used to describe an isolated endogenous or synthetic polynucleotide (or oligonucleotide) that is free of additional substituents. In another embodiment, CpG oligonucleotides are bound to one or more compounds to increase the efficiency of cellular uptake. Alternatively, or in addition, CpG oligonucleotides are bound to one or more compounds to increase the stability of the oligonucleotide within the scaffold and/or dendritic cell.

CpG oligonucleotides are condensed prior to cellular uptake. In one preferred embodiment, CpG oligonucleotides are condensed using polyethylimine (PEI), a cationic polymer that increases the efficiency of cellular uptake into dendritic cells.

CpG oligonucleotides of the present invention can be divided into multiple classes. For example, exemplary CpG-ODNs encompassed by compositions, methods and devices of the present invention are stimulatory, neutral, or suppressive. The term "stimulatory" used herein is meant to describe a class of CpG-ODN sequences that activate TLR9. The term "neutral" used herein is meant to describe a class of CpG-ODN sequences that do not activate TLR9. The term "suppressive" used herein is meant to describe a class of CpG-ODN sequences that inhibit TLR9. The term "activate TLR9" describes a process by which TLR9 initiates intracellular signaling.

Simulatory CpG-ODNs can further be divided into three types A, B and C, which differ in their immune-stimulatory activities. Type A stimulatory CpG ODNs are characterized by a phosphodiester central CpG-containing palindromic motif and a phosphorothioate 3' poly-G string. Following activation of TLR9, these CpG ODNs induce high IFN-α production from plasmacytoid dendritic cells (pDC). Type A CpG ODNs weakly stimulate TLR9-dependent NF-κB signaling.

Type B stimulatory CpG ODNs contain a full phosphorothioate backbone with one or more CpG dinucleotides. Following TLR9 activation, these CpG-ODNs strongly activate B cells. In contrast to Type A Cpg-ODNs, Type B CpG-ODNS weakly stimulate IFN-α secretion.

Type C stimulatory CpG ODNs comprise features of Types A and B. Type C CpG-ODNs contain a complete phosphorothioate backbone and a CpG containing palindromic motif. Similar to Type A CpG ODNs, Type C CpG ODNs induce strong IFN-α production from pDC. Simlar to Type B CpG ODNs, Type C CpG ODNs induce strong B cell stimulation.

Exemplary stimulatory CpG ODNs comprise, but are not limited to, ODN 1585, ODN 1668, ODN 1826, ODN 2006, ODN 2006-G5, ODN 2216, ODN 2336, ODN 2395, ODN M362 (all InvivoGen). The present invention also encompasses any humanized version of the preceding CpG ODNs. In one preferred embodiment, compositions, methods, and devices of the present invention comprise ODN 1826 (the sequence of which from 5' to 3' is tccatga**cg**ttcctga**cg**tt, wherein CpG elements are bolded, SEQ ID NO: 10).

Neutral, or control, CpG ODNs that do not stimulate TLR9 are encompassed by the present invention. These ODNs comprise the same sequence as their stimulatory counterparts but contain GpC dinucleotides in place of CpG dinucleotides.

Exemplary neutral, or control, CpG ODNs encompassed by the present invention comprise, but are not limited to, ODN 1585 control, ODN 1668 control, ODN 1826 control, ODN 2006 control, ODN 2216 control, ODN 2336 control, ODN 2395 control, ODN M362 control (all InvivoGen). The present invention also encompasses any humanized version of the preceding CpG ODNs.

Suppressive CpG ODNs that inhibit TLR9 are encompassed by the present invention. Exemplary potent inhibitory sequences are $(TTAGGG)_4$ (ODN TTAGGG, InvivoGen, SEQ ID NO: 11), found in mammalian telomeres and ODN 2088 (InvivoGen), derived from a murine stimulatory CpG ODN by replacement of 3 bases. Suppressive ODNs disrupt the colocalization of CpG ODNs with TLR9 in endosomal vesicles without affecting cellular binding and uptake. Suppressive CpG ODNs encompassed by the present invention are used to fine-tune, attenuate, reverse, or oppose the action of a stimulatory CpG-ODN. Alternatively, or in addition, compositions, methods, or devices of the present invention comprising suppressive CpG ODNs are used to treat autoimmune conditions or prevent immune responses following transplant procedures.

Cancer Antigens

Compositions, methods, and devices of the present invention comprise cancer antigens with means to vaccinate and/or provide protective immunity to a subject to whom such a device was administered. Cancer antigens are used alone or in combination with GM-CSF, CpG-ODN sequences, or immunomodulators. Moreover, cancer antigens are used simultaneously or sequentially with GM-CSF, CpG-ODN sequences, or immunomodulators.

Exemplary cancer antigens encompassed by the compositions, methods, and devices of the present invention include, but are not limited to, tumor lysates extracted from biopsies, irradiated tumor cells, MAGE series of antigens (MAGE-1 is an example), MART-1/melana, tyrosinase, ganglioside, gp100, GD-2, O-acetylated GD-3, GM-2, MUC-1, Sos1, Protein kinase C-binding protein, Reverse transcriptase protein, AKAP protein, VRK1, KIAA1735, T7-1, T11-3, T11-9, Homo Sapiens telomerase ferment (hTRT), Cytokeratin-19 (CYFRA21-1), SQUAMOUS CELL CARCINOMA ANTIGEN 1 (SCCA-1), (PROTEIN T4-A), SQUAMOUS CELL CARCINOMA ANTIGEN 2 (SCCA-2), Ovarian carcinoma antigen CA125 (1A1-3B) (KIAA0049), MUCIN 1 (TUMOR-ASSOCIATED MUCIN), (CARCINOMA-ASSOCIATED MUCIN), (POLYMORPHIC EPITHELIAL MUCIN),(PEM),(PEMT),(EPISIALIN), (TUMOR-ASSOCIATED EPITHELIAL MEMBRANE ANTIGEN),(EMA),(H23AG), (PEANUT-REACTIVE URINARY MUCIN), (PUM), (BREAST CARCINOMA- ASSOCIATED ANTIGEN DF3), CTCL tumor antigen se1-1, CTCL tumor antigen se14-3, CTCL tumor antigen se20-4, CTCL tumor antigen se20-9, CTCL tumor antigen se33-1, CTCL tumor antigen se37-2, CTCL tumor antigen se57-1, CTCL tumor antigen se89-1, Prostate-specific membrane antigen, 5T4 oncofetal trophoblast glycoprotein, Orf73 Kaposi's sarcoma-associated herpesvirus, MAGE-C1 (cancer/testis antigen CT7), MAGE-B1 ANTIGEN (MAGE-XP ANTIGEN) (DAM10), MAGE-B2 ANTIGEN (DAM6), MAGE-2 ANTIGEN, MAGE-4a antigen, MAGE-4b antigen, Colon cancer antigen NY-CO-45, Lung cancer antigen NY-LU-12 variant A, Cancer associated surface antigen, Adenocarcinoma antigen ART1, Paraneoplastic associated brain-testis-cancer antigen (onconeuronal antigen MA2; paraneoplastic neuronal antigen), Neuro-oncological ventral antigen 2 (NOVA2), Hepatocellular carcinoma antigen gene 520, TUMOR-ASSOCIATED ANTIGEN CO-029, Tumor-associated antigen MAGE-X2, Synovial sarcoma, X breakpoint 2, Squamous cell carcinoma antigen recognized by T cell, Serologically defined colon cancer antigen 1, Serologically defined breast cancer antigen NY-BR-15, Serologically defined breast cancer antigen NY-BR-16, Chromogranin A;

parathyroid secretory protein 1, DUPAN-2, CA 19-9, CA 72-4, CA 195, Carcinoembryonic antigen (CEA).

Immunomodulators

Compositions, methods, and devices of the present invention comprise immunomodulators including, but not limited to, TLR ligands, growth factors, and products of dying cells, e.g. heat shock proteins, with means to stimulate dendritic cell activation. Immunomodulators are used alone or in combination with GM-CSF, CpG-ODN sequences, or cancer antigens. Immunomodulators are used simultaneously or sequentially with GM-CSF, CpG-ODN sequences, or cancer antigens.

All known TLR ligands found either on a cell surface or an internal cellular compartment are encompassed by the compositions, methods, and devices of the present invention. Exemplary TLR ligands include, but are not limited to, triacyl lipoproteins (TLR1); lipoproteins, gram positive peptidoglycan, lipteichoic acids, fungi, and viral glycoproteins (TLR2); double-stranded RNA, poly I:C (TLR 3); lipopolysaccaride, viral glycoproteins (TLR 4); flagellin (TLR5); diacyl lipoproteins (TLR6); small synthetic compounds, single-stranded RNA (TLR7 and TLR 8); unmethylated CpG DNA (TLR9); Profilin (TLR11). Also included as TRL ligands are host molecules like fibronectin and heat shock proteins (HSPs). Host TLR ligands are also encompassed by the present invention. The role of TLRs in innate immunity and the signaling molecules used to activate and inhibit them are known in the art (for a review, see Holger K. Frank B., Hessel E., and Coffman RL. Therapeutic targeting of innate immunity with Toll-like receptor agonists and antagonists. Nature Medicine 13, 552-559 (2007), herein incorporated by reference).

All known growth factors are encompassed by the compositions, methods, and devices of the present invention. Exemplary growth factors include, but are not limited to, transforming growth factor beta (TGF-β), granulocyte-colony stimulating factor (G-CSF), granulocyte-macrophage colony stimulating factor (GM-CSF), nerve growth factor (NGF), neurotrophins, Platelet-derived growth factor (PDGF), erythropoietin (EPO), thrombopoietin (TPO), myostatin (GDF-8), growth differentiation factor-9 (GDF9), acidic fibroblast growth factor (aFGF or FGF-1), basic fibroblast growth factor (bFGF or FGF-2), epidermal growth factor (EGF), hepatocyte growth factor (HGF). The present invention encompasses cytokines as well as growth factors for stimulating dendritic cell activation. Exemplary cytokines include, but are not limited to, IL-1, IL-2, IL-3, IL-4, IL-5, IL-6, IL-8, IL-10, IL-12 1L-15, 1L-17, 1L-18, TNF-α, IFN-γ, and IFN-α.

Indications of cell death and products of dying cells stimulate dendritic cell activation. As such, all products of dying cells are encompassed by the compositions, methods, and devices of the present invention. Exemplary cell death products include, but are not limited to, any intracellular feature of a cell such as organelles, vesicles, cytoskeletal elements, proteins, DNA, and RNA. Of particular interest are heat shock proteins expressed when a cell is under stress and which are released upon cell death. Exemplary heat shock proteins include, but are not limited to, Hsp10, Hsp20, Hsp27, Hsp33, Hsp40, Hsp60, Hsp70, Hsp71, Hsp72, Grp78, Hsx70, Hsp84, Hsp90, Grp94, Hsp100, Hsp104, Hsp110.

Microenvironments and Vaccine Efficiency

The devices/scaffold described herein represent an infection-mimicking microenvironment. Each device constitutes a factory that attracts/accepts, educates/stimulates and sends forth to surrounding bodily tissues activated dendritic cells that are capable of stimulating/enhancing an immune response to a particular antigen. Specifically, the scaffold devices are implanted or coated with pathogenic molecules to mimic and infectious microenvironment to further activate the dendritic cell response.

Appropriately mimicking aspects of infection with material systems dramatically impacts tumor progression when applied as cancer vaccines by continuously recruiting, activating and homing DCs to LNs. The first PLG vaccine, using GM-CSF alone, led to a batch process where host DCs were recruited by GM-CSF to reside at a site of tumor antigen presentation, and were trapped until GM-CSF levels fell and the cells could become activated and disperse (see U.S.S.N. 11/638,796; herein incorporated by reference). Temporal variation of the local GM-CSF concentration allowed control over the number of recruited DCs, and the timing of their activation and dispersement. Although the best GM-CSF-based vaccine was able to confer protective immunity in nearly a quarter of the animals tested, approximately 26% of the recruited DCs were activated (~240,000 DCs) and approximately 6% of DCs dispersed to the LNs. High levels of GM-CSF recruited large numbers of DC, but also limited DC activation, leaving potentially therapeutic DCs entrapped within scaffolds. These results motivated the development of an improved system that mimicked bacterial infection by locally presenting CpG-ODNs as an overriding 'danger signal', that opposed GM-CSF inhibition of DC activation and dispersement. These devices described herein represent significant advances by mediating increased and continuous egress of DCs.

CpG-ODN molecules were condensed with PEI to not only promote ODN uptake into DCs and localization to its TLR-9 receptor (Fig 3), but also to electrostatically immobilize it

in PLG matrices to be presented simultaneously with tumor antigens (Fig 6). *In vitro* results indicated that PEI-CpG-ODN condensates can decondense within DCs and stimulate TLR signaling that promoted DC activation and dispersement toward the lymph node derived chemokine, CCL19, in the presence of inhibitory levels of GM-CSF (500ng/ml).

In vivo, appropriately designed infection-mimics mediated a continuous process that shuttled DCs through an infectious-like microenvironment via recruitment with GM-CSF, followed by immediate activation of resident DCS via condensed CpG-ODN presentation, and subsequent release. An *in vivo* screen of the dose effects of combined CpG-ODN delivery revealed differential effects on DC activation, with an unusual decoupling of CCR7 and MHCII expression, at high CpG-ODN (>50μg) and GM-CSF (> 1μg) doses, whereas optimal CpG-ODN doses (10-25μg) induced significant DC activation (44%, and $1.5x10^6$ cells) even when opposed by high GM-CSF levels (3 μg, *in vivo*). Therefore, optimal CpG-ODN presentation can activate large numbers of DCs recruited by strong GM-CSF pulses *in situ*, and these numbers exceed the numbers often programmed and transplanted in *ex vivo* protocols (Fig 7).

This DC programming process proved to be continuous as DCs were shuttled through an infectious-like microenvironment via recruitment with intense pulses of GM-CSF, followed by the subsequent programming and release of resident DCS via condensed CpG-ODN stimulation. The percentage of DCs that homed to the LNs approximately doubled from 6% to 13% (U.S.S.N. 11/638,796 and Fig 8), which corresponded to 180,000 programmed DCs (~4-fold enhancement compared to devices without CpG-ODN) being dispersed to the lymph nodes, with infection-mimics (Fig 7 and 8). Strikingly, the lymph nodes in this condition were markedly enlarged (Figure 8) and loaded with large numbers of DCs at sacrifice, supporting the conclusion that an infection-mimic was created in those animals.

The ability of these infectious-material systems to continuously control DC trafficking and activation translated to a regulation over the efficacy of the cancer vaccine. As the numbers of material-resident, activated DCs that were programmed and dispersed to the lymph nodes increased, the efficacy increased from 0 to 23 and finally 50%. Host T-cells mediated the immune protection, and a clear relation between the numbers of CD-4 and CD-8 lymphocytes (~50% increase due to infection mimicking) in the tumors that did form (Figure10) and vaccine efficacy was found. These results are qualitatively consistent with an ex vivo vaccine developed using irradiated tumor cells engineered to secrete GM-CSF, as that

system was previously found to stimulate a potent, specific, and long-lasting anti-tumor immunity (Akira S, Takeda K, Kaisho T. Nature Immunol, 2, 675-80, 2001). In contrast, though, the infection-mimicking material system programmed DCs *in situ*, and bypassed all *ex vivo* cell manipulation and transplantation, and provided tight control over the number of DCs recruited, activated and dispersed to the lymph nodes (LNs).

These results indicate the value of finely controlling cell behavior and programming *in situ*. The mechanism behind vaccine efficacy in these studies was clearly the appropriate control over the number and timing of DC mobilization and programming. Infection-mimics are a useful tool for the development of vaccines with means to create immunity against otherwise lethal infection, cancers and autoimmunity.

Scaffold Compositions and Architecture

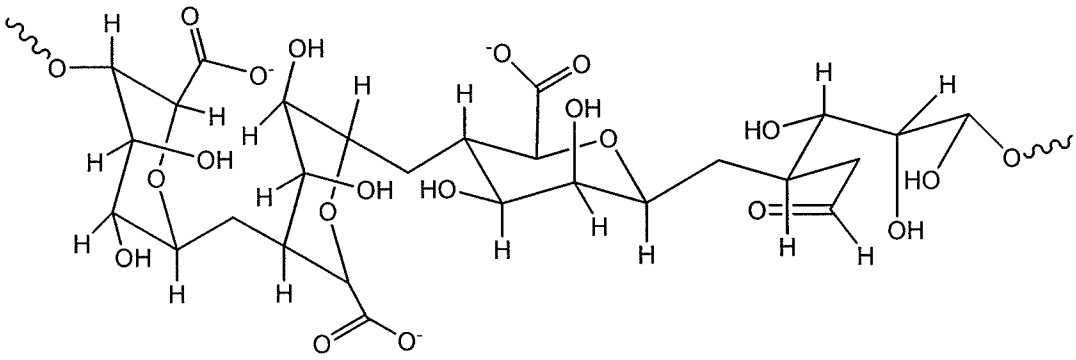
Components of the scaffolds are organized in a variety of geometric shapes (e.g., discs, beads, pellets), niches, planar layers (e.g., thin sheets). For example, discs of about 0.1-200 millimeters in diameter, e.g., 5, 10, 20, 40, 50 millimeters are implanted subcutaneously. The disc may have a thickness of 0.1 to 10 milimeters, e.g., 1, 2, 5 milimeters. The discs are readily compressed or lyophilized for administration to a patient. An exemplary disc for subcutaneous administration has the following dimensions: 8 milimeters in diameter and 1 milimeter in thickness. Multicomponent scaffolds are optionally constructed in concentric layers each of which is characterized by different physical qualities (% polymer, % crosslinking of polymer, chemical composition of scaffold, pore size, porosity, and pore architecture, stiffness, toughness, ductility, viscoelasticity, and or composition of bioactive substances such as growth factors, homing/migration factors, differentiation factors. Each niche has a specific effect on a cell population, e.g., promoting or inhibiting a specific cellular function, proliferation, differentiation, elaboration of secreted factors or enzymes, or migration. Cells incubated in the scaffold are educated and induced to migrate out of the scaffold to directly affect a target tissue, e.g., and injured tissue site. For example, stromal vascular cells and smooth muscle cells are useful in sheetlike structures are used for repair of vessel-like structures such as blood vessels or layers of the body cavity. For example, such structures are used to repair abdominal wall injuries or defects such as gastroschisis. Similarly, sheetlike scaffolds seeded with dermal stem cells and/or keratinocytes are used in bandages or wound dressings for regeneration of dermal tissue. The device is placed or transplanted on or next to a target tissue, in a protected location in the body, next to blood vessels, or outside the body as in the case of an external wound dressing.

Devices are introduced into or onto a bodily tissue using a variety of known methods and tools, e.g., spoon, tweezers or graspers, hypodermic needle, endoscopic manipulator, endo- or trans-vascular- catheter, stereotaxic needle, snake device, organ-surface-crawling robot (United States Patent Application 20050154376; Ota et al., 2006, Innovations 1:227-231), minimally invasive surgical devices, surgical implantation tools, and transdermal patches. Devices can also be assembled in place, for example by senquentially injecting or inserting matrix materials. Scaffold devices are optionally recharged with cells or with bioactive compounds, e.g., by sequential injection or spraying of substances such as growth factors or differentiation factors.

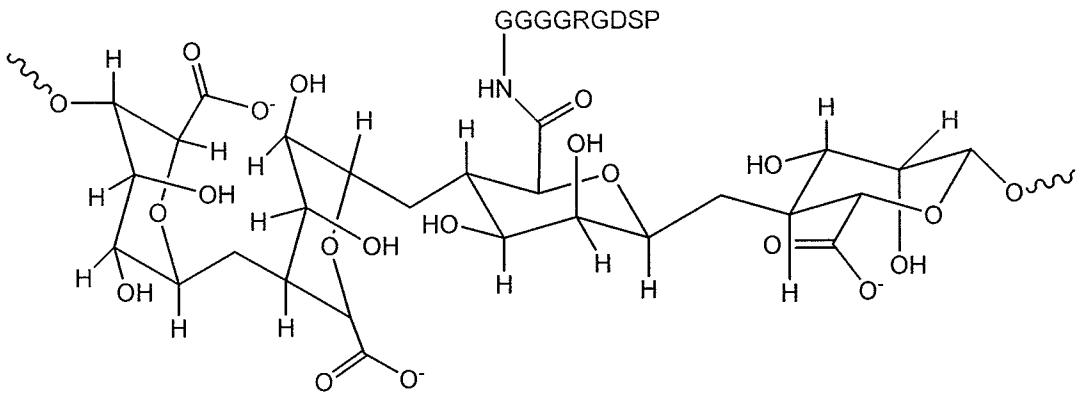
A scaffold or scaffold device is the physical structure upon which or into which cells associate or attach, and a scaffold composition is the material from which the structure is made. For example, scaffold compositions include biodegradable or permanent materials such as those listed below. The mechanical characteristics of the scaffold vary according to the application or tissue type for which regeneration is sought. It is biodegradable (e.g., collagen, alginates, polysaccharides, polyethylene glycol (PEG), poly(glycolide) (PGA), poly(L-lactide) (PLA), or poly(lactide-co-glycolide) (PLGA), poly lactic-coglycolic acid, or permanent (e.g., silk). In the case of biodegradable structures, the composition is degraded by physical or chemical action, e.g., level of hydration, heat or ion exchange or by cellular action, e.g., elaboration of enzyme, peptides, or other compounds by nearby or resident cells. The consistency varies from a soft/pliable (e.g., a gel) to glassy, rubbery, brittle, tough, elastic, stiff. The structures contain pores, which are nanoporous, microporous, or macroporous, and the pattern of the pores is optionally homogeneous, heterogenous, aligned, repeating, or random.

Alginates are versatile polysaccharide based polymers that may be formulated for specific applications by controlling the molecular weight, rate of degradation and method of scaffold formation. Coupling reactions can be used to covalently attach bioactive epitopes, such as the cell adhesion sequence RGD to the polymer backbone. Alginate polymers are formed into a variety of scaffold types. Injectable hydrogels can be formed from low MW alginate solutions upon addition of a cross-linking agents, such as calcium ions, while macroporous scaffolds are formed by lyophilization of high MW alginate discs. Differences in scaffold formulation control the kinetics of scaffold degradation. Release rates of morphogens or other bioactive substances from alginate scaffolds is controlled by scaffold formulation to present morphogens in a spatially and temporally controlled manner. This

controlled release not only eliminates systemic side effects and the need for multiple injections, but can be used to create a microenvironment that activates host cells at the implant site and transplanted cells seeded onto a scaffold.



Partially oxidized alginate



RGD-modified alginate

The scaffold comprises a biocompatible polymer matrix that is optionally biodegradable in whole or in part. A hydrogel is one example of a suitable polymer matrix material. Examples of materials which can form hydrogels include polylactic acid, polyglycolic acid, PLGA polymers, alginates and alginate derivatives, gelatin, collagen, agarose, natural and synthetic polysaccharides, polyamino acids such as polypeptides particularly poly(lysine), polyesters such as polyhydroxybutyrate and poly-epsilon.-caprolactone, polyanhydrides; polyphosphazines, poly(vinyl alcohols), poly(alkylene oxides) particularly poly(ethylene oxides), poly(allylamines)(PAM), poly(acrylates), modified

styrene polymers such as poly(4-aminomethylstyrene), pluronic polyols, polyoxamers, poly(uronic acids), poly(vinylpyrrolidone) and copolymers of the above, including graft copolymers.

The scaffolds are fabricated from a variety of synthetic polymers and naturally-occurring polymers such as, but not limited to, collagen, fibrin, hyaluronic acid, agarose, and laminin-rich gels. One preferred material for the hydrogel is alginate or modified alginate material. Alginate molecules are comprised of (1-4)-linked β-D-mannuronic acid (M units) and α L-guluronic acid (G units) monomers, which can vary in proportion and sequential distribution along the polymer chain. Alginate polysaccharides are polyelectrolyte systems which have a strong affinity for divalent cations (e.g. Ca^{+2}, Mg^{+2}, Ba^{+2}) and form stable hydrogels when exposed to these molecules. See Martinsen A., et al., Biotech. & Bioeng., 33 (1989) 79-89.) For example, calcium cross-linked alginate hydrogels are useful for dental applications, wound dressings chondrocyte transplantation and as a matrix for other cell types.

An exemplary device utilizes an alginate or other polysaccharide of a relatively low molecular weight, preferably of size which, after dissolution, is at the renal threshold for clearance by humans, e.g., the alginate or polysaccharide is reduced to a molecular weight of 1000 to 80,000 daltons. Prefereably, the molecular mass is 1000 to 60,000 daltons, particularly preferably 1000 to 50,000 daltons. It is also useful to use an alginate material of high guluronate content since the guluronate units, as opposed to the mannuronate units, provide sites for ionic crosslinking through divalent cations to gel the polymer. U.S. Patent Number 6,642,363, incorporated herein by reference discloses methods for making and using polymers containing polysachharides such as alginates or modified alginates that are particularly useful for cell transplantation and tissue engineering applications.

Useful polysaccharides other than alginates include agarose and microbial polysaccharides such as those listed in the table below.

Polysaccharide Scaffold Compositions

Polymers[a]	Structure
Fungal	
Pullulan (N)	1,4-;1,6-α-D-Glucan
Scleroglucan (N)	1,3;1,6- α -D-Glucan
Chitin (N)	1,4-β-D-Acetyl Glucosamine
Chitosan (C)	1,4- β.-D-N-Glucosamine
Elsinan (N)	1,4-;1,3- α -D-Glucan
Bacterial	
Xanthan gum (A)	1,4- β.-D-Glucan with D-mannose;

	D-glucuronic Acid as side groups
Curdlan (N)	1,3- β.-D-Glucan (with branching)
Dextran (N)	1,6- α -D-Glucan with some 1,2;1,3-; 1,4-α- linkages
Gellan (A)	1,4- β.-D-Glucan with rhamose, D-glucuronic acid
Levan (N)	2,6- β -D-Fructan with some β -2,1-branching
Emulsan (A)	Lipoheteropolysaccharide
Cellulose (N)	1,4- β-D-Glucan

[a] N-neutral, A = anionic and C=cationic.

The scaffolds of the invention are porous or non-porous. For example, the scaffolds are nanoporous having a diameter of less than about 10 nm; microporous wherein the diameter of the pores are preferably in the range of about 100 nm-20 μm; or macroporous wherein the diameter of the pores are greater than about 20 μm, more preferably greater than about 100 μm and even more preferably greater than about 400μm. In one example, the scaffold is macroporous with aligned pores of about 400-500μm in diameter. The preparation of polymer matrices having the desired pore sizes and pore alignments are described in the Examples. Other methods of preparing porous hydrogel products are known in the art. (U.S. Pat. No. 6,511,650 incorporated herein by reference).

Bioactive compositions

The device includes one or more bioactive compositions. Bioactive compositions are purified naturally-occurring, synthetically produced, or recombinant compounds, e.g., polypeptides, nucleic acids, small molecules, or other agents. For example, the compositions include GM-CSF, CpG-ODN, and tumor antigens or other antigens. The compositions described herein are purified. Purified compounds are at least 60% by weight (dry weight) the compound of interest. Preferably, the preparation is at least 75%, more preferably at least 90%, and most preferably at least 99%, by weight the compound of interest. Purity is measured by any appropriate standard method, for example, by column chromatography, polyacrylamide gel electrophoresis, or HPLC analysis.

Coupling of the polypeptides to the polymer matrix is accomplished using synthetic methods known to one of ordinary skill in the art. Approaches to coupling of peptides to polymers are discussed in Hirano and Mooney, *Advanced Materials*, p.17-25 (2004). Other useful bonding chemistries include those discussed in Hermanson, *Bioconjugate Techniques*, p. 152-185 (1996), particularly by use of carbodiimide couplers, DCC and DIC (Woodward's

Reagent K). Polypeptides contain a terminal amine group for such carbodiimide bonding. The amide bond formation is preferably catalyzed by 1-ethyl-3-(3-dimethylaminopropyl)carbodiimide (EDC), which is a water soluble enzyme commonly used in peptide synthesis.

Control of release kinetics of bioactive compositions

The release profile of bioactive compositions such as GM-CSF is controlled using a number of different techniques, e.g., encapsulation, nature of attachment/association with the scaffold, porosity of the scaffold, and particle size of the bioactive compositions.

For example, GM-CSF is encapsulated as one means by which to incorporate GM-CSF into the scaffolds. GM-CSF was first encapsulated into PLG microspheres, and then these GM-CSF loaded microspheres were then in a gas foaming process to develop macroporous PLG scaffolds. The incorporation of GM-CSF into the microspheres causes the GM-CSF to be more deeply embedded into the polymer, which causes the device to sustain the initial pulse of GM-CSF delivery over days 1-5. Other incorporation methods are optionally used to alter or fine tune the duration of the GM-CSF pulse as desired, which would in turn change the kinetics of DC recruitment. For example, foaming PLG particles mixed with lyophilized GM-CSF results in GM-CSF that is associated more with the surface of the polymer scaffold, and the protein diffuses more quickly.

Alternative methods for scaffold fabrication that modify release kinetics include modifying the physical structure of the scaffolds pores, thereby leading to different degradation times and release kinetics (change pore size or total porosity as a percentage of volume), e.g., as described in Riddle et al., Role of poly(lactide-co-glycolide) particle size on gas-foamed scaffolds. J Biomater Sci Polym Ed. 2004;15(12):1561-70. Another way to alter release kinetics is to modify the composition, i.e., the raw materials from which the scaffold is made, thereby altering the release properties. For example, different polymers, e.g. alginate, PLA, PGA, or using PLGA are used. Also, use of the polymers with different ratios of glycolic and lactic acid) leads to different release profiles. For example, a variety of PLGs, differing in composition (lactide to glycolide ratio) and molecular weight are used to prepare microspheres (5-50 μm) using known double emulsion (water/oil/water) process, followed by preparation of scaffolds using particulate PLG and PLG microspheres using gas foaming/particulate leaching techniques (Ennett et al., Temporally regulated delivery of VEGF in vitro and in vivo. J Biomed Mater Res A. 2006 Oct;79(1). Another technique

involves incorporating the protein into different compartments (e.g., encapsulating proteins PLG microspheres or simple mixing and lyophilizing with the polymer before foaming).

Charging and /or recharging the device

A bioactive composition such as GM-CSF is incorporated within different layers/compartments of the device, thereby allowing multiple pulses of GM-CSF to be delivered. Each pulse charges (or recharges) the device with an influx of DCs. Scaffolds are fabricated using a variety of methods to create multiple pulses of GM-CSF (or other bioactive agents). For example, such devices are made by incorporating the protein into different compartments (e.g encapsulating proteins PLG microspheres or simple mixing and lyophilizing with the polymer before foaming) thereby creating 2 or more distinct release profiles (i.e. pulses) of the protein (e.g., as described in Richardson et al., Polymeric system for dual growth factor delivery. Nat Biotechnol. 2001 Nov;19(11)).

Alternatively, the protein is encapsulated in fast degrading PLG microspheres (e.g. low MW, 50:50 ratio) and slow degrading PLG microspheres (high MW, 85:15 ratio). Then these microspheres are mixed together to be used later to fabricate the scaffolds. Therefore, the protein is encapsulated in both fast a degrading polymer and a slow degrading polymer, thereby resulting in at least 2 distinct releases kinetics and pulses of delivery. This method is utilized to create 3, 4, 5, or more different kinds of microspheres, the ratiometric characteristics of which differ, thereby leading to 3, 4, 5 or more pulses of release of the bioactive composition such as GM-CSF.

Another approach to making a device that delivers more than one pulse is to fabricate a layered scaffold. Layered scaffolds are made by compression molding on different scaffold formulations with another. For example, the raw materials (sucrose + PLG1 + Protein) is compressed in a mold and a slightly varied formulation (sucrose + PLG2 + Protein) is also compressed in a mold. Then these two layers are compressed together and then foamed, resulting in a bilayered scaffold with distinct spatial control of the concentration of the protein, e.g., as described in Chen et al., Pharm Res. Spatio-temporal VEGF and PDGF delivery patterns blood vessel formation and maturation. 2007 Feb;24(2):258-64).

Device construction

The scaffold structure is constructed out of a number of different rigid, semi-rigid, flexible, gel, self-assembling, liquid crystalline, or fluid compositions such as peptide polymers, polysaccharides, synthetic polymers, hydrogel materials, ceramics (e.g., calcium phosphate or hydroxyapatite), proteins, glycoproteins, proteoglycans, metals and metal

alloys. The compositions are assembled into cell scaffold structures using methods known in the art, e.g., injection molding, lyophillization of preformed structures, printing, self-assembly, phase inversion, solvent casting, melt processing, gas foaming, fiber forming/processing, particulate leaching or a combination thereof. The assembled devices are then implanted or administered to the body of an individual to be treated.

The device is assembled *in vivo* in several ways. The scaffold is made from a gelling material, which is introduced into the body in its ungelled form where it gels *in situ*. Exemplary methods of delivering device components to a site at which assembly occurs include injection through a needle or other extrusion tool, spraying, painting, or methods of deposit at a tissue site, e.g., delivery using an application device inserted through a cannula. In one example, the ungelled or unformed scaffold material is mixed with bioactive substances and cells prior to introduction into the body or while it is introduced. The resultant *in vivo/in situ* assembled scaffold contains a mixture of these substances and cells.

I*n situ* assembly of the scaffold occurs as a result of spontaneous association of polymers or from synergistically or chemically catalyzed polymerization. Synergistic or chemical catalysis is initiated by a number of endogenous factors or conditions at or near the assembly site, e.g., body temperature, ions or pH in the body, or by exogenous factors or conditions supplied by the operator to the assembly site, e.g., photons, heat, electrical, sound, or other radiation directed at the ungelled material after it has been introduced. The energy is directed at the scaffold material by a radiation beam or through a heat or light conductor, such as a wire or fiber optic cable or an ultrasonic transducer. Alternatively, a shear-thinning material, such as an ampliphile, is used which re-cross links after the shear force exerted upon it, for example by its passage through a needle, has been relieved.

Suitable hydrogels for both *in vivo* and *ex vivo* assembly of scaffold devices are well known in the art and described, e.g., in Lee et al., 2001, Chem. Rev. 7:1869-1879. The peptide amphiphile approach to self-assembly assembly is described, e.g., in Hartgerink et al., 2002, Proc. Natl. Acad. Sci. U. S. A. 99:5133-5138. A method for reversible gellation following shear thinning is exemplied in Lee et al., 2003, Adv. Mat. 15:1828-1832.

A multiple compartment device is assembled *in vivo* by applying sequential layers of similarly or differentially doped gel or other scaffold material to the target site. For example, the device is formed by sequentially injecting the next, inner layer into the center of the previously injected material using a needle, forming concentric spheroids. Non-concentric compartments are formed by injecting material into different locations in a previously

injected layer. A multi-headed injection device extrudes compartments in parallel and simultaneously. The layers are made of similar or different scaffolding compositions differentially doped with bioactive substances and different cell types. Alternatively, compartments self-organize based on their hydro-philic/phobic characteristics or on secondary interactions within each compartment.

Compartmentalized device

In certain situations, a device containing compartments with distinct chemical and/or physical properties is useful. A compartmentalized device is designed and fabricated using different compositions or concentrations of compositions for each compartment.

Alternatively, the compartments are fabricated individually, and then adhered to each other (e.g., a "sandwich" with an inner compartment surrounded on one or all sides with the second compartment). This latter construction approach is accomplished using the intrinsic adhesiveness of each layer for the other, diffusion and interpenetration of polymer chains in each layer, polymerization or cross-linking of the second layer to the first, use of an adhesive (e.g., fibrin glue), or physical entrapment of one compartment in the other. The compartments self-assemble and interface appropriately, either *in vitro* or *in vivo*, depending on the presence of appropriate precursors (e.g., temperature sensitive oligopeptides, ionic strength sensitive oligopeptides, block polymers, cross-linkers and polymer chains (or combinations thereof), and precursors containing cell adhesion molecules that allow cell-controlled assembly).

Alternatively, the compartmentalized device is formed using a printing technology. Successive layers of a scaffold precursor doped with bioactive substances is placed on a substrate then cross linked, for example by self-assembling chemistries. When the cross linking is controlled by chemical-, photo- or heat-catalyzed polymerization, the thickness and pattern of each layer is controlled by a masque, allowing complex three dimensional patterns to be built up when un-cross-linked precursor material is washed away after each catalyzation. (WT Brinkman et al., Photo-cross-linking of type 1 collagen gels in the presence of smooth muscle cells: mechanical properties, cell viability, and function. *Biomacromolecules,* 2003 Jul-Aug;4(4): 890-895.; W. Ryu et al., The construction of three-dimensional micro-fluidic scaffolds of biodegradable polymers by solvent vapor based bonding of micro-molded layers. *Biomaterials,* 2007 Feb;28(6): 1174-1184; Wright, Paul K. (2001). *21st Century manufacturing.* New Jersey: Prentice-Hall Inc.) Complex, multi-compartment layers are also built up using an inkjet device which "paints" different doped-

scaffold precursors on different areas of the substrate. Julie Phillippi (Carnegie Mellon University) presentation at the annual meeting of the American Society for Cell Biology on December 10, 2006; Print me a heart and a set of arteries, Aldhouse P., New Scientist 13 April 2006 Issue 2547 p 19.; Replacement organs, hot off the press, C. Choi, New Scientist, 25 Jan 2003, v2379. These layers are built-up into complex, three dimensional compartments. The device is also built using any of the following methods: Jetted Photopolymer, Selective Laser Sintering, Laminated Object Manufacturing, Fused Deposition Modeling, Single Jet Inkjet, Three Dimensional Printing, or Laminated Object Manufacturing.

The release profiles of bioactive substances from scaffold devices is controlled by both factor diffusion and polymer degradation, the dose of the factor loaded in the system, and the composition of the polymer. Similarly, the range of action (tissue distribution) and duration of action, or spatiotemporal gradients of the released factors are regulated by these variables. The diffusion and degradation of the factors in the tissue of interest is optionally regulated by chemically modifying the factors (e.g., PEGylating growth factors). In both cases, the time frame of release determines the time over which effective cell delivery by the device is desired.

The bioactive substances are added to the scaffold compositions using known methods including surface absorption, physical immobilization, e.g., using a phase change to entrap the substance in the scaffold material. For example, a growth factor is mixed with the scaffold composition while it is in an aqueous or liquid phase, and after a change in environmental conditions (e.g., pH, temperature, ion concentration), the liquid gels or solidifies thereby entrapping the bioactive substance. Alternatively, covalent coupling, e.g., using alkylating or acylating agents, is used to provide a stable, long term presentation of a bioactive substance on the scaffold in a defined conformation. Exemplary reagents for covalent coupling of such substances are provided in the table below.

Methods to covalently couple peptides/proteins to polymers

Functional Group of Polymer	Coupling reagents and cross-linker	Reacting groups on proteins/peptides
-OH	Cyanogen bromide (CNBr) Cyanuric chloride 4-(4,6-Dimethoxy-1,3,5-triazin-2-yl)-4-methyl-morpholinium chloride (DMT-MM)	$-NH_2$
$-NH_2$	Diisocyanate compounds Diisothoncyanate compounds Glutaraldehyde Succinic anhydride	$-NH_2$ -OH
$-NH_2$	Nitrous Acid Hydrazine + nitrous acid	$-NH_2$ -SH -Ph-OH

$-NH_2$	Carbodiimide compounds (e.g., EDC, DCC)[a] DMT-MM	-COOH
-COOH	Thionyl chloride N-hydroxysuccinimide N-hydroxysulfosuccinimide + EDC	$-NH_2$
-SH	Disulfide compound	-SH

[a] EDC: 1-ethyl-3-(3-dimethylaminopropyl) carbodiimide hydrochloride; DCC: dicyclohexylcarbodiimide

Bioactive substances suitable for use in the present invention include, but are not limited to: interferons, interleukins, chemokines, cytokines, colony stimulating factors, chemotactic factors, granulocyte/macrophage colony stimulating factor (GMCSF). Splice variants of any of the above mentioned proteins, and small molecule agonists or antagonists thereof that may be used advantageously to activate dendritic cells are also contemplated herein.

Examples of cytokines as mentioned above include, but are not limited to IL-1, IL-2, IL-3, IL-4, IL-5, IL-6, IL-7, IL-8, IL-10, IL-12, IL-15, IL-17, IL-18, granulocyte-macrophage colony stimulating factor (GM-CSF), granulocyte colony stimulating factor (G-CSF), interferon-γ (γ-IFN), IFN-α, tumor necrosis factor (TNF), TGF-β, FLT-3 ligand, and CD40 ligand.

Scaffolds of the invention optionally comprise at least one non-viral gene therapy vector such that either the transplanted cells or host cells in the vicinity of the implant would take up and express gene that lead to local availability of the desired factor for a desirable time frame. Such non-viral vectors include, but are not limited to, cationic lipids, polymers, targeting proteins, and calcium phosphate.

Scaffold Fabrication.

A 85:15, 120 kD copolymer of D,L-lactide and glycolide (PLG) (Alkermes, Cambridge, MA) was utilized in a gas-foaming process to form scaffolds with open, interconnected pores (Cohen S., Yoshioka T., Lucarelli, M., Hwang L.H., and Langer R. Pharm. Res. 8,713-720 (1991); herein incorporated by reference). PLG microspheres encapsulating GM-CSF were made using standard double emulsion (Harris, L.D., Kim, B.S., and Mooney, D.J. J. Biomed.Mater. Res. 42,396-402 (1998); herein incorporated by reference). 16 mg of PLG microspheres were then mixed with 150 mg of the porogens, NaCl or sucrose (sieved to a particle size between 250 μm and 425 μm), and compression molded. The resulting disc was allowed to equilibrate within a high-pressure CO_2 environment, and a rapid reduction in pressure causes the polymer particles to expand and fuse into an interconnected structure. The NaCl was leached from the scaffolds by immersion in water

yielding scaffolds that were 90% porous. To incorporate tumor lysates into PLG scaffolds, biopsies of B16-F10 tumors, that had grown subcutaneously in the backs of C57BL/6J mice (Jackson Laboratory, Bar Harbor Maine), were digested in collagenase (250 U/ml) (Worthington, Lakewood, NJ) and suspended at a concentration equivalent to 10^7 cells per ml after filtration through 40 μm cell strainers. The tumor cell suspension was subjected to 4 cycles of rapid freeze in liquid nitrogen and thaw (37°C) and then centrifuged at 400 rpm for 10 min. The supernatant (1ml) containing tumor lysates was collected and lyophilized with the PLG microspheres and the resulting mixture was used to make PLG scaffold-based cancer vaccines. To incorporate CpG-ODNs into PLG scaffolds, PEI-CpG-ODN condensate solutions were vortexed with 60 μl of 50% (wt/vol) sucrose solution, lyophilized and mixed with dry sucrose to a final weight of 150 mg. The sucrose containing PEI-CpG-ODN condensate was then mixed with blank, GM-CSF and/or tumor lysate loaded PLG microspheres to make PLG cancer vaccines.

Scaffold compositions of the present invention comprise GM-CSF and CpG-ODN sequences. A range of concentrations of each element are contemplated. In a preferred embodiment, the scaffold composition comprises PLG. With respect to GM-CSF, per 40 mg polymeric scaffold composition, 0-100 μg of GM-CSF polypeptide is incorporated into or coated onto the scaffold composition. Alternatively, doses comprising 0-50 μg, 0-25μg, 0-10μg, 0-5μg, and 0-3μg of GM-CSF are incorporated into the scaffold composition. In a preferred embodiment, 0-3μg of GM--CSF are incorporated into the scaffold composition. With respect to CpG-ODN sequences, or PEI-CpG-ODN condensates, per 40 mg polymeric scaffold composition, 0-1000 μg of PEI-CpG-ODN is incorporated into or coated onto the scaffold composition. Alternatively, doses comprising 0-500 μg, 0-250 μg, 0-100 μg, 0-50 μg, 0-25 μg, 0-10 μg, and 0-5 μg of PEI-CpG-ODN are incorporated into the scaffold composition. In a preferred embodiment, 0-50 μg of PEI-CpG-ODN are incorporated into the scaffold composition.

CpG-ODN incorporation and *in vitro* release studies

To determine the incorporation efficiency of CpG-ODN incorporation, PLG scaffolds were prepared with 50 ug of CpG-ODN and digested in 1 ml of chloroform (Sigma Aldrich, and washed with 2 mls of aqueous buffer. The aqueous phase was isolated and the amount of CpG-ODN incorporated was determined by absorbance readings (260/280 and 260/230 ratios calculated at 0.2 mm pathlength) using a Nanodrop instrument, ND1000 (Nanodrop technologies, Wilmington, DE). Similarly, to determine CpG-ODN release kinetics CpG-

ODN loaded scaffolds were placed in 1 ml of Phosphate Buffer Solution (PBS) in an incubator (37°C). At various timepoints, the PBS release media was collected and replaced with fresh media. The total amount of CpG-ODN incorporated into PLG scaffolds and released into PBS over time was analyzed and recorded.

In vitro DC migration assays and DC activation

A DC line, JAWSII (ATCC, Manassas, VA) was used for *in vitro* experiments and was maintained in α-MEM (Invitrogen, Carlsbad, CA) supplemented with 20% FBS (Invitrogen, Carlsbad, CA) and 5ng/ml of GM-CSF. To determine the *in vitro* effects of CpG-rich oligonucleotides (CpG-ODN) on DC activation, JAWSII cells were cultured with 5μg/ml of CpG-ODN 1826, 5'-tcc atg acg ttc ctg acg tt-3', (SEQ ID NO: 12; Invivogen, San Diego, CA) for 24 hours, and in the presence of 0, 50 or 500 ng/ml GM-CSF for 12 hours. To assess the effects of condensing CpG-ODN on DC activation, CpG ODN was condensed with PEI molecules by dropping ODN-1826 solutions into PEI solution, while vortexing the mixture (Huang YC, Riddle F, Rice KG, and Mooney DJ. Hum Gene Ther. 5, 609-17. (2005); herein incorporated by reference). The charge ratio between PEI and CpG-ODN (NH3+:PO4–) was kept constant at 7 during condensation. As a positive control for DC activation, DCs were also cultured with the stimulatory factors, TNF-α (10 ng/ml) (Peprotech, Rocky Hill, NJ) and LPS (10 ng/ml) (Sigma-Aldrich, St. Louis, MO). The DCs were then harvested and stained with primary antibodies (BD Pharmingen, San Diego, CA): PE-conjugated CD86 (B7, costimulatory molecule), FITC-conjugated CCR7, and FITC-conjugated MHCII. Cells were analyzed by FACS and gated according to positive FITC, and PE using isotype controls, and the percentage of cells staining positive for each surface antigen was recorded.

Migration assays were performed with 6.5 mm transwell dishes (Costar, Cambridge, MA) with a pore size of 5 μm. To test whether CpG-ODN stimulation may affect DC chemotaxis towards CCL19 (Peprotech, Rocky Hill, NJ) in the presence of GM-CSF, $5x10^5$ DCs stimulated with either 5μg/ml of CpG-ODN or PEI-CPG-ODN (Charge Ratio of 7), and 0, 50 and 500 ng/ml GM-CSF were placed in the top wells and 300 ng/ml of CCL19 was placed in the bottom well. After 12 hours the cells that migrated into the bottom wells of the chamber were harvested and counted using a coulter counter. Dispersement of DCs from PEI-CpG-ODN loaded PLG matrices toward CCL19 was assessed by incorporating 5, 50 and 500 μg of condensates into PLG scaffolds (13 mm diameter, 2mm thick that were quartered) seeded with $1x10^6$ DCs and fixed onto transwells using bovine collagen (BD Biosciences,

San Jose, CA). To test the effects of CpG stimulaton in the presence of GM-CSF, 500 ng/ml of GM-CSF was supplemented into the media of the top wells with scaffolds containing 25 μg of PEI-CpG-ODN. At various timepoints, the cells that migrated into the bottom wells of the chamber were harvested and counted using a coulter counter.

In vivo DC migration and activation assays

Blank scaffolds and scaffolds containing GM-CSF with or without 10 μg PEI-ODN control (5'- tcc atg agc ttc ctg agc tt -3') or 10 μg PEI-CpG-ODN condensate loaded scaffolds were implanted into subcutaneous pockets on the back of 7-9 week old male C57BL/6J mice. For histological examination scaffolds were excised and fixed in Z-fix solution, embedded in paraffin, and stained with hematoxylin and eosin. To analyze DC recruitment, scaffolds were excised and the ingrown tissue was digested into single cell suspensions using a collagenase solution (Worthingtion, 250 U/ml) that was agitated at 37°C for 45 minutes. The cell suspensions were then poured through a 40μm cell strainer to isolate cells from scaffold particles and the cells were pelleted and washed with cold PBS and counted using a Z2 coulter counter (Beckman Coulter). The resultant cell populations were then stained with primary antibodies (BD Pharmingen, San Diego, CA) conjugated to fluorescent markers to allow for analysis by flow cytometry. APC-conjugated CD11c (dendritic cell marker) and PE-conjugated CD86 (B7, costimulatory molecule) stains were conducted for DC recruitment analysis, and APC-conjugated CD11c, FITC-conjugated CCR7, and PE-conjugated MHCII stains were conducted for DC programming analysis. Cells were gated according to positive FITC, APC and PE using isotype controls, and the percentage of cells staining positive for each surface antigen was recorded. To track in vivo DC emigration from scaffolds toward the inguinal lymph nodes, 250 μg of lyophilized fluoroscein isothiocyanate (FITC) (Molecular Probes, Carlsbad, CA) was incorporated into scaffolds by mixing with PLG microspheres before scaffold processing, and FITC was also applied by incubating scaffolds with 330 ul of 3% FITC solution for 30 min. FITC painted scaffolds were then implanted subcutaneously into the left flank of C57BL/6J mice and the inguinal lymph nodes (LNs) were harvested at various time-points after scaffold implantation. Cell suspensions from LNs were prepared by digestion in collagenase for 30 min and pressing of the tissue through 70 μm cell strainers, and examined for CD11c(+)FITC(+) cell numbers by flow cytometry.

Tumor growth assays

PLG scaffolds with melanoma tumor lysates and various dosages of GM-CSF and/or 10μg PEI-CpG-ODN condensates were implanted subcutaneously into the lower left flank of

C57BL/6J mice. Animals were challenged 14 days later with a subcutaneous injection of 10^5 B16-F10 melanoma cells (ATCC, Manassas, NJ) in the back of the neck. Animals were monitored for the onset of tumor growth (approximately $1mm^3$) and sacrificed for humane reasons when tumors grew to 20 - 25 mm (longest diameter). For histological examination, tumors were biopsied at days 20-25 after injection and fixed in Z-fix (Anatech, Battle Creek, MI) and stained for hematoxylin and eosin. To examine tumor tissue for T-cell infiltration, immunoperoxidase staining was performed using the avidin-biotin-peroxidase Vectastain Elite ABC kit (Vector Laboratories). The primary antibodies used were GK 1.5 (CD4), and 53-6.72 (CD8) and staining was developed using DAB+ substrate chromogen (DAKO, Carpinteria, CA). Sections from tumor samples (n=3 or 4) were visualized at 40x and 100x with a Nikon light microscope (Indianapolis, IN) and positively stained T-cells were counted manually. PLG cancer vaccines were also compared to a common cell-based vaccine using B16-F10 melanoma cells that were genetically modified to express GM-CSF, and subsequently irradiated (3500rad) as described previously (Dranoff G., et al. Proc. Natl. Acad. Sci. USA. 90, 3539-3543(1993); herein incorporated by reference).The irradiated tumor cells ($5x10^5$ cells) were then injected subcutaneously into C57BL/6J mice that were challenged 14 days later with 10^5 B16-F10 melanoma cells.

Statistical analysis

All values in the present study were expressed as mean ± S.D. The significant differences between the groups were analyzed by a Student's *t* test and a *P* value of less than 0.05 was considered significant.

Vaccine device

The biocompatible scaffolds are useful as delivery vehicles for cancer vaccines. The cancer vaccine stimulates an endogenous immune response against cancer cells. Currently produced vaccines predominantly activate the humoral immune system (i.e., the antibody dependent immune response). Other vaccines currently in development are focused on activating the cell-mediated immune system including cytotoxic T lymphocytes which are capable of killing tumor cells. Cancer vaccines generally enhance the presentation of cancer antigens to both antigen presenting cells (e.g., macrophages and dendritic cells) and/or to other immune cells such as T cells, B cells, and NK cells. Although cancer vaccines may take one of several forms, their purpose is to deliver cancer antigens and/or cancer associated antigens to antigen presenting cells (APC) in order to facilitate the endogenous processing of such antigens by APC and the ultimate presentation of antigen presentation on the cell

surface in the context of MHC class I molecules. One form of cancer vaccine is a whole cell vaccine which is a preparation of cancer cells which have been removed from a subject, treated *ex vivo* and then reintroduced as whole cells in the subject. These treatments optionally involve cytokine exposure to activate the cells, genetic manipulation to overexpress cytokines from the cells, or priming with tumor specific antigens or cocktails of antigens, and expansion in culture. Dendritic cell vaccines activate antigen presenting cells directly, and their proliferation, activation and migration to lymph nodes is regulated by scaffold compositions to enhance their ability to elicit an immune response. Types of cancers to be treated include central nervous system (CNS) cancers, CNS Germ Cell tumor, lung cancer, Leukemia, Multiple Myeloma, Renal Cancer, Malignant Glioma, Medulloblastoma, and Melanoma.

For the purpose of eliciting an antigen-specific immune response, a scaffold device is implanted into a mammal. The device is tailored to activate immune cells and prime the cells with a specific antigen thereby enhancing immune defenses and destruction of undesired tissues and targeted microorganisms such as bacterial or viral pathogens. The device attracts appropriate immune cells, such as macrophages, T cells, B cells, NK cells, and dendritic cells, by containing and/or releasing signaling substances such as GM-CSF. These signaling substances are incorporated in the scaffold composition in such a way as to control their release spatially and temporally using the same techniques used to integrate other bioactive compounds in the scaffold composition.

Once the immune cells are inside the device, the device programs the immune cells to attack or cause other aspects of the immune system to attack undesired tissues (e.g., cancer, adipose deposits, or virus-infected or otherwise diseased cells) or microorganisms. Immune cell activation is accomplished by exposing the resident immune cells to preparations of target-specific compositions, e.g,. ligands found on the surface of the undesired tissues or organisms, such as cancer cell surface markers, viral proteins, oligonucleatides, peptide sequences or other specific antigens. For example, useful cancer cell-specific antigens and other tissue or organism-specific proteins are listed in the table below.

The device optionally contains multiple ligands or antigens in order to create a multivalent vaccine. The compositions are embedded in or coated on the surface of one or more compartments of the scaffold composition such that immune cells migrating through the device are exposed to the compositions in their traverse through the device. Antigens or other immune stimulatory molecules are exposed or become exposed to the cells as the

scaffold composition degrades. The device may also contain vaccine adjuvants that program the immune cells to recognize ligands and enhance antigen presentation. Exemplary vaccine adjuvants include chemokines/cytokines, CpG rich oligonucleotides. or antibodies that are exposed concurrently with target cell-specific antigens or ligands.

The device attracts immune cells to migrate into a scaffold where they are educated in an antigen-specific manner and activated. The programmed immune cells are then induced to egress towards lymph nodes in a number of ways. The recruitment composition and deployment signal/composition, e.g., a lymph node migration inducing substance, is released in one or more bursts, programmed by the method of incorporation and/or release from the scaffold material, or controlled by the sequential degradation of scaffold compartments which contain the attractant. When a burst dissipates, the cells migrate away. Compartments containing repulsive substances are designed to degrade and release the repulsive substance in one or more bursts or steadily over time. Relative concentration of the repulsive substances cause the immune cells to migrate out of the device. Alternatively, cells which have been placed in or have migrated into the device are programmed to release repulsive substances or to change their own behavior. For example, localized gene therapy is carried out by cell exposure to plasmid DNA attached to the scaffold. Useful repulsive substances include chemokines and cytokines. Alternatively, the device may cause immune cells to egress by degrading and releasing them.

Target disease states, stimulatory molecules and antigens useful in vaccine device construction are listed below.

Bioactive factors to promote immune responses

a. Interleukins: IL-1, IL-2, IL-3, IL-4, IL-5, IL-6, IL-8, IL-10, IL-12 1L-15, 1L-17, 1L-18 etc.
b. TNF-α
c. IFN-γ
d. IFN-α
e. GM-CSF
f. G-CSF
g. Ftl-3 ligand
h. MIP-3 β (CCL19)
i. CCL21
j. M-CSF
k. MIF
l. CD40L
m. CD3
n. ICAM
o. Anti CTLA-4 antibodies
p. TGF-β

q. CPG rich DNA or oligonucleotides
r. Sugar moieties associated with Bacteria: Lipopolysacharides (LPS) is an example
s. Fas ligand
t. Trail
u. Lymphotactin
v. Mannan (M-FP)
w. Heat Shock Proteins (apg-2, Hsp70 and Hsp 90 are examples)

Diseases and antigens - vaccination targets

a. Cancer: antigens and their sources
i. Tumor lysates extracted from biopsies
ii. Irradiated tumor cells
iii. Melanoma
1. MAGE series of antigens (MAGE-1 is an example)
2. MART-1/melana
3. Tyrosinase
4. ganglioside
5. gp100
6. GD-2
7. O-acetylated GD-3
8. GM-2

iv. Breast cancer
1. MUC-1
2. Sos1
3. Protein kinase C-binding protein
4. Reverse trascriptase protein
5. AKAP protein
6. VRK1
7. KIAA1735
8. T7-1, T11-3, T11-9

v. Other general and specific cancer antigens
1. Homo Sapiens telomerase ferment (hTRT)
2. Cytokeratin-19 (CYFRA21-1)
3. SQUAMOUS CELL CARCINOMA ANTIGEN 1 (SCCA-1), (PROTEIN T4-A)
4. SQUAMOUS CELL CARCINOMA ANTIGEN 2 (SCCA-2)
5. Ovarian carcinoma antigen CA125 (1A1-3B) (KIAA0049)
6. MUCIN 1 (TUMOR-ASSOCIATED MUCIN), (CARCINOMA-ASSOCIATED MUCIN), (POLYMORPHIC EPITHELIAL MUCIN),(PEM),(PEMT),(EPISIALIN), (TUMOR-ASSOCIATED EPITHELIAL MEMBRANE ANTIGEN),(EMA),(H23AG), (PEANUT-REACTIVE URINARY MUCIN), (PUM), (BREAST CARCINOMA-ASSOCIATED ANTIGEN DF3)
7. CTCL tumor antigen se1-1
8. CTCL tumor antigen se14-3
9. CTCL tumor antigen se20-4
10. CTCL tumor antigen se20-9
11. CTCL tumor antigen se33-1
12. CTCL tumor antigen se37-2
13. CTCL tumor antigen se57-1

14. CTCL tumor antigen se89-1
15. Prostate-specific membrane antigen
16. 5T4 oncofetal trophoblast glycoprotein
17. Orf73 Kaposi's sarcoma-associated herpesvirus
18. MAGE-C1 (cancer/testis antigen CT7)
19. MAGE-B1 ANTIGEN (MAGE-XP ANTIGEN) (DAM10)
20. MAGE-B2 ANTIGEN (DAM6)
21. MAGE-2 ANTIGEN
22. MAGE-4a antigen
23. MAGE-4b antigen
24. Colon cancer antigen NY-CO-45
25. Lung cancer antigen NY-LU-12 variant A
26. Cancer associated surface antigen
27. Adenocarcinoma antigen ART1
28. Paraneoplastic associated brain-testis-cancer antigen (onconeuronal antigen MA2; paraneoplastic neuronal antigen)
29. Neuro-oncological ventral antigen 2 (NOVA2)
30. Hepatocellular carcinoma antigen gene 520
31. TUMOR-ASSOCIATED ANTIGEN CO-029
32. Tumor-associated antigen MAGE-X2
33. Synovial sarcoma, X breakpoint 2
34. Squamous cell carcinoma antigen recognized by T cell
35. Serologically defined colon cancer antigen 1
36. Serologically defined breast cancer antigen NY-BR-15
37. Serologically defined breast cancer antigen NY-BR-16
38. Chromogranin A; parathyroid secretory protein 1
39. DUPAN-2
40. CA 19-9
41. CA 72-4
42. CA 195
43. Carcinoembryonic antigen (CEA)

b. AIDS (HIV associated antigens)

i. Gp120
ii. SIV229
iii. SIVE660
iv. SHIV89.6P
v. E92
vi. HC1
vii. OKM5
viii. FVIIIRAg
ix. HLA-DR (Ia) antigens
x. OKM1
xi. LFA-3

c. General infectious diseases and associated antigens

i. Tuberculosis
1. Mycobacterium tuberculosis antigen 5
2. Mycobacterium tuberculosis antigen 85
3. ESAT-6

4. CFP-10
5. Rv3871
6. GLU-S

ii. Malaria

1. CRA
2. RAP-2
3. MSP-2
4. AMA-1

iii. Possible mutant influenza and meningitis strains

d. Neuro protection - protect against neurological diseases (e.g., Alzheimer's, Parkinsons, Prion disease)

1. Classes of self CNS antigens
2. human alpha-synuclein (Parkinson's)
3. beta amyloid plaques (Alzheimer's)

e. Autoimmune Diseases (multiple sclerosis, Rheumatoid arthritis etc)

i. Disease linked MHC antigens
ii. Different classes of Self antigens
iii. Insulin
iv. Insulin peptide B9-23
v. glutamic acid
vi. decarboxylase 65 (GAD 65)
vii. HSP 60

Disease linked T-cell receptor (TCR)

In situ Regulation of DC Subsets and T Cells Mediates Tumor Regression in Mice

Prior vaccines have been largely ineffective for patients with established cancer, as advanced disease requires potent and sustained activation of $CD8^+$ cytotoxic T lymphocytes (CTLs) to kill tumor cells and clear the disease. Subsets of dendritic cells (DCs) specialize in antigen cross-presentation and in the production of cytokines, which regulate both CTLs and T regulatory (Treg) cells that shut down effector T cell responses. Coordinated regulation of a DC network, and plasmacytoid DCs (pDCs) and $CD8^+$ DCs in particular, enhances host immunity in mice. Functionalized biomaterials incorporating various combinations of an inflammatory cytokine, immune danger signal, and tumor lysates were used to control the activation and localization of host DC populations *in situ*. The numbers of pDCs and $CD8^+$ DCs, and the endogenous production of interleukin-12, all correlated strongly with the magnitude of protective antitumor immunity and the generation of potent $CD8^+$ CTLs. Vaccination by this method maintained local and systemic CTL responses for extended periods while inhibiting FoxP3 Treg activity during antigen clearance, resulting in complete regression of distant and established melanoma tumors. The efficacy of this vaccine as a monotherapy against large invasive tumors is a result of the local activity of pDCs and $CD8^+$

DCs induced by persistent danger and antigen signaling at the vaccine site. These results indicate that a critical pattern of DC subsets correlates with the evolution of therapeutic antitumor responses. Provision of secondary immunostimulatory site of tumor antigen presentation allows one to manipulate the *in situ* generation of a heterogeneous DC network capable of CTL induction, and activate robust CD8 T cell effector responses to established tumors.

Described herein is the *in situ* generation of a heterogeneous DC network capable of CTL induction to activate robust CD8+ T cell effector responses to established tumors, by providing a secondary immunostimulatory site of tumor antigen presentation. Inflammation or infection produces DC populations that are not found in the steady state (K. Shortman, S. H. Naik, Steady-state and inflammatory dendritic-cell development. *Nat. Rev. Immunol.* 7, 19–30 (2007)), suggesting that stimuli in tissue microenvironments provoke a response from the network of DCs. The cytokine granulocyte-macrophage colony-stimulating factor (GM-CSF) is present at increased concentrations during inflammation (J. A. Hamilton, GM-CSF in inflammation and autoimmunity. *Trends Immunol.* 23, 403–408 (2002); M. C. Dieu, B. Vanbervliet, A. Vicari, J. M. Bridon, E. Oldham, S. Aït-Yahia, F. Brière, A. Zlotnik, S. Lebecque, C. Caux, Selective recruitment of immature and mature dendritic cells by distinct chemokines expressed in different anatomic sites. *J. Exp. Med.* 188, 373–386 (1988)), which causes the recruitment of both monocytes and DCs while inducing local monocytes to differentiate into DCs (G. Dranoff, E. Jaffee, A. Lazenby, P. Golumbek, H. Levitsky, K. Brose, V. Jackson, H. Hamada, D. Pardoll, R. C. Mulligan, Vaccination with irradiated tumor cells engineered to secrete murine granulocyte-macrophage colony-stimulating factor stimulates potent, specific, and long-lasting anti-tumor immunity. *Proc. Natl. Acad. Sci.* U.S.A. 90, 3539–3543 (1993); B. Pulendran, J. Banchereau, S. Burkeholder, E. Kraus, E. Guinet, C. Chalouni, D. Caron, C. Maliszewski, J. Davoust, J. Fay, K. Palucka, Flt3-ligand and granulocyte colony-stimulating factor mobilize distinct human dendritic cell subsets *in vivo*. *J. Immunol.* 165, 566–572 (2000)).

Implantable synthetic polymer matrices (antigen-loaded acellular biomaterial device) that spatially and temporally control the *in vivo* presentation of cytokines, tumor antigens, and danger signals were utilized herein. GM-CSF is released from these polylactide-co-glycolide (PLG) [a Food and Drug Administration (FDA)–approved biomaterial] matrices into the surrounding tissue to recruit DC precursors and DCs. CpG-rich oligonucleotides are immobilized on the matrices as danger signals, and antigen (tumor lysates) is released to

matrix-resident DCs to program DC development and maturation. These matrices quantitatively regulate DC activation and trafficking *in situ* and induce prophylactic immunity against inoculations of murine B16-F10 melanoma cells (P. Schnorrer, G. M. Behrens, N. S. Wilson, J. L. Pooley, C. M. Smith, D. El-Sukkari, G. Davey, F. Kupresanin, M. Li, E. Maraskovsky, G. T. Belz, F. R. Carbone, K. Shortman, W. R. Heath, J. A. Villadangos, The dominant role of $CD8^+$ dendritic cells in cross-presentation is not dictated by antigen capture. *Proc. Natl. Acad. Sci.* U.S.A. 103, 10729–10734 (2006)). As described herein, this system administered repeatedly over time to controls the recruitment and activation of multiple DC and T cell subsets and is effective as a therapeutic vaccine against established tumors.

The following materials and methods were used to generate the data described herein.

Matrix fabrication

An 85:15, 120-kD copolymer of $_{D,L}$-lactide and glycolide (PLG) (Alkermes) was utilized in a gas-foaming process to form porous PLG matrices (L. D. Harris, B. S. Kim, D. J. Mooney, Open pore biodegradable matrices formed with gas foaming. *J. Biomed. Mater. Res.* 42, 396–402 (1998)). In brief, PLG microspheres encapsulating GM¬CSF were first made with standard double emulsion (S. Cohen, T. Yoshioka, M. Lucarelli, L. H. Hwang, R. Langer, Controlled delivery systems for proteins based on poly(lactic/glycolic acid) microspheres. *Pharm. Res.* 8, 713–720 (1991)). PLG micro-spheres were then mixed with 150 mg of the porogen, sucrose (sieved to a particle size between 250 and 425 mm), and compression molded. The resulting disc was allowed to equilibrate within a high-pressure CO_2 environment, and a rapid reduction in pressure causes the polymer particles to expand and fuse into an interconnected structure. The sucrose was leached from the scaffolds by immersion in water, yielding scaffolds that were 90% porous. To incorporate tumor lysates into PLG scaffolds, the biopsies of B16-F10 tumors that had grown subcutaneously in the backs of C57BL/6J mice (Jackson Laboratory) were digested in collagenase (250 U/ml) (Worthington) and suspended at a concentration equivalent to 10^7 cells per milliliter after filtration through 40-μm cell strainers. The tumor cell suspension was subjected to four cycles of rapid freeze in liquid nitrogen and thaw (37°C) and then centrifuged at 400 rpm for 10 min. The supernatant (1 ml) containing tumor lysates was collected, incubated with the PLG microspheres, and lyophilized, and the resulting mixture was utilized in the high-pressure CO_2 process to foam macroporous PLG matrices incorporating tumor lysates. To incorporate CpG-ODNs into PLG scaffolds, CpG-ODN 1826, 5′-tccatgacgttcctgacgtt-3′

(Invivogen) was condensed with PEI (M_n ~60,000) molecules by dropping ODN 1826 solutions into PEI solution while vortexing the mixture (L. D. Harris, B. S. Kim, D. J. Mooney, Open pore biodegradable matrices formed with gas foaming. J. Biomed. Mater. Res. 42, 396–402 (1998); S. Cohen, T. Yoshioka, M. Lucarelli, L. H. Hwang, R. Langer, Controlled delivery systems for proteins based on poly(lactic/glycolic acid) microspheres. Pharm. Res. 8, 713–720 (1991); Y. C. Huang, M. Connell, Y. Park, D. J. Mooney, K. G. Rice, Fabrication and *in vitro* testing of polymeric delivery system for condensed DNA. J. Biomed. Mater. Res. A 67, 1384–1392(2003)). The charge ratio between PEI and CpG-ODN (NH_3^+:PO_4^-) was kept constant at 7 during condensation. PEI-CpG-ODN condensate solutions were then vortexed with 60 μl of 50% (w/v) sucrose solution, lyophilized, and mixed with dry sucrose to a final weight of 150 mg. The sucrose containing PEI-CpG-ODN condensate was then mixed with blank, GM-CSF, and/or tumor lysate–loaded PLG microspheres to make PLG cancer vaccines.

In situ identification of DC subsets and T cells

Blank PLG matrices and matrices containing 3000 ng of GM-CSF alone or in combination with either 1, 10, 50, or 100 μg of CpG-ODN (studies were also performed with tumor lysates copresented with either 3000 ng of GM-CSF or 100 μg of CpG-ODN alone or in combination) were implanted into subcutaneous pockets on the back of 7- to 9-week-old male C57BL/6J mice. For histological examination, scaffolds were excised and fixed in Z-fix solution (Anatech), embedded in paraffin, and stained with hematoxylin and eosin (H&E). To analyze DC recruitment, scaffolds were excised at various time points and digested the ingrown tissue into single-cell suspensions with a collagenase solution (250 U/ml; Worthington) that was agitated at 37°C for 45 min. The cell suspensions were then poured through a 40-μm cell strainer to isolate cells from scaffold particles, and the cells were pelleted and washed with cold PBS and counted with a Z2 coulter counter (Beckman Coulter). To assess DC infiltration and activation, subsets of the total cell population isolated from PLG matrices were stained with primary antibodies (BD Pharmingen) conjugated to fluorescent markers to allow for analysis by flow cytometry. Allophycocyanin (APC)–conjugated CD11c (DC marker) and phycoerythrin (PE)–conjugated CD86 (B7, costimulatory molecule) stains were conducted for DC recruitment analysis, and APC-conjugated CD11c, fluorescein isothiocyanate (FITC)–conjugated CCR7, and PE-conjugated MHCII stains were conducted for DC programming analysis. To further delineate the presence of specific DC subsets, cells were stained with APC-conjugated CD11c and PE-

conjugated PDCA-1 (pDC marker), APC-conjugated CD11c and PE-conjugated CD8 (CD8 DCs), or APC-conjugated CD11c and FITC-conjugated CD11b (CD11b DCs). To assess T cell infiltration, PE-Cy7–conjugated CD3 stains were performed in conjunction with APC-conjugated CD8a (CD8 T cells), FITC-conjugated CD4 (CD4 T cells), and PE-conjugated FoxP3 (Treg) and analyzed with flow cytometry. Cells were gated according to positive FITC, APC, and PE with isotype controls, and the percentage of cells staining positive for each surface antigen was recorded.

Tumor growth assays, protective cytokines, and TRP2 pentamer analysis

PLG scaffolds with melanoma tumor lysates and various dosages of GM-CSF and/or various quantities of PEI-CpG-ODN condensates were implanted subcutaneously into the lower left flank of C57BL/6J mice. For prophylactic vaccinations, animals were challenged 14 days later with a subcutaneous injection of 10^5 B16-F10 melanoma cells [American Type Culture Collection (ATCC)] in the back of the neck. Animals were monitored for the onset of tumor growth (~1 mm^3) and killed for humane reasons when tumors grew to 20 to 25 mm (longest diameter).

To assess PLG vaccine efficacy in the therapeutic setting, C57BL/6J mice were challenged with a subcutaneous injection of 5×10^5 B16-F10 melanoma cells (ATCC) in the back of the neck. At either day 9 or day 13 after tumor challenge, PLG vaccines loaded with 3000 ng of GM-CSF, 100 μg of CpG-ODN, and tumor lysates were implanted subcutaneously into the lower left flank of C57BL/6J mice. A subset of mice was vaccinated again at 10 days after the initial vaccination (days 19 and 23).

To determine *in vivo* IL-12p70, IFN-α, IFN-γ, and TGF-β concentrations at the matrix implant site, the adjacent tissue was excised and digested with tissue protein extraction reagent (Pierce). After centrifugation, the concentrations of IL-12, IFN- α, IFN- γ, and TGF-β in the supernatant were then analyzed with enzyme-linked immunosorbent assay (R&D Systems) according to the manufacturer's instructions.

To determine the generation of TRP2-specific CTLs, single-cell suspensions were prepared from the spleens of mice immunized with PLG vaccines (lysate + 3000 ng of GM-CSF + 100 μg of CpG) at various time points. These cells were initially stained with APC-H-2Kb–TRP2 pentamers (Proimmune) and subsequently stained with PE-conjugated monoclonal antibody to CD8 (BD Pharmingen) before being analyzed by flow cytometry.

The data indicate that an implanted copolymer matrix (antigen-loaded acellular biomaterial device) that incorporates inflammatory cytokines, immune danger signal, and tumor antigens elicits an immune response network that eradicates established tumors *in vivo*.

Statistical analysis

All values in the present study were expressed as mean ± SD. The significant differences between the groups were analyzed by a Student's *t* test and a *P* value of <0.05 was considered significant.

Local GM-CSF delivery promotes recruitment of CD11 b^+ DCs

Macroporous PLG matrices were fabricated for GM-CSF release to recruit DCs and with an interconnected porous structure facilitates cell infiltration. Matrices were loaded with 0, 3000, and 7000 ng of GM-CSF and implanted into the subcutaneous pockets of C57BL/6J mice. Histological analysis at day 14 after implantation of PLG matrices loaded with 3000 ng of GM-CSF revealed enhanced cellular infiltration when compared to blank controls. Fluorescence-activated cell sorting (FACS) analysis for CD11c DCs showed that GM-CSF delivery recruited significantly more DCs (a factor of ~8 increase) than blank PLG matrices. The matrix-resident DCs were almost exclusively CD11b^+ (~87%), in accordance with other studies of GM-CSF effects on DC recruitment *in vivo* (N. Mach, S. Gillessen, S. B. Wilson, C. Sheehan, M. Mihm, G. Dranoff, Differences in dendritic cells stimulated *in vivo* by tumors engineered to secrete granulocyte-macrophage colonystimulating factor or Flt3-ligand. Cancer Res. 60, 3239–3246 (2000); E. Daro, B. Pulendran, K. Brasel, M. Teepe, D. Pettit, D. H. Lynch, D. Vremec, L. Robb, K. Shortman, H. J. McKenna, C. R. Maliszewski, E. Maraskovsky, Polyethylene glycolmodified GM-CSF expands CD11bhighCD11chigh but not CD11blowCD11chigh murine dendritic cells *in vivo*: A comparative analysis with Flt3 ligand. J. Immunol. 165, 49–58 (2000)). The total number of DCs recruited and their expression of the costimulatory molecule CD86 increased with GM-CSF delivery in a dose-dependent manner. However, the highest dose (7000 ng) of GM-CSF reduced the number of activated DCs at the implant site, as indicated by diminished major histocompatibility complex class II (MHCII) and CCR7 expression at day 14 after implantation. Because total DC recruitment and activation both peaked at 3000 ng of GM-CSF, this dose was utilized to recruit and generate DCs. GM-CSF delivery promoted greater cellular penetration into and association with the PLG material, as indicated by histological analysis and measurement of DC numbers, allowing for the subsequent programming of resident DC precursors and DCs.

In situ delivery of CpG-oligodeoxynucleotide promotes pDC recruitment and IFN production

The ability of local presentation of danger signals to regulate the ratio of distinct DC subtypes was next examined by immobilizing TLR-activating, polyethylenimine (PEI)–condensed CpG-oligodeoxynucleotide (ODN) molecules into the matrices. Condensation of oligonucleotides with the polycationic polymer PEI results in positively charged particles that bind electrostatically to the anionic PLG matrix. PLG matrices incorporating CpG-ODN alone recruited $CD11c^+$-$PDCA\text{-}1^+$- pDCs to the PLG matrix. This effect was enhanced with coadministration of GM-CSF. The dose of CpG-ODN presented in combination with 3000 ng of GM-CSF was altered to regulate the numbers of resident pDCs, resulting in 190,000, 520,000, and 1,200,000 cells at doses of 0, 10, and 100 μg of CpG-ODN, respectively. Copresentation of CpG-ODN had little effect on the ability of GM-CSF to enhance $CD11c^+$-$CD11b^+$ cDCs. High doses of CpG-ODN promoted the local production of IFN-α (~1010 pg/ml) and IFN-γ (~600 pg/ml) independently of the presence of GM-CSF. These results indicate that controlled GM-CSF and CpG-ODN danger signaling from synthetic extracellular matrices cooperates to regulate resident pDC and $CD11c^+CD1\ 1b^+$ cDC numbers, along with the production of protective cytokines commonly linked to TH1 and CTL immunity.

Tumor lysate co-delivery with CpG-ODN and GM-CSF stimulates CD8+ generation and IL-12 production

Experiments were carried out to determine whether co-presenting cancer antigens with CpG-ODNs to matrix-resident DCs would promote further DC development, activation, and CTL antigen sensitization. In this context, necrotic tumor cells may be particularly immunostimulatory, as they release a variety of endogenous mediators (for example, heat shock proteins and damaged nucleic acids) that trigger innate immune recognition (C. Fonseca, G. Dranoff, Capitalizing on the immunogenicity of dying tumor cells. *Clin. Cancer Res.* 14, 1603–1608 (2008)). Thus, freeze-thaw lysates of B16 melanomas were prepared, and antigen-presenting matrices were fabricated by encapsulating these lysates into the PLG material, resulting in localized and sustained antigen presentation to the infiltrating cell population (O. A. Ali, N. Huebsch, L. Cao, G. Dranoff, D. J. Mooney, Infection-mimicking materials to program dendritic cells *in situ*. *Nat. Mater.* 8, 151–158 (2009)). These antigen-presenting matrices unexpectedly stimulated $CD8^+$ DC generation *in situ*). On viral invasion, $CD8^+CD11c^+$ cDCs are especially efficient at cross-presenting exogenous antigen on MHCII molecules (J. D. Farrar, H. Asnagli, K. M. Murphy, T helper subset development: Roles of instruction, selection, and transcription. *J. Clin. Invest.* 109, 431–435 (2002); D. Skokos, M.

C. Nussenzweig, CD8 DCs induce IL-12–independent Th1 differentiation through Delta 4 Notch-like ligand in response to bacterial LPS. *J. Exp. Med.* 204, 1525–1531 (2007); J. M. den Haan, S. M. Lehar, M. J. Bevan, $CD8^+$ but not $CD8^-$ dendritic cells cross-prime cytotoxic T cells *in vivo*. *J. Exp. Med.* 192, 1685–1696 (2000)) and at producing the T_H1-promoting cytokine IL-12 (M. Moser, K. M. Murphy, Dendritic cell regulation of TH1-TH2 development. *Nat. Immunol.* 1, 199–205 (2000); D. Jankovic, M. C. Kullberg, S. Hieny, P. Caspar, C. M. Collazo, A. Sher, In the absence of IL-12, CD4+ T cell responses to intracellular pathogens fail to default to a Th2 pattern and are host protective in an $IL\text{-}10^{-/-}$ setting. *Immunity* 16, 429–439 (2002); V. E. Schijns, B. L. Haagmans, C. M. Wierda, B. Kruithof, I. A. Heijnen, G. Alber, M. C. Horzinek, Mice lacking IL-1 2 develop polarized Th1 cells during viral infection. *J. Immunol.* 160, 3958–3964 (1998); J. Magram, J. Sfarra, S. Connaughton, D. Faherty, R. Warrier, D. Carvajal, C. Y. Wu, C. Stewart, U. Sarmiento, M. K. Gately, IL-12-deficient mice are defective but not devoid of type 1 cytokine responses. *Ann. N.Y. Acad. Sci.* 795, 60–70 (1996)), which are two mechanisms that aid in priming CTL immunity to viruses and tumors. This activity, however, is normally associated with lymphoid tissues. Co-presentation of tumor lysates with CpG-ODN led to the presence of 200,000 $CD8^+$ DCs, which increased to ~670,000 (a factor of 9 increase over blank matrices) when GM-CSF was added to stimulate recruitment. Additionally, tumor lysate in combination with GM-CSF and CpG enhanced the numbers of recruited pDCs at day 10 after implantation by a factor of 2 over matrices without lysate and by a factor of 10 over blank controls. No significant difference in pDC numbers was observed with tumor lysate in combination with only GM-CSF or CpG signaling. The $CD11c^+CD11b^+$DC population at the vaccine site depended on GM-CSF alone, as tumor lysate or CpG signaling alone or in combination had no significant effect on the recruitment and expansion of these DCs.

In situ production of the T cell growth factor IL-12 at matrices that deliver both tumor lysate and CpG-ODN to cell populations recruited by GM-CSF was about four times at blank matrices and at least twice at all other matrix formulations. However, tumor lysates in the matrix did not increase the high concentrations of IFN-α and IFN-γ induced by CpG-ODN alone. These results indicate that the engineered matrices manipulated both the number and the function of specific DC subsets, as well as the accompanying CTL-polarizing activity.

PLG matrices co-delivering GM-CSF, CpG-ODN, and tumor lysates stimulate potent local and systemic CD8+ cytotoxic T cells

To elucidate the adaptive immune mechanisms induced by PLG vaccines that deliver tumor lysate, GM-CSF, and CpG-ODN, the activity of both local and systemic CTLs was

examined. Flow cytometric analysis of cells infiltrating the vaccine site revealed a significant $CD3^+CD8^+$ T cell response by day 5 (representative sample: ~1.9×10^5 cells), which peaked at day 12 when a relatively large proportion of the matrix-resident cells were CTLs (representative sample: 8.5% of cells; ~8.5×10^5 cells). Local $CD8^+$ T cell numbers dropped sharply by day 16 and were negligible at day 21 likely because of antigen clearance. PLG vaccines containing tumor lysates, GM-CSF, and CpG-ODN preferentially tuned and promoted $CD8^+$ cytotoxic immune responses relative to other matrix formulations devoid of CpG. Further, the activation and persistence of systemic CTL responses was monitored by staining splenocytes with MHCII–tyrosinase-related protein 2 (TRP2) peptide pentamers to identify CTLs with specificity to TRP2, which is a major antigenic target of melanoma vaccines in mice and humans. A significant expansion of TRP2-specific CTLs was observed in the spleens of vaccinated mice by day5, which continued and peaked between days 7 and 16 before falling at days 21 to 28, indicating that systemic anti-melanoma responses were being generated and sustained for extended periods.

Tumor protection induced by PLG matrices correlated with DC subsets and IL-12 production

This system is capable of generating prophylactic immunity against poorly immunogenic B16-F10 melanoma (O. A. Ali, N. Huebsch, L. Cao, G. Dranoff, D. J. Mooney, Infection-mimicking materials to program dendritic cells *in situ*. *Nat. Mater.* 8, 151–158 (2009)). The relation of this antitumor efficacy to the specific DC networks invoked by various vaccine formulations was investigated. C57BL/6J mice were vaccinated with PLG-based matrices incorporating B16 tumor lysates, GM-CSF, and CpG-ODN in varying combinations and then challenged with live B16-F10 melanoma tumor cells at day 14 after vaccination. PLG vaccines with both B16- F10 tumor lysates and either 1, 10, 50, or 100 mg doses of CpG-ODN danger signaling allowed 10 to 30% of the vaccinated mice to survive, tumor-free, after an otherwise lethal cell challenge, whereas 100% of unvaccinated mice were killed by day 23 due to tumor burden. When GM-CSF–mediated DC recruitment was combined with lysate and CpG-ODN delivery, the mice showed significant protection from tumor-induced lethality. CpG-ODN doses of 10, 50, and 100 μg resulted in 50%, 60%, and 90% survival rates, respectively.

The ability of vaccine systems to create a heterogeneous DC population correlated with the marked increase in antitumor efficacy. In comparison to antigen matrices delivering GM-CSF alone, the antigen-loaded matrices delivering CpG and GM-CSF together resulted in a higher proportion of pDCs (~31% versus 7%) and $CD8^+$ cDCs (~14% versus 5.5%),

which correlated with a significant enhancement in mouse survival (90% versus 20%), although total DC numbers *in situ* were statistically similar (3.0 ± 0.6 versus 4.2 ± 0.9 million DCs; two-tailed Student's *t* test, $n = 5$). Survival rates were proportional to the number of pDCs and $CD8^+$ cDCs, but not $CD11b^+$ DCs, generated at the PLG vaccine site at day 10. Additionally, the endogenous production of IL-12 was correlated with animal survival, indicating the importance of cross-presentation and T_H1-promoting cytokines to vaccine efficacy.

Engineered PLG matrices incorporating CpG-ODN attenuate immune regulation by FoxP3 Treg number and immunosuppressive cytokines

Although several vaccines designed to program DCs either *ex vivo* or *in situ* have achieved significant and long-term prophylactic protection in mouse models of cancer, eradication of invasive and well-established tumors has not been achieved without adoptive T cell transfer or systemic therapies (W. W. Overwijk, M. R. Theoret, S. E. Finkelstein, D. R. Surman, L.A. de Jong, F. A. Vyth-Dreese, T. A. Dellemijn, P. A. Antony, P. J. Spiess, D. C. Palmer, D. M. Heimann, C. A. Klebanoff, Z. Yu, L. N. Hwang, L. Feigenbaum, A. M. Kruisbeek, S. A. Rosenberg, N. P. Restifo, Tumor regression and autoimmunity after reversal of a functionally tolerant state of self-reactive $CD8^+$ T cells. *J. Exp. Med.* 198, 569–580 (2003); Y. Tamura, P. Peng, K. Liu, M. Daou, P. K. Srivastava, Immunotherapy of tumors with autologous tumor-derived heat shock protein preparations. *Science* 278, 117–120 (1997)). This limitation might reflect, at least in part, the ability of DC-based vaccines to stimulate Treg cells (S. A. Quezada, K. S. Peggs, M. A. Curran, J. P. Allison, CTLA4 blockade and GM-CSF combination immunotherapy alters the intratumor balance of effector and regulatory T cells. *J. Clin. Invest.* 116, 1935–1945 (2006); M. Jinushi, Y. Nakazaki, M. Dougan, D. R. Carrasco, M. Mihm, G. Dranoff, MFG-E8–mediated uptake of apoptotic cells by APCs links the pro- and antiinflammatory activities of GM-CSF. *J. Clin. Invest.* 117, 1902–1 913 (2007)) that attenuate the cytotoxic activity of adaptive immune responses. Thus, the impact of the engineered matrices on the induction of immunosuppressive pathways was examined. Monitoring $CD4^+$ T cell responses to antigen-presenting matrices with GM-CSF and CpG revealed peak activity at days 5 and 7, which decreased to negligible concentrations by day 12 after implantation. By contrast, matrices containing GM-CSF and tumor lysate led to a significant enhancement of CD4 T cell infiltration at day 12, and these cells likely contribute to regulation of CTL responses. Incorporation of GM-CSF and tumor lysate into the vaccine matrix led to a factor of 10 increase in TGFβ concentrations and a significant increase in IL-10 at the vaccine site; these are cytokines commonly associated

with Treg activity and immunosuppression. Further, as observed previously in GM-CSF–based vaccines, GM-CSF cosignaling with tumor antigens resulted in a significant $CD3^+FoxP3^+$ response at the vaccine site when compared to all other matrix formulations, resulting in an almost even ratio of $CD8^+$ effectors and FoxP3 Treg cells. CpG-ODN presentation in concert with both tumor lysate and GM-CSF counteracted these immunosuppressive mechanisms, as TGFβ and IL-10 concentrations and Treg activity were not enhanced over the control matrices, and CD8 CTLs outnumbered FoxP3 T cells by a factor of ~25 at day 12 after implantation. These findings indicate that the vaccine system promotes and extends CTL responses through naïve T cell differentiation induced by pDCs and $CD8^+$ DCs, the corresponding production of type 1 IFNs and IL-12, and inhibition of negative feedback mechanisms.

EXAMPLES

Example 1: PLG devices loaded with GM-CSF

PLG matrices loaded with 3 μg of GM-CSF were implanted into the subcutaneous pockets of C57BL/6J mice. The macroporous PLG matrix presents GM-CSF, danger signals, and cancer antigens in a defined spatiotemporal manner *in vivo*, and serves as a residence for recruited DCs as they are programmed. These matrices released approximately 60% of their bioactive GM-CSF load within the first 5 days, followed by slow and sustained release of bioactive GM-CSF over the next 10 days (Figure 11A) to effectively recruit resident DCs.

The matrices were made as follows. A 85:15, 120 kD copolymer of D,L-lactide and glycolide (PLG) (Alkermes, Cambridge, MA) was utilized in a gas-foaming process to form macroporous PLG matrices (Harris, L.D., Kim, B.S., and Mooney, D.J. Open pore biodegradable matrices formed with gas foaming. J. Biomed.Mater. Res. 42,396-402 (1998)). GM-CSF was encapsulated (54% efficiency) into PLG scaffolds using a high pressure CO_2 foaming process. PLG microspheres encapsulating GM-CSF were made using standard double emulsion (Cohen S., Yoshioka T., Lucarelli, M., Hwang L.H., and Langer R. Controlled delivery systems for proteins based on poly(lactic/glycolic acid) microspheres. Pharm. Res. 8,713-720 (1991)). To incorporate tumor lysates, biopsies of B16-F10 tumors that had grown subcutaneously in the backs of C57BL/6J mice (Jackson Laboratory, Bar Harbor Maine), were digested in collagenase (250 U/ml) (Worthington, Lakewood, NJ), and subjected to 4 cycles of rapid freeze in liquid nitrogen and thaw (37°C) and then centrifuged at 400 rpm for 10 min. The supernatant containing tumor lysates was collected and lyophilized with the PLG microspheres and the resulting mixture was used to make PLG

scaffold-based cancer vaccines. To incorporate CpG-ODNs into PLG scaffolds, CpG-ODN 1826, 5'-tcc atg acg ttc ctg acg tt-3', (SEQ ID NO: 12; Invivogen, San Diego, CA) was first condensed with poly(ethylenimine) (PEI, *M*w ~25,000 g mol–1, Sigma Aldrich) molecules by dropping ODN-1826 solutions into PEI solution, while vortexing the mixture. The charge ratio between PEI and CpG-ODN (NH3+:PO4–) was kept constant at 7 during condensation. PEI-CpG-ODN condensate solutions were then vortexed with 60 μl of 50% (wt/vol) sucrose solution, lyophilized and mixed with dry sucrose to a final weight of 150 mg. The sucrose containing condensates was then mixed with blank, GM-CSF and/or tumor lysate loaded PLG microspheres to make PLG cancer vaccines.

Following administration to the animals, histological analysis was carried out at day 14. The analysis revealed that the total cellular infiltration into scaffolds was significantly enhanced compared to control (no incorporated GM-CSF) (Figure 11B). Analysis for DCs specifically (cells positive for cell surface antigens CD11c and CD86) showed that GM-CSF increased not just the total resident cell number, but also the percentage of cells that were DCs (Figure 11C). The number of DCs residing in the material as a result of GM-CSF delivery was approximately the same or better than the number of DCs that are commonly programmed and administered by *ex vivo* protocols (~10^6 cells), and enhanced DC numbers were sustained in the material over time. The effects of GM-CSF on *in vivo* DC recruitment were time and dose-dependent (Figure 11D).

The dose of GM-CSF delivered from the PLG scaffolds was altered to provide distinct *in vivo* concentration profiles in the surrounding tissue, and regulate DC maturation and dispersion of resident DCs (Figure 11E). Implantation of scaffolds with no GM-CSF led to moderate local levels immediately after implantation that subsequently fell to low levels by day 1-2, and then peaked again at day 5, likely due to the inflammatory response to the surgery and implanted PLG. Delivery of GM-CSF from the PLG scaffolds led to a similar GM-CSF concentration profile over time, but at much higher local concentrations. By approximately doubling the initial dose of GM-CSF, the system attained an order of magnitude difference in the peak levels of GM-CSF *in vivo*, likely due to endogenous GM-CSF production by resident DCs and leukocytes. The secondary peak for GM-CSF was found at day 5 for the 3000 ng dose, and at day 7 for the 7000 ng dose (Figure 11E). Regardless of whether 3000 or 7000 ng doses of GM-CSF were utilized, the activation state of DCs peaked when GM-CSF levels began to subside (at days 10 and 28, respectively) and enter into the optimal concentration range for DC programming.

The ability of the pulse of GM-CSF to recruit and subsequently release a batch of activated DCs to home to the lymph nodes was then tested. Fluorescein isocyanate (FITC) was incorporated into and painted onto PLG scaffolds, as DCs recruited to the scaffold ingest this label. The label can be later used to identify these cells following their trafficking to the inguinal lymph nodes. At day 2, the 3000 ng dose of GM-CSF led to an inhibition of lymph node homing, likely due to the high initial levels of GM-CSF that entrap DCs at the scaffold site (Figure 11F). However, as GM-CSF levels subsided, a batch of the recruited, FITC-positive DCs were released from the matrices, resulting in a superior and a sustained DC presence in the lymph nodes.

As temporally controlling the local GM-CSF concentration in turn controls recruitment, and dispersement of a batch of DCs, the utility of these cells as a cancer vaccine was evaluated by immobilizing melanoma tumor lysates into the matrices to load resident DCs with tumor antigens. These PLG cancer vaccines were implanted into C57BL/6J mice, and 14 days later these mice were injected with highly aggressive and metastatic B16-F10 melanoma cells. All mice implanted solely with blank PLG scaffolds had appreciable tumors within 18 days and had to be euthanized by day 23, due to the aggressiveness of these cells. Delivery of antigen alone from the PLG scaffolds slightly improved the fate of the mice, as some mice in this group survived until day 40. Surprisingly, co-delivery of GM-CSF with antigen dramatically decreased tumor formation, and the optimal GM-CSF dose delayed tumor formation by approximately 40 days in 50% of the animals, and cured 23% of animals. Moreover, localized tumor antigen presentation in combination with optimal GM-CSF exposure (400ng) increased the average time before tumor formation by 3-fold as compared to antigen alone, and by nearly 2-fold over non-optimal GM-CSF exposure.

Analysis of T-cell infiltration into tumor tissue by immunohistochemistry was next performed to determine if programmed DCs were capable of inducing T-cell activation and homing to tumors. Vaccination with antigen alone resulted in CD4(+) T-cell infiltrates. Notably, recruiting and programming a batch of DCs in situ with appropriate GM-CSF presentation resulted in a 2-fold increase in CD8(+) cytotoxic T-cell numbers over blank controls. The vaccine's efficacy was attenuated in CD8 and CD4 T-cell knock-out mice, attesting to the specific role of CD4 and CD8 T-cells in the immune protection.

A continuous process of *in situ* DC programming is achieved by presenting additional cues that released the DCs from GM-CSF inhibition once they reside in the matrices. In particular, the presentation of synthetic CpG-ODN with exogenous GM-CSF provides a

mimic of bacterial infections, in which cells recruited by inflammatory cytokines are stimulated by local toll-like receptor activating "danger signals", such as CpG-ODN present in bacteria. CpG-ODN was immobilized to the PLG matrices by first condensing nucleotides with polyethylenimine (PEI) to form cationic nanoparticles. Following foaming of a combination of CpG-ODN and PLG particles, the CpG-ODN was largely retained in the matrices (>80% over 25 days) due to electrostatic interactions with the anionic PLG material. The CpG-ODN immobilization allows for host DCs, recruited by GM-CSF, to uptake these nucleotides locally as they reside in the matrices. Surprisingly, this approach resulted in approximately 2.5 and 4.5 fold increases in the numbers of activated DCs (positive for MHCII and CCR7) in the scaffolds, respectively, over GM-CSF or CpG-ODN delivery alone. CpG-ODN presentation enhanced DC activation in the presence of inhibitory GM-CSF levels (>40 ng/ml) *in situ*, indicating a more continuous process of DC recruitment and activation. This infection-mimicking system reliably generated activated DCs'. The magnitude of the immune response with this infection-mimic was confirmed grossly, as the lymph nodes of these animals were markedly enlarged. Most importantly, a 6-fold increase in the number of DCs that were first recruited to the matrices and subsequently dispersed to the lymph nodes was achieved with this system.

The ability of continuous DC recruitment, and programming to generate an immune response was next tested in the melanoma model. The vaccine provided significant protection, and the level of protection correlated with the CpG dose. Animal survival increased from 23% to 50% and finally 90% at CpG doses of 0 μg, 10μg and 100μg, respectively. This material infection-mimic induced equivalent or better immune protection than that obtained with exsiting cell-based therapy. Materials presenting CpG-ODN with lysates alone had only a 20% survival, indicating the benefit of recruiting DCs with GM-CSF. The benefit of providing a residence for recruited DCs while they are programmed was demonstrated by the failure of vaccine formulations consisting of bolus injections of tumor lysates, CpG-ODN, with and without 3000ng of GM-CSF. Moreover, injecting GM-CSF loaded PLG microspheres to provide sustained GM-CSF delivery without providing a residence for recruited cells, with bolus CpG-ODN and tumor lysate delivery resulted in little immune protection and animals did not survive over 35 days.

To further examine the mechanism of immune protection with this material system, the subsets of DCs and the endogenous production of cytokines by these cells in materials presenting GM-CSF and CpG-ODN alone or together were analyzed, along with the

specificity of the immune response. The delivery of GM-CSF alone enhanced the recruitment of CD11c(+)CD11b(+) myeloid DCs, whereas CpG-ODN delivery alone had little effect on the overall numbers of this subset. CpG-ODN delivery did, though, increase the number of plasmacytoid DCs at the site, which have been described to predominantly secrete Thelper(Th)-1 cytokines, especially type1 interferons and interleukin(IL)-12 that can promote CD8(+), cytotoxic T cell immunity in response to CpG-ODN presentation with antigen. Accordingly, CpG signaling not only upregulated the expression of activation markers on resident DCs, but also induced IFN-γ and IL-12 production at the vaccine site, as expected from the increased presence of plasmacytoid DCs. Moreover, analysis of T cell infiltrates into tumors that formed in the subset of animals that were not completely protected (infection mimics; 10 μg CpG-ODN dose) revealed that, even in these animals, DC programming with CpG-ODN resulted in an almost 3-fold increase in CD8(+) T-cell infiltration over controls. Further, tyrosinase-related protein (TRP)-2 is a main antigenic target of the immune response elicited by melanoma vaccines in both mice (including B16 whole cell vaccines) and humans, and staining cells isolated from spleens with MHC class I/TRP2 peptide pentamers revealed a dramatic expansion of TRP2-specific CD8 T cells in vaccinated mice. These antigen-specific T cells are involved in the killing of tumor cells, and facilitated immune protection after vaccination. Additionally, 33% of surviving mice developed patches of skin and hair depigmentation starting at the sites of tumor inoculation (back of neck). Depigmentation, which likely involves T cell responses to melanocyte antigens, has been correlated to improved clinical responses in human melanoma patients, and, in these studies, was only observed in mice treated with infection mimics .

These results indicate that mimicking aspects of infection with polymeric material systems dramatically impacts tumor progression by effectively recruiting, activating and homing DCs to lymph nodes. The first approach utilized a pulse of GM-CSF alone to recruit DCs to the tumor-antigen presenting material. The DCs subsequently resided within the material and were trapped until GM-CSF levels fell and cells could become activated and disperse. The specific concentration and duration of GM-CSF are critical to its effects. A continuous process was subsequently developed to shuttle DCs through an infectious-like microenvironment via recruitment with GM-CSF, followed by activation of resident DCs via CpG-ODN presentation, and subsequent release. The presentation of PEI condensed CpG-ODN from the material dramatically increased not only the numbers of activated, host DCs residing in the material, but also the percentage and total numbers of programmed DCs that

emigrated to the lymph nodes. Further, CpG-ODN signaling selected for specific DC subsets and DC functions associated with protective immune responses.

The system's quantitative control over DC trafficking and activation translated to a regulation over the efficacy of the cancer vaccine. As the numbers of DCs that were programmed and dispersed to the lymph nodes increased, the survival increased from 0 to 25 and finally 90%. T-cells mediated immune protection, as a clear relation between the numbers of T cells in the tumors that did form and vaccine efficacy was found, and infection mimics induced the generation of melanoma-antigen specific T cells. The matrix structure was necessary to produce long-lasting immunity, as vaccines delivered in bolus form and sustained release without provision of a cell residence failed to produce significant protective immunity. Although reports concluded that either cell transplantation or multiple systemic injections are necessary to promote protective immunity in clinically relevant tumor models, the data indicate that devices comprising functional polymeric residence materials provide significant and specific immune protection that is equal to or superior to previous systems, even with single application at vastly reduced total drug doses (e.g., 3 μg in the scaffold system vs. 100's μg total dose in repeated, systemic injections).

These data have significant clinical relevance, as the material system programmed DCs *in situ*, and not only bypassed the complication and cost of *ex vivo* cell manipulation and transplantation, but also provided tight control over the number of DCs recruited, activated and dispersed to the lymph nodes. Patients are treated with and the devices provide an alternative to current cancer vaccines, or are used in concert with those and other approaches.

The system is applicable to other situations in which one desires to promote a destructive immune response (e.g., eradicate infectious diseases) or to promote tolerance (e.g., subvert autoimmune disease). The use of polymers as a temporary residence for *in situ* cell programming is a powerful alternative to current cell therapies that depend on *ex vivo* cell manipulation (e.g., stem cell therapies).

Example 2: Condensation of Synthetic CpG-ODN molecules increases cellular uptake

Synthetic CpG-ODN molecules were condensed with PEI, which resulted in positively charged, small PEI-CpG-ODN condensates that facilitates cellular internalization via promoting association with the cell membrane and enhancing transmembrane transport (Fig 2). ODN Condensation at charge ratios of 7 and 15, between the amine groups of PEI and the phosphate groups of ODNs, resulted in optimal particle sizes and positive charge (Fig 2B and C), but a charge ratio of 7 was utilized in experiments due to PEI toxicity at high

doses.

PEI condensation of CpG-ODN dramatically enhanced nucleotide uptake into DCs *in vitro* (Fig 3A-C). Quantification of CpG-ODN uptake into DCs revealed orders of magnitude differences (up to ~100-fold) between ODN condensates and naked ODN, which were maintained for extended time periods (>80hrs) *in vitro* (Fig 3C). The complexes subsequently decondense (Figure 3D) allowing for CpG-ODN localization to its intercellular receptor, TLR-9, which has been previously demonstrated to be present in endosomes.

Example 3: CpG-ODN induced DC activation and DC mobilization

Because effective CpG stimulation of DCs requires intercellular localization, the effects of PEI-condensation were evaluated on DC activation. DCs stimulated with PEI-CpG-ODN *in vitro* exhibited enhanced levels of CD86, MHCII and CCR7 expression, in comparison to those stimulated with naked CpG-ODN, which correlated strongly with DC uptake of condensates (Fig 4A and B). DCs exhibited an activated morphology, upon cellular uptake of PEI-CpG-ODN including the development of fine needle-like dendrites and large membrane expansion, which allows mature DCs to "wrap-up" T-cells promoting strong cell-cell interactions. The activation states of PEI-CpG-ODN stimulated DCs mirrored or surpassed that of positive controls stimulated with TNF-α and LPS (Fig 3C) and PEI-CpG-ODN condensates promoted a 3-fold increase in DC migration toward CCL19 *in vitro*, over unstimulated DCs (Fig 4D).

PEI-CpG-ODN condensates also released DCs from GM-CSF inhibition, as significant DC activation was noted in cells exposed to both condensed oligonucleotides and high levels of GM-CSF (Figure 5A). Additionally, PEI-CpG-ODN stimulation also promoted DC migration away from high GM-CSF sources (500 ng/ml) toward CCL19 (Figure 5B).

A PLG system was developed that effectively immobilized and presented PEI-CpG-ODN condensates (Figure 6A) to resident DCs to stimulate DC activation and mobilization. Local PEI-CpG-ODN presentation promoted DC mobilization *in vitro* (Fig 6). Interestingly, there is an optimal dose range, 5-50 μg, of PEI-CpG-ODN that enhanced DC emigration from PLG matrices toward CCL19, but high doses (500 μg) had no effect on DC migration (Figure 6B and C). A 25μg of PEI-CpG-ODN also counteracted the suppressive effects that high GM-CSF levels had on DC migration, in this model (Fig 6C). These results indicate that appropriate CpG-ODN presentation provides an avenue to continuously program and disperse host DCs that are recruited and otherwise trapped by high levels of GM-CSF *in situ*.

Example 4: Infection-mimics continuously program and disperse DCs *in vivo*

An infection-mimicking system to continuously recruit and program DCs was created by simultaneous release of GM-CSF to attract host DCs to PLG matrices, while the PEI-CpG-ODN condensates were largely retained in the matrix (>80% over 25 days) (Figure 6), likely via electrostatic interactions as has been shown for plasmid DNA, allowing for recruited DCs to uptake the complexes locally. Strikingly, when optimized, this approach resulted in approximately 2.5 and 4.5 fold increases in the numbers of MHCII and CCR7 expressing DCs resident in the matrices in situ, respectively (over GM-CSF or CpG-ODN delivery alone) (Figure 7A and B). Interestingly, high doses of PEI-CpG-ODN (>50 μg) resulted in relatively low MHCII expression and enhanced CCR7 expression, indicating differential regulation of DC function in comparison to low doses (Fig 7A). Optimum CpG-ODN signaling (~10-25 μg) enhanced DC activation in the presence of inhibitory GM-CSF levels (>40 ng/ml) *in situ*, and this infection-mimicking system generated the numbers of activated DCs (>10^6) (Figure 7A and B) commonly administered in *ex vivo* protocols.

Most importantly, a 6-fold increase in the number of DCs that were first recruited to the matrices and subsequently dispersed to the lymph nodes was achieved with this system (Figure 8 A). The magnitude of the immune response with infection-mimics could even be appreciated grossly, as the lymph nodes of these animals were markedly enlarged (Figure8B and C). As characterized by infectious responses, these swollen lymph nodes contained greater numbers of immune cells including DCs (Figure 8C and D).

Example 5: Infection-mimicking microenvironment confers potent anti-tumor immunity.

The ability of continuous DC recruitment, and programming to generate an immune response was next tested in the melanoma model. This vaccine provided significant protection, as 50% of the animals did not form tumors over an 80 day time frame (Fig 9), and this result was remarkably similar to that obtained with a widely investigated cell-based therapy (Figure 9). Animals receiving lys + CpG were 37.5% tumor free 140 days after treatment and achieved protective immunity.

Furthermore, analysis of T-cell infiltrates into tissue of tumors that formed in the subset of animals that were not completely protected revealed that, even in these animals, DC programming with CpG-ODN resulted in an almost 3-fold increase in CD8(+) T-cell infiltration over controls (Fig 10). Thus, all animals receiving the Lys-GM-CpG treatment demonstrated a therapeutic benefit.

Example 6: Tumor protection is regulated by CpG-ODN presentation and plasmacytoid DC (pDC) enrichment

Hematopoetic precursor cells of both the myeloid and lymphoid lineage have the capacity to differentiate into two main categories of DCs, plasmacytoid DCs (pDCs) and conventional DCs (cDCs), each of which are equipped with specific defense mechanisms capable of propagating specific responses to invading pathogens. This plasticity likely allows for the recruitment and generation of the DC subset(s) most proficient at eliciting the desired immune response. cDCs include $CD11c^{+}CD11b^{+}$ and $CD11c^{+}CD8\alpha^{+}$ cells exhibiting classical DC morphology with the long, protruding dendrites that make them especially adept at antigen processing and antigen presentation to T cells. pDCs are round non-dendritic cell capable of producing large amounts of type-1 interferons in response to 'danger signals', such as unmethylated CpG dinucleotide sequences in bacterial or viral DNA.

pDC derived type 1 interferons (IFN) link innate and adaptive immunity to viral infection by triggering antigen cross presentation to CD8+ T cells and interleukin production (e.g. IL-12) by cDCs that facilitate the clonal expansion of cytotoxic T cells. Type 1 IFNs also act to directly induce naïve T cell differentiation to T helper 1 cells. In addition to producing potent IFNs, pDCs stimulated by inflammatory stimuli and microbial infection differentiate into a dendritic form capable of processing and presentating antigen to prime T cell responses. pDCs and cDCs cooperate to perform specialized functions that initiate distinct cellular and molecular events leading to protective immunity.

Many cell-based vaccines for cancer fail to incorporate the different components of the DC network. Cancer vaccines are frequently developed using easily accessible, patient-derived blood monocytes that are transformed into DCs *ex vivo* using cytokine mixtures and pulsed with tumor antigens to promote antigen presentation. These antigen-loaded DCs are then injected back into cancer patients with the goal of inducing anti-tumor immune responses mediated primarily by Th1 cells and CTLs. While initial trials utilizing *ex vivo* DC vaccines in advanced cancer patients have resulted in antigen-specific T-cell expansion and the production of protective cytokines, many vaccines have failed to show survival advantage over traditional treatments (e.g., chemotherapy) and have failed to gain FDA approval. These cell-based vaccines provide no control over the in vivo function of the transplanted DCs and only incorporates one DC type into the vaccine, which may not be the most potent. Therefore, the rate-limiting step is likely the inability to fully recapitulate *ex vivo* the development of immunocompetent DCs, in particular the processes of DC activation and specialization during the generation of immune responses. The devices and methods

described herein overcome the shortcomings of such earlier approaches, and therefore, haver several advantages over earlier systems.

The devices comprise an implantable, synthetic extra-cellular matrix (ECM) that controls the *in situ* recruitment and generation of a heterogenous DC network to produce protective immune responses to tumors. GM-CSF was incorporated into polylactide-co-glycolide (an FDA approved biomaterial) matrices to recruit DC precursors and DCs, as the cytokine is released from the material into the surrounding tissue. These macroporous matrices present immobilized tumor antigens and CpG-rich oligonucleotides as danger signals, capable of programming DC development and maturation as cells reside within the material. The distribution of the DC subsets generated at the vaccine site is regulated by modifying cancer-antigen presentation by the material and the dosages of danger signals, which significantly affected the magnitude of the protective immune response to tumors when tested in an art recognized B16-F10 tumor model.

Matrices were made to release a pulse of GM-CSF to recruit DCs, and were loaded with 0, 3000, and 7000 ng of GM-CSF, and implanted into the subcutaneous pockets of C57BL/6J mice. A GM-CSF gradient formed in the surrounding tissue, which peaked at 12 hours post-implantation as the GM-CSF concentration reached 100 μg/ml and 30 μg/ml (>30 fold difference over no incorporated GM-CSF) at distances of 1-3mm and 3-5mm, respectively, from the implant site. Elevated GM-CSF levels were maintained for extended periods (approximately 10 days) while the factor was released from the PLG to the neighboring tissue. Histological analysis at day 14 post-implantation of PLG matrices loaded with 3000 ng of GM-CSF revealed enhanced cellular infiltration over blank controls, and FACS analysis for the CD11c(+) DC population showed that GM-CSF delivery recruited significantly more DCs (~8 fold increase) than blank controls. The total number of DCs recruited and their expression of the co-stimulatory molecule CD86 increased with GM-CSF delivery in a dose dependent manner.

PLG matrices were then modified to immobilize TLR-activating, PEI-condensed CpG-ODN molecules and present them as danger signals to DC populations recruited by GM-CSF. Provision of condensed CpG-ODN signaling with GM-CSF dramatically enhanced cellular infiltration into PLG matrices, as revealed by histological analysis at Day 10 post-implantation. Importantly, CpG-ODN presentation from PLG matrices regulated the local presence of specific DC subsets and the resulting production of protective cytokines. Stimulation of the DC infiltrate recruited by GM-CSF with CpG-ODN enriched the PLG

matrix with CD11c(+)PDCA-1(+) plasmacytoid DCs (pDCs), a DC subset exhibiting enhanced type 1 IFN production that are associated with t-helper 1 (Th1) immunity.

CpG-ODN leads to preferential recruitment and expansion of pDCs to the tumor site. The dose of CpG-ODN is controlled to regulate the numbers of resident pDCs, which increased from 190,000, to 520,000, to 1,100,000 cells at doses of 0, 10 and 100 μg of CpG-ODN, respectively. GM-CSF delivery alone significantly enhanced the numbers of CD11c(+)CD11b(+) cDCs recruited to the matrices, but co-presentation of CpG-ODN had little effect on either mDC populations or Cd11c(+)CD8(+) DCs. High doses of CpG-ODN promoted the local production of IFN-α (~1010 pg/ml), IFN-γ (~600 pg/ml) and, to a lesser degree, IL-12 (150 pg/ml) at the implant site, which correlated with the increased pDC numbers at this condition. The recruitment of DCs by GM-CSF was required for CpG-ODN signaling to have a significant effect, in terms of expansion of pDC populations and production of Th1 cytokines. These results indicate that controlled GM-CSF and CpG-ODN danger signaling from synthetic extra-cellular matrices can effectively regulate resident pDC and CD11c(+)CD11b(+) cDC numbers along with the production of Th1 cytokines.

Studies were carried out to determine wheather co-presenting cancer antigens with CpG-ODNs to matrix-resident DCs would promote further DC development, activation and antigen sensitization, leading to protective tumor immunity and cytotoxic T cell responses. Antigen-presenting matrices were fabricated by encapsulating B16-F10 melanoma tumor lysates into the PLG matrices. Controlled antigen presentation in combination with GM-CSF and CpG signaling enhanced the numbers of resident pDCs at Day 10 post-implantation by 2-fold over matrices without antigen, and by 10-fold over blank controls (Fig 12A). No significant difference in pDC numbers was observed with antigen presentation in combination with GM-CSF or CpG signaling alone, indicating the benefit of both GM-CSF-mediated recruitment and CpG-ODN activation of matrix-resident DCs. The CD11c(+)CD11b(+) DC population at the vaccine site depended on GM-CSF delivery alone (Figure 12B), as antigen or CpG signaling alone or in combination had no significant effect on the recruitment and expansion of these cDCs (Figure 12B). Antigen and CpG-ODN presenting matrices led to the presence of 200,000 CD11c(+)CD8(+) cDCs, which increased to approximately 670,000 (9-fold increase over blank matrices) with GM-CSF-mediated recruitment (Figure 12C). Analysis of the endogenous production of IFNs and IL-12 revealed that antigen stimulation in combination with GM-CSF promoted endogenous IFN-α and IFN-γ production that was similar to CpG-ODN induction (Figure 12D-E). Additionally,

the *in situ* production of the T-cell growth factor, IL-12, at matrices presenting both antigen and CpG-ODN to cell populations recruited by GM-CSF was approximately 4-fold higher than blank matrices at least 2-fold higher all other matrix formulations (Fig 3F). Remarkably, a significant percentage (10.3%) of the total cells at the site of antigen presenting matrices were CD8(+) (cDC subset and cytotoxic T-cells) (Figure 12G), which was in correlation with both the number of CD11c(+)CD8(+) cDCs and the concentration of IL-12 (Figures 12C, F,G). These results indicate that immune responses sensitive to cancer antigen presentation were generated by manipulating both the number and function of specific DC subsets *in situ*, including CD8(+)DCs, which was accompanied by CD8+ T cell activity.

C57BL/6J mice were vaccinated using melanoma antigens (e.g., B16-F10 tumor lysates) presented from PLG-based vaccines that differentially regulated the generation and function of specific DC subsets *in situ* (varying GM-CSF and CPG-ODN combinations), and challenged with B16-F10 melanoma tumor cells at D14 post-vaccination. PLG vaccines presenting both B16-F10 tumor lysates and either 1, 10, 50 or100 μg doses of CpG-ODN danger signaling led to approximately 10 -30% of the vaccinated mice surviving, tumor-free (Figure 13A), after an otherwise lethal dose while 100% of unvaccinated mice were euthanized by day 23 due to tumor burden. Surprisingly, GM-CSF mediated DC recruitment combined with antigen and CpG-ODN presentation generated significant tumor protection. CpG-ODN doses of 10, 50, and 100 μg resulted in 50, 60 and 90% survival rates (Figure 13B). Survival rates correlated strongly with the number of pDCs generated at the PLG vaccine site at day 10, but did not correlate with the total CD11c(+)CD11b(+) DC numbers recruited. Additionally, high survival rates (60% and 90%) were attained with PLG systems that generated relatively high numbers of CD11c(+)CD8(+) DCs (~$2x10^5$ cells) (Figure 13E) and increased IFN-α, IFN-γ, and IL-12 production *in situ.*

The ability of vaccine systems to recruit a hetereogenous DC network also had a profound effect on vaccine efficacy, as the DC population generated by CpG and GM-CSF loaded scaffolds compared to GM-CSF loaded scaffolds resulted in a higher proportion of pDCs (~38% vs. 7%) and CD8+ cDCs (~9.4% vs. 5.5%) (Figure 13F), leading to a significant enhancement in mouse survival (90% vs. 20%), even though total DC numbers *in situ*, were statistically similar (3.05±0.55 vs. 2.67 ±0.64 million DCs). Moreover, tyrosinase-related protein (TRP)-2 is a main antigenic target of the immune response elicited by melanoma vaccines in both mice (including B16 whole cell vaccines) and humans, and staining splenocytes with MHC class I/TRP2 peptide pentamers revealed a significant

expansion of TRP2-specific CD8 T cells in mice vaccinated with GM-CSF, antigen and 100 μg of CpG-ODN (0.55% splenocytes, $1.80x10^5 \pm 0.6x10^4$ cells) in comparison to matrices presenting lower CpG doses, either 0 or 50 μg (0.2% and 0.3% splenocytes). The development and expansion of these antigen-specific T cells were induced by the promotion of pDC activation and their corresponding production of type 1 IFNs. These cytotoxic T cells were in turn involved in the killing of tumor cells, which facilitated immune protection after vaccination. These results indicate that devices (PLG matrices) described herein precisely regulate the *in situ* recruitment and expansion of specialized DC subsets. This preferential recruitment and expansion of pDCs dramatically improves immune responses to cancer antigens, reduces tumor progression, and improves survival of cancer patients compared to previous vaccine approaches.

Figures 14A-B show survival of mice vaccinated with PLG vaccines versus controls in a therapeutic model. Mice were innoculated with $5x10^5$ tumor cells and tumors were allowed to grow for 7 days in mice until palpable (1-3 mm^3). Mice were vaccinated (at Day 7) with PLG scaffolds containing 3 μg GM-CSF, tumor lysates and 100 μg CpG-ODN. Survival data was obtained using mice (n=10) with established tumors (7 days after tumor inoculation). PLG vaccines containing GM-CSF, lysates and CpG-ODN were using for the vaccination.

[02] The macroporous, synthetic ECMs described herein provided control over the presentation of inflammatory and infectious signaling agents creating microenvironments capable of generating distinct DC networks *in situ*. The total cell number and heterogeneity of these DC networks correlated with the magnitude of immune responses to cancer antigens in B16 melanoma models. GM-CSF was released quickly from PLG-based ECMs to recruit and house host DC precursors and DCs in its macroporous structure. CpG-ODNs were then immobilized within the GM-CSF-secreting matrices to direct pDC development *in situ*, and, indeed, the CpG signaling not only enhanced CD11c(+)PDCA-1(+) pDC numbers at the implant site, but also enriched the site with pDCs in a dose dependent manner. When tumor antigen was incorporated into PLG matrices, enhancement of activity and enrichment of CD11c+CD8+ cDCs at the vaccine site was observed. The provision of cancer antigens resulted in an enhancement of the total CD8+ cell population, indicating that Cd8+ DCs and Cd8+ T cells responded *in situ* to the antigen-presenting material and that the immune response had cytotoxic components. Cytokine analysis at the vaccine implant site indicated that DC subsets act in a cooperative fashion to generate an effective immune response. pDC

numbers correlated strongly with the presence of type-1 IFNs, which aided the activation of and antigen cross-presentation by CD11c(+)CD11b(+) cDCs to enhance CTL priming by these cells. Additionally, pDCs and CD8+ cDC numbers correlated with IL-12 production, which promotes antigen expression and cross-presentation by matrix resident DCs and the development and growth of CTLs.

Tumor growth and T-cell analysis indicated that as the heterogeneity of the DC network increased *in situ,* so did vaccine efficacy. Although total DC numbers remained statistically similar with GM-CSF signaling, provision of CpG-ODN danger signaling increased pDC numbers in a dose dependent manner, which strongly correlated to animal survival after a B16-F10 tumor challenge. CpG-ODN doses of 10, 50 and 100 μg (in GM-CSF secreting matrices) along with melanoma antigen presentation from PLG vaccines resulted in 45%, 60% and 90% survival in mice. Removal of GM-CSF signaling from PLG vaccines sharply reduced the total numbers of DCs generated *in situ*, which resulted in survival dropping to 10%, whereas removal of CpG-ODN signaling reduce pDC numbers *in situ*, as a majority of the DCs (87.4%) were CD11b+ CDCs. The minimum number of DCs required to induce protective immunity was determined for each DC subset, as approximately 600,000 pDCs and 200,000 CD8+ cDCs (~30% of total DCs) were required to cooperate with approximately 2,000,0000 CD11b+ cDCs to achieve greater than 50% survival after tumor challenge.

The results are clinically significant as the devices and methods demonstrated the ability to quantitatively target and employ DC subsets *in vivo* for the generation of immunity, resulting in distinct and protective immune responses.

Example 7: Presentation of TLR agonists in structural polymeric devices

Materials & Methods

Mice

C57BL/6 mice and *Batf3-/-* knockout mice (6-8-week-old female; Jackson Laboratories) were used in the studies described in Example 7.

Matrix Fabrication

A 85:15, 120 kD copolymer of D,L-lactide and glycolide (PLG) (Alkermes, Cambridge, MA) was utilized in a gas-foaming process to form porous PLG matrices (Harris et al., 1998 J. Biomed. Mater. Res., 42: 396–402). PLG microspheres encapsulating GM-CSF were first made using standard double emulsion (Cohen et al., 1991 Pharm. Res., 8: 713–720). The double emulsion process was also utilized to fabricate PLG microspheres

containing MPLA (Avanti Polar Lipids, Alabaster, AL) as an adjuvant. PLG microspheres were then mixed with 150 mg of the porogen, sucrose (sieved to a particle size between 250 μm and 425 μm), and compression molded, thereby yielding a disc device with open, interconnected pores that are generally of the size range of the porogen. The resulting disc was allowed to equilibrate within a high-pressure CO_2 environment, and a rapid reduction in pressure causes the polymer particles to expand and fuse into an interconnected structure (Harris et al., 1998 J. Biomed. Mater. Res., 42: 396–402). The sucrose was leached from the scaffolds by immersion in water yielding scaffolds that were 90% porous.

To incorporate tumor lysates into PLG scaffolds, biopsies of B16-F10 tumors that had grown subcutaneously in the backs of C57BL/6J mice (Jackson Laboratory, Bar Harbor Maine), were digested in collagenase (250 U/ml) (Worthington, Lakewood, NJ) and suspended at a concentration equivalent to 10^7 cells per ml after filtration through 40 μm cell strainers. The tumor cell suspension was subjected to 4 cycles of rapid freeze in liquid nitrogen and thaw (37°C) and then centrifuged at 400 rpm for 10 min. The supernatant (1ml) containing tumor lysates was collected, incubated with the PLG microspheres and lyophilized and the resulting mixture was used to make PLG scaffoldbased cancer vaccines.

To incorporate CpG-ODNs and P(I:C) into PLG scaffolds, CpG-ODN 1826, 5'- tcc atg acg ttc ctg acg tt-3', (SEQ ID NO: 12; Invivogen, San Diego, CA) or P(I:C) (high molecular weight; Invivogen, Sand Diego, CA) was first condensed with poly(ethylenimine) (PEI, *Mn* ~60,000, Sigma Aldrich) molecules by dropping ODN-1826 solutions into a PEI solution, while vortexing the mixture (Huang, et al., 2003 J. Biomed. Mater. Res., A 67: 1384–1392). The charge ratio between PEI and CpG-ODN (NH3+:PO4–) was kept constant at 7 during condensation. The charge ratio between PEI and P(I:C) (NH3+:PO4-) was kept constant at 3 during condensation. The condensate solutions were then vortexed with 60 μl of 50% (wt/vol) sucrose solution, lyophilized and mixed with dry sucrose to a final weight of 150 mg. The sucrose containing PEI-CpGODN condensate was then mixed with blank, GM-CSF and/or tumor lysate loaded PLG microspheres to make PLG cancer vaccines.

In situ identification of DCs and T cells

GM-CSF loaded PLG matrices and matrices containing GM-CSF in combination with either 100 μg of CpG-ODN, MPLA, or P(I:C) were implanted into subcutaneous pockets on the back of 7-9 week old male C57BL/6J mice. To analyze DC recruitment, scaffolds were excised at various time-points and the ingrown tissue was digested into single cell suspensions using a collagenase solution (Worthington, 250 U/ml) that was agitated at 37°C

for 45 minutes. The cell suspensions were then poured through a 40μm cell strainer to isolate cells from scaffold particles and the cells were pelleted and washed with cold PBS and counted using a Z2 coulter counter (Beckman Coulter). To assess, DC infiltration and activation, subsets of the total cell population isolated from PLG matrices were then stained with primary antibodies (BD Pharmingen, San Diego, CA) conjugated to fluorescent markers to allow for analysis by flow cytometry. APC-conjugated CD11c (dendritic cell marker), FITC-conjugated MHCII and PE-conjugated CD86 (B7, costimulatory molecule) stains were conducted for DC recruitment and activation analysis. To further delineate the presence of specific DC subsets, cells were also stained with APC-conjugated CD11c and PE-conjugated PDCA-1 (plasmacytoid DC marker) or APC-conjugated CD11c and PE-conjugated CD8 (CD8 DCs). To assess Tcell infiltration PE-Cy7 conjugated CD3 stains were performed in conjunction with APC-conjugated CD8a (CD8 T cells), and PE-conjugated FoxP3 (Treg) and analyzed with flow cytometry. Cells were gated according to single positive FITC, APC and PE stainings and using isotype controls. The percentage of cells staining positive for each surface antigen was recorded.

Tumor growth assays, protective cytokines and Trp2 pentamer analysis

PLG scaffolds with melanoma tumor lysates and GM-CSF in combination with CpG-ODN, MPLA, or P(I:C) were implanted subcutaneously into the lower left flank of C57BL/6J mice. For prophylactic vaccinations, animals were challenged 14 days later with a subcutaneous injection of 10^5 B16-F10 melanoma cells (ATCC, Manassas, NJ) in the back of the neck. Animals were monitored for the onset of tumor growth (approximately $1mm^3$) and sacrificed for humane reasons when tumors grew to 20 - 25 mm (longest diameter).

To assess PLG vaccine efficacy in the therapeutic setting, C57/BL6J mice were challenged with a subcutaneous injection of $5x10^5$ B16-F10 melanoma cells (ATCC, Manassas, NJ) in the back of the neck. At day 9 after tumor challenge PLG vaccines loaded with 3000ng GM-CSF in combination with 100 μg of CpG-ODN, MPLA or P(I:C), and tumor lysates were implanted subcutaneously into the lower left flank of C57BL/6J mice. A subset of mice were vaccinated again 10 days after the initial vaccination (Days 19 and 23).

To determine *in vivo* IL-12p70 concentration at the matrix implant site, adjacent tissue was excised and digested with tissue protein extraction reagent. After centrifugation, the concentrations of IL-12, in the supernatant were then analyzed with ELISA (R&D systems), according to the manufacturers instructions.

To determine the generation of TRP-2-specific cytotoxic T lymphocytes, single cell suspensions were prepared from the spleens of mice immunized with PLG vaccines [Antigen + 3000ng GM-CSF + 100μg (CpG or MPLA or P(I:C)] at various timepoints. These cells were initially stained with PE-H-2Kb/TRP2 pentamers (Sigma Aldrich), and subsequently stained with FITC-anti-CD8 and PE-CY7 CD3 mAb (mAb (BD Pharmingen, San Diego) before being analyzed using flow cytommetry.

Tumor infiltrating leukocyte (TIL) characterization

On the indicated days, B16-F10 tumors were removed from mice, and digested in 1 mg/mL collagenase II (250 U/ml) (Worthington, Lakewood, NJ) and 0.1 mg/mL DNase for 1 hour at 37°C. Dissociated cells were filtered through a 40-μm filter, and directly stained with antibodies for phenotype characterization by fluorescence-activated cell sorting (FACS) analysis. APC-anti-CD8 and PE-Cy7-anti CD3 were used to identify T cells isolated from the B16F10 tumors. These TILs were also costained with FITC-anti-IFNγ, and PE-anti-CD107a. All antibodies were obtained from eBioscience, San Diego, CA.

Statistical analysis

All values in the present study were expressed as mean ± S.D. The significant differences between the groups were analyzed by a Student's *t* test and a *P* value of less than 0.05 was considered significant.

Controlled GM-CSF and TLR agonist presentation

Macroporous, poly-lactide-co-glycolide (PLG) matrices (Figure 15F) were designed to quickly release GM-CSF (Ali et al., 2009 Nat Mater, 2: 151–8), approximately 60% of the protein was released by day 10 (Figures 15A, 15B, and 15E), to induce the recruitment of DCs or their precursors. GM-CSF loaded PLG scaffolds were also modified to present TLR-activating, CpG-ODN, MPLA and P(I:C) molecules, as danger signals. The *in vitro* release kinetics of GM-CSF were similar in all conditions (Figures 15A, 15B, and 15E). TLR agonists were more stably associated with scaffolds, as approximately 20-30% of incorporated CpG-ODN, P(I:C) and MPLA was released over the first 10 days *in vitro*, followed by slow and sustained release of danger signals over the next 14 days. Presentation of the TLR agonists was designed to provide a long-term, local signal to activate DCs. Importantly, the relatively high molecular weight and composition of the particular PLG chosen to fabricate scaffolds results in slow scaffold degradation, allowing for long-term analysis of the vaccine site and its regulation over DC activation and T cell immunity.

Controlled DC generation and activation *in vivo*

To examine the ability of PLG matrices to recruit and activate dendritic cells *in vivo*, matrices delivering GM-CSF in combination with danger signals were implanted subcutaneously into the backs of C57BL/6J mice. The magnitude of DC infiltration and activation into the matrices was determined by FACS analysis of cell populations isolated from the polymeric material after 7 days. Control matrices delivering GM-CSF alone contained $2.41 + 0.24 \times 10^5$ CD11c(+) (Figures 16E and 16F) cells, with relatively low expression levels of the activation markers, MHCII (2.57% of total CD11c(+) cells) and CD86 (4.58% of CD11c(+) cells). Inclusion of TLR-activating danger signals into PLG matrices dramatically enhanced dendritic cell generation and activation *in situ*. Presentation of CpG-ODN, MPLA and P(I:C) enhanced the total number of recruited DCs by 2.5, 1.9, and 2.2 fold, respectively (Figure 16F), as compared to GM-CSF delivery alone. Analysis of the activation state of matrix-resident DCs revealed that local TLR induction produces significant percentages of activated DCs, as CD11c(+) cells positive for MHCII(+) and CD86(+), comprised approximately 30%, 19%, and 28% of the total cells recruited to CpG, MPLA and P(I:C) loaded matrices, respectively. Matrices presenting TLR agonists mediated approximately 15 (MPLA) to 20 (P(I:C)) to 23-fold (CpG-ODN) increases in the total number of activated DCs at the implant site relative to control matrices devoid of this signaling (Figure 16F).

Stimulation of the cells which infiltrated PLG matrices with CpGODN, MPLA or P(I:C) enriched the numbers of CD11c(+)PDCA-1(+) pDCs and CD11c(+)CD8(+) cDCs (Figure 16G) relative to controls. The danger signals increased the numbers of pDCs at the implant site by approximately 4-fold relative to control matrices, with an average pDC number of 140,000 cells residing in the scaffolds presenting any of the TLR agonists (Figure 16G). CD8(+) DCs were also present at the implant site at approximately 5-fold higher levels with MPLA and P(I:C) presentation and at a 9-fold higher number when utilizing CpG-ODN as a stimulant. Strikingly, the local delivery of TLR-activating agents promoted the local production of IL-12 (200-400 ng/ml) at the implant site (Figure 16H), with CpG and P(I:C) inducing the highest levels. The IL-12 concentration correlated with the increased numbers of activated DCs and DC subsets in these conditions (Figure 16H). Additionally, the concentrations of a panel of candidate inflammatory cytokines were assayed at the vaccine site. Similar elevated levels of IFN-α (Figure 21A) resulted from CpG-ODN and P(I:C) induction while MPLA had no effect on IFN-α concentration. However, MPLA

led to 4-fold higher levels of TNF-α (Figure 21B). IL-12 concentrations at MPLA loaded matrices were 2-fold lower than CpG-ODN and P(I:C). TNF-α inhibits monocyte and DC derived IFN-γ, IL-12, and T cell priming (Hodge-Dufour et al., 1998 Proc. Natl. Acad. Sci. USA, 95: 13806–13811) and the aforementioned cytokine profiles, suggesting that MPLA loaded matrices are less efficient at stimulating anti-tumor T cell responses compared to matrices incorporating CpG-ODN and P(I:C) signaling.

Prophylactic vaccination and correlates to its efficacy

Since PLG matrices presenting TLR agonists generate distinct and activated DC populations *in situ* and potent cytokine production, the anti-tumor efficacy of these systems were tested in the poorly immunogenic, B16-F10 melanoma model. B16 tumor lysates were used to act as a source of tumor antigen in vaccine formulations. Prophylactic PLG-based vaccines presenting both B16-F10 tumor lysates and GM-CSF resulted in 10% of the vaccinated mice surviving, tumor-free (Fibure 17A), after an otherwise lethal cell challenge at day 14 post-vaccination. Importantly, antigen loaded matrices with GM-CSF in combination with TLR agonists produced significant, and long-term tumor protection. CpG-ODN, MPLA and P(I:C) presentation from PLG vaccines resulted in 90, 80 and 70% survival rates (Figure 19B). Regression analysis was subsequently performed to determine whether induction of long-term survival was related to pDC, CD8(+), and IL-12 levels at the vaccine site: previously published data using various doses of CpG-ODN were included in the analysis. Strikingly, animal survival rates were strongly correlated with the numbers of pDCs, CD8(+) DCs and with endogenous IL-12 generated by PLG vaccines (Figures 17A-C). These findings demonstrate the importance of antigen cross-presentation by CD8(+) DCs and the Th1-promoting cytokine, IL-12 to vaccine efficacy.

Therapeutic vaccination and anti-tumor T cell activity

As specific vaccine formulations containing various TLR agonists produced significant numbers of activated DCs and conferred prophylactic immunity, studies were carred out to determined whether the vaccines would lead to superior therapeutic responses and cytotoxic T-cell responses. Mice challenged with 5 x 10^5 B16-F10 melanoma cells were subsequently vaccinated at days 9 and 19, after tumors were established. All tumor-bearing mice implanted with control PLG matrices demonstrated rapid tumor growth and required euthanasia by Day 24, as expected (Figures 19A B) PLG vaccines presenting MPLA as an adjuvant decreased the rate of tumor progression (Figures 19A), and a slight increase in mean survival time (~1.5 fold increase) over controls was found (Figures 19A and B). Complete

tumor regression (Tumors < 36 mm^2) and long term survival of mice (33% survival) was achieved in the subset of mice vaccinated with PLG vaccines exploiting P(I:C) and CpG-ODN as an adjuvant.

FACs analysis was used to characterize the numbers of B16-F10 tumor-infiltrating leukocytes (TILs) induced by the various vaccines. Significantly greater numbers of CD8(+) CTLs per 1×10^6 tumor cells were present in animals treated with TLR-agonist-loaded vaccines, as compared with control animals (Figures 19C-D). CD8(+) T cell infiltrates were further characterized for IFNγ expression and expression of CD107a, a marker for cytotoxic-associated cell degranulation. These cell populations were markedly enhanced in vaccine treated animals (Figures 19C-D). Vaccines featuring CpGODN, P(I:C) and MPLA signaling resulted in approximately 6.1, 3.1 and 1.4 fold increases in IFNγ(+), CD107a(+) TILs in comparison to controls. Moreover, CpG loaded vaccines resulted in significantly higher numbers of activated TILs in comparison to their P(I:C) and MPLA counterparts (Figure 19D).

The activation of systemic CTL responses was also monitored by staining splenocytes with MHC class I/TRP2 peptide pentamers to identify CTLs with specificity to tyrosinase-related protein (TRP)-2. This is a main antigenic target of melanoma vaccines in mice and humans. A significant expansion of TRP2 specific CTLs was observed in the spleens of mice vaccinated with CpG-ODN, MPLA and P(I:C) loaded vaccines, in comparison to controls devoid of TLR agonists (Figure 19E). Taken together, these data indicate that vaccine formulations containing various TLR agonists produce significant and systemic anti-melanoma CTLs in correlation with the activation of specific DC subsets and reduce tumor burden.

Vaccine efficacy is impaired in mice lacking CD8(+) DCs

Since PLG vaccines incorporating TLR agonists were capable of generating CD8(+) DC populations *in situ*, which correlated to potent anti-tumor CTL responses and survival (Figure 17 and 19), studies were carried out to examine whether these cells were required to confer anti-tumor immunity in vivo. Batf3-/- transgenic mice were used in these experiments, as lack CD8(+) DCs, without exhibiting abnormalities in other hematopoietic cell types or tissue architecture (Hildner et al., 2008 Science, 322: 1097–1100). Wild-type and Batf3-/- mice were vaccinated with CpG-ODN loaded PLG vaccines and challenged with B16-F10 cells 14 days later. Vaccination of wildtype mice promoted complete protection against tumor growth and long-term survival (100% surivival), as expected, but vaccinated

Batf3-/- were not protected and tumor growth rates were similar to untreated, wild-type animals (Figure 20A). Moreover, vaccinated Batf3-/- failed to produce the local CTL responses observed in wild-type mice, and a 3-fold decrease in TRP2 specific cytotoxic T cells coincided with higher ratios of FoxP3(+) T regulatory (Tregs) cells at the vaccine site in this condition (Figure 20B). These results indicated that a lack of CD8(+) DCs resulted in limited cytotoxicity and allowed regulatory pathways mediated by Tregs to potentially extinguish the vaccine mediated, immune response.

Wild type mice were also able to induce the production of the T cell growth factor, IL-12, at the vaccine site at 5-fold higher levels than found in vaccinated Batf3-/- mice (Figure 20C). The partial loss of IL-12 production in CD8(+) DC knock-out mice indicates that these cells are important producers or mediators of this Th1-polarizing cytokine. The vaccine sites of CD8(+) T cell knock out mice also showed decreased levels of IL-12 and IFN-γ (Figure 21C and D). The IL-12-IFNγ pathway is a positive feedback mechanism with each cytokine augmenting production of its counterpart. The data with Batf3-/- mice and CD8(+) T cell knock-out mice indicate that the immune response resulting from vaccination in normal mice may be amplified by cytokine mediated cross talk between DCs and CTLs. Finally, the systemic production of anti-tumor CTLs was also impaired in Batf3-/-, as a 3 fold reduction in Trp2 specific CTLs was measured in the spleens of these mice in comparison to wild-type controls (Figure 20D). These results indicate that vaccine efficacy in this system is critically regulated by CD8 DCs, via their ability to cross present tumor antigens, to produce Th-1 induction factors such as IL-12, and to generate and interact with CTLs.

To address the limitations of earlier cancer vaccines, a PLG matrix was utilized that controls the the presentation of tumor lysate, GM-CSF and TLR agonists to create a vaccine node that recruits and activates multiple DC subsets in situ. The contribution of DC subsets to vaccine efficacy was analyzed and it was demonstrated that effective tumor cell killing required the participation of CD8(+) DCs, with strong correlations to pDCs and IL-12. These components were critical to the vaccine results regardless of the type or dose of stimulant incorporated within the scaffolds.

Inclusion of TLR agonists was required to activate DCs, in general, increasing their surface expression of MHCII and the costimulatory molecule, CD86 (Figure 16) indicating an enhanced capacity to present antigen and activate T cell populations. In particular, appropriate TLR signaling enhanced the generation of CD8(+) and pDC subsets at the

vaccine site and stimulated the production of IFNs and the potent T cell growth factor, IL-12. Moreover, removal of TLR agonists from the system resulted in decreased numbers of Trp2 specific, cytotoxic CD8(+) T cells locally at the vaccine site and systemically in spleens and tumors and this coincided with reduced survival in vaccine studies. PLG vaccines presenting P(I:C) or CpG-ODN induced potent tumor rejection in therapeutic models of B16-F10 melanoma, causing complete tumor regression in over a third of vaccinated animals and eradicating tumors reaching $35mm^2$ in size. Analysis of the tumor sites in vaccinated animals demonstrated intense and activated CD8(+), cytotoxic T cell infiltrates likely effecting tumor-cell killing. These systems outperformed the preclinical results of current vaccine modalities extensively studied in the clinic, including irradiated tumor cell vaccines and DC based vaccines (Gilboa E, 2007 J Clin Invest, 117: 1195-1203; Banchereau J. and Steinman R.M. 2007 Nature, 49: 419-426; Ali et al., 2009 Sci Transl Med, 1: 8–19; Rosenberg et al., 2004 Nat Med, 10: 909-915; Klebanoff et al., 2006 Immunol Rev, 211: 214–224). Vaccines presenting MPLA signaling also slowed tumor growth rates, but did not cause tumors to completely regress. This may be explained by the fact that, CpG-ODN and P(I:C) signaling outperformed MPLA in terms of promoting higher average levels of cell surface activation markers on DCs and cytokine profiles that promote Th-1 polarization and CTL responses. Additionally, MPLA was a strong inducer of TNF-α, in comparison to CPG-ODN and P(I:C), which can inhibit IL-12, and IFN pathways priming CTL responses (Hodge-Dufour et al., 1998 Proc. Natl. Acad. Sci. USA, 95: 13806–13811). Thus, the differential effects of TLR agonists on survival rates are consistent with the numbers and subsets of activated DCs produced at the vaccine site and cytotoxic T-cell activity. Combinations of TLR agonists, e.g., poly (I:C) and CpG or poly (I:C) and MPLA, lead to a synergistic anti-tumor effect.

All vaccinated mice without the CD8(+) DC compartment, Batf3-/- mice, generated tumors in prophylactic models that produced 90% tumor-free survival rates in wild-type mice. Cytokine analysis of the vaccine site of these animals revealed that local IL-12 levels, and CTL responses were markedly reduced indicating that CD8(+) DCs are an important source of IL-12, and Th-1 polarization. Without CD8(+) DC participation, vaccination not only resulted in reduced cytotoxic, CD8(+) T cell activity (at tumor site and spleen) it also allowed the progression of Treg activity. High FoxP3(+) Treg to CD8(+) Tcell ratios indicates unbalanced immunosuppression that extinguishes vaccine efficacy and promotes tumor growth (Quezada et al., 2006 J. Clin. Invest., 116: 1935–1945; Hodi et al., 2008 Proc. Natl. Acad. Sci. U.S.A., 105: 3005–3010). CD8(+) DCs and IL-12 can cause Tregs inhibition

or their conversion to IFNγ-producing, effector T cells (Wei et al., 2009 Immunity, 30: 155–167; Zhou et al., 2009 Nat Immunol., 10: 1000–1007; Oldenhove et al., 2009 Immunity, 31: 772–786), and these mechanisms are potentially critical to the efficacy of material-based cancer vaccines.

An interesting aspect of these systems is CTL homing to the vaccine site due to long term antigen presentation, and knocking out CD8(+) T cells resulted in a significant reduction of local levels of IFNγ and IL-12 (S3 &S4). T cell derived IFNγ enhances DC expression of IL-12 and costimulatory molecules creating a feedback loop that amplifies CTL-mediated responses to infection. In this setting, after vaccine priming, T cells that home back to the antigen-presenting vaccine site may be important vaccine components themselves as they may sustain and amplify CTL responses via IFNγ-mediated DC activation and IL-12 production. These findings provide evidence that CD8(+) DCs, pDCs and IL-12, or their equivalent functionally (i.e., appropriate antigen presentation, and Th1 polarization) lead to improved material-based cancer vaccines. The methods and devices described herein are also useful for other clinical indications, such as infectious and autoimmune disease.

As described above, three different types of pathogen associated molecular patterns (PAMPs) were incorporated into or onto structural polymeric devices such as PLG disc structures/scaffolds to act as adjuvants in vaccines (3 types; a short oligonucleotide (CpG-ODN); a synthetic RNA - (Poly(I:C); P(I:C)), a synthetic lipid (monophosphoryl lipid A; MPLA) (Figures 15A-D). Such vaccine formulations recruit and activate dendritic cells in situ, which was quantitatively assessed (Figures 16A-D).

Vaccine-dependent survival in an aggressive melanoma cancer model correlates strongly with the ability of the vaccine to specifically activate 2 subsets of dendritic cells – CD8(+) DCs and plasmacytoid DCs – regardless of the adjuvant utilized in the vaccine system (Figures 17A-C). This correlation has been confirmed utilizing 4 different vaccine adjuvants in the PLG vaccine. These vaccines induce potent tumor rejection in a therapeutic model of melanoma, by activating specific T cell responses that have been detected at the vaccine site and at tumors (Figures 18A-D and 19A-D). These findings demonstrate the PLG vaccine system's versatility in incorporating different types of agonists that stimulate different pathways in innate and adaptive immune responses (Figures 15A-D).

DC subsets that are critical for anti-tumor immune responses were identified. Subsets of DCs include myeloid dendritic cell (mDC), plasmacytoid DCs, and CD8+ DCs. mDCs ar most similar to monocytes. mDC are made up of at least two subsets: (1) the more common

mDC-1, which is a major stimulator of T cells; and (2) the extremely rare mDC-2, which may have a function in fighting wound infection. mDCs secrete IL-12 and are characterized by TLR 2 and TLR4. Plasmacytoid DCs look like plasma cells, but have certain characteristics similar to myeloid dendritic cells, can produce high amounts of interferon-alpha, and are characterized by TLR7 and TLR9. The TLR agonist, CpG, binds to TLR9. CD8+ DCs in mice are equivalent to CD141+ dendritic cells.

CD141+ DCs are found in human lymph nodes, bone marrow, tonsil, and blood. They are characterized by high expression of toll-like receptor 3 (TLR3), production of IL-12p70 and IFN-β, and superior capacity to induce T helper 1 cell responses, when compared with the more commonly studied CD1c+ DC subset. Polyinosine-polycytidylic acid (poly I:C)–activated CD141+ DCs have a superior capacity to cross-present antigens to CD8+ cytotoxic T lymphocytes than poly I:C–activated CD1c+ DCs. Thus CD141+ DC subset represents an important functionally distinct human DC subtype with characteristics similar to those of the mouse CD8α+ DC subset. CD141+ DCs play a role in the induction of cytotoxic T lymphocyte responses and their activation is important for vaccination against cancers, viruses, and other pathogens.

CD141+ DCs and plasmacytoid DCs are critical for successful cancer vaccination (prophylactic and therapeutic). The results described herein indicate that p(I:C) in vaccine device stimulates CD141+ DCs in humans (CD8+ DCs in mice) and CpG stimulates plasmacytoid DCs. Devices with one or both of these TLR agonists lead to potent DC activation and the generation of significant prophylactic and therapeutic anti-tumor immune responses. A combination of different TLR agonists, e.g., a combination of p(I:C) and CpG, in a device leads to a synergistic effect in the activation of a DC immune response against tumors. CD141+ DCs and plasmacytoid DCs have not been specifically utilized or targeted in current clinical trials. The data obtained from these experiments was used to design cancer vaccine systems and provide a more informed translation of immune response data from mouse to humans.

Synergistic effect of P(I:C) + CpG ODN on tumor inhibition

Figure 22 shows the results of a vaccine experiment where P(I:C) and CpG-ODN in combination were examined versus the CpG-ODN and P(I:C) alone. As shown in Figure 22, the combination of the TLR agonists P(I:C) and CpG-ODN outperformed the vaccines incorporating CpG-ODN or P(I:C) alone. Specifically, PLG vaccines incorporating CpG-ODN and P(I:C) act synergistically to generate significant tumor inhibition, reduced tumor

burden, and to generate improved anti-tumor immune responses.

Figure 22 shows the overall survival of mice bearing melanoma tumors, and treated with either blank matrices [Blank] or matrices loaded with CpG-ODN or P(I:C) alone or in combination [CpG-ODN + P(I:C)] (n=8). Mice were challenged with $5x10^5$ B16-F10 cells and vaccinated 3 days later with PLG vaccines. Total dose of TLR agonist was approximately 100 μg in all vaccines.

Example 8: Inflammatory cytokines presented from polymer matrices differentially generate and activate DCs in situ

During infection, inflammatory cytokines mobilize and activate dendritic cells (DCs), which are essential for efficacious T cell priming and immune responses that clear the infection. Described herin is the design of macroporous poly(lactide-co-glycolide) (PLG) matrices that release the inflammatory cytokines GM-CSF, Flt3L and CCL20, in order to mimic infection-induced DC recruitment. The ability of these infection mimics to function as cancer vaccines was examined via induction of specific, anti-tumor T cell responses. As described in detail below, all vaccine systems tested were able to confer specific anti-tumor T cell responses and long-term survival in a therapeutic, B16-F10 melanoma model. However, GM-CSF and Flt3L vaccines resulted in similar survival rates, and outperformed CCL20 loaded scaffolds, even though they had differential effects on DC recruitment and generation. GM-CSF signaling was identified as the most potent chemotactic factor for conventional DCs and significantly enhanced surface expression of MHC(II) and CD86(+), which are utilized for priming T cell immunity. In contrast, Flt3L vaccines led to greater numbers of plasmacytoid DCs (pDCs), correlating with increased levels of T cell priming cytokines that amplify T cell responses. These results demonstrate that 3D polymer matrices modified to present inflammatory cytokines are utilized to effectively mobilize and activate different DC subsets in vivo for immunotherapy.

An exemplary amino acid sequence of human Flt3 is provided below (GenBank Accession No.: P49771.1 (GI:1706818), incorporated herein by reference; SEQ ID NO: 13):

```
  1 mtvlapawsp ttyllllll ssglsgtqdc sfqhspissd favkirelsd yllqdypvtv
 61 asnlqdeelc gglwrlvlaq rwmerlktva gskmqgller vnteihfvtk cafqpppscl
121 rfvqtnisrl lqetseqlva lkpwitrqnf srclelqcqp dsstlpppws prpleatapt
181 apqpplllll llpvgllila aawclhwqrt rrrtprpgeq vppvpspqdl llveh
```

An exemplary amino acid sequence of human CCL20 is provided below (GenBank Accession No.: AAH20698.1 (GI:18088857), incorporated herein by reference; SEQ ID NO: 14):

```
 1 mcctksllla almsvlllhl cgeseasnfd cclgytdril hpkfivgftr qlanegcdin
61 aiifhtkkkl svcanpkqtw vkyivrllsk kvknm
```

Materials & Methods

Mice

C57BL/6 mice (6-8-week-old female; Jackson Laboratories) were used in the experiments described in Example 8.

Primary cells (DCs) isolation and culture

Primary bone-marrow-derived dendritic cells (BMDCs) were flushed from the femurs of C57BL/6 mice and cultured in 100-mm bacteriological petri dishes (Falcon number 1029/Becton Dickinson). Cell culture medium RPMI-1640 (R10) (Sigma) was supplemented with 1% Penicillin-Streptomycin (Invitrogen), 2 mM l-Glutamine (Invitrogen), 50 μM 2-mercaptoethanol (Sigma) and 10% heat-inactivated fetal bovine serum (FBS, Invitrogen). At day 0, bone marrow leukocytes were seeded at 2×10^6 cells per 100-mm dish in 10 ml R10 medium containing 20 ng/ml granulocyte-macrophage colony-stimulating factor (GM-CSF) (Peprotech). At day 3, another 10 ml R10 medium containing 20 ng/mL GM-CSF was added to the plates. At days 6 and 8, half of the culture supernatant was collected and centrifuged, the cell pellet was resuspended in 10 ml fresh R10 containing 20 ng/mL GM-CSF, and placed back into the original plate. The non-adherent cell population in the culture supernatant was used between days 8 and 12 for all the experiments.

Transwell migration studies for chemotaxis and chemokinesis

Transwell migration studies were performed by plating bone marrow derived dendritic cells in the top well of 6.5 mm transwell dishes (Costar, Cambridge, MA) with a pore size of 5 μm. The chemotactic effects of GM-CSF, FL (Flt3), and CCL20 on the migration of BMDCs was assessed by placing 500 ng/ml of recombinant murine GM-CSF, FL or CCL20 (Peprotech, Rocky Hill, NJ) in the bottom wells and $3x10^5$ DCs in the top wells. For chemokinesis studies, the concentration of cytokine in each compartment was equal at 500 ng/ml and $3x10^5$ DCs were added to the top wells. The number of cells that migrated from the top well to the bottom well through the porous membrane was counted at the end of 12 h to quantify migration. Cells that had migrated to the bottom well were collected by treatment with 0.25% trypsin-0.03% ethylenediaminetetraacetic acid (EDTA, Invitrogen) and counted with a Z2 coulter counter (Beckman Coulter, Inc).

Matrix Fabrication

A 85:15, 120 kD copolymer of D,L-lactide and glycolide (PLG) (Alkermes,

Cambridge, MA) was utilized in a gas-foaming process to form porous PLG matrices. PLG microspheres encapsulating GM-CSF, FLt3L, or CCL20 were first made using standard double emulsion, incorporating approximately 170 ng/mg of protein PLG microspheres. PLG microspheres were then mixed with 150 mg of the porogen, sucrose (sieved to a particle size between 250 μm and 425 μm), and compression molded. The resulting disc was allowed to equilibrate within a high-pressure CO_2 environment, and a rapid reduction in pressure causes the polymer particles to expand and fuse into an interconnected structure. The sucrose was leached from the scaffolds by immersion in water yielding scaffolds that were 90% porous.

To incorporate tumor lysates into PLG scaffolds, biopsies of B16-F10 tumors that had grown subcutaneously in the backs of C57BL/6J mice (Jackson Laboratory, Bar Harbor Maine), were digested in collagenase (250 U/ml) (Worthington, Lakewood, NJ) and suspended at a concentration equivalent to 10^7 cells per ml after filtration through 40 μm cell strainers. The tumor cell suspension was subjected to 4 cycles of rapid freeze in liquid nitrogen and thaw (37°C) and then centrifuged at 400 rpm for 10 min. The supernatant (1ml) containing tumor lysates was collected, incubated with the PLG microspheres and lyophilized and the resulting mixture was used to make PLG scaffold-based cancer vaccines.

To incorporate CpG-ODNs into PLG scaffolds, CpG-ODN 1826, 5'-tcc atg acg ttc ctg acg tt-3', (Invivogen, San Diego, CA; SEQ ID NO: 12) was first condensed with poly(ethylenimine) (PEI, *Mn* ~60,000, Sigma Aldrich) molecules by dropping ODN-1826 solutions into PEI solution, while vortexing the mixture. The charge ratio between PEI and CpG-ODN (NH3+:PO4–) was kept constant at 7 during condensation. The condensate solutions were then vortexed with 60 μl of 50% (wt/vol) sucrose solution, lyophilized and mixed with dry sucrose to a final weight of 150 mg. The sucrose containing PEI-CpG-ODN condensate was then mixed with blank, GM-CSF and/or tumor lysate loaded PLG microspheres to make PLG cancer vaccines.

<u>In situ identification of DCs and T cells</u>

GM-CSF loaded PLG matrices containing approximately 3 μg of GM-CSF, Flt3L, or CCL20 in combination with 100 μg of CpG-ODN were implanted into subcutaneous pockets on the back of 7-9 week old male C57BL/6J mice. To analyze DC recruitment by FACS analysis, scaffolds were excised and the ingrown tissue was digested into single cell suspensions using a collagenase solution (Worthingtion, 250 U/ml) that was agitated at 37°C for 45 minutes. The cell suspensions were then poured through a 40μm cell strainer to isolate

cells from scaffold particles and the cells were pelleted and washed with cold PBS and counted using a Z2 coulter counter (Beckman Coulter). To assess, DC infiltration and activation, subsets of the total cell population isolated from PLG matrices were then stained with primary antibodies (BD Pharmingen, San Diego, CA) conjugated to fluorescent markers to allow for analysis by flow cytometry. APC-conjugated CD11c (dendritic cell marker), FITC-conjugated MHCII and PE-conjugated CD86 (B7, costimulatory molecule) stains were conducted for DC recruitment and activation analysis. To delineate the presence of the plasmacytoid DC subset, cells were also stained with APC-conjugated CD11c and PE-conjugated PDCA-1 (plasmacytoid DC marker). Cells were gated according to single positive FITC, APC and PE stainings using isotype controls. The percentage of cells staining positive for each surface antigen was recorded.

For the immunostaining of DC infiltrates in paraffin sections of scaffolds, samples were prepared and re-hydrated according to standard procedures. Antigen retrieval was performed with citrate buffer in a pressurized cooker (10mM Sodium Citrate, 0.05% Tween 20, pH 6.0, for 5 min in 950C). After brief washes with PBST buffer (0.01% Tween-20), samples were blocked with 5% goat serum in staining buffer (5%BSA, 2% Fetal Bovine Serum in PBST, pH 7.4) for 1 hour in ambient temperature. Anti-CD11c Armenian Hamster IgG (20 mg/ml, Abcam, Cambridge, MA) was diluted in staining buffer and allowed to bind overnight at 40C in a humidified chamber. After washing 3 times with PBST, Alexa®594 Goat anti-Hamster (5 mg/ml, Life Technologies, Grand Island, NY) secondary IgG was diluted in staining buffer and applied for 1h at RT. After three washes with PBS, samples were air-dried and mounted with ProLong Gold Antifade reagent with DAPI for nuclear staining (Life Technologies, Grand Island, NY). Confocal tile scans were obtained and processed with Zeiss LSM 710 laser-scanning microscope and bundled software (Zeiss, Thornwood, NY).

Tumor growth assays, protective cytokines and Trp2 pentamer analysis

PLG scaffolds containing B16-F10 melanoma tumor lysates, 100 μg CpG-ODN in combination with 3μg GM-CSF, Flt3L or CCL20 were implanted subcutaneously into the lower left flank of C57BL/6J mice to act as cancer vaccines. To assess PLG vaccine efficacy in the therapeutic setting, C57/BL6J mice were challenged with a subcutaneous injection of $5x10^5$ B16-F10 melanoma cells (ATCC, Manassas, NJ) in the back of the neck, and 3 days after tumor challenge PLG vaccines were implanted subcutaneously into the lower left flank. Animals were monitored for the onset of tumor growth (approximately $1mm^3$) and sacrificed

for humane reasons when tumors grew to 20 - 25 mm (longest diameter).

To determine the *in vivo* IL-12p70 and IFN-γ concentration at the matrix implant site, adjacent tissue was excised and digested with tissue protein extraction reagent at Day 10 after implantation (Pierce). After centrifugation, the concentrations of IL-12 and IFN-γ, in the supernatant were then analyzed with ELISA (R&D systems), according to the manufacturers instructions. To determine the generation of TRP-2-specific cytotoxic T lymphocytes, single cell suspensions were prepared at Day 10 from the spleens of mice immunized with PLG vaccines. These cells were initially stained with PE-H-2Kb/TRP2 pentamers (Sigma Aldrich), and subsequently stained with FITC-anti-CD8 and PE-CY7 CD3 mAb (mAb (BD Pharmingen, San Diego) before being analyzed using flow cytometry.

The role of dendritic cells in the immune response

Dendritic cells (DCs) orchestrate immune responses to infection and tumors by priming and propagating specific, cytotoxic T lymphocyte (CTL) responses. Immature DCs residing in peripheral tissue detect foreign substances (i.e. antigens) unique to invading pathogens, and are activated by stimuli, such as pathogen associated molecular patterns (PAMPs) or products of dying cells (i.e. "danger signals"), originating during pathogen induced inflammatory responses. Maturing DCs mature both process and present antigens on major histocompatibility complexes (MHC) receptors, and express the costimulatory molecules CD80 and CD86, both of which are required for effector T-cell stimulation. Another important result of DC maturation by 'danger signaling', is that DCs acquire the ability to home to the lymph nodes to engage and activate naive T-cells, enabling the T cells to recognize the antigens DCs are presenting.

The ability of particular DCs to initiate and control immune responses is a consequence of both their localization within tissues and their specialized capacity for mobilization. DCs originate from pluripotent stem cells in the bone marrow, enter the blood stream and localize into almost all organs. Based on the relative expression of a series of surface markers, different subsets of DCs or DC precursors can be identified in peripheral blood, including plasmacytoid DCs (pDCs) and conventional DCs (cDCs)2. pDCs are major type I interferon (IFN) producers, and specialize in activating adaptive immune responses to virus challenge via cytokine signaling. CD11c(+) cDCs, such as epidermal DCs, are especially adept at antigen presentation and co-stimulation of T cells.

Upon microbial invasion and inflammation, DCs rapidly migrate into the draining lymph nodes and primary sites of infection at rates that vastly outnumber other APCs, such as

macrophages. The production of most DC subsets, including (pDCs) is controlled in the steady state by the cytokine Fms-related tyrosine kinase 3 ligand ligand (FL). Other cytokines, such as GM-CSF and CCL20, released by damaged or infected cells, actively recruit and localize cDCs to the sites of inflammation. In inflammatory models, both in vivo and in vitro, these inflammatory cytokines have been shown to also enhance DC migration and proliferation and may regulate DC activation state. The quantity of DCs activated during infection or within tumors is correlated with the strength of the subsequent immune response and disease prognosis.

To generate sufficient numbers of dendritic cells (DCs) for immunotherapy, laboratory-based culture of DC precursors with inflammatory cytokines, such as granulocyte macrophage-colony stimulating factor (GM-CSF) and FL (Flt3) has often been used. DCs modified *in vitro* to present tumor antigens are capable of eliciting antitumor effects in murine models upon transplantation. Initial clinical testing of *ex vivo* DC-based vaccines has revealed the induction of tumor regression in a subset of cancer patients, but little survival benefit. Protocols involving the *ex vivo* manipulation of DCs are limited by the quantities and types of DCs that can be produced, poor engraftment efficiency and LN homing, and loss of DC activation upon injection in the *in vivo* environment.

To address these limitations, infection-mimicking materials were developed to present inflammatory cytokines in combination with a danger signal to recruit and activate DCs in vivo. As described below, the abilities of multiple inflammatory cytokines, GM-CSF, FL (Flt3), and CCL20 to recruit and activate DCs when delivered from macroporous, implantable polymer scaffolds was examined. Also, nanoparticles containing cytosine-guanosine (CpG) rich oligonucleotide (CpG-ODN) sequences were immobilized onto scaffolds, as CpG-ODN are expressed in bacterial DNA, and are potent danger signals that can stimulate activation of matrix resident DCs. Finally, the ability of these systems to prime anti-tumor T cell responses and confer tumor protection via presentation of cancer antigens was examined.

In vitro chemotaxis and chemokinesis of cytokines

In vitro transwell studies were conducted to investigate the chemotaxis and chemokinesis effects of bone-marrow derived DCs in response to GM-CSF, FL and CCL20. GM-CSF gradients promoted significant DC chemotaxis, as DC migration in this condition was approximately 50% higher than the control condition (Figure 23A). Similar effects on chemokinesis were observed, as GMCSF exposure promoted a similar 50% increase in the

number of migrated cells in response to homogenous levels of the cytokine (Figure 23B). In contrast, FL and CCL20 had no effect on the chemotaxis or chemokineses of DCs in these assays (Figure 23). These results indicate that GM-CSF has a superior effect on DC mobilization and recruitment in comparison to FL and CCL20.

Controlled release of cytokines and in vivo DC recruitment

Macroporous, poly-lactide-co-glycolide (PLG) matrices were designed to provide long-term and sustained release of GM-CSF, FL, and CCL20 (Figure 23A) and to house DCs for activation. These PLG scaffolds were 80-90% porous with an average pore size between 125-200 um to facilitate dendritic cell infiltration. The *in vitro* release kinetics for the three cytokines were similar, as the matrices quickly released protein with a burst over the first 5 days followed by sustained release over the next several weeks (Figure 24A). The scaffolds released approximately 43, 36, and 26% of the incorporated GMCSF, FL and CCL20, respectively, by day 4 followed by approximately 0.9% daily release of protein over the next 23 days (Figure 24A).

To examine the ability of PLG matrices loaded with inflammatory cytokines to recruit and activate dendritic cells *in vivo*, PLG matrices delivering GM-CSF, FL and CCL20 were implanted subcutaneously into the backs of C57BL/6J mice and removed at day 7 after implantation. Immunohistochemical analysis revealed intense CD11c(+) DC infiltrates penetrating the porous network of all the scaffolds releasing cytokines, and GM-CSF mediated the most dense DC clustering (Figure 24B). The magnitude of DC infiltration and activation into the matrices was quantified by FACS analysis of cell populations isolated from the polymeric material. Blank PLG matrices recruited approximately 190,000 CD11c(+) DCs, whereas scaffolds delivering GM-CSF recruited approximately 960,000 DCs, equating to over a 5-fold difference in cell recruitment (Figure 24C). Scaffolds presenting FL and CCL20 recruited 2.5 fold more DCs than control conditions, but significantly less than GM-CSF presenting scaffolds (Figure 24C). These results are consistent with the *in vitro* results that identified GM-CSF as the most potent mobilizing and chemotactic factor for DCs, in comparison to FL and CCL20.

In Vivo DC Activation

PLG scaffolds were modified to present nanoparticles containing TLR-activating, CpG-ODN, as an infection-mimicking danger signal in concert with delivery with inflammatory cytokines. This dramatically enhanced DC activation *in situ* over control conditions lacking cytokine signaling (Figure 25A). Analysis of the activation state of

matrix-resident DCs revealed that GM-CSF induced recruitment in combination with CpG-ODN produced significant percentages of activated DCs, as MHCII(+) and CD86(+) DCs comprised approximately 54-66% of the total DCs recruited to scaffolds. Approximately 8-fold, 4-fold, and 4-fold increases in the total number of activated DCs were found with GM-CSF, at the implant site relative to control matrices devoid of cytokines (Figure 25B).

FL presentation in combination with CpG-ODN enriched the PLG matrix with the highest average number of CD11c(+)PDCA-1(+) pDCs (Fig 1C), generating over 160,000 resident pDCs. Strikingly, approximately 22% of the total cells resident in these scaffolds consisted of this DC subset (Figure 25A). This indicates that FL is a strong mobilizing agent for pDCs. Scaffolds presenting GM-CSF and CCL20 also significantly enhanced pDC generation, leading to approximately 110,000 resident pDCs. The pDC subset has been associated with the induction of t-helper 1 (Th1) immunity via its capacity to induce IL-12 and type-1 interferons (IFNs), which are critical to propagating CTL responses to infections and tumors. These data indicate that while the three cytokines tested all enhanced DC recruitment and activation, GM-CSF signaling in combination with CpG-ODN produced the highest numbers of activated cDCs, while FL led to the greatest number of resident pDCs.

Induction of T cell immunity and Therapeutic Vaccination

B16-F10 tumor lysates were incorporated into PLG matrices as tumor antigens. IL-12 and IFN-γ secretion by activated DCs can prime CTL-mediated immune responses and tumor cell death. Thus, the presence of these Th-1 inducers at the scaffold implant site was quantified. PLG vaccines presenting FL in combination with CpG-ODN enhanced the local concentration of IL-12 and IFN-γ by 8 and 13-fold, respectively, over control scaffolds (Figure 26A and 26B). GM-CSF release resulted in approximately 3 and 6-fold increases in the local concentration of IL-12 and IFN-γ (Figure 26A and 26B). CCL20 release from PLG vaccines led to a 2-fold increase in IL-12 concentration, and no effect on IFN-γ levels at the vaccine site (Figure 26A and 26B).

The activation of systemic CTL responses was monitored by staining isolated splenocytes with MHC class I/TRP2 peptide pentamers. This allows one to identify CTLs with specificity to tyrosinase-related protein (TRP)-2, which is a main antigenic target of melanoma vaccines in mice and humans. A significant expansion of TRP2 specific CTLs was observed in the spleens of mice vaccinated with scaffolds incorporating all three cytokines (Figure 26C). Vaccines incorporating FL and GMCSF led to approximately 5 and 4-fold higher numbers of Trp2 specific CTLs than control vaccines, which was a significantly

greater effect than found with CCL20 vaccines (Figure 26C). Taken together, these data indicate that vaccine formulations containing various inflammatory agents are capable of producing significant and systemic anti-melanoma CTLs and the local production of Th1 cytokines.

The anti-tumor efficacy of these vaccines were then tested in the poorly immunogenic, B16-F10 melanoma, model. C57BL/6J mice were challenged with 10^5 tumor cells, and then vaccinated with PLG vaccines three days later. Animals treated with control scaffolds required euthanization after 30 days due to progressive disease. PLG vaccines loaded with cytokines induced long-term tumor protection in a significant subset of animals (Figure 26D). GMCSF, FL and CCL20 presentation from PLG vaccines resulted in 88, 75 and 62% long-term survival rates (Figure 26D).

Controlled mobilization and activation of DCs and DC precursors is of particular interest in the development of *ex vivo* DC based vaccines, and more generally the design of material systems that activate the immune system *in vivo*. As described herein, polymers which mimic key aspects of microbial infection effectively recruit DCs for cancer vaccination. PLG scaffolds engineered to release GM-CSF, FL, and CCL20 led to significant numbers of resident DCs, and the co-presentation of danger signals led to DC maturation. Even though all vaccine formulations were capable of inducing tumor protection in a therapeutic model of B16-F10 melanoma, GM-CSF and FL vaccines produced more antigen specific CTLs, higher levels of Th1 priming cytokines, and greater survival rates when compared to CCL20 (Figure 26D).

While GM and FL releasing PLG vaccines resulted in statistically similar T cell and anti-tumor responses, they had differential effects on DC recruitment and activation. *In vitro* tests indicated that GM-CSF was the most potent chemotactic factor for cDCs (Figure 23). This finding was consistent with the ability of GM-CSF releasing matrices to recruit significantly more total DCs (~10^6, on par with ex vivo DC based protocols) and activated DCs, in comparison to FL scaffolds (Figures 24-25). In contrast, and in agreement with other reports, FL vaccines led to more matrix-resident pDCs when combined with CpG-ODN danger signaling. pDCs are an important source of Th1 priming cytokines that amplify CTL responses, and increased pDCs numbers likely contributed to the enhanced local production of IL-12 and IFNγ at the vaccine site. As described herein, GM and FL are combined in material systems to exploit GMCSF mediated activation of cDCs and FL mediated generation of pDCs. This creates a superior DC network that is employed for cancer vaccination and

immunotherapy.

The results presented herein indicate that pDCs, and their cDC counterparts are targeted to exploit their specialized abilities to mediate anti-tumor T cell responses. In contrast to nanoparticle targeting systems, the polymer systems described herein not only serve as a antigen delivery devices to recruit and activate DCs, but also serve as a physical structure where DCs temporarily reside while they are activated.

The systems described herein demonstrated significant anti-tumor activity. In addition to the polymers, e.g., PLG, described herein, matrices are optionally fabricated from other more inflammatory polymers to boost immune responses and DC mobilization. Another important aspect of subsequent T cell priming by these cells is LN homing. The exit or dispersement of DCs after antigen exposure is optimized by incorporating different adjuvants into the material to activate migratory function. Alternatively, other matrix properties, including degradation kinetics and porosity are altered to promote further control over DC trafficking.

Altogether, these findings provide evidence that FL, CCL20 and GM-CSF are utilized in biomaterial systems to mimic infection-induced recruitment of DCs *in situ*. As described herein, infection-mimicking porous devices are effective as therapeutic cancer vaccines.

OTHER EMBODIMENTS

While the invention has been described in conjunction with the detailed description thereof, the foregoing description is intended to illustrate and not limit the scope of the invention, which is defined by the scope of the appended claims. Other aspects, advantages, and modifications are within the scope of the following claims.

The patent and scientific literature referred to herein establishes the knowledge that is available to those with skill in the art. All United States patents and published or unpublished United States patent applications cited herein are incorporated by reference. All published foreign patents and patent applications cited herein are hereby incorporated by reference. Genbank and NCBI submissions indicated by accession number cited herein are hereby incorporated by reference. All other published references, documents, manuscripts and scientific literature cited herein are hereby incorporated by reference.

While this invention has been particularly shown and described with references to preferred embodiments thereof, it will be understood by those skilled in the art that various changes in form and details may be made therein without departing from the scope of the invention encompassed by the appended claims.

What is claimed is:

CLAIMS

1. A device comprising a porous polymeric structure composition, a disease-associated antigen, and a toll-like receptor (TLR) agonist, wherein said TLR agonist preferentially binds to TLR3.

2. The device of claim 1, wherein said disease-associated antigen comprises a tumor antigen.

3. The device of claim 1, wherein said polymeric structure composition comprises poly-lactide-co-glycolide (PLG).

4. The device of claim 1, wherein said TLR agonist comprises a TLR3 agonist.

5. The device of claim 1, wherein said TLR3 agonist comprises polyinosine-polycytidylic acid (poly I:C) or PEI- poly (I:C).

6. The device of claim 1, wherein said TLR agonist further comprises pathogen associated molecular patterns (PAMPs).

7. The device of claim 1, wherein said TLR agonist comprises a nucleic acid.

8. The device of claim 1, wherein said TLR agonist further comprises a TLR9 agonist.

9. The device of claim 8, wherein said TLR9 agonist comprises a cytosine-guanosine oligonucleotide (CpG-ODN) or a PEI-CpG-ODN.

10. The device of claim 1, wherein said device further comprises a recruitment composition.

11. The device of claim 11, wherein said recruitment composition comprises granulocyte macrophage colony stimulating factor (GM-CSF), Flt3L, or CCL20.

12. The device of claim 10, wherein said recruitment composition comprises encapsulated GM-CSF.

13. The device of claim 2, wherein said tumor antigen comprises a tumor lysate, purified protein tumor antigen, or synthesized tumor antigen.

14. The device of claim 6, wherein said PAMPs comprises a monophosphoryl lipid A (MPLA).

15. The device of claim 1, wherein said device comprises a combination of TLR agonists, said combination comprising a TLR3 agonist and a TLR9 agonist.

16. The device of claim 15, wherein said TLR3 agonist comprises poly (I:C) and said TLR9 agonist comprises CpG-ODN.

17. The device of claim 1, wherein said device comprises a combination of TLR agonists, said combination comprising a TLR3 agonist and a TLR4 agonist.

18. The device of claim 17, wherein said TLR3 agonist comprises poly (I:C) and said TLR4 agonist comprises MPLA.

19. The device of claim 1, wherein said TLR3 agonist is present in an amount to preferentially stimulate CD8+ dendritic cells or CD141+ dendritic cells.

20. A device comprising a polymeric structure composition, a tumor antigen, and a combination of TLR agonists, wherein said TLR agonist is selected from the group consisting of TLR1, TLR2, TLR3, TLR4, TLR5, TLR6, TLR7, TLR8, TLR9, TLR10, TLR11, TLR12, and TLR13.

21. A method for eliciting an anti-tumor immune response, comprising contacting or implanting into a subject device comprising a polymeric structure composition, a tumor antigen, and a TLR agonist, wherein said TLR agonist preferentially binds to TLR3.

22. The method of claim 21, wherein said TLR agonist comprises a TLR3 agonist.

23. The method of claim 21, wherein said TLR agonist comprises a TLR3 agonist and a TLR9 agonist.

24. The method of claim 21, wherein said anti-tumor immune response comprises activation of a CD8+ dendritic cell or a CD141+ dendritic cell.

25. The method of claim 23, wherein said anti-tumor immune response comprises activation of a plasmacytoid dendritic cell or a CD141+ dendritic cell.

26. The method of claim 23, wherein said anti-tumor immune response comprises a reduction in tumor burden.

27. The method of claim 21, wherein said TLR agonist is present at a concentration effective to induce production of interleukin-12 (IL-12) by dendritic cells.

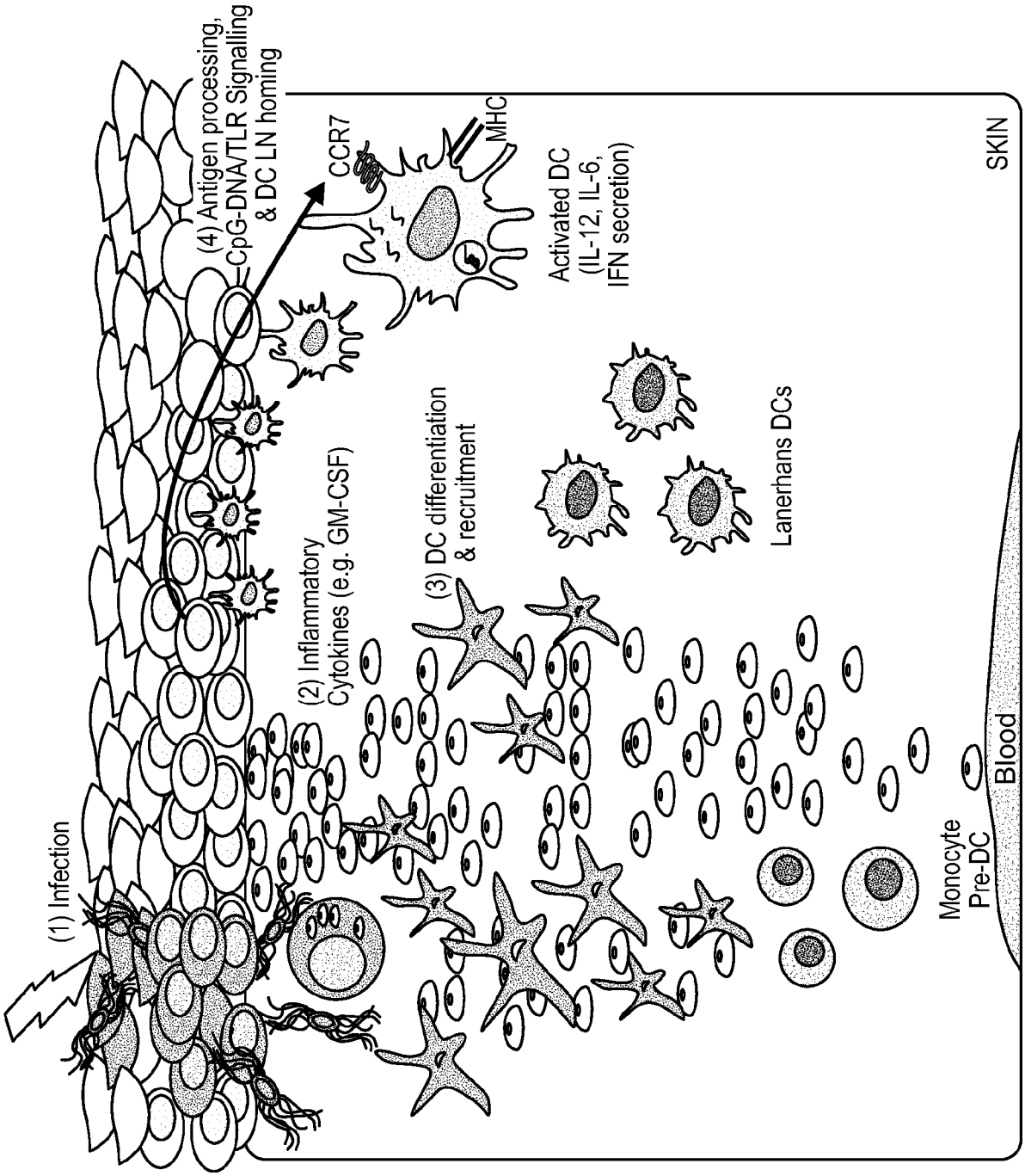
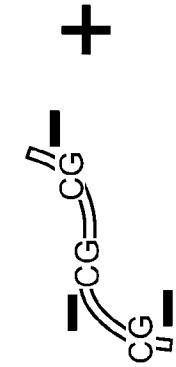
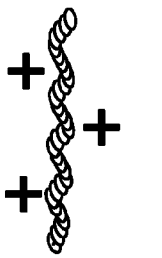

(1) Infection
(2) Inflammatory Cytokines (e.g. GM-CSF)
(3) DC differentiation & recruitment
(4) Antigen processing, CpG-DNA/TLR Signalling & DC LN homing
CCR7
MHC
Activated DC (IL-12, IL-6, IFN secretion)
Lanerhans DCs
Monocyte Pre-DC
Blood
SKIN

FIG. 1

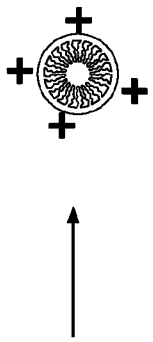
FIG. 2A



CpG-ODN



Polyethylenimine (PEI)



PEI-CpG ODN Condensate

FIG. 2B

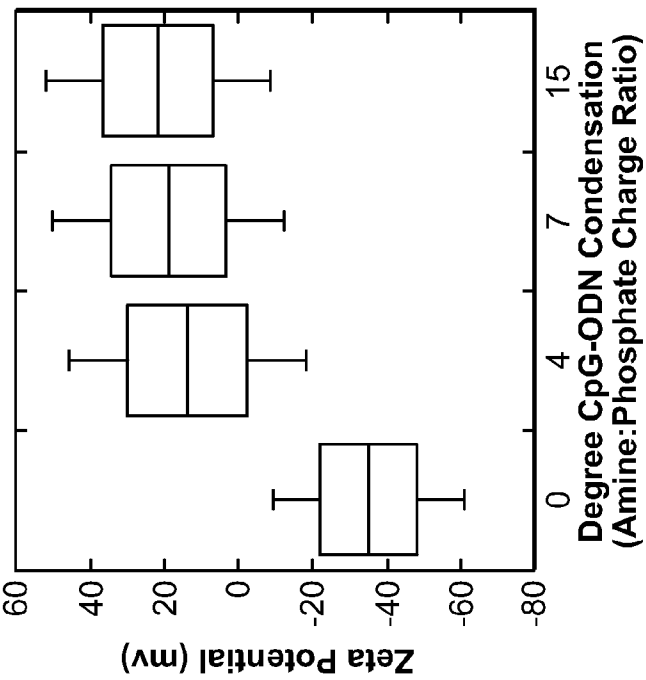


FIG. 2C

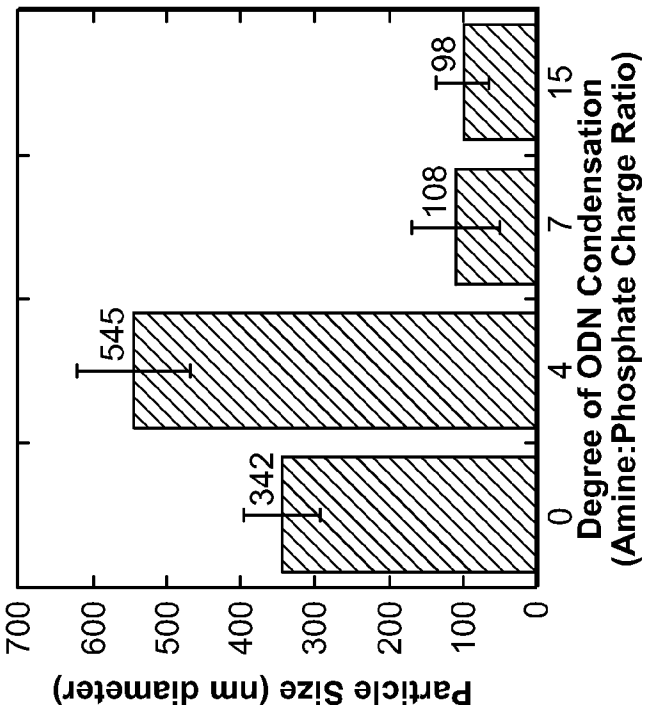


FIG. 3A

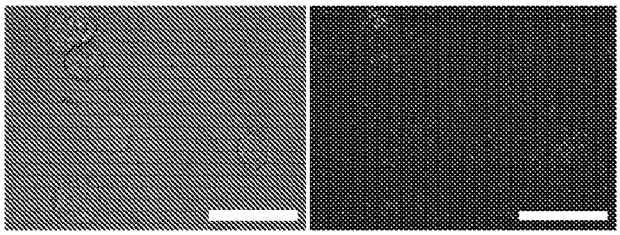


FIG. 3B

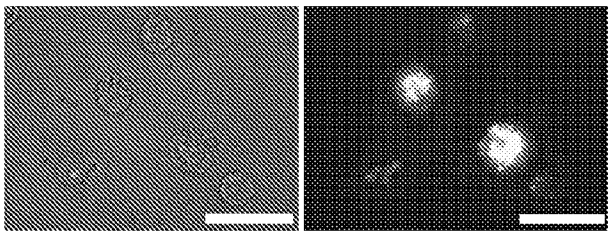


FIG. 3C

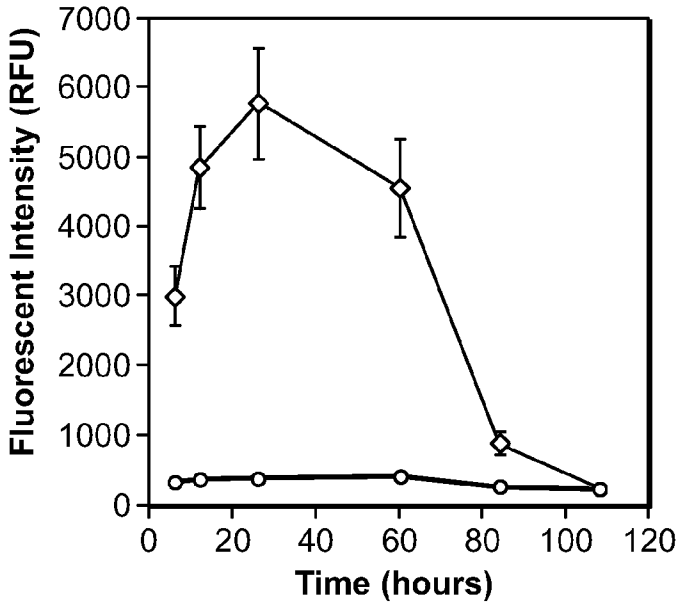


FIG. 3D

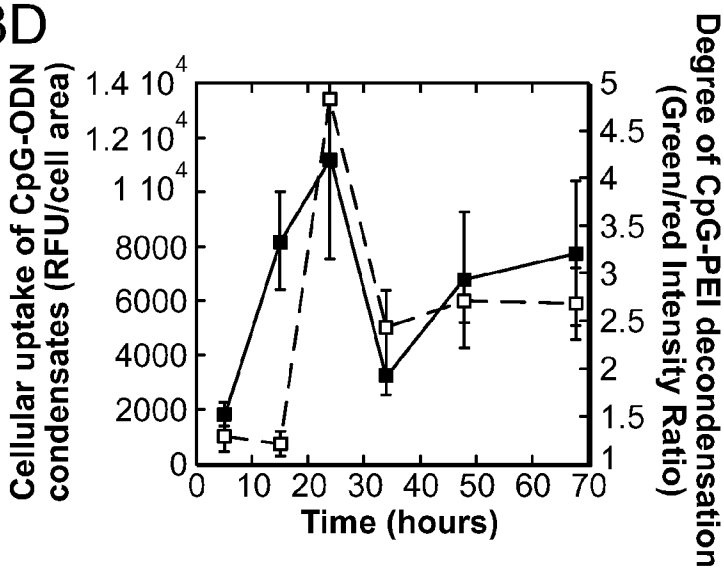


FIG. 4A

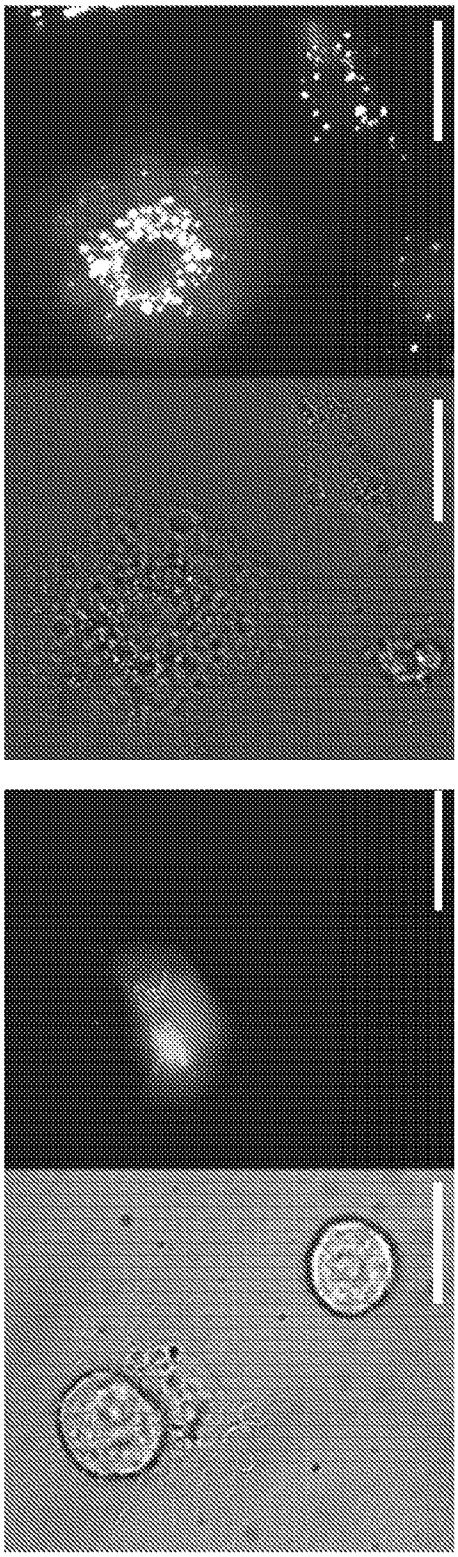
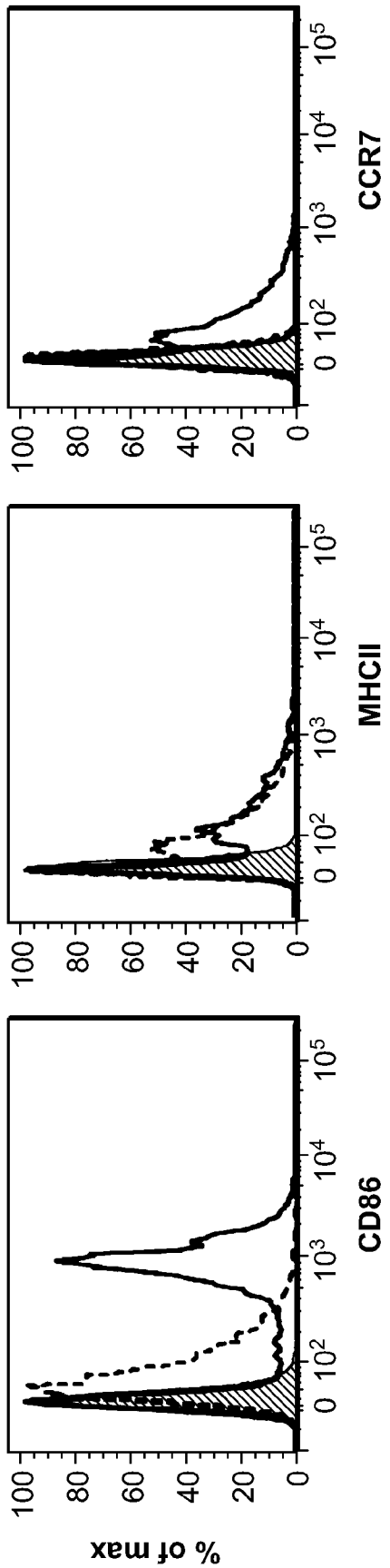


FIG. 4B



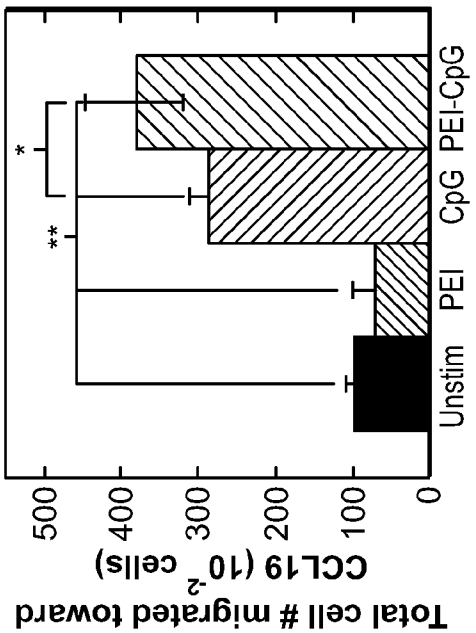


FIG. 4D

	No Stim	TNF-alpha/LPS	CpG-ODN	Cond oligo
CCR7	23.5±4.3	27.4±2.0	25.6±4.2	**34.8±7.1**
MHCII	22.6±3.6	31.1±8.3	39.9±0.55	**48.8±1.7**
CD86	20.0±4.3	67.5±10	38.1±2.3	**57.3±2.8**

FIG. 4C

FIG. 5A

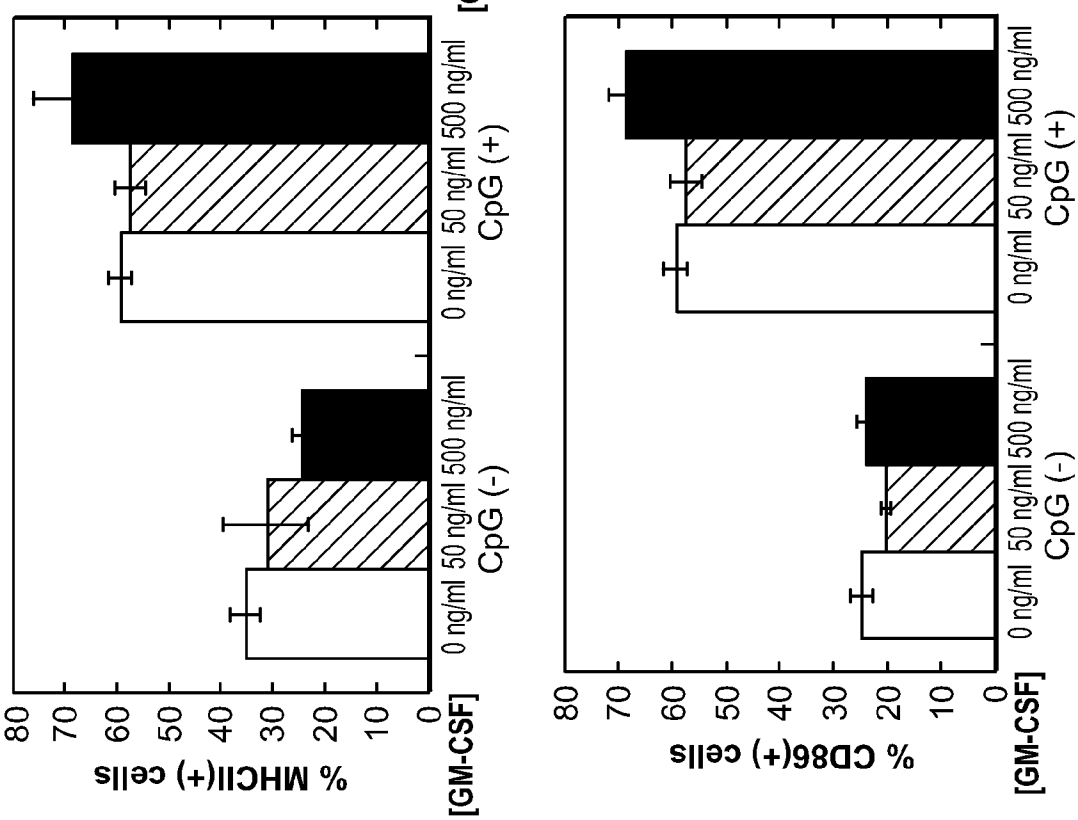

% MHCII(+) cells
% CCR7(+) cells
% CD86(+) cells
[GM-CSF]
0 ng/ml
50 ng/ml
500 ng/ml
CpG (-)
CpG (+)

FIG. 5B

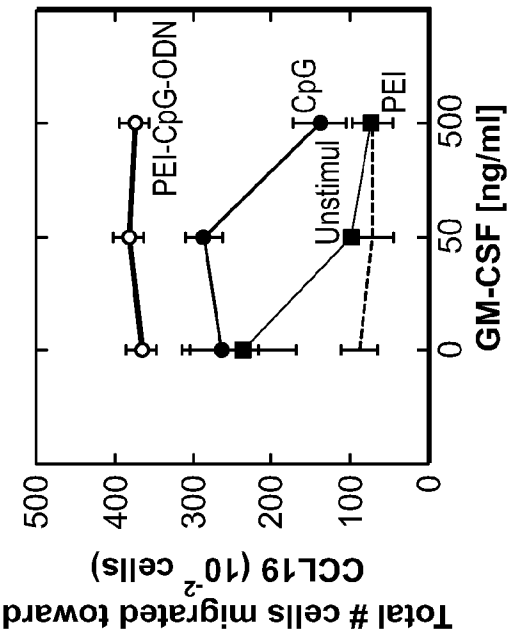

Total # cells migrated toward CCL19 (10^2 cells)
PEI-CpG-ODN
Unstimul
CpG
PEI
GM-CSF [ng/ml]

FIG. 6A

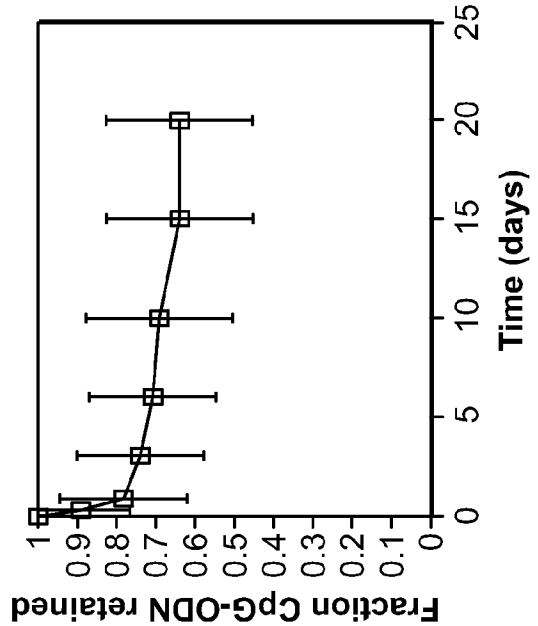


FIG. 6B

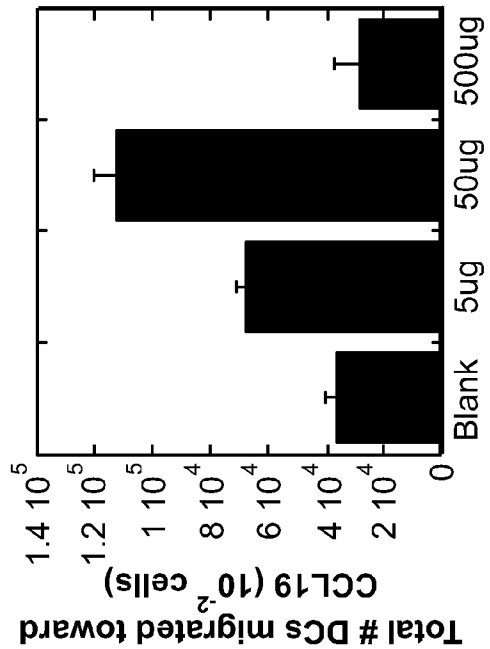


FIG. 6C

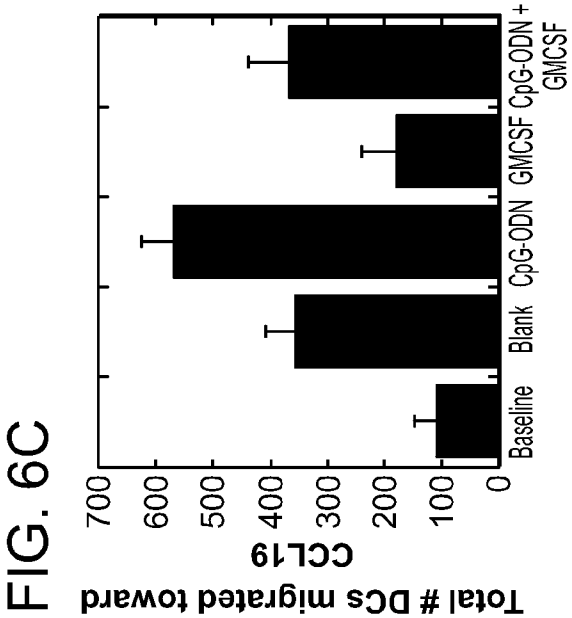
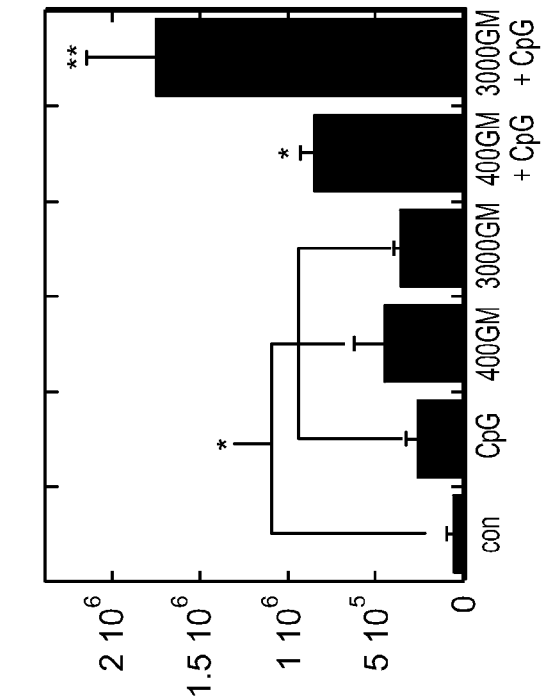
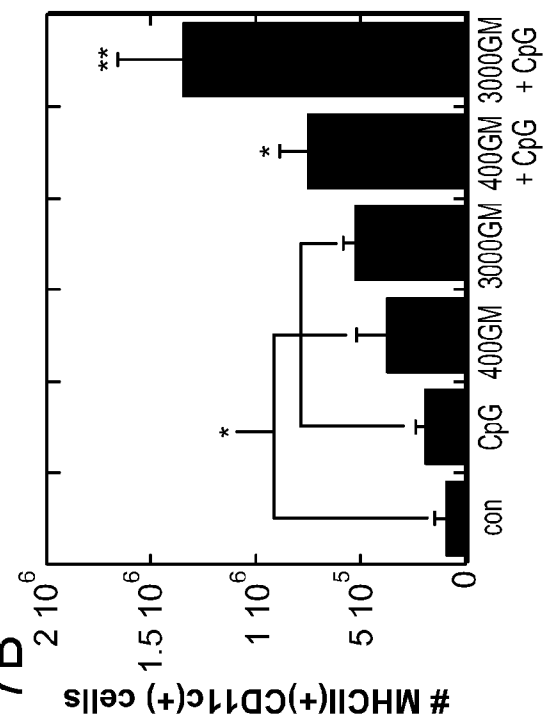


FIG. 7A

Conditions	CpG-ODN (ug)	GM-CSF (ng)	Total Cell (10^{-6} cells)	CD11c(+)DCs (10^{-6} cells)	CD11c(+)MHCII(+) (%)	CD11c(+)CCR7(+) (%)
1	-	400	2.37 ± 0.53	0.51 ± 0.06	18 ± 4.3	22 ± 4.5
2	10	-	1.32 ± 0.24	0.46 ± 0.09	35 ± 10	28 ± 7.6
3	**10**	**3**	**3.25 ± 0.65**	**1.48 ± 0.17**	**46 ± 6.7**	**53 ± 3.2**
4	10	7	5.43 ± 1.76	1.39 ± 0.23	26 ± 3.5	47 ± 2.4
5	10	400	1.12 ± 0.68	0.51 ± 0.47	44 ± 12	50 ± 6.5
6	25	400	2.3 ± 0.89	0.75 ± 0.07	33 ± 6.4	43 ± 7.6
7	50	400	3.35 ± 0.86	0.81 ± 0.17	3.0 ± 0.6	4.1 ± 2.3
8	100	400	4.23 ± 1.88	0.45 ± 0.09	6.7 ± 0.2	10 ± 5.6
9	50	1000	5.12 ± 2.34	3.32 ± 0.74	10 ± 1.2	65 ± 1.4
10	50	3000	5.59 ± 3.65	2.51 ± 0.63	12 ± 3.4	45 ± 2.4
11	50	7000	6.51 ± 2.58	3.91 ± 0.78	11 ± 2.4	60 ± 7.8

FIG. 7B





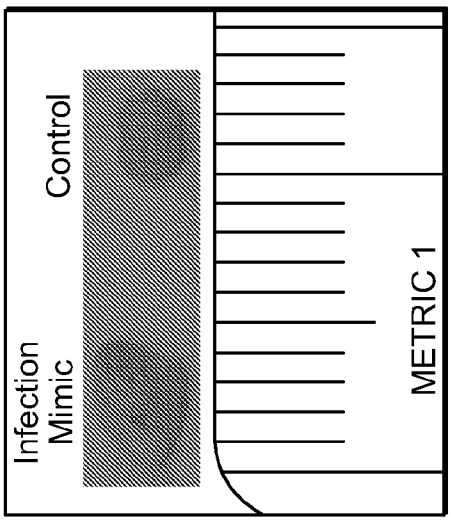


FIG. 8B

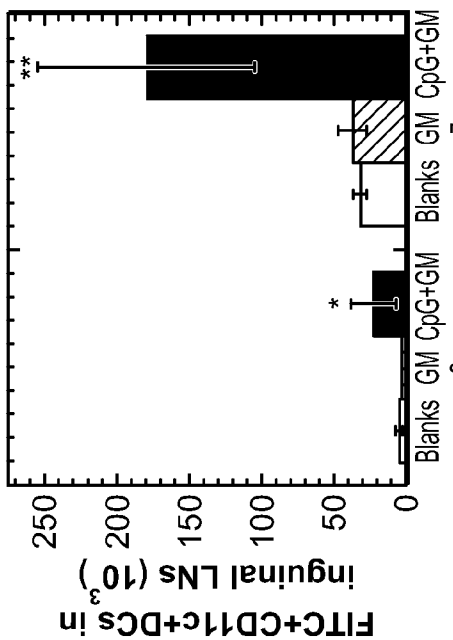


FIG. 8A

FIG. 8D

FIG. 8C

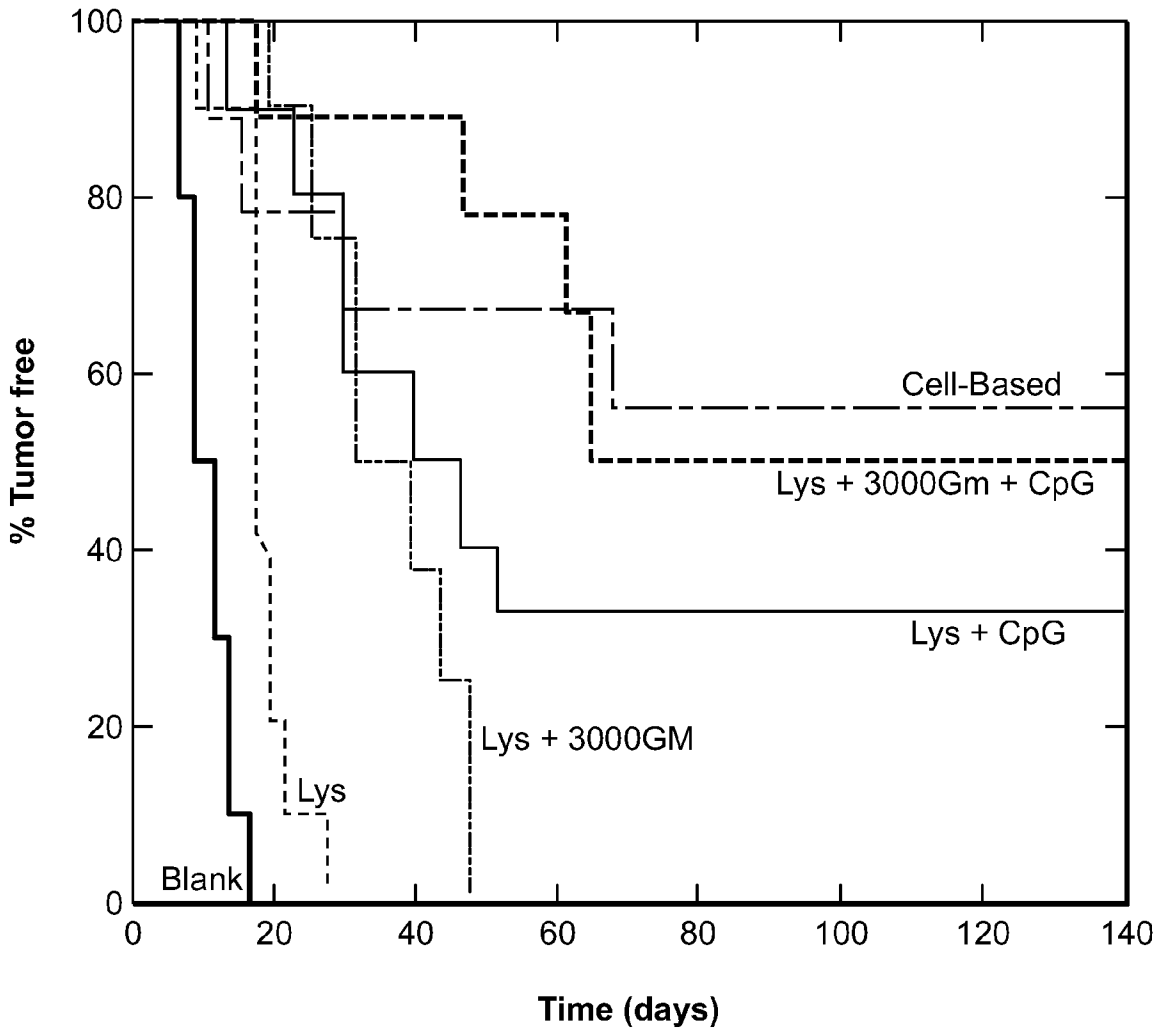

100
80
60
40
20
0
% Tumor free
0
20
40
60
80
100
120
140
Time (days)
Cell-Based
Lys + 3000Gm + CpG
Lys + CpG
Lys + 3000GM
Lys
Blank

FIG. 9

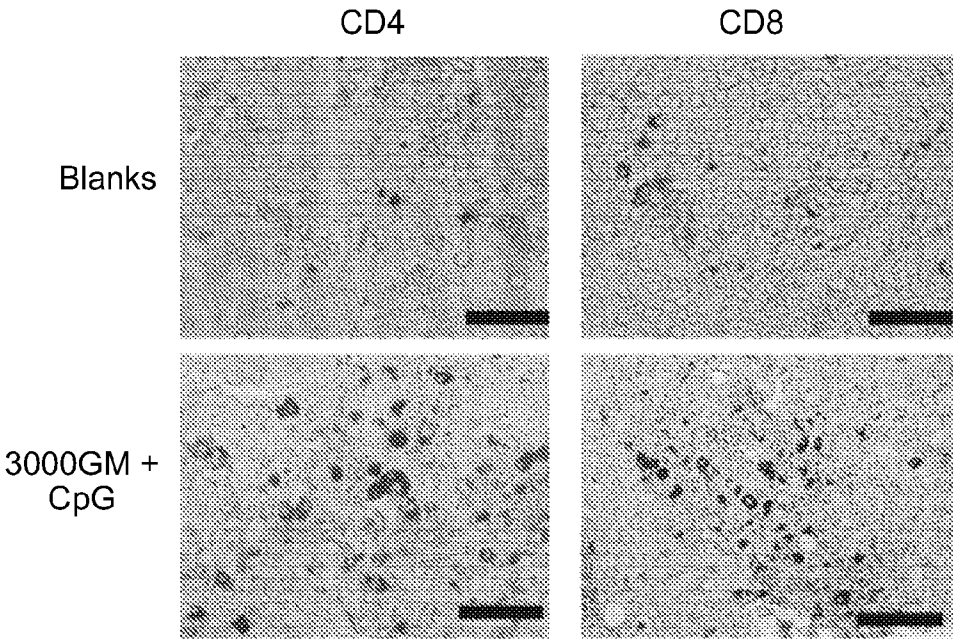


FIG. 10A

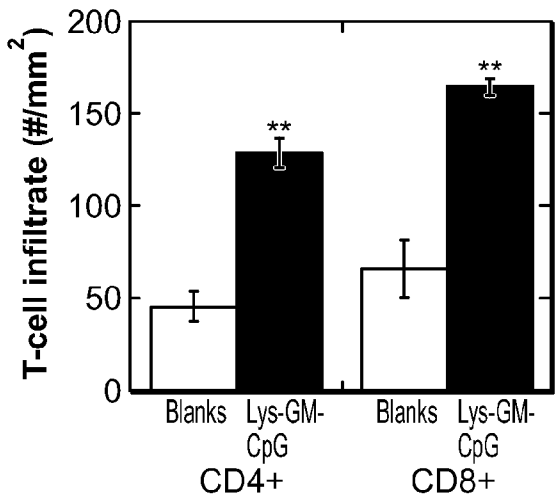


FIG. 10B

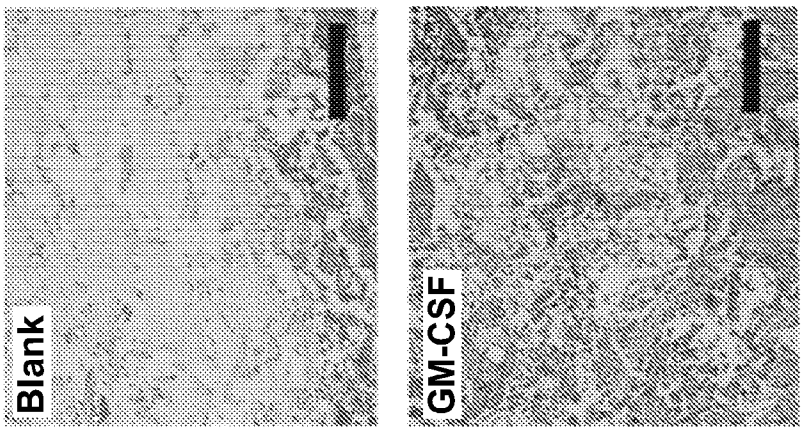


FIG. 11B

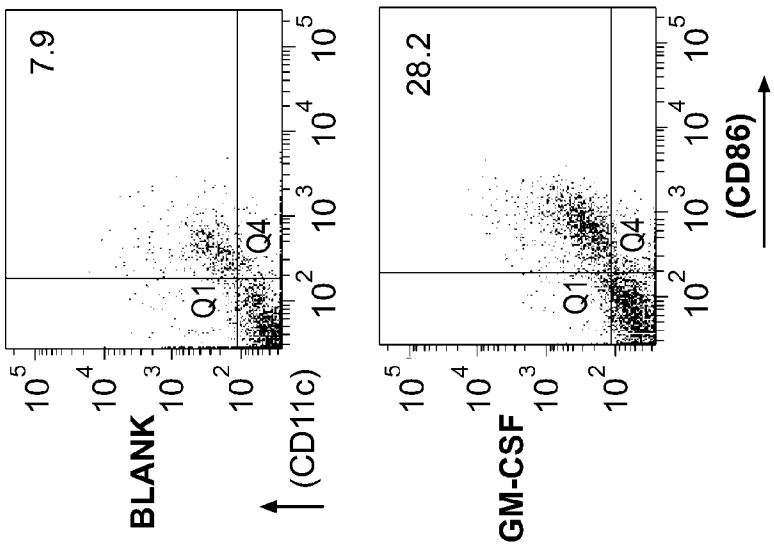


FIG. 11C

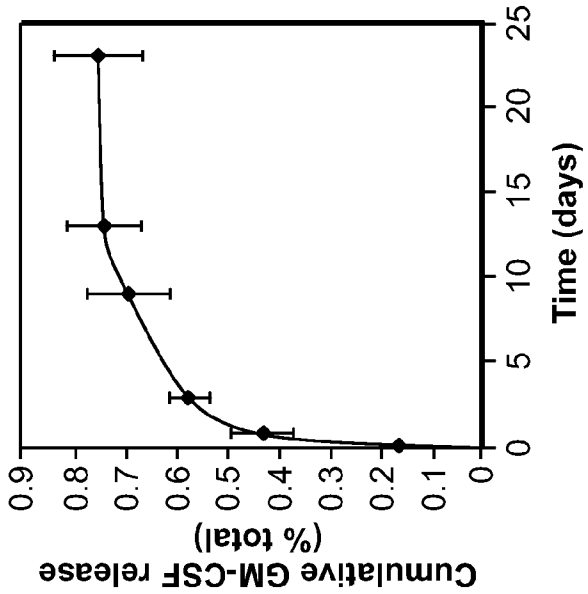


FIG. 11A

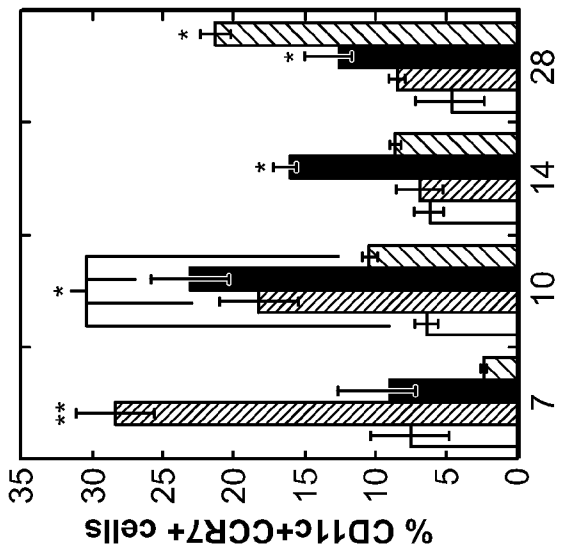


FIG. 11F

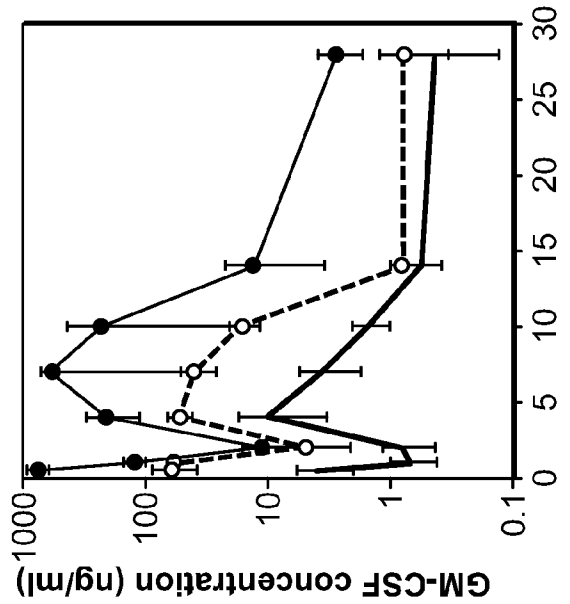


FIG. 11E

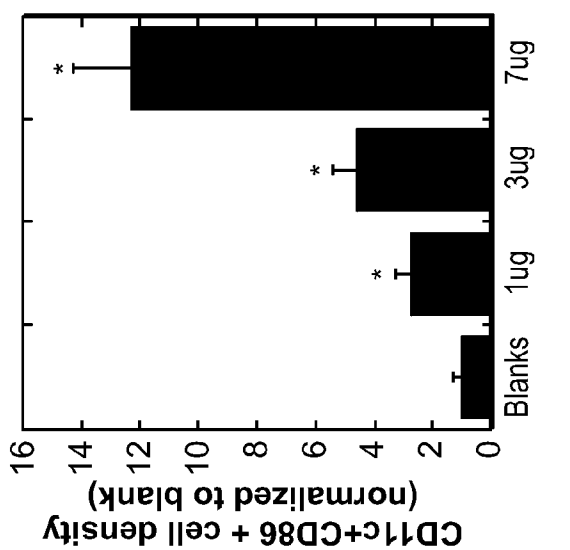


FIG. 11D

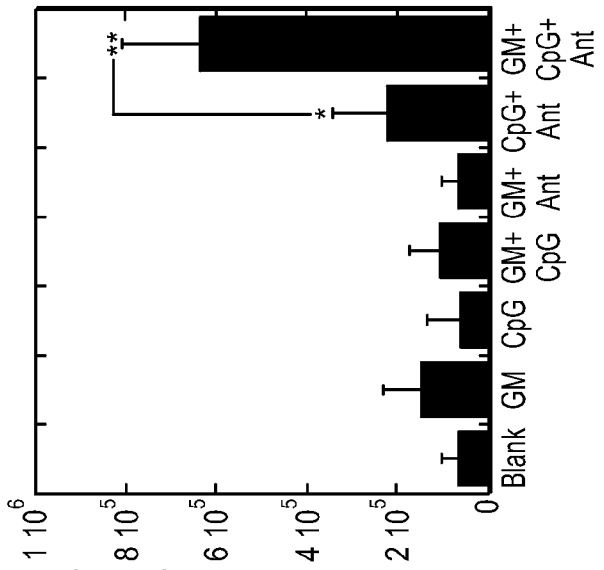


FIG. 12C

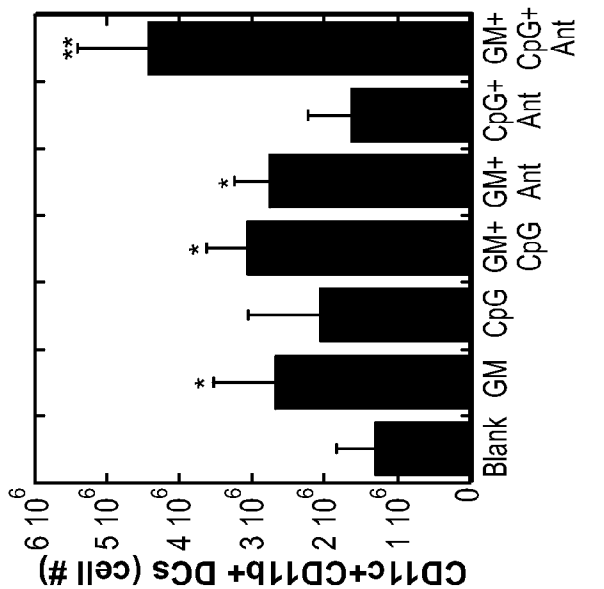


FIG. 12B

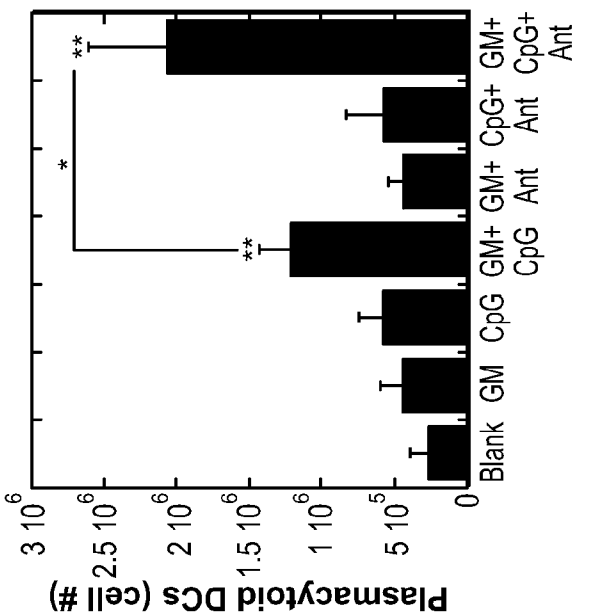
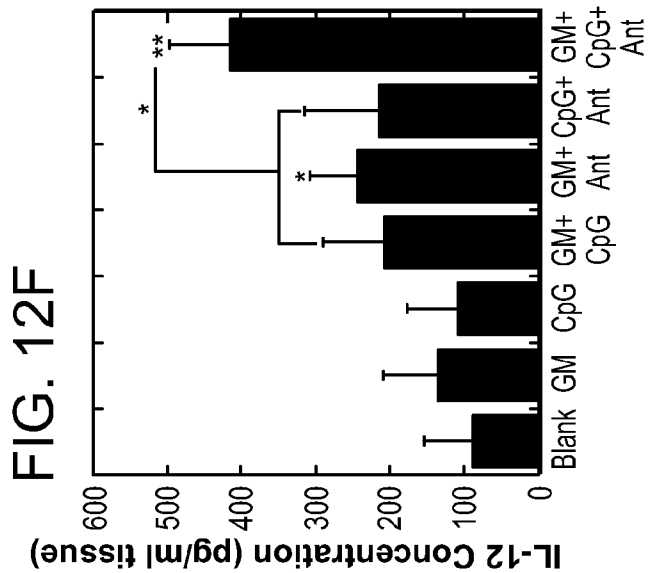
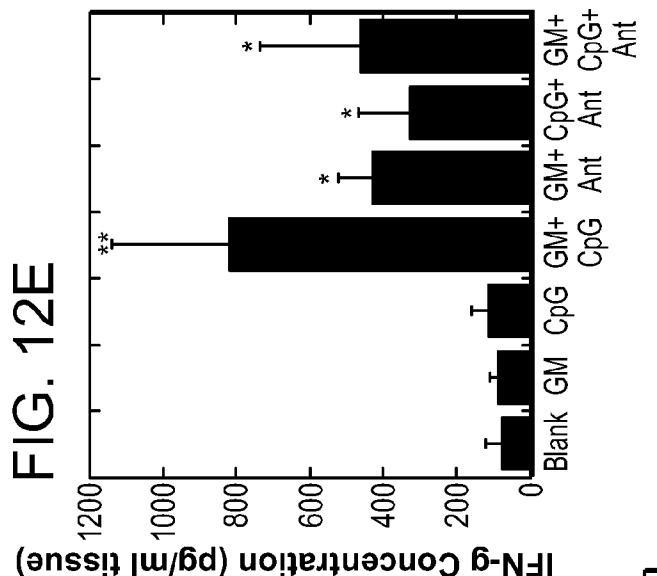
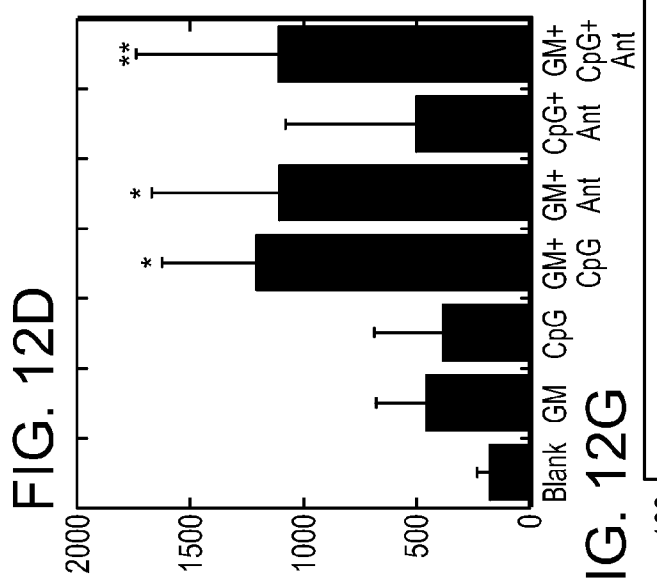
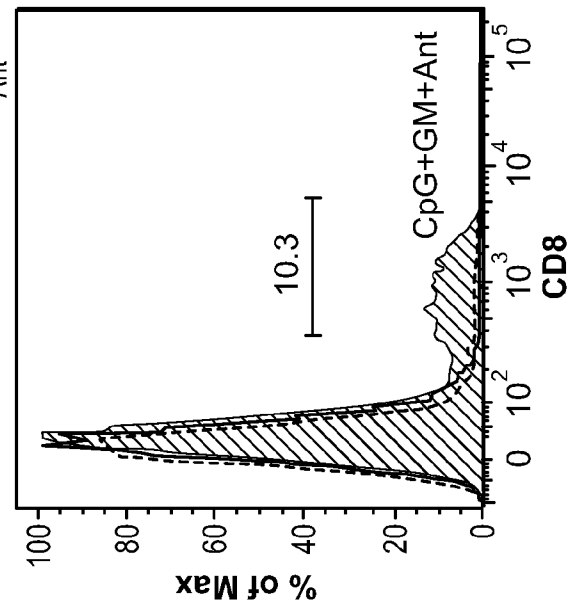


FIG. 12A


FIG. 12F
IL-12 Concentration (pg/ml tissue)
0
100
200
300
400
500
600
Blank
GM
CpG
GM+ CpG
GM+ Ant
CpG+ Ant
GM+ CpG+ Ant
*
*
**


FIG. 12E
IFN-g Concentration (pg/ml tissue)
0
200
400
600
800
1000
1200
Blank
GM
CpG
GM+ CpG
GM+ Ant
CpG+ Ant
GM+ CpG+ Ant
**
*
*
*


FIG. 12D
IFN-a Concentration (pg/ml tissue)
0
500
1000
1500
2000
Blank
GM
CpG
GM+ CpG
GM+ Ant
CpG+ Ant
GM+ CpG+ Ant
*
*
**


FIG. 12G
% of Max
0
20
40
60
80
100
0
10^2
10^3
10^4
10^5
CD8
10.3
CpG+GM+Ant

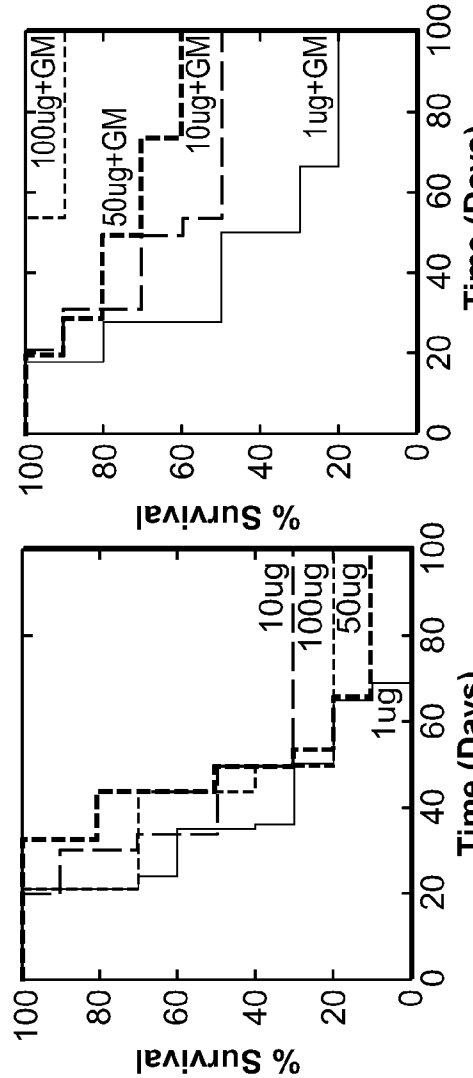


FIG. 13A

FIG. 13B

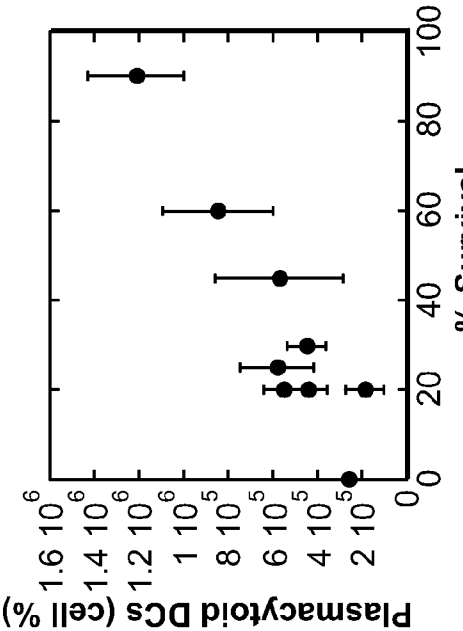


FIG. 13C

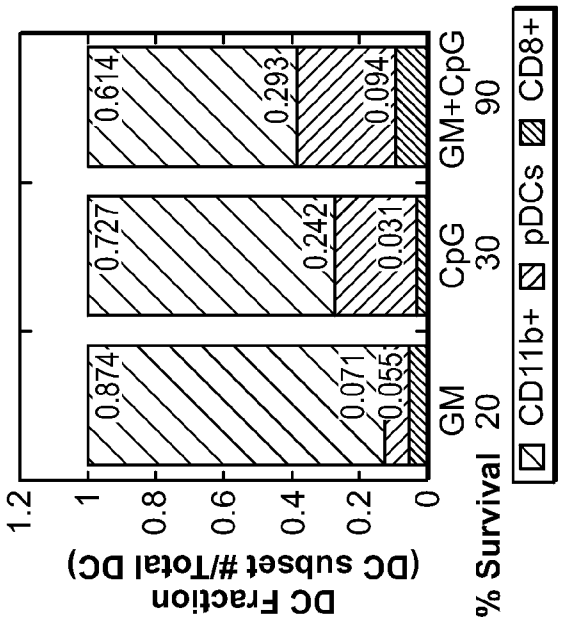


FIG. 13F

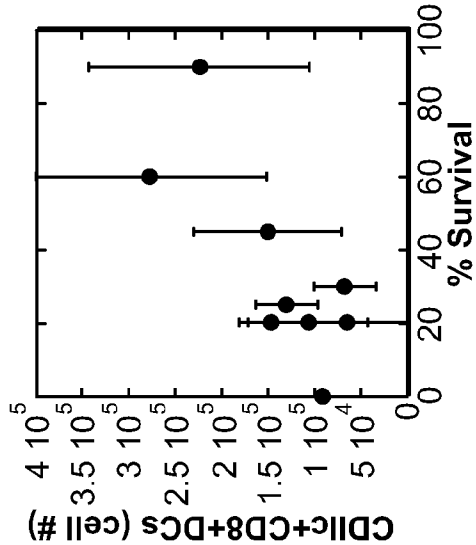


FIG. 13E

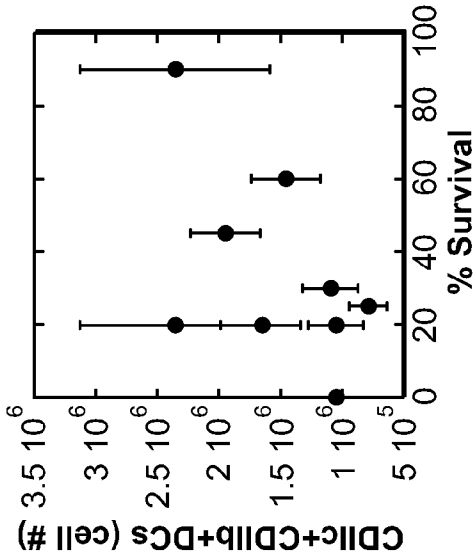


FIG. 13D

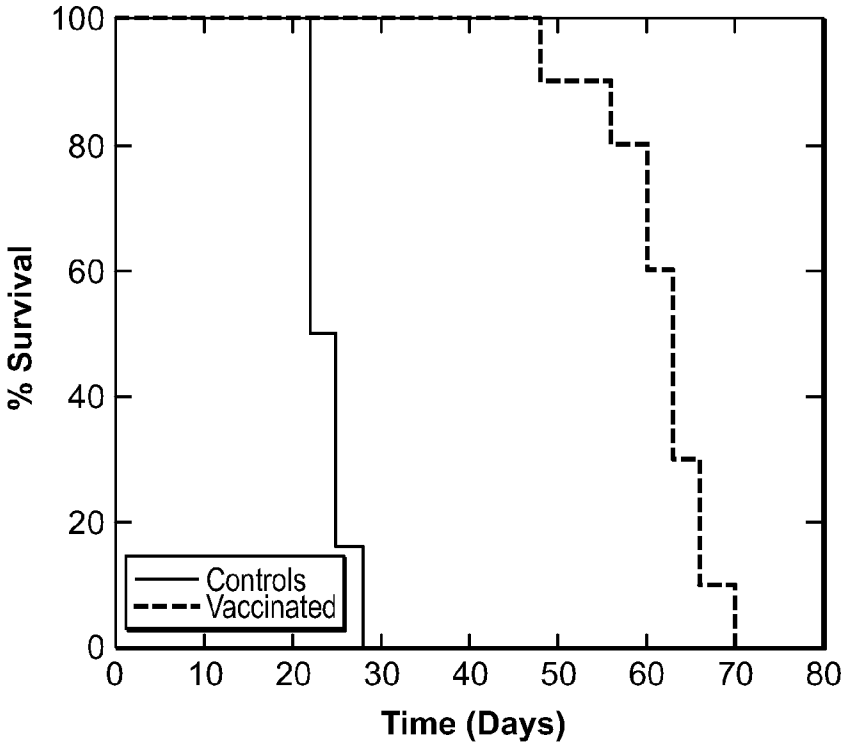


FIG. 14A

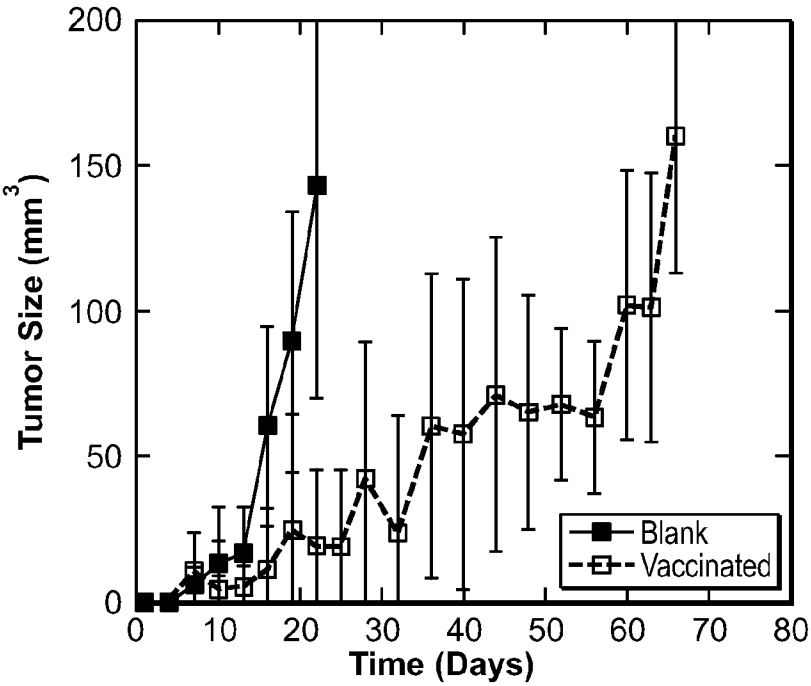


FIG. 14B

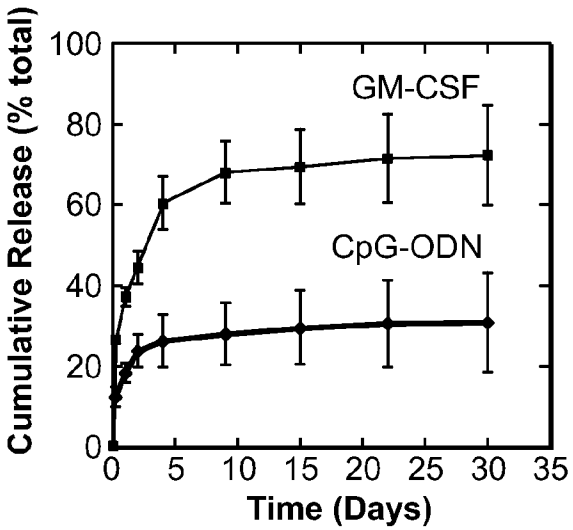


FIG. 15A

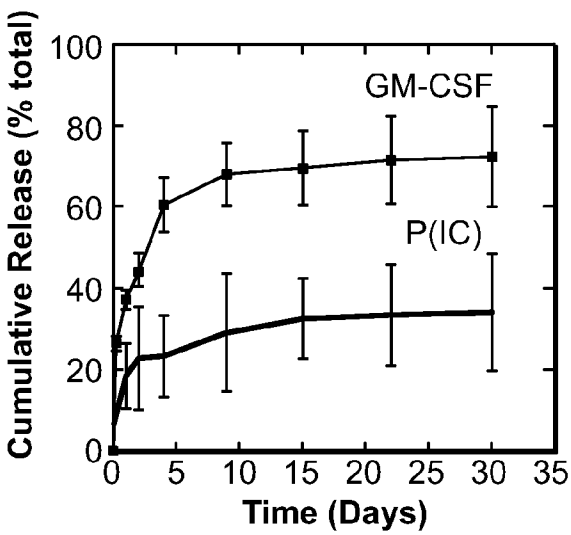


FIG. 15B

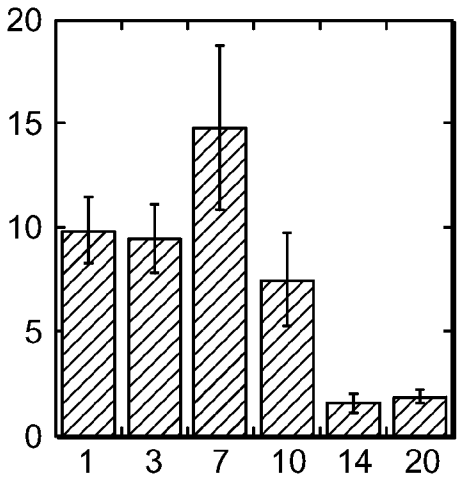


FIG. 15C

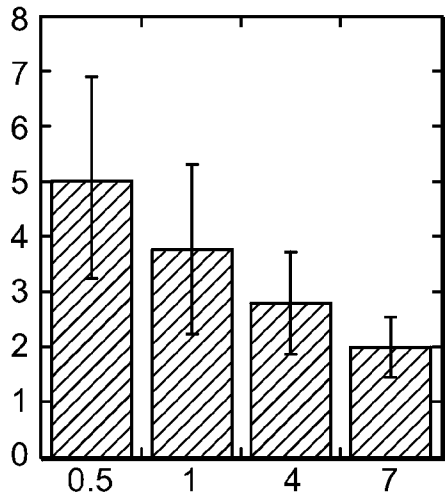


FIG. 15D

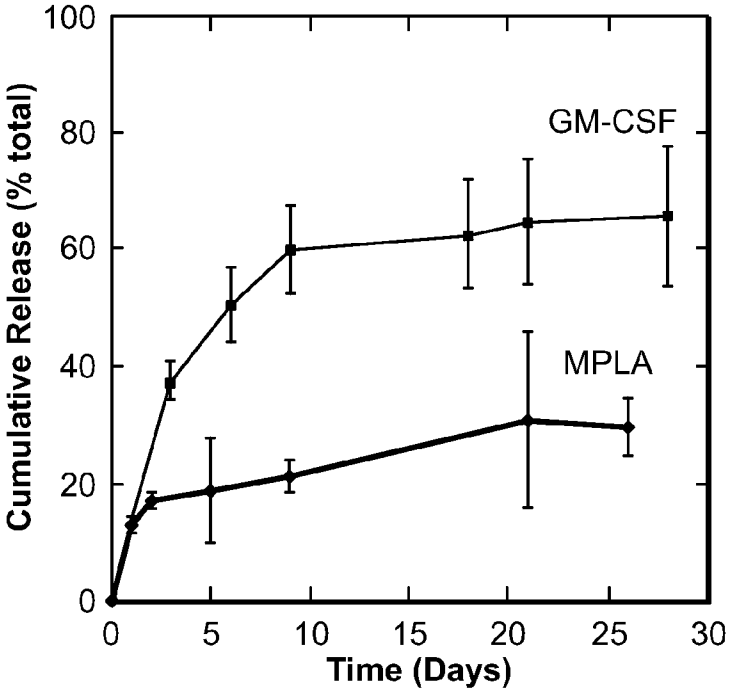


FIG. 15E

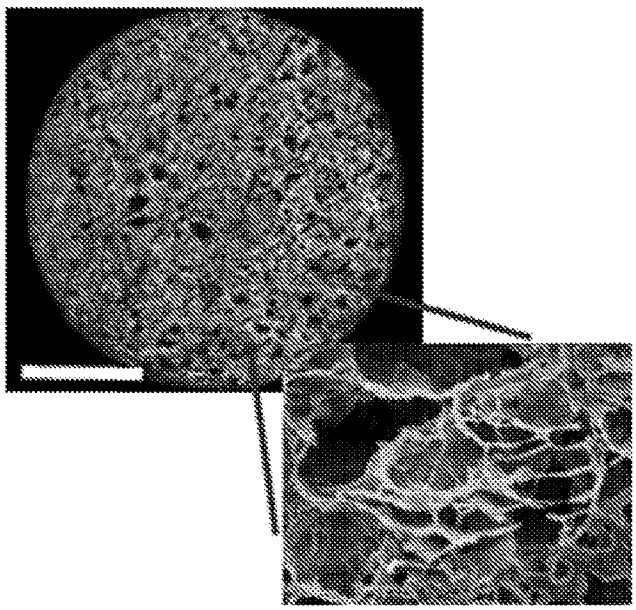


FIG. 15F

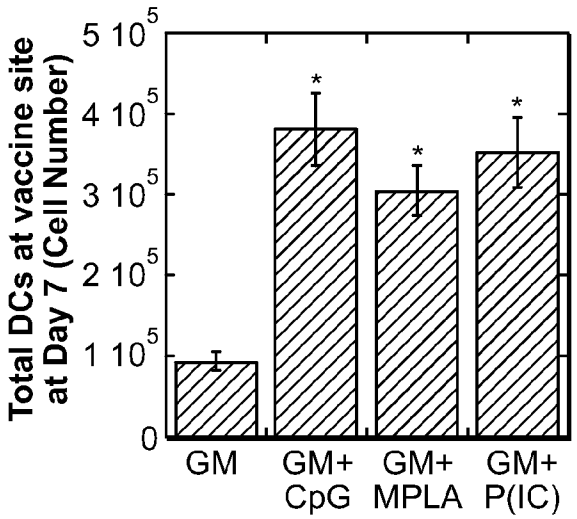


FIG. 16A

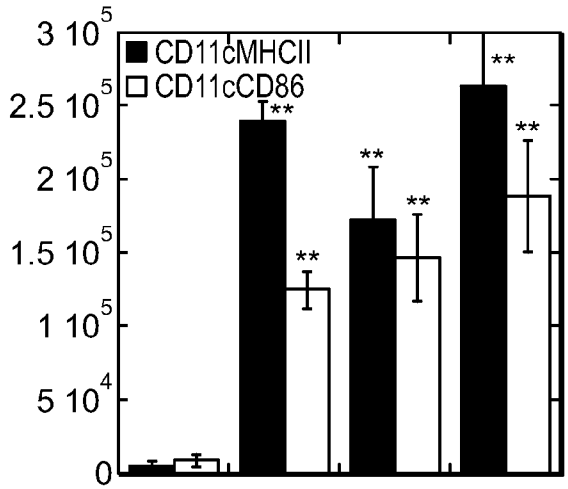


FIG. 16B

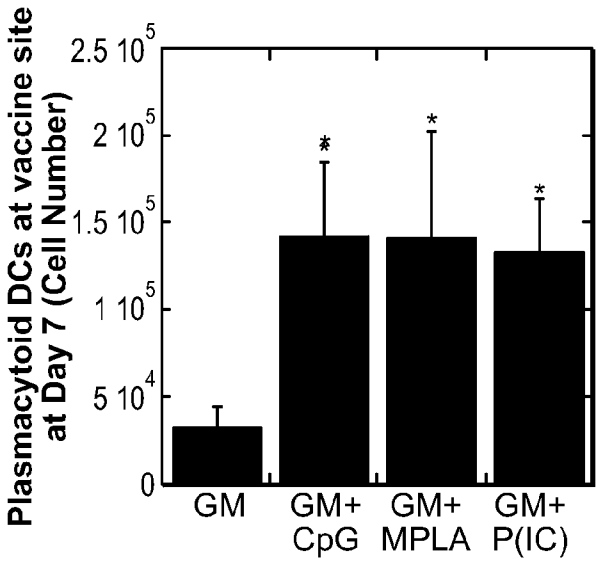


FIG. 16C

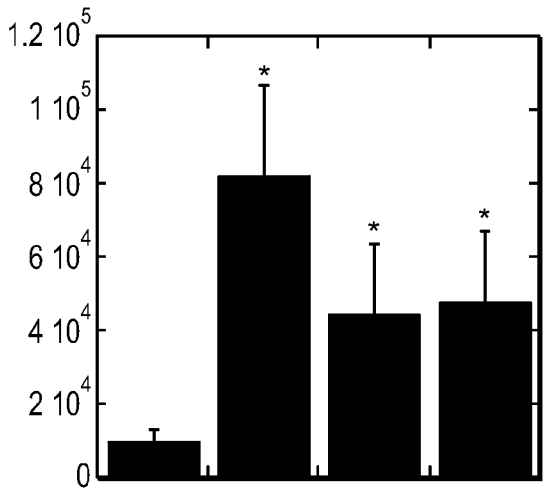
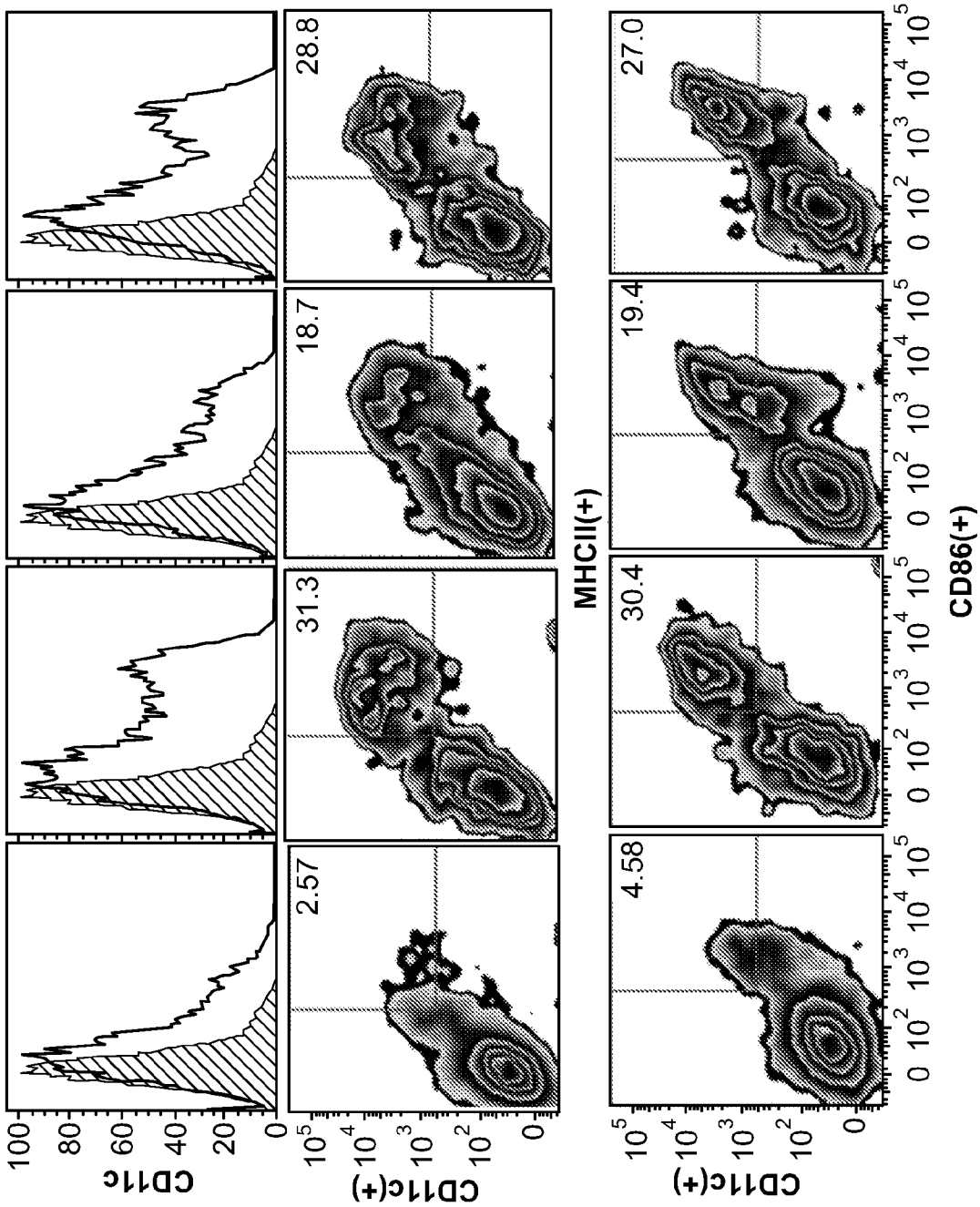


FIG. 16D

FIG. 16E


Control
CpG
MPLA
P(IC)
CD11c
CD11c(+)
MHCII(+)
CD86(+)
2.57
31.3
18.7
28.8
4.58
30.4
19.4
27.0

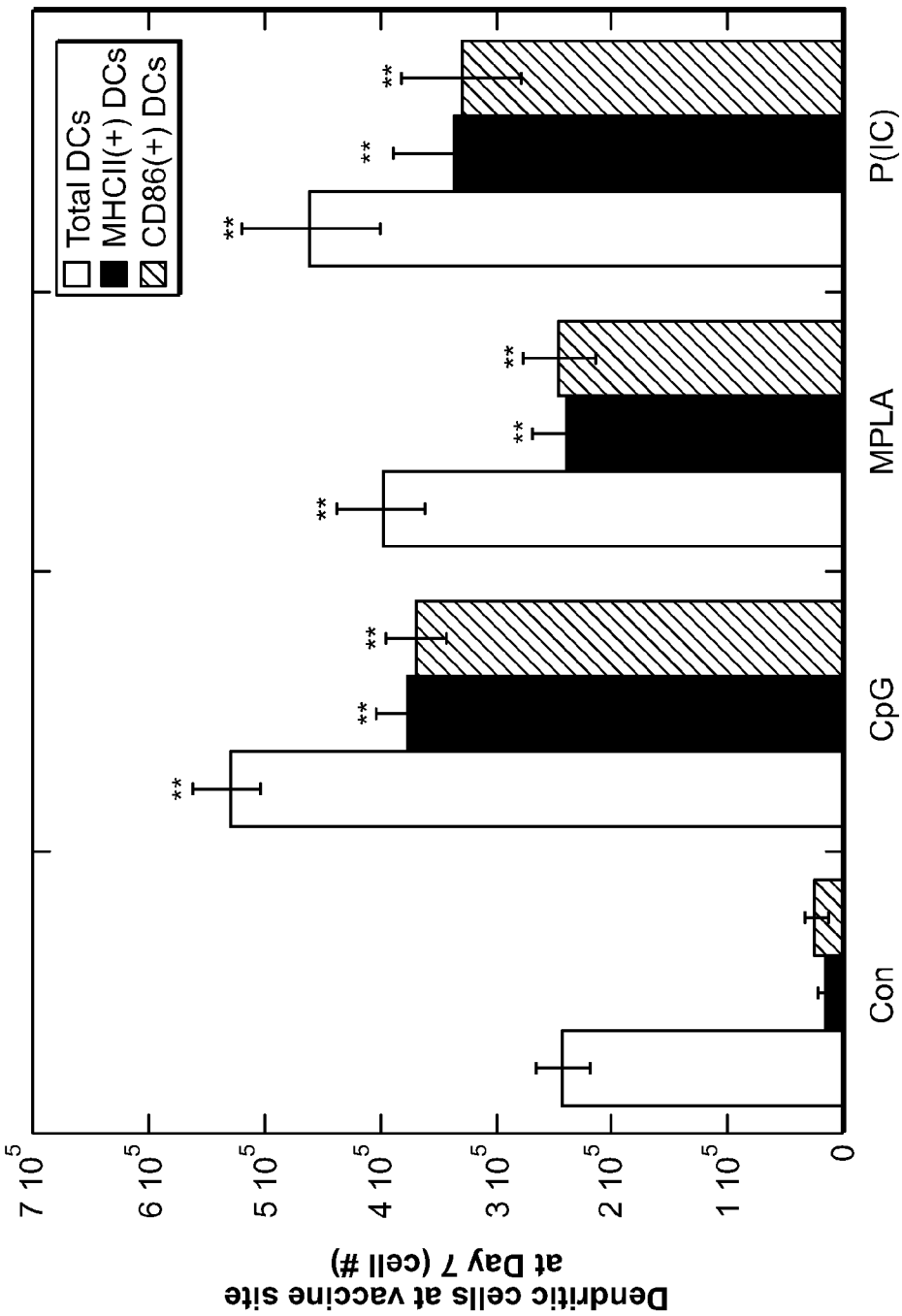

Dendritic cells at vaccine site
at Day 7 (cell #)
7 10^5
6 10^5
5 10^5
4 10^5
3 10^5
2 10^5
1 10^5
0
Con
CpG
MPLA
P(IC)
Total DCs
MHCII(+) DCs
CD86(+) DCs
**

FIG. 16F

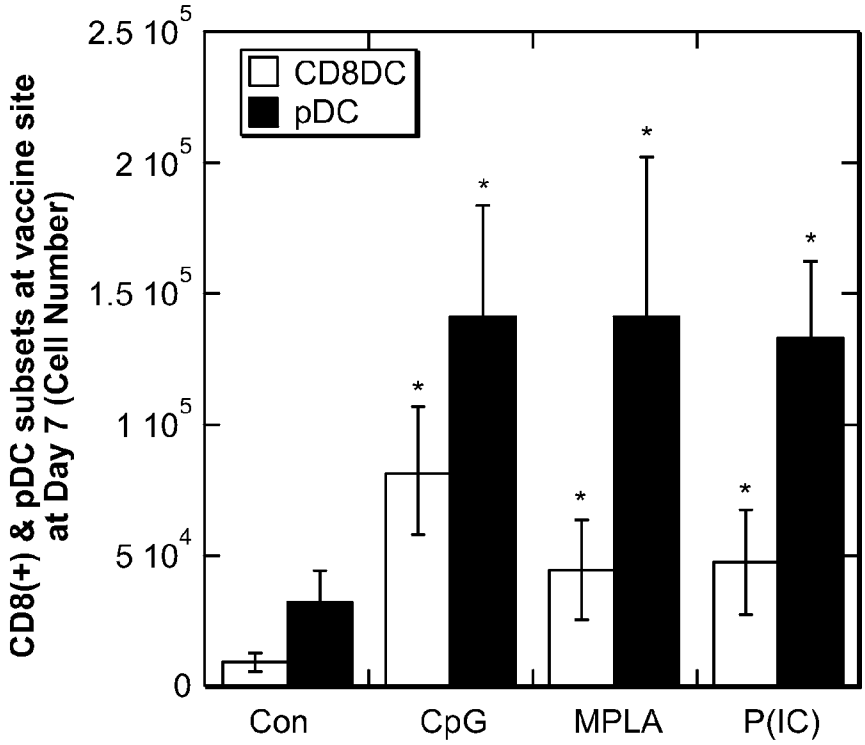


FIG. 16G

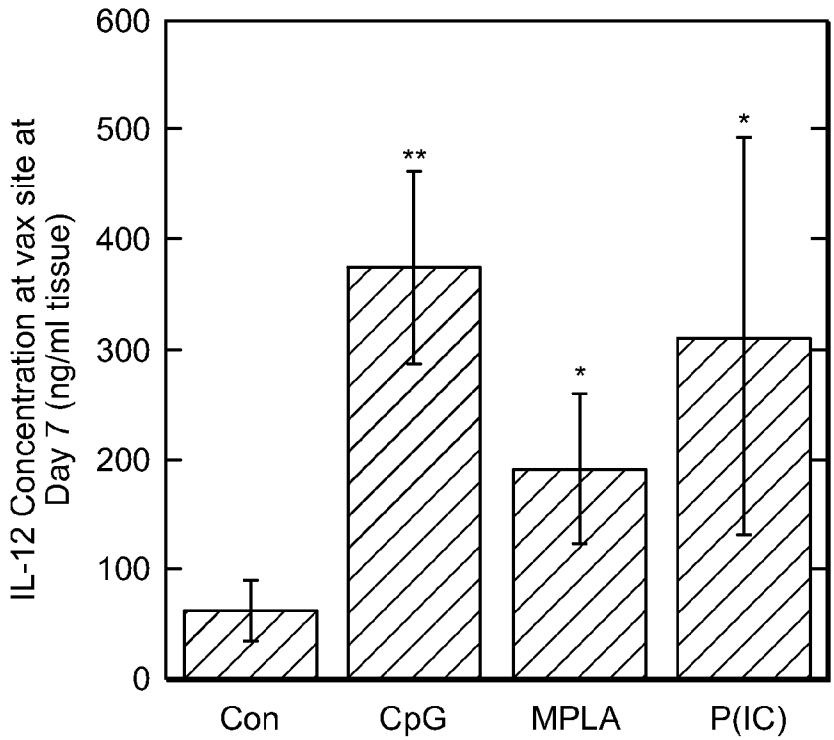


FIG. 16H

FIG. 17A

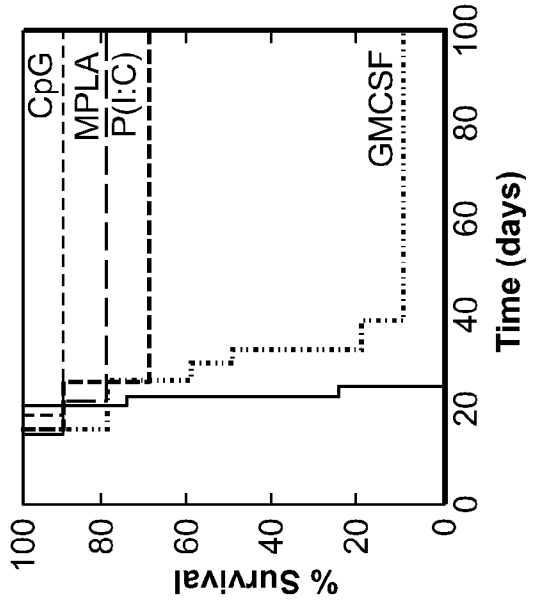


FIG. 17B

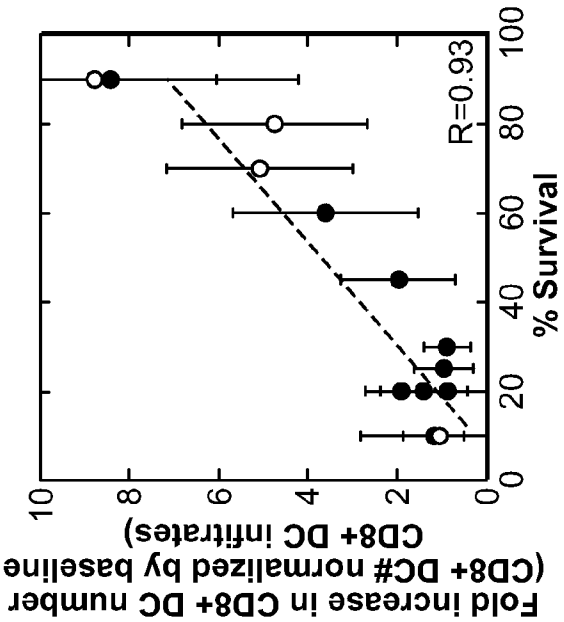


FIG. 17C

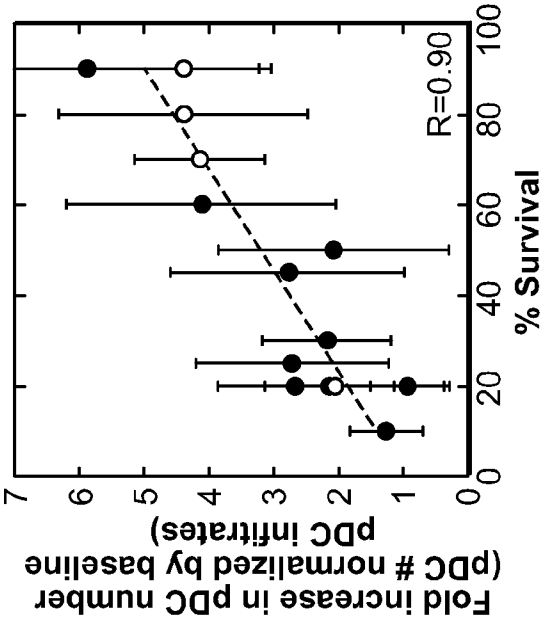
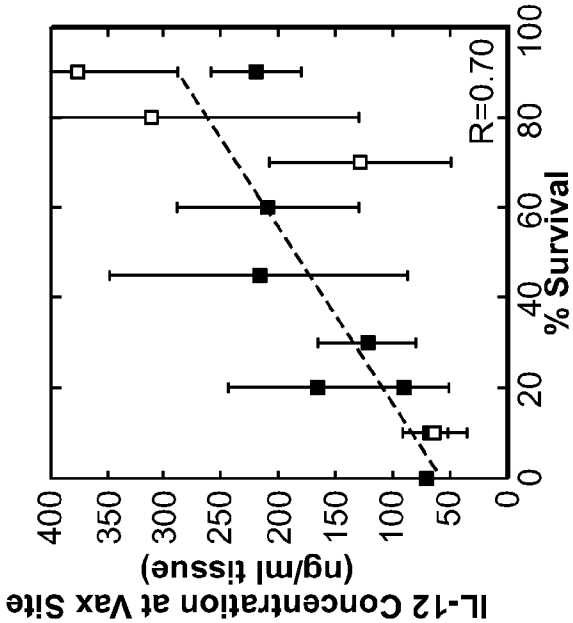


FIG. 17D



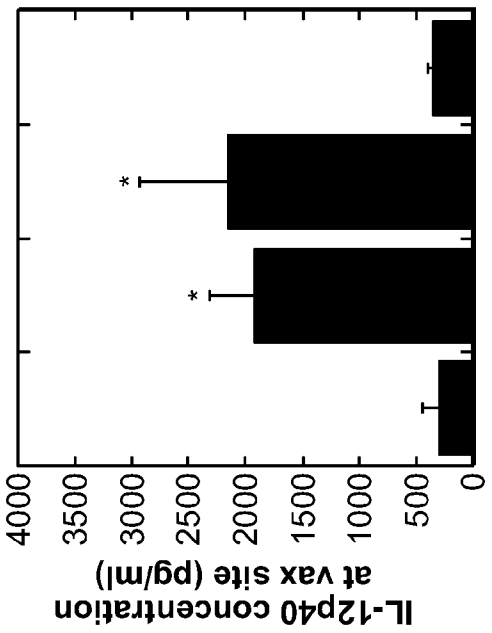


FIG. 18B

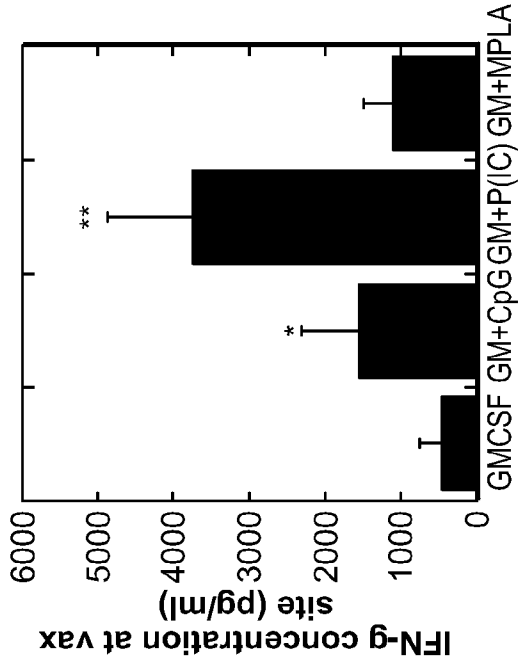


FIG. 18D

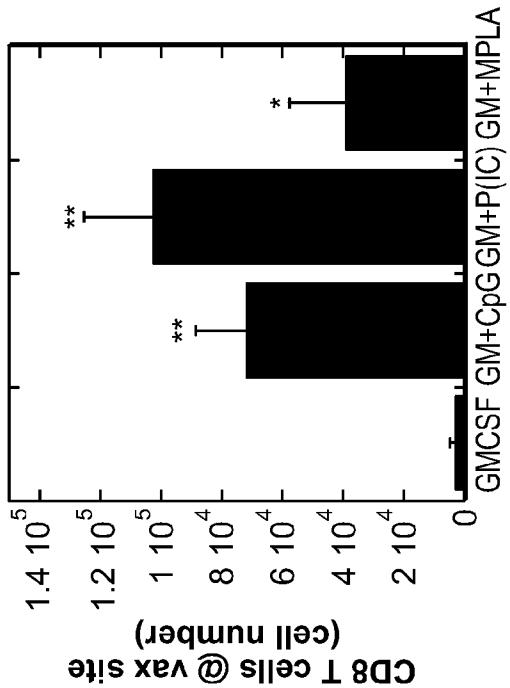


FIG. 18A

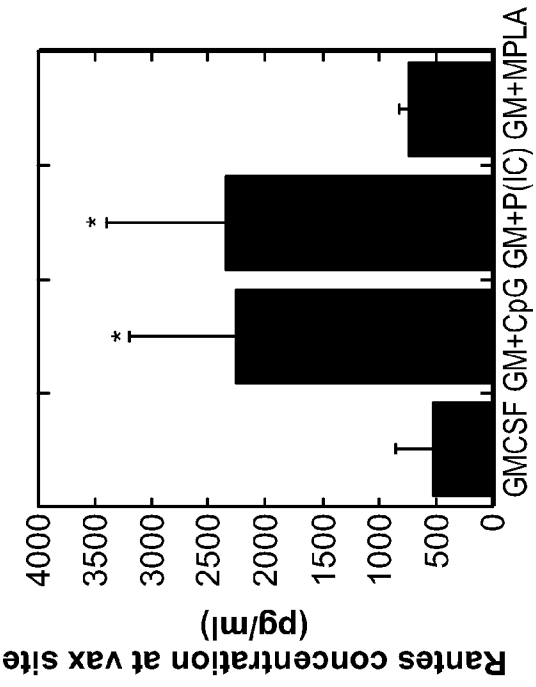


FIG. 18C

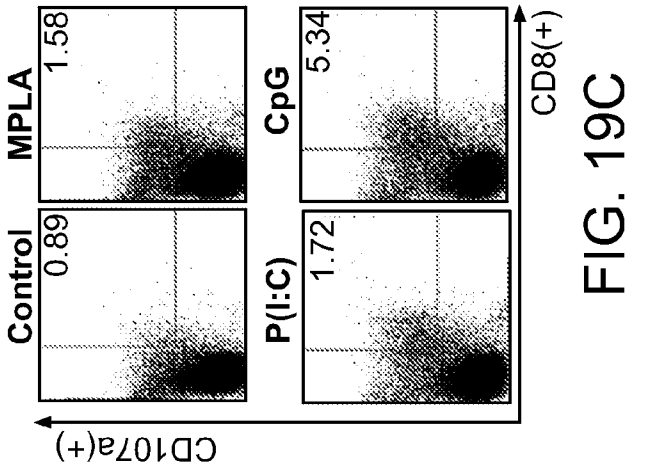


FIG. 19C

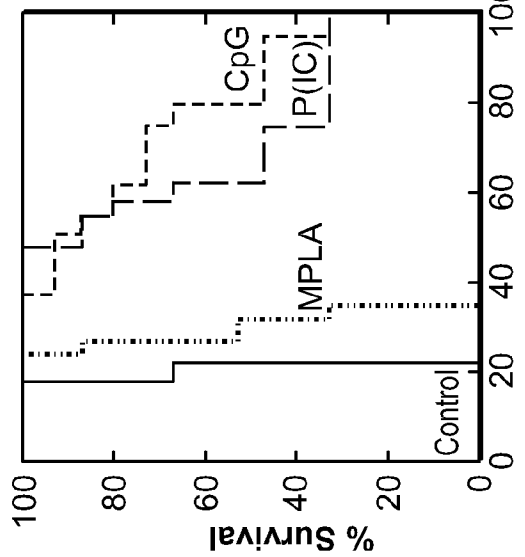


FIG. 19B

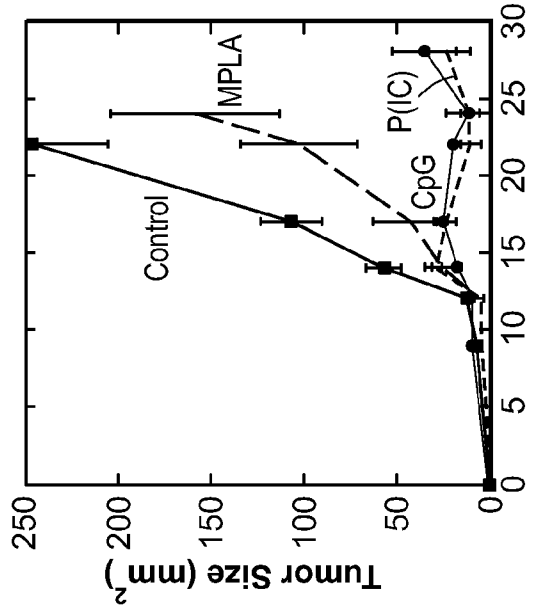


FIG. 19A

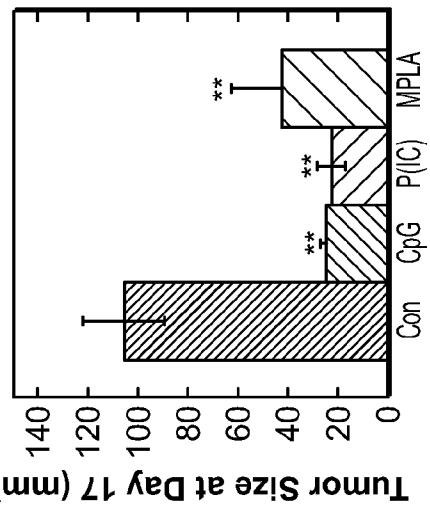


FIG. 19F

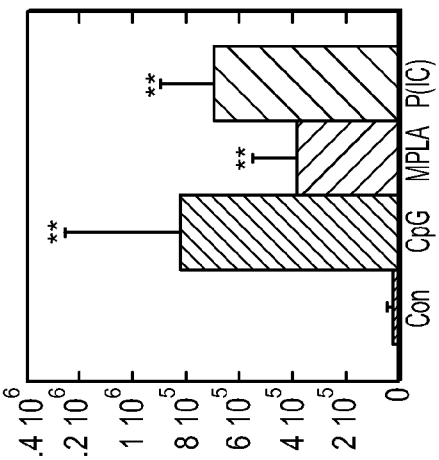


FIG. 19E

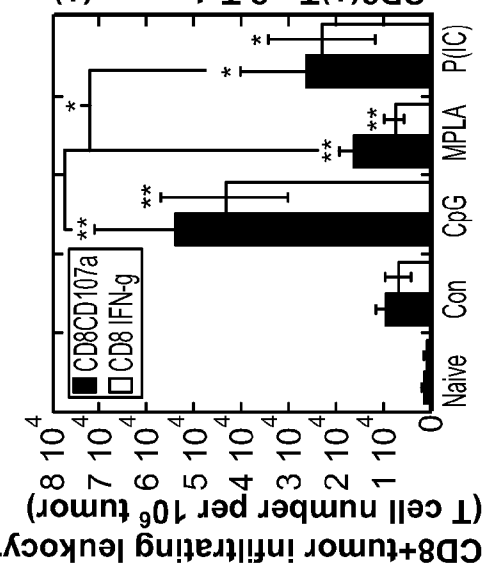


FIG. 19D

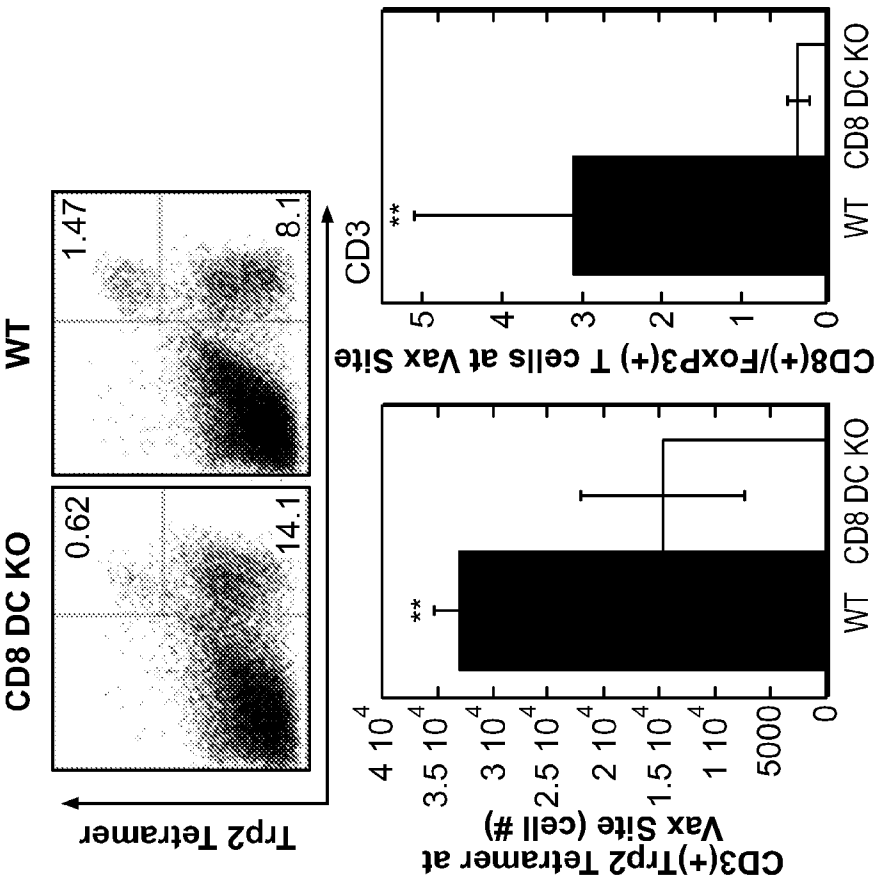


FIG. 20B

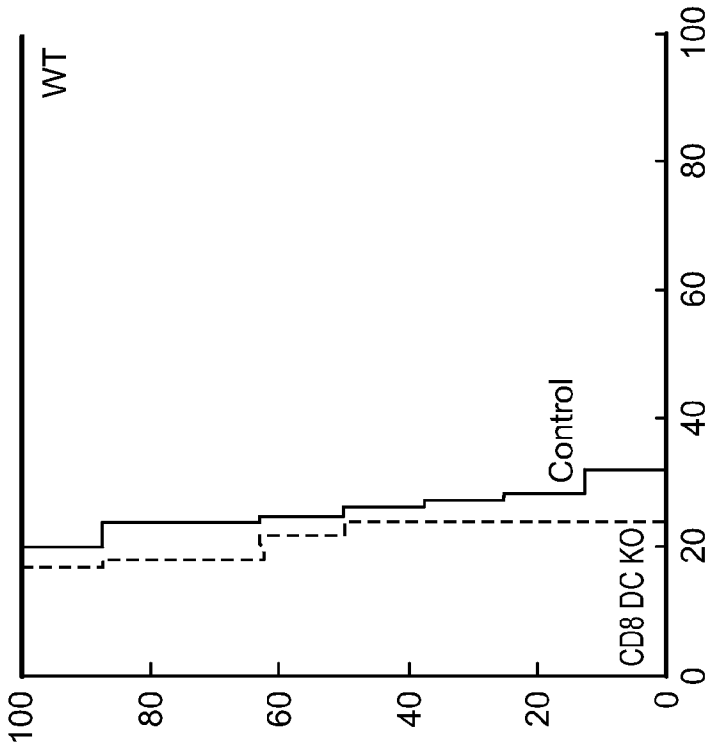


FIG. 20A

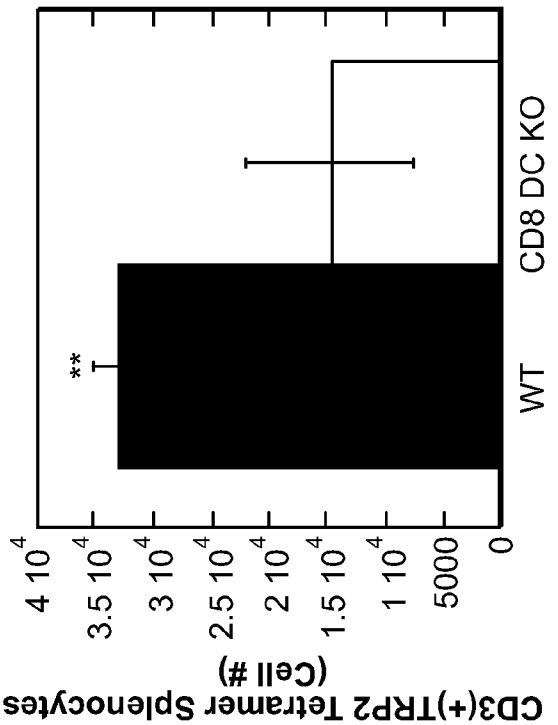


FIG. 20D

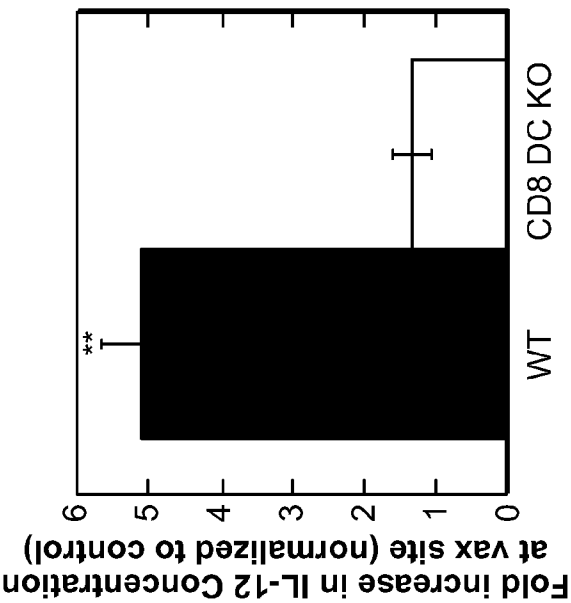


FIG. 20C

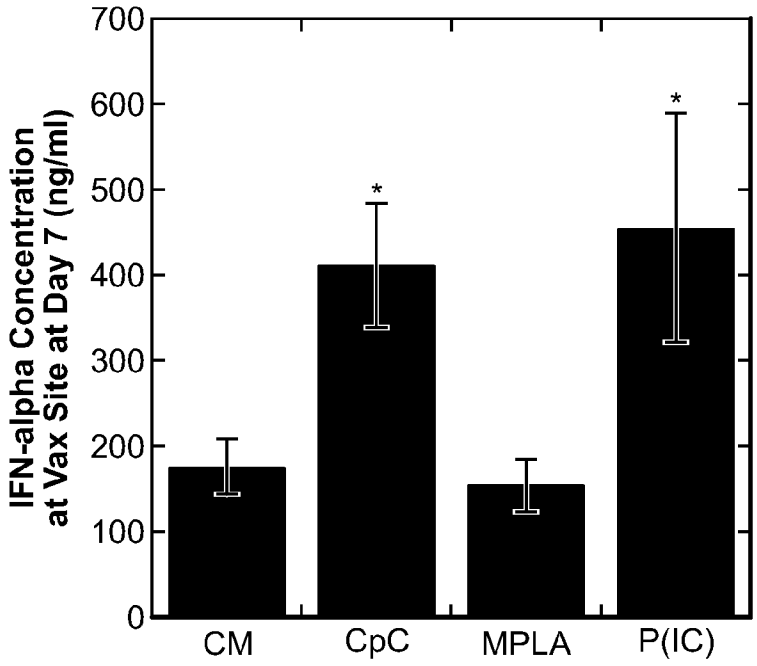


FIG. 21A

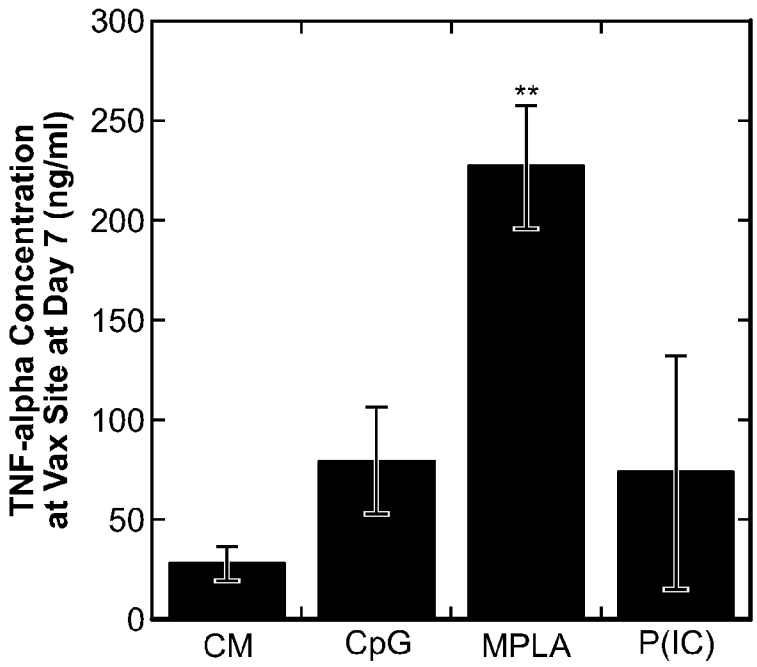


FIG. 21B

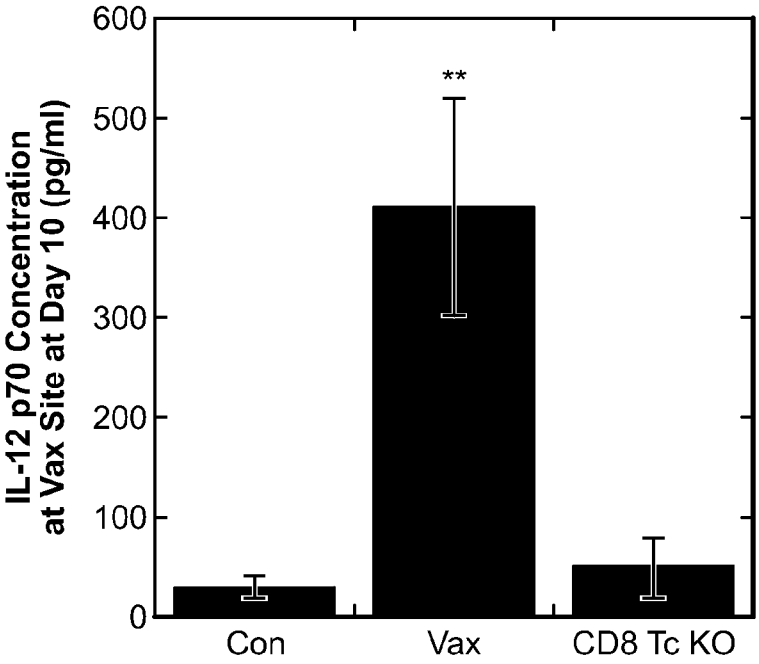


FIG. 21C

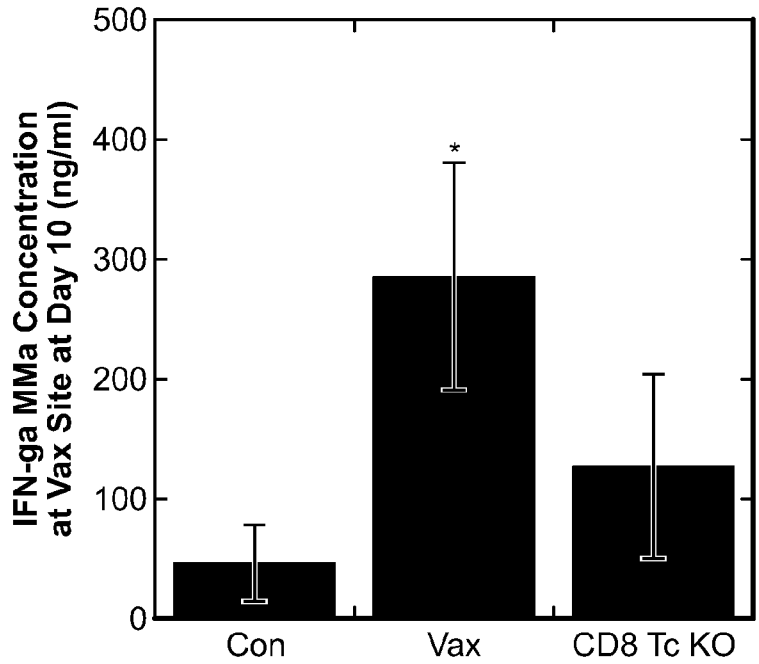


FIG. 21D

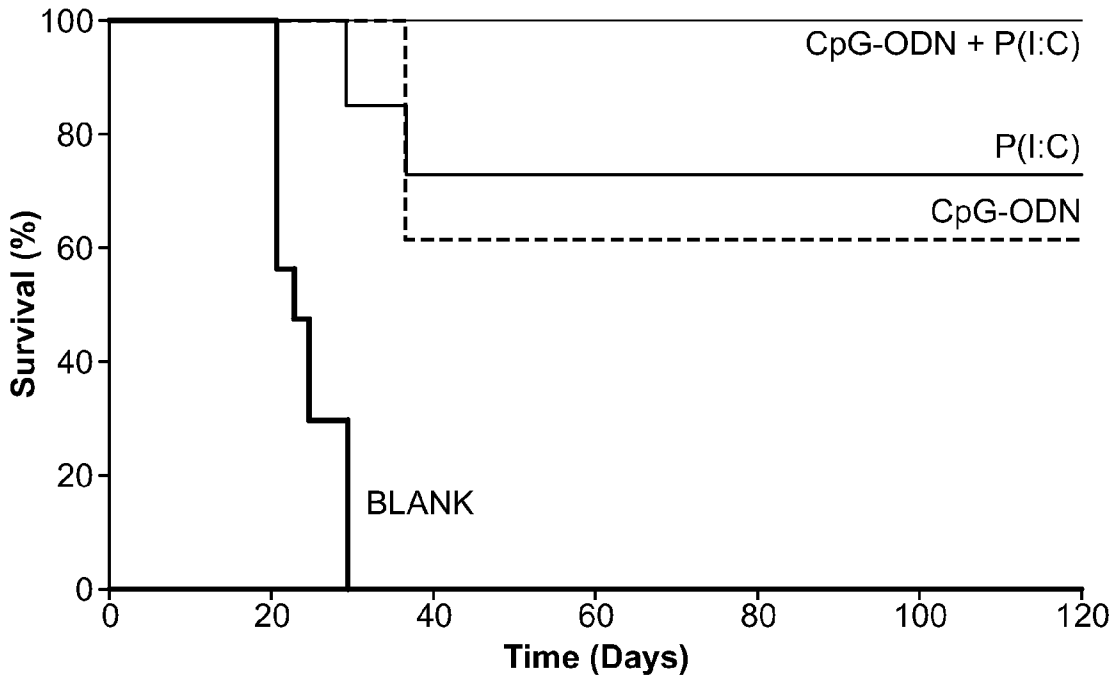

100
80
60
40
20
0
Survival (%)
0
20
40
60
80
100
120
Time (Days)
CpG-ODN + P(I:C)
P(I:C)
CpG-ODN
BLANK

FIG. 22

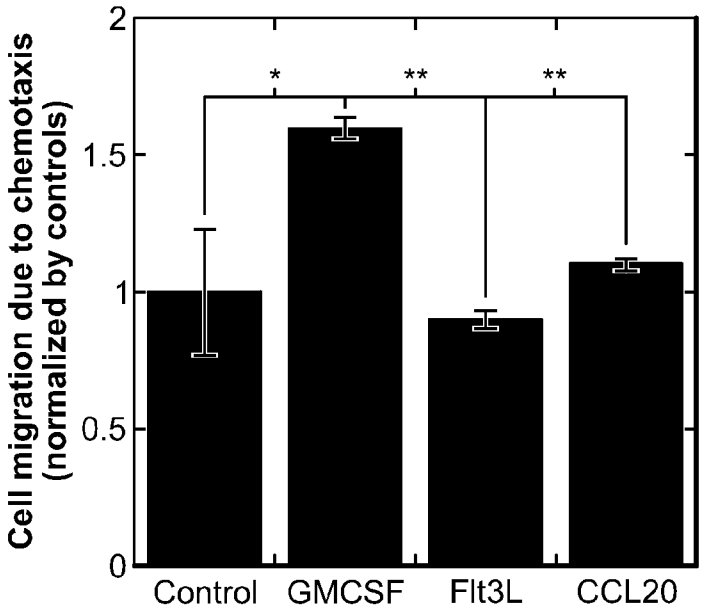


FIG. 23A

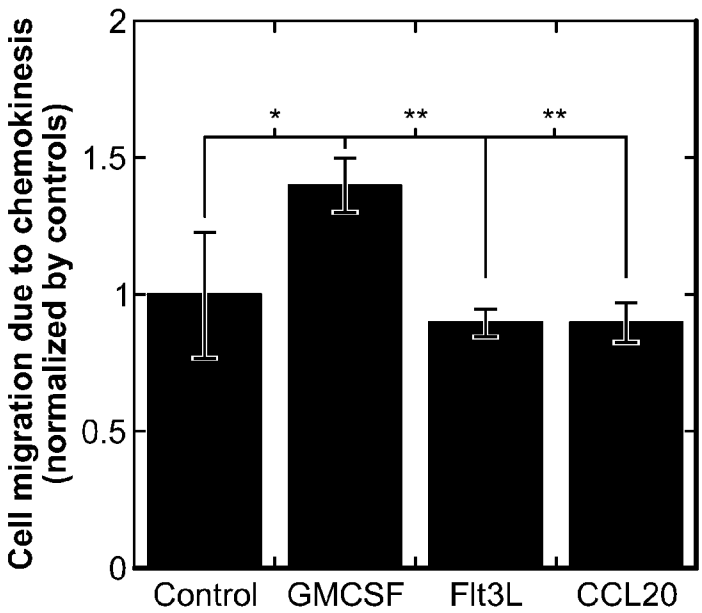


FIG. 23B

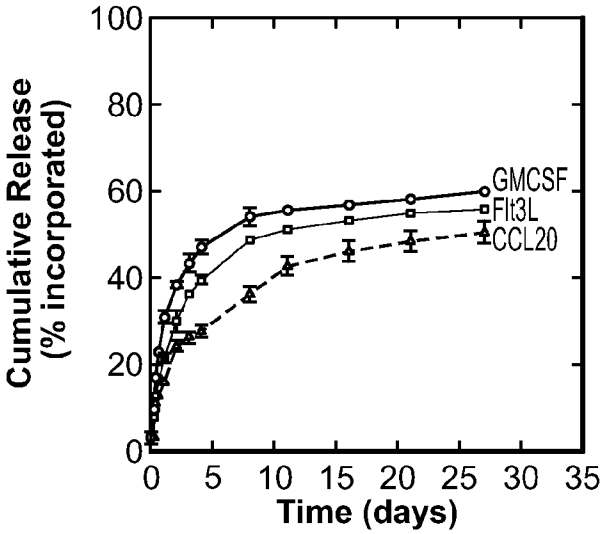


FIG. 24A

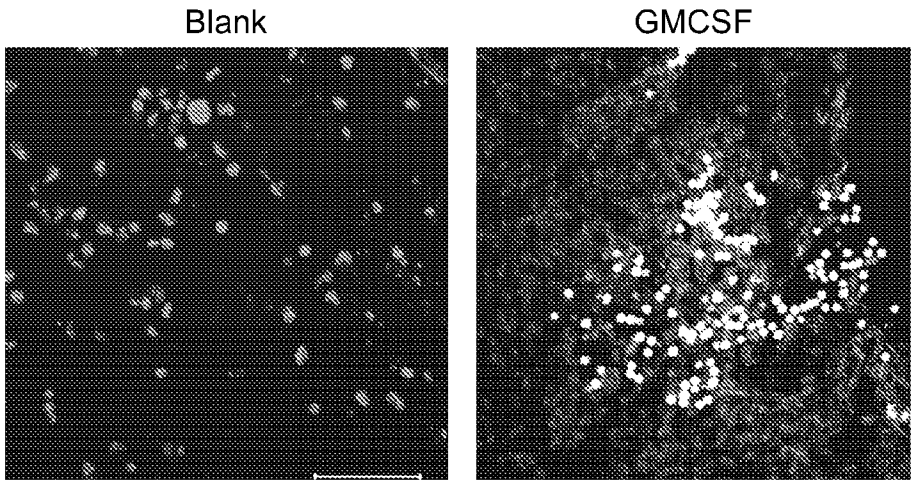


FIG. 24B

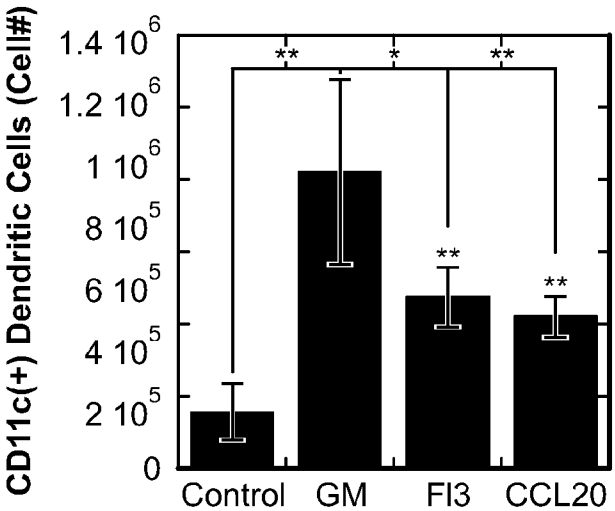


FIG. 24C

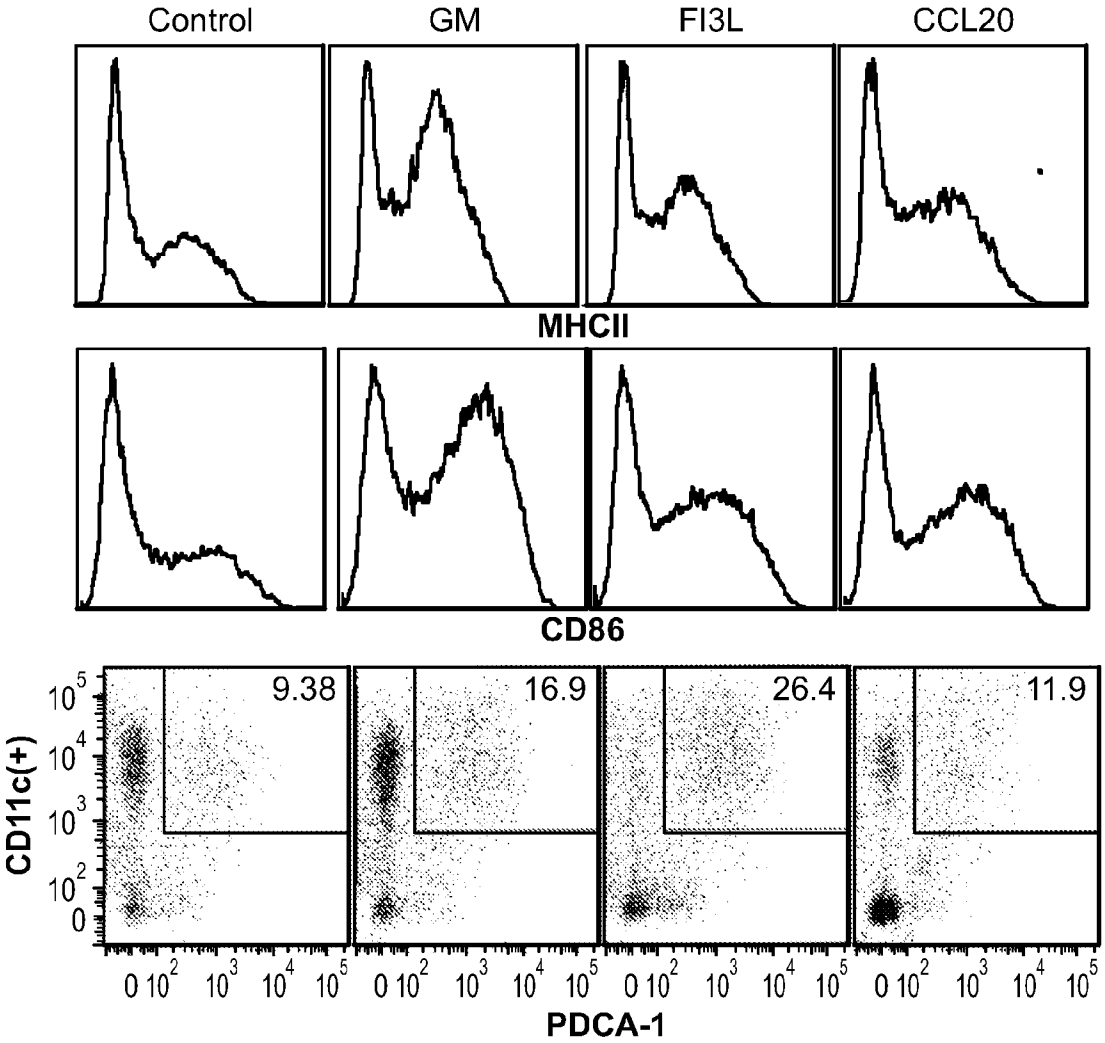


FIG. 25A

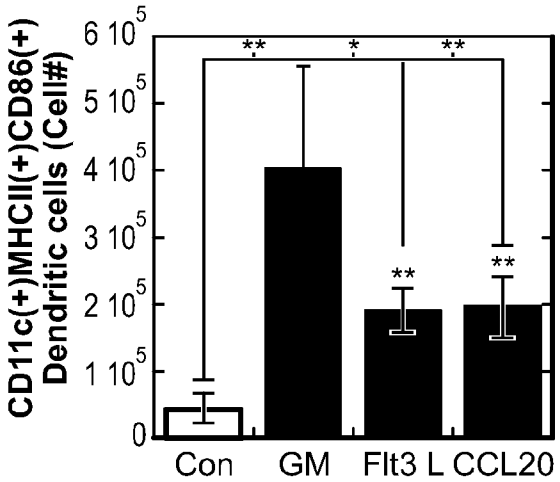


FIG. 25B

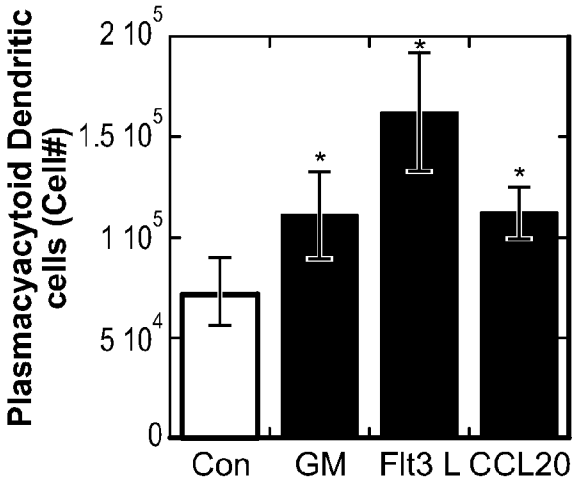


FIG. 25C

FIG. 26A

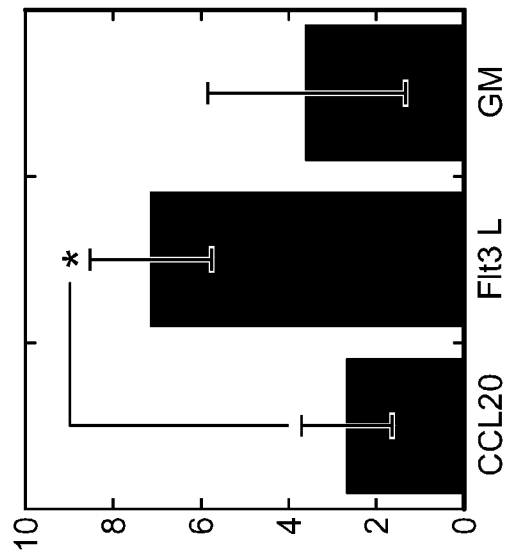


FIG. 26B

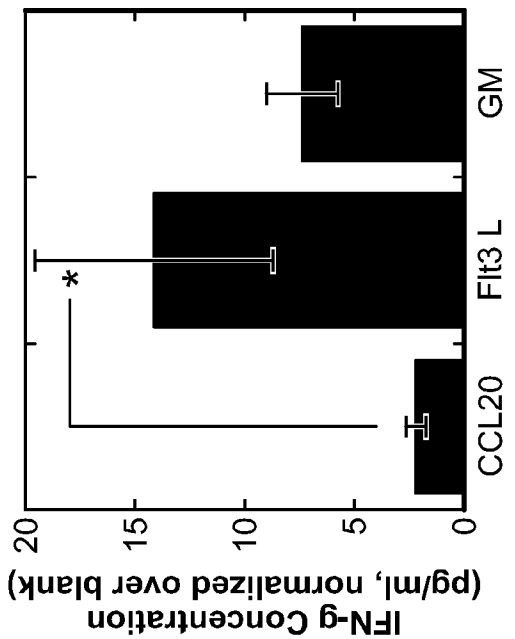


FIG. 26C

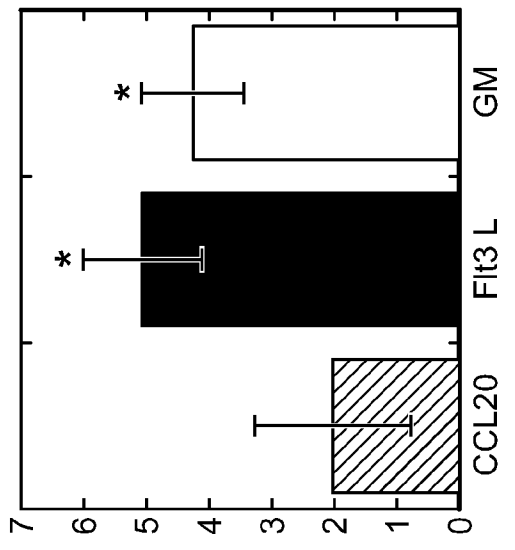
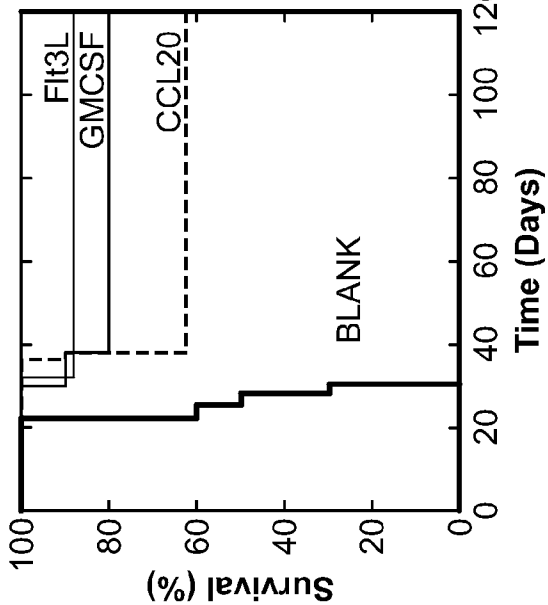


FIG. 26D



INTERNATIONAL SEARCH REPORT

International application No
PCT/US2013/021478

A. CLASSIFICATION OF SUBJECT MATTER
INV. A61K39/39 A61K9/16
ADD.

According to International Patent Classification (IPC) or to both national classification and IPC

B. FIELDS SEARCHED

Minimum documentation searched (classification system followed by classification symbols)
A61K

Documentation searched other than minimum documentation to the extent that such documents are included in the fields searched

Electronic data base consulted during the international search (name of data base and, where practicable, search terms used)
EPO-Internal, WPI Data, BIOSIS, EMBASE, INSPEC

C. DOCUMENTS CONSIDERED TO BE RELEVANT

Category*	Citation of document, with indication, where appropriate, of the relevant passages	Relevant to claim No.
X,P	WO 2012/009611 A2 (UNIV JOHNS HOPKINS [US]; FUCHS EPHRAIM JOSEPH [US]; UNIV YALE [US]; FA) 19 January 2012 (2012-01-19) the whole document	1-27
X	WO 2005/072088 A2 (SCIPERIO INC [US]; HIGBEE RUSSELL G [US]; BARBER GLEN N [US]; KACHURIN) 11 August 2005 (2005-08-11) abstract page 15, lines 15-22 claims; examples	1-27
X	WO 2011/150240 A1 (SELECTA BIOSCIENCES INC [US]; BRATZLER ROBERT L [US]; JOHNSTON LLOYD [) 1 December 2011 (2011-12-01) page 3, lines 1-26 page 4, lines 12-24 examples	1-27

-/--

[X] Further documents are listed in the continuation of Box C.

[X] See patent family annex.

* Special categories of cited documents :

"A" document defining the general state of the art which is not considered to be of particular relevance

"E" earlier application or patent but published on or after the international filing date

"L" document which may throw doubts on priority claim(s) or which is cited to establish the publication date of another citation or other special reason (as specified)

"O" document referring to an oral disclosure, use, exhibition or other means

"P" document published prior to the international filing date but later than the priority date claimed

"T" later document published after the international filing date or priority date and not in conflict with the application but cited to understand the principle or theory underlying the invention

"X" document of particular relevance; the claimed invention cannot be considered novel or cannot be considered to involve an inventive step when the document is taken alone

"Y" document of particular relevance; the claimed invention cannot be considered to involve an inventive step when the document is combined with one or more other such documents, such combination being obvious to a person skilled in the art

"&" document member of the same patent family

Date of the actual completion of the international search	Date of mailing of the international search report
12 April 2013	23/04/2013

Name and mailing address of the ISA/	Authorized officer
European Patent Office, P.B. 5818 Patentlaan 2 NL - 2280 HV Rijswijk Tel. (+31-70) 340-2040, Fax: (+31-70) 340-3016	Villa Riva, A

INTERNATIONAL SEARCH REPORT

International application No
PCT/US2013/021478

C(Continuation). DOCUMENTS CONSIDERED TO BE RELEVANT

Category*	Citation of document, with indication, where appropriate, of the relevant passages	Relevant to claim No.
X	WO 2011/151431 A1 (GLAXOSMITHKLINE BIOLOG SA [BE]; OUAKED NADIA [CA]; PLANTE MARTIN [CA];) 8 December 2011 (2011-12-08) the whole document	1-27
X	US 2010/272771 A1 (HARLOW ED [US] ET AL) 28 October 2010 (2010-10-28) paragraphs [0085], [0156], [0175], [0210] claims	1-27
X	WO 2009/102465 A2 (HARVARD COLLEGE [US]; DANA FARBER CANCER INST INC [US]; MOONEY DAVID J) 20 August 2009 (2009-08-20) cited in the application the whole document	1-27
X	KRISHNAMACHARI YOGITA ET AL: "PLGA microparticles that co-deliver antigen and toll like receptor ligand adjuvants for applications in cancer immunotherapy", INTERNET CITATION, 11 November 2009 (2009-11-11), page 1, XP002670678, Retrieved from the Internet: URL:http://abstracts.aapspharmaceutica.com /ExpoAAPS09/CC/forms/attendee/index.aspx?c ontent=sessionInfo&sessionId=2176 [retrieved on 2012-03-01] abstract	1-27
Y	AIALA SALVADOR ET AL: "Combination of immune stimulating adjuvants with poly(lactide-co-glycolide) microspheres enhances the immune response of vaccines", VACCINE, ELSEVIER LTD, GB, vol. 30, no. 3, 15 November 2011 (2011-11-15), pages 589-596, XP028348171, ISSN: 0264-410X, DOI: 10.1016/J.VACCINE.2011.11.057 [retrieved on 2011-11-22] figures 2-4; tables 1,2 page 595, right-hand column, lines 4-12	1-27
Y	MARIE-LUCE DE TEMMERMAN ET AL: "Particulate vaccines: on the quest for optimal delivery and immune response", DRUG DISCOVERY TODAY, vol. 16, no. 13, July 2011 (2011-07), pages 569-582, XP028231719, ISSN: 1359-6446, DOI: 10.1016/J.DRUDIS.2011.04.006 [retrieved on 2011-05-04] the whole document	1-27

-/--

INTERNATIONAL SEARCH REPORT

International application No
PCT/US2013/021478

C(Continuation). DOCUMENTS CONSIDERED TO BE RELEVANT

Category*	Citation of document, with indication, where appropriate, of the relevant passages	Relevant to claim No.
Y	SAMAR HAMDY ET AL: "Targeting dendritic cells with nano-particulate PLGA cancer vaccine formulations", ADVANCED DRUG DELIVERY REVIEWS, ELSEVIER BV, AMSTERDAM, NL, vol. 63, no. 10, 9 May 2011 (2011-05-09), pages 943-955, XP028277027, ISSN: 0169-409X, DOI: 10.1016/J.ADDR.2011.05.021 [retrieved on 2011-06-06] figure 3; table 2 Page 950-951, Section 4.4 -----	1-27

INTERNATIONAL SEARCH REPORT

Information on patent family members

International application No
PCT/US2013/021478

Patent document cited in search report	Publication date	Patent family member(s)	Publication date
WO 2012009611 A2	19-01-2012	AU 2011279024 A1	21-02-2013
		WO 2012009611 A2	19-01-2012
WO 2005072088 A2	11-08-2005	AU 2004314706 A1	11-08-2005
		CA 2548992 A1	11-08-2005
		EP 1697511 A2	06-09-2006
		JP 4772693 B2	14-09-2011
		JP 2007517774 A	05-07-2007
		JP 2011173909 A	08-09-2011
		US 2005244505 A1	03-11-2005
		US 2010285132 A1	11-11-2010
		WO 2005072088 A2	11-08-2005
WO 2011150240 A1	01-12-2011	AU 2011258147 A1	01-11-2012
		AU 2011258156 A1	08-11-2012
		AU 2011258165 A1	08-11-2012
		AU 2011258171 A1	08-11-2012
		CA 2798323 A1	01-12-2011
		CA 2798493 A1	01-12-2011
		CA 2798739 A1	01-12-2011
		CA 2798994 A1	01-12-2011
		CN 102905728 A	30-01-2013
		CN 102905729 A	30-01-2013
		CN 102917731 A	06-02-2013
		EP 2575773 A2	10-04-2013
		EP 2575876 A1	10-04-2013
		EP 2575886 A1	10-04-2013
		EP 2582393 A1	24-04-2013
		US 2011293700 A1	01-12-2011
		US 2011293701 A1	01-12-2011
		US 2011293723 A1	01-12-2011
		US 2012027806 A1	02-02-2012
		WO 2011150240 A1	01-12-2011
		WO 2011150249 A1	01-12-2011
		WO 2011150258 A1	01-12-2011
		WO 2011150264 A2	01-12-2011
WO 2011151431 A1	08-12-2011	AU 2011260215 A1	17-01-2013
		CA 2801266 A1	08-12-2011
		CN 102905726 A	30-01-2013
		EP 2575871 A1	10-04-2013
		SG 185729 A1	28-12-2012
		WO 2011151431 A1	08-12-2011
US 2010272771 A1	28-10-2010	US 2010272771 A1	28-10-2010
		US 2010272776 A1	28-10-2010
WO 2009102465 A2	20-08-2009	AU 2009215188 A1	20-08-2009
		CA 2715460 A1	20-08-2009
		CN 102006891 A	06-04-2011
		EP 2254602 A2	01-12-2010
		JP 2011511834 A	14-04-2011
		US 2012100182 A1	26-04-2012
		WO 2009102465 A2	20-08-2009